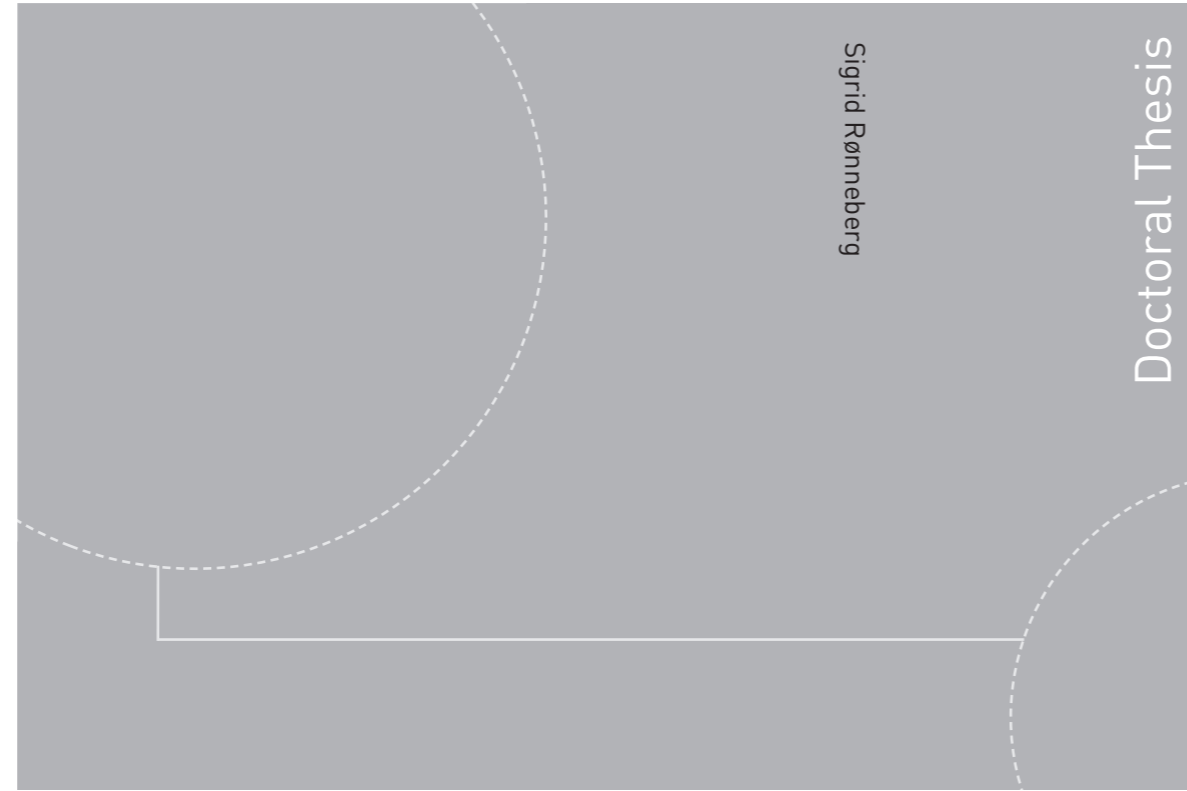


ISBN 978-82-326-4527-8 (printed version)
ISBN 978-82-326-4524-5 (electronic version)
ISSN 1503-8181



Doctoral theses at NTNU, 2020:87

Sigrød Rønneberg

Fundamental Mechanisms of Ice Adhesion

Doctoral theses at NTNU, 2020:87

NTNU
Norwegian University of
Science and Technology
Faculty of Engineering
Department of Structural Engineering

 **NTNU**
Norwegian University of
Science and Technology

 NTNU

 **NTNU**
Norwegian University of
Science and Technology

Sigrid Rønneberg

Fundamental Mechanisms of Ice Adhesion

Thesis for the degree of Philosophiae Doctor

Trondheim, 05.03.2020

Norwegian University of Science and Technology
Faculty of Engineering
Department of Structural Engineering



Norwegian University of
Science and Technology

NTNU

Norwegian University of Science and Technology

Thesis for the degree of Philosophiae Doctor

Faculty of Engineering

Department of Structural Engineering

© Sigrid Rønneberg

ISBN 978-82-326-4527-8 (printed version)

ISBN 978-82-326-4524-5 (electronic version)

ISSN 1503-8181

Doctoral theses at NTNU, 2020:87



Printed by Skipnes Kommunikasjon as

Beautiful!
Powerful!
Dangerous!
Cold!
Ice has a magic, can't be controlled

This icy force both foul and fair
Has a frozen heart worth mining!

There's beauty and there's danger here
Split the ice apart!

Frozen Heart by Kristen Anderson-Lopez and Robert Lopez

Now suppose that there were many possible ways in which water could crystallize, could freeze. Suppose that the sort of ice we skate upon and put into highballs - what we might call *ice-one* - is only one of several types of ice. And suppose that there were one form - which we will call *ice-nine*, with a melting point of 50°C. (...)

I tried to alarm them about *ice-nine* being a means to ending life on earth. (...)

It was winter now, and forever.

Cat's Cradle by Kurt Vonnegut

Abstract

Unwanted icing cause daily problems, as well as dangerous situations and costly repairs. Both de-icing and anti-icing techniques are applied to mitigate unwanted ice formation, and the most promising technique is the development of low ice adhesion surfaces. At present, there exists several types of such low ice adhesion surfaces. Although research of low ice adhesion strength continuously increases, there is no unified definition of icephobicity and the fundamental mechanisms of ice adhesion and ice detachment are largely unknown. Furthermore, each research group creates its own experimental set-up to generate ice and test the ice adhesion strength of their developed surfaces. As a result, the reported ice adhesion strength values are not comparable.

Ice is an inherently chaotic substance, and the properties and interaction of ice situated on a surface depends greatly on the environmental conditions and ice formation process. It is the forces and interactions on atomic level which determine the ice adhesion strength. Of these, the electrostatic forces are the most prominent in ice-solid adhesion processes. In order to lower the ice adhesion strength, the forces at the ice-solid interface must be minimised. However, different icing conditions result in different types of ice, which leads to different ice adhesion mechanisms.

There are several different types of ice, which are neither agreed upon nor uniformly defined. As each ice type has very different properties, such a lack of agreement might result in misunderstandings and challenge the comparability of research performed at different facilities. In this thesis, the ice adhesion strength of three types of ice on bare aluminium surfaces were investigated. The three ice types were precipitation ice, in-cloud ice and bulk water ice, and the ice adhesion strength was measured with a centrifugal adhesion test. The results showed a significant difference when comparing the ice adhesion strength of the three ice types. Precipitation ice has a higher ice adhesion strength than the other two, and bulk water ice is the easiest to remove. Bulk water ice only displays 40% of the ice adhesion of precipitation ice under similar conditions, and the standard deviation is quite high for all three ice types. The difference is thought to result from differences in the density of the ice types, due to mechanical properties of the ice based on their formation process.

As there is no available and recognised standard today, all quantitative ice adhesion strength results need to be adjusted in order to be directly comparable. In this thesis, it has been shown that the reported ice adhesion strengths are very sensitive to measurement set-up in addition to the ice type. Due to the many different applications of low ice adhesion surfaces and coatings, an ideal standard measurement technique for ice adhesion strength may never exist. However, with

a common reference test, a specific comparison between both past and present reported values of ice adhesion strength may be compared to each other. We suggest such a reference test as a horizontal shear test with bulk water ice on a bare aluminium surface under given atmospheric conditions. By establishing a database of reported ice adhesion strengths from this reference set-up, and testing the experimental parameters individually, the effect of changing these parameters can be determined.

To further explore the effect of changing ice adhesion strength test methods and experimental set-ups, an interlaboratory study between two facilities researching ice adhesion strength has been performed as part of this thesis. This study found that there are significant differences between the ice adhesion strength obtained from different ice adhesion tests, but that the same trends are apparent. From this study, it can be concluded that the most important property of a test well suited to measure ice adhesion strength is repeatability, due to the large effect of experimental outliers where the ice adhesion strength differ from normal values.

Through atomistic simulations, it is possible to visualise and investigate the ice-solid detachment mechanisms at nanoscale and investigate fundamental relations governing ice-solid adhesion. Through such simulations, this thesis has validated the thermodynamic theory concerning the relation between water wettability and ice adhesion strength for ideal systems. This theory is not agreed upon from experiments, but the simulations indicate that this disagreement is due to surface material deformations and other experimental factors which may be controlled, and not the properties of water and ice. The reproduction of the nanoscale theory is interesting and important due to the gap in understanding between experimental observations and theoretical models. The results represents a step towards a more thorough understanding of the fundamental mechanisms of ice adhesion, and its relation to water wettability.

With improved communication of experimental conditions, and thus enhanced comparability, the multitude of developed low ice adhesion surfaces may be discussed and compared with a common framework and demands. By further investigating the fundamental mechanisms of ice adhesion for different ice types, and determining their detachment process from a solid surface, we will be a large step closer to understanding the theory behind ice-solid adhesion, and thus to design surfaces that truly minimises the ice adhesion.

Summary for the general public

Unwanted icing cause daily problems, as well as dangerous situations and costly repairs. To avoid such icing, several types of anti-ice surface coating has been developed where ice does not stick to the surface, but rather slides right off. These surfaces are denoted as low ice adhesion surfaces. However, although several such low ice adhesion surfaces have been developed over the past decades, the mechanisms governing the ice removal are still unknown. As a result, the development of new surfaces is performed by a trial-and-error approach.

In this thesis, the focus has been to examine the underlying mechanisms of detachment of ice from a surface. It has been discovered that the type of ice to be removed, for instance clear ice or frost, has a great impact on the difficulty of removing the ice. Furthermore, the method of ice removal during the testing of the developed surfaces impacts how difficult the ice is to remove. When experimental equipment is custom-made at each laboratory, these differences lead to a profound lack of comparability between developed low ice adhesion surfaces. This thesis proposes a common reference that all future and past low ice adhesion surfaces may be compared to. The key point of such a reference is the repeatability of the experiments, and it will include both the type of ice tested, and the ice removal method.

By computational simulations, it is also possible to investigate what actually happens to the molecules of ice and water when situated on the surface. Through such simulations, it has been shown that the shape of water droplets on a surface might predict the difficulty of ice removal of the same surface, as stated by thermodynamics. As experimental studies disagree upon the existence of the relationship, the simulations indicate that the disagreement is not due to the properties and interactions of ice and water, but rather experimental factors such as surface properties and material deformations.

The only feasible strategy to develop fully automated ice removal through low ice adhesion surfaces is to understand what is happening during ice removal. This thesis represents a large step towards this fundamental understanding.

Generelt sammendrag

Uønsket ising skaper daglig problemer og situasjoner som kan være både farlige og kostbare. For å unngå slik ising har det blitt utviklet flere typer anti-is overflater som hindrer is i å feste seg på overflaten og heller sklir rett av. Disse overflatene har dermed lav isvedheft. Dessverre er mekanismene for hvordan disse overflatene virker i stor grad ukjente, selv om det er blitt forsket på dem i flere tiår. Dette gjør at utviklingen av nye overflater ofte gjennomføres med prøve- og feilemetoden.

I denne avhandlingen har fokuset vært på å undersøke de underliggende mekanismene for hvordan is løsner fra en overflate. Nye funn er at typen is som skal fjernes, enten det er for eksempel rim eller klar is, betyr mye for hvor vanskelig isen er å fjerne. Videre betyr også metoden brukt for å fjerne isen mye for hvor vanskelig isen er å fjerne fra overflaten. Når eksperimentelt utstyr spesialbygges på hvert laboratorium, fører de overnevnte forskjellene til en grunnleggende mangel på sammenlignbarhet mellom ulike typer overflater med lav isvedheft. Denne avhandlingen foreslår en felles referanse som alle fremtidige og tidligere overflater med lav isvedheft kan sammenlignes med. Den viktigste egenskapen til denne referansen er repeterbarheten, og referansen inkluderer både typen is testet og isfjerningsmetoden.

Ved å bruke datasimuleringer er det også mulig å undersøke vannmolekylene i vann og is på en overflate. Gjennom slike atomsimuleringer har det blitt vist at formen på vandrdåper på en overflate kan forutsi hvor lett is kan fjernes fra overflaten, slik som forutsett av termodynamisk teori. Ettersom eksperimentelle resultater ikke enes om den samme sammenhengen, indikerer simuleringene at uenigheten er på grunn av eksperimentelle faktorer, og ikke på grunn av vannet eller isen og dets egenskaper.

Den eneste gjennomførbare strategien for å utvikle fullt automatiserte systemer for isfjerning gjennom overflater med lav isvedheft er å forstå hva som skjer når isen løsner fra overflaten. Denne avhandlingen representerer et stort steg mot denne underliggende forståelsen.

List of contributions

Included papers

Paper 1: The effect of ice type on ice adhesion

Sigrid Rønneberg, Caroline Laforte, Christophe Volat, Jianying He, and Zhiliang Zhang. 2019. "The effect of ice type on ice adhesion", AIP Advances, 9: 055304. [1]

To lower the ice adhesion strength is the most efficient technique for passive ice removal for several applications. In this paper, the effect of different types of ice on the ice adhesion strength was investigated. The ice types precipitation ice, in-cloud ice and bulk water ice on the same aluminum substrate and under similar environmental conditions were investigated. The ice adhesion strength was measured with a centrifugal adhesion test and varied from 0.78 ± 0.10 MPa for precipitation ice, 0.53 ± 0.12 MPa for in-cloud ice to 0.28 ± 0.08 MPa for bulk water ice. The results indicate that the ice adhesion strength inversely correlates with the density of ice. The results inspire a new strategy in icephobic surface development, specifically tailored to the relevant ice type.

Co-author contributions

The experiments were conducted by Sigrid Rønneberg and Caroline Laforte with help from Caroline Blackburn at the Anti-icing Materials International Laboratory (AMIL) facilities in Chicoutimi, Quebec, Canada. The results were analysed by Sigrid Rønneberg, who also wrote the draft. All authors contributed to the idea of the study, as well as the final preparation of the manuscript.

Paper 2: The need for standards in low ice adhesion surface research: A critical review

Sigrid Rønneberg, Jianying He, and Zhiliang Zhang. 2019. "The need for standards in low ice adhesion surface research: a critical review", *Journal of Adhesion Science and Technology*: 1-29. [2]

Low ice adhesion surfaces are a promising anti-icing strategy. However, experimentally obtained ice adhesion strengths are so far not transferable or comparable, and they are very sensitive to the experimental set-up and type of accreted ice. This critical review describes both the widely used ice adhesion measurement techniques and ice generation methods, before discussing why the results cannot be directly compared. The ice adhesion measurement techniques included are horizontal and vertical shear tests, centrifugal ice adhesion tests and tensile tests. The ice generation methods included in the review are icing by freezing drizzle, wind tunnel icing and bulk water icing, and definitions of other ice types are included. Special challenges for low ice adhesion surfaces have been discussed, as well as the effect of ice sample size and the impact from gravity. A future standard within ice adhesion research should be able to directly compare different experimental results, and should, therefore, include all relevant parameters and currently available methods. Due to the large variation of available ice adhesion set-ups, it is recommended that a reference test and ice type is established for enhanced comparability. The reference suggested is a horizontal shear test with bulk water ice, and defined experimental parameters. A continuing focus on the fundamental mechanisms of ice adhesion is needed to identify the important contributions to the large variations in reported ice adhesion strengths.

Co-author contributions:

The literature review was conducted by Sigrid Rønneberg, who also wrote first draft. All authors contributed equally to the development of the idea as well as revision and writing of the final manuscript.

Paper 3: Interlaboratory Study of Ice Adhesion Using Different Techniques

Sigrid Rønneberg, Yizhi Zhuo, Caroline Laforte, Jianying He, and Zhiliang Zhang. 2019. "Interlaboratory Study of Ice Adhesion Using Different Techniques", *Coatings*, 9: 678. [3]

Low ice adhesion surfaces are a promising anti-icing strategy. However, reported ice adhesion strengths cannot be directly compared between research groups. This study compares results obtained from testing the ice adhesion strength on two types of surfaces at two different laboratories, testing two different types of ice with different ice adhesion test methods at temperatures of -10°C and -18°C . One laboratory used the centrifuge adhesion test and tested precipitation ice and bulk water ice, while the other laboratory used a vertical shear test and tested only bulk water ice. The surfaces tested were bare aluminum and a commercial icephobic coating, with all samples prepared in the same manner. The results showed comparability in the general trends, surprisingly, with the greatest differences for bare aluminum surfaces at -10°C . For bulk water ice, the vertical shear test resulted in systematically higher ice adhesion strength than the centrifugal adhesion test. The standard deviation depends on the surface type and seems to scale with the absolute value of the ice adhesion strength. The experiments capture the overall trends in which the ice adhesion strength surprisingly decreases from -10°C to -18°C for aluminum and is almost independent of temperature for a commercial icephobic coating. In addition, the study captures similar trends in the effect of ice type on ice adhesion strength as previously reported and substantiates that ice formation is a key parameter for ice adhesion mechanisms. Repeatability should be considered a key parameter in determining the ideal ice adhesion test method.

Co-author contributions:

The experiments at AMIL facilities were performed by Caroline Laforte, while the experiments at NTNU were performed by Yizhi Zhuo and Sigrid Rønneberg. The analysis of the data and the writing of the first draft was performed by Sigrid Rønneberg. All authors contributed to the idea, as well as the revision and writing of the final manuscript.

Paper 4: Nanoscale Correlations of Ice Adhesion Strength and Water Contact Angle

Sigrid Rønneberg, Senbo Xiao, Jianying He, and Zhiliang Zhang. 2020. "Nanoscale Correlations of Ice Adhesion Strength and Water Contact Angle", Submitted.

Surfaces with low ice adhesion represent a promising strategy to achieve passive anti-icing performance. However, as a successful and robust low ice adhesion surface must be tested under realistic conditions at low temperatures and for several types of ice, the initial screening of potential low ice adhesion surfaces requires large resources. A theoretical relation between ice adhesion and water wettability in the form of water contact angle exists, but there is disagreement on whether this relation holds for experiments. In this study, we utilise molecular dynamics simulations to examine the fundamental relations between ice adhesion and water contact angle on an ideal graphene surface. The results show a significant correlation according to the theoretic predictions, indicating that the theoretical relation holds for the ice and water when discarding surface material deformations and other experimental factors. The reproduction of the thermodynamic theory at the nanoscale is important due to the gap between experimental observations and theoretical models. The results in this study represent a step forward towards understanding the fundamental mechanisms of water-solid and ice-solid interactions, and the relationship between them.

Co-author contributions:

The atomistic simulation systems were created by Senbo Xiao, while all simulations were performed by Sigrid Rønneberg, who also analysed the data and wrote the first draft. All authors contributed to the idea, as well as the revision and writing of the final manuscript.

Other publications

Book chapter: Comparison of icephobic materials through interlaboratory studies

Sigrid Rønneberg, Caroline Laforte, Jianying He, and Zhiliang Zhang. 2020. "Comparison of icephobic materials through interlaboratory studies." in Kash Mittal and Chang-Hwan Choi (eds.), *Ice Adhesion: Mechanism, Measurement and Mitigation* (Wiley).

Conference paper: Standardizing the testing of low ice adhesion surfaces

Sigrid Rønneberg, Jianying He, and Zhiliang Zhang. 2019. "Standardizing the testing of low ice adhesion surfaces." In *International Workshops on Atmospheric Icing of Structures (IWAIS)*, Reykjavik, Iceland. [4].

Conference presentations

Sigrid Rønneberg, Zhiwei He, Senbo Xiao, Jianying He, Zhiliang Zhang. (2017) *Fundamental Characteristics of Surfaces with Low Ice Adhesion*. International Workshop on Surface Icing and Assessment of De-Icing / Anti-Icing Technologies. Fraunhofer IFAM; Bremen. 2017-01-24 - 2017-01-25.

Sigrid Rønneberg, Caroline Laforte, Christophe Volat, Jianying He, Zhiliang Zhang. (2018) *The Effect of Ice Type on Ice Adhesion*. 14th International Conference on the Physics and Chemistry of Ice. Paul Scherrer Institut; Zürich. 2018-01-08 - 2018-01-12.

Sigrid Rønneberg, Jianying He, Zhiliang Zhang. (2019) *Ice ice baby – Variations in ice type for low ice adhesion surfaces*. International Symposium on Materials for Anti-Icing . NTNU Nanomechanical Lab; Trondheim. 2019-05-27 - 2019-05-28.

Sigrid Rønneberg, Jianying He, Zhiliang Zhang. (2019) *Standardizing the testing of low ice adhesion surfaces*. International Workshop on Atmospheric Icing of Structures (IWAIS); Reykjavik. 2019-06-23 - 2019-06-28.

Sigrid Rønneberg, Senbo Xiao, Jianying He, Zhiliang Zhang. (2019) *Ice adhesion and wettability at nanoscale*. Norwegian Nanosymposium 2019. NTNU Nano; Trondheim. 2019-10-16 - 2019-10-17.

Other contributions

Selected popular science presentations

Sigrid Rønneberg. (2018) Superglatte overflater for isfjerning. Forsker Grand Prix / Researchers Grand Prix, Trondheim 2018 . Forskningsdagene; Trondheim, Byscenen. 2018-09-27.

Sigrid Rønneberg. (2019) Anti-is mysteriet. Researcher's Night 2019 . NTNU; Trondheim. 2019-09-27 - 2019-09-27.

Co-authored publications and presentations

Tong Li, Yizhi Zhuo, Verner Håkonsen, Sigrid Rønneberg, Jianying He, Zhiliang Zhang. (2019) Epidermal Gland Inspired Self-Repairing Slippery Lubricant-Infused Porous Coatings with Durable Low Ice Adhesion. *Coatings*. vol. 9 (10).

Verner Håkonsen, Zhiwei He, Sigrid Rønneberg, Yizhi Zhuo, Senbo Xiao, Jianying He, Zhiliang Zhang. (2018) Fundamental icephobicity - Recent studies and findings. NATO STO AVT PBM meeting. NATO STO; Athens. 2018-12-10 - 2018-12-14.

Per-Olaf Borrebæk, Sigrid Rønneberg, Tong Li, Bjørn Petter Jelle, Alex Klein-Paste, and Zhiliang Zhang. 2020. "Snow adhesion on icephobic surfaces", Submitted.

Per-Olaf Borrebæk, Sigrid Rønneberg, Bjørn Petter Jelle, Alex Klein-Paste, Jianying He, and Zhiliang Zhang. 2020. "A classifying framework for cold precipitation", In preparation.

Acknowledgements

A PhD is not a one person task. Luckily, I have had the help of some great people.

First and foremost, I want to thank my supervisors, professor Zhiliang Zhang and professor Jianying He. Thank you for always believing in me, and for your unfaltering support. You have given me inspiration and space to work on my own ideas, no matter that it differed from what I was meant to research. Without your vast knowledge and experience, this thesis or the research within would never have seen the light of day or been completed. To Zhiliang, thank you for the close supervision throughout the past three years, and especially for your fast responses these past few weeks. You have given me the guidance I needed when I was faltering, and you have given me focus. To Jianying, thank you for all your encouragement and for our talks when I have felt close to drowning.

I also want to thank the rest of the anti-icing team at the Nanomechanical Lab (NML) at NTNU: Senbo Xiao, Zhiwei He, Verner Håkonsen, Yizhi Zhuo, Tong Li and Feng Wang, as well as Per-Olof Borrebæk at the Department of Civil Engineering. For our fruitful discussions, for your cooperation, and for your help when I became stuck. For Senbo in particular, thank you for creating the simulation systems I was always meant to focus on in my research, and which are the topic of the final paper of this thesis. I got to them in the end!

A special thank you to Caroline Laforte at the Anti-icing Materials International Laboratory (AMIL) in Chicoutimi, Canada. Thank you for agreeing with me that different types of ice were interesting, and for allowing me to come and visit your lab and cooperate with you on the projects in this thesis. It is amazing that one conversation at a conference in January 2017 turned into a book chapter and two journal papers, as well as lots of inspiration for future international collaborations.

To the rest of my colleagues at NML, thank you for your friendship, both past and present. To my previous officemates Merete and Sandra, and office neighbours Ingrid and Susanne, thank you for being someone to take coffee breaks with and for seeing a friendly face at work each day. Thank you also to all friends in Trondheim, who have kept me functioning during the past months by helping with social interactions and food.

Finally, thank you to my family. My parents, who have always believed in me and who allowed me to question the world and discussed it with me from an early age. I would not have been here without you, and I would not have had the confidence to start a PhD without you. I would also not have been able to finish my PhD while moving from Trondheim to Oslo without your help. Last, but not least, to Knut. Thank you for staying with me through the hardships, and for helping me celebrate milestones. You have kept me sane these three years. All the best ideas in this project has been born in conversations with you, and you have made sure

xvi

my grammar was on point. The best part of the past three and a half years has been marrying you.

Contents

Abstract	iii
Summary for the general public	v
Generelt sammendrag	vii
List of contributions	ix
Acknowledgements	xv
List of Figures	xix
List of Tables	xxi
Preface	xxiii
1 Introduction	1
1.1 De-icing and anti-icing	2
1.2 Low ice adhesion surfaces	4
1.3 Unanswered questions	6
2 Background	9
2.1 Definitions	9
2.2 Forces and interactions	12
2.3 Ice adhesion models	14
2.4 Ice as a material	16
2.5 Wettability	17
3 Finding ice adhesion	21
3.1 Measurement techniques	21
3.1.1 Comparisons	23
3.1.2 Recommendations	27
3.2 Types of ice	29

3.2.1	Size and density of impact ices	32
3.2.2	Ice type and ice adhesion strength	34
3.3	Future comparability and standardisation	36
4	Results and findings	41
4.1	Effect of ice type	41
4.2	The need for standards	44
4.3	Interlaboratory study	46
4.4	Nanoscale correlations	48
5	Discussion and concluding remarks	53
5.1	Answers to fundamental questions	53
5.2	Future work	59
5.3	Concluding remarks	61
	Bibliography	63
I	Included papers	75
A	Paper 1	77
B	Paper 2	95
C	Paper 3	127
D	Paper 4	151
II	Other publications	193
E	Book chapter	195
F	Conference paper	227
III	Extra appendices	235
G	Future work	237
H	Publication list	247

List of Figures

1.1	Overview of available publications including the phrase "ice adhesion", found with a simple literature search performed at Sciencedirect and Scopus at December 7 2019. No further classification was applied, and no other key words were included.	7
2.1	Illustration of the most general water contact angle θ . The surface energies γ correspond to the parameters of Young's equation in equation (2.4). Figure also appears in Paper 4 (Appendix D). . . .	18
3.1	Schematic illustration of the four most widely used tests methods for ice adhesion strength measurements: a) Horizontal shear test b) Vertical shear test c) Tensile test d) Centrifugal adhesion test. For all methods, ice is blue and the fixed surface is grey, with the applied force on the ice illustrated by a green arrow. The counterweight in d) is red. Figure from Paper 2 (Appendix B). . . .	23
3.2	Illustration of the effect of gravity on the measured ice adhesion strength, given by the self-removed ice adhesion strength τ' divided by the measured ice adhesion strength τ for several generic low ice adhesion surfaces as a function of the height of the ice sample. The self-removed ice adhesion strength is given in equation (3.1). Figure from Paper 2 (Appendix B).	25
3.3	Ice adhesion strength of bulk water ice measured with vertical shear test at NTNU and centrifugal adhesion test at AMIL. AI denotes the bare aluminium surface, while IC represents the icephobic coating. Both surfaces were tested at temperatures of both -10°C and -18°C .	26
3.4	Overview of different types of ice and precipitation by droplet size. Overview based on droplet measurement techniques [141].	33
3.5	Images of the different ice types investigated in Paper 1.	35
3.6	Selected elements and parameters of the proposed reference data bank to enable comparison of differently obtained ice adhesion values. Figure from Paper 4 (Appendix D).	38

3.7	Schematic drawing of the proposed reference test for increased comparability within ice adhesion research. Figure from Paper 2 (Appendix B).	39
4.1	Ice adhesion strength obtained with the centrifugal test for the three ice types described in Table 4.1 at temperatures of -10°C on an aluminium surface.	42
4.2	Mean ice adhesion strength per ice type as a function of mass per ice thickness, i.e. apparent density, with standard deviations included. The linear fitting is given by equation (4.1), and is calculated from all experimental data.	43
4.3	Measured ice adhesion strengths. Aluminium surfaces as denoted as Al, while the surfaces with icephobic coating are denoted IC. Precipitation ice is denoted as PI while bulk water ice is denoted BWI. AMIL tests were performed with centrifuge adhesion test, while NTNU tests were performed with vertical shear test. All results for tests on bulk water ice are shown in Figure 3.3.	47
4.4	Ice adhesion strength as function of the contact angle θ as described by the general relation between ice adhesion strength τ and water contact angle on a generic surface with properties C_0 . The relation is described by equation (4.3).	50
4.5	Illustration of the normalised ice adhesion strength and water contact angle for all four systems investigated in the simulations, with the theoretical relation from equation (4.3) included together with the significance of the fitting.	51
G.1	Example of a system where the equilibrium properties of water and ice might be investigated, here by a water layer on an ideal graphene surface.	244

List of Tables

1.1	Unanswered questions within ice adhesion research.	8
2.1	Parameters from equations (2.2) and (2.3), describing two models for ice adhesion strength. Parameters in alphabetical order, units not included. For more details, see original references.	15
3.1	Overview of different ice adhesion tests covered by previous reviews, with Paper 2 from this thesis included. Year of publication is included.	22
3.2	Ice adhesion strength and experimental conditions of several studies of low ice adhesion surfaces utilising a shear test and the same type of ice, namely bulk water ice (see Section 3.2).	28
3.3	Alphabetical selection of definitions of icing and ice types from different references within several applications for anti-icing and ice mitigation.	30
3.4	Typical properties of accreted atmospheric ice on structures, as defined by ISO 12494 [17].	33
3.5	Typical processes of in-cloud icing with densities [142]. Condensation is ice formation by the deposition and freezing of super cooled droplets of vapour, while de-sublimation is the formation of ice crystals bypassing the liquid phase.	33
3.6	Six main classifications of accreted ice by densities and appearance, as described by [97, 143]. The top three ices are in the glaze family, while the bottom three are in the rime family.	34
3.7	Results of ice adhesion tests for the three different ice types, including the number of samples tested with each ice type. Data taken from Paper 1 (Appendix A).	35
4.1	Definition of ice types and ice generation methods.	41
4.2	Different definitions of glaze ice as applied to ice adhesion research.	45
4.3	Overview of the different simulation systems investigated in this study.	50

G.1 Overview of projects for future work to uncover further fundamental mechanisms of ice adhesion strength, divided in experimental and atomistic studies. 239

Preface

Winter has always been my favourite season of the year. So when I applied for a PhD position before finishing my Master degree, it was a big plus that the work entailed anti-icing. Although I had to switch to a new field of research, I am extremely happy with my project, and the path it has lead me on.

I have become completely fascinated by ice in the course of the past years. This incredible substance that is so common in Norway during winter, that enables skating and skiing and cold drinks during summer, that can be either white or transparent or any shade in between, and that we still do not know everything about. There are more than 15 different types of ice crystals, and an almost infinite amount of combinations of the one type of ice crystals that we see on Earth which gives the ice different properties.

My fascination with ice has greatly impacted the PhD project. Instead of doing mainly molecular dynamics simulations and multiscale modelling, as was detailed in my job description, I have spent my time investigating ice as a material. I have had a complete freedom of topic in my research, and have loved (almost) every minute of it. I now have an album where I store pictures of ice found in nature, which has been added to by family and friends.

Ice research is worldwide, and international. Through my years as a PhD candidate, I have met a great deal of interesting people, many of whom love ice as much as me. Ice is all around, and the work of understanding this mysterious substance never ends. There is always more to discover, and for someone like me who is driven by curiosity of the world around us, ice is the perfect research topic.

This PhD thesis has been a part of a project from the Norwegian Research Council called *Towards Design of Super-Low Ice Adhesion Surfaces (SLICE)*, project number 250990. Thank you for giving me the opportunity to discover my unknown passion for this cold substance that so impacts our daily life.

Chapter 1

Introduction

Ice and frost often cause inconvenience for the daily life of human beings [5–8]. In transport, icing and snowing on roads may cause slippery surfaces and lead to accidents [9, 10], and icing on the wings and surface of aircrafts may cause loss of lift, increase in drag, faults in gauge readings, and great risk of stalling and potentially fatal crashes [11–15].

Two particular problems in unwanted icing are atmospheric icing and icing on structures. Atmospheric icing, which is a general expression for any process of ice build-up and snow accretion on the surface of an object exposed to the atmosphere [16], may especially lead to numerous problems in telecommunications [15–17]. Atmospheric icing on structures can cause failure from static ice loads, dynamic effects, wind action, and damage caused by falling ice [17], and both wind turbines and power transmission lines are negatively impacted by icing [16–23]. For instance, icing of power transmission lines during winter storms is a persistent problem that causes outages and costs millions of dollar in repair expenses [7, 24, 25], and ice induced cascade failure events of power line towers, such as those in Canada in 1996 and in China 2008, have had catastrophic consequences [16, 26, 27].

As unwanted icing remains an important issue to solve for both daily life and industrial purposes, particularly for Arctic purposes, several different methods and research topics focus on ice mitigation. In this thesis, the focus will be on anti-icing technology in the form of low ice adhesion surfaces, and the fundamental mecha-

nisms governing the interaction of ice with different surfaces and the measurement of these. The scope of the thesis will be further defined in Section 1.3.

1.1 De-icing and anti-icing

To remove or mitigate unwanted ice, both de-icing techniques and anti-icing techniques are in use. De-icing techniques remove existing ice, while anti-icing techniques stop the accretion and formation of ice [28]. At present, three types of de-icing methods are in use to remove or prevent the formation of unwanted icing. These techniques are categorised as either thermal, mechanical or chemical de-icing methods [15, 29]. Thermal de-icing methods are the most used in both automotive and aerospace applications, where the iced elements cover relatively small areas [15]. The most common thermal methods apply thermal heating elements and fluids at high temperature. For marine applications, heating of the vessel and the application of hot water are commonly used methods for avoiding icing [29, 30]. The most common chemical de-icing methods utilise commercial fluids or salts that lower the freezing point of water, thereby reducing icing [10, 15]. These methods are important for both aircrafts and other transportation. Mechanical de-icing methods employing pneumatic boots, piezoelectric cells or manual de-icing are also widely in use [29].

Although the traditional methods for ice removal are functioning, they are either inefficient or expensive, in addition to often being environmentally hazardous. Due to the high amount of heat required to melt ice, thermal ice removal requires large amount of energy and effective strategies for removing the resulting water [29]. Mechanical ice removal may cause damage to the structure as well as pose a hazard by itself, for instance when icing on power lines are removed with helicopters [31]. Chemical methods for ice removal often cause risks to the environment, such as around airports or increased amount of salt around roads.

Anti-icing methods, as compared to de-icing methods, are often more efficient than de-icing methods as they ensure that no icing will take place. Such anti-icing methods are either active, which means that they utilise energy such as warmth to mitigate ice formation, or passive, which means that the anti-icing system do not require external input of energy to induce early ice detachment or mitigate ice

formation. Such passive anti-icing materials are also called icephobic coatings. By employing the natural forces such as gravity, natural wind, or surface tension, the passive icephobic coating ensures that accreted ice never forms on the exposed surface or structure.

The term icephobic is chosen from the word *phobia*, Latin for fear of a specific substance. As expected, icephobic surfaces thus show little or no interaction with ice [15]. The ideal icephobic surface is solid, durable, easy to apply, inexpensive, efficient in a wide range of icing conditions, and applicable for several anti-icing applications. However, to date no material has been identified which is efficient enough to ensure adequate protection against ice accumulation, nor durable enough to be economically viable [15]. Furthermore, there is no exact thermodynamic definition of icephobicity in the literature [32, 33].

There are three main pathways to icephobic surfaces, in term of three different properties that are often associated with icephobicity. These are 1) the prevention of water accumulation on the surface, 2) the delay of freezing of accumulated water, and 3) the lowering of the ice-solid adhesion so that ice can be easily removed [5, 25, 32, 34–36]. Any icephobic surface must display at least one of these properties to successfully mitigate hazardous icing.

The first property, the prevention of water accumulation on the surface, is often achieved by the use of superhydrophobic surfaces as defined in Section 2.1. Such surfaces display very high water contact angles, and facilitate the bouncing of incoming water droplets [34, 37]. It follows that if there is no water on the surface, there will be no ice formation. However, although superhydrophobic surfaces and icephobic surfaces have several important characteristics in common, it has been concluded that they are not directly correlated [32, 38–40]. Furthermore, superhydrophobic surfaces for icephobic applications have been found to degrade in high humidity environments and in low temperatures due to mechanical interlocking and frost formation [41, 42].

The second property, the delay of freezing of accumulated water, has been almost equally investigated as the removal of water on the surfaces. With a delay in nucleation of incoming water, the water may be removed with other means prior to freezing [25, 43]. This nucleation delay may be achieved with superhydrophobic surfaces or other methods of surface texturing [25, 36], or by the use of ice-binding

molecules, which are also called anti-freeze proteins [44].

The third property is the lowering of the ice-solid adhesion, such that the ice is removed easily from the surface after formation. At sufficiently low temperatures, the formation of ice is inevitable [41]. As a result, it might be unreliable to base an anti-icing strategy on the avoidance of ice. Following this uncertainty, the reduction of ice adhesion strength is probably the most promising overall anti-icing strategy. With a sufficiently low ice adhesion, the ice accreted on a surface might be shed merely due to its own weight or a natural wind action [39, 45].

1.2 Low ice adhesion surfaces

In extreme conditions, the lowering of ice adhesion strength is clearly the most promising strategy to avoid unwanted icing. Due to the high demands for durability and low uncertainty, to trust anti-icing surfaces relying on the removal of water or delay of ice nucleation is risky. In addition, degrading of the surface structure and anti-ice properties during icing and de-icing cycles are more common for anti-icing surfaces based on the removal of water or delay of ice nucleation. Thus, anti-icing surfaces with low ice adhesion strength are more likely to display a sufficiently long durability, although such surfaces can also potentially degrade during ice removal.

Low ice adhesion surfaces are often defined by an ice adhesion strength below 60 kPa [46]. With an ice adhesion strength below about 20 kPa, the ice formed on the surface can be shed by natural vibrations, its own weight or a natural wind [39, 45]. Surfaces with ice adhesion strength below 10 kPa, which enables an ice sample of dimensions $1\text{ m} \times 1\text{ m} \times 1\text{ m}$ to fall off by its own weight, are defined as super-low ice adhesion surfaces [35].

There are several types of low ice adhesion surfaces, with different underlying mechanisms. In the following paragraphs, a few such strategies for designing low ice adhesion surfaces are described. The strategies included are only a selection of some possible low ice adhesion surfaces, and not an exhaustive list.

Although superhydrophobic and icephobic surfaces are not directly related, the use of hydrophobic and hydrophilic sections of a surface have been utilised to create low ice adhesion surfaces in so-called amphiphilic coatings [47]. Analogous,

a super-repellent surface coating has been proposed with contact angles above 150° for most liquids which also states ice adhesion strengths below 10 kPa [48]. However, this publication does not give sufficient information to be able to reproduce their ice adhesion tests. Furthermore, as stated previously, surface designs applying superhydrophobic properties degrade quickly in certain atmospheric conditions, and the values of ice adhesion strength on superhydrophobic surfaces increase due to water condensation both on top of and between surface asperities [49].

Another type of low ice adhesion surfaces are lubricating coatings. One type of such coatings are Slippery Liquid Infused Porous Surfaces (SLIPS), where lubricant is trapped within the pores of a solid material, resulting in a smooth and slippery surface [25]. SLIPS coatings are more promising than superhydrophobic surfaces [25], and have been extensively investigated in realistic conditions with respect to durability [50]. Lubricated surfaces has been prepared with several different lubricants. Golovin et al. [51, 52] has investigated the effect of interfacial slippage in oil-infused polymeric coatings, and achieved ice adhesion strengths below 0.2 kPa. Wang et al. [53] created an organogel coating with paraffin as lubricating layer and achieved ice adhesion strengths of 1.7 kPa at temperatures of -30°C . However, a major drawback of utilising SLIPS as low ice adhesion surfaces is the durability, as the lubricant layer is depleted gradually [25]. This challenge has been attempted to solve by adding an aqueous lubricating layer that can be replenished directly with water [54], self-healing elastomeric coatings [55], solid phase-transitioning lubricants [56], and coatings inspired by epidermal glands in the skin to include an evaporation-induced phase separation [57, 58].

As durability is a key factor in low ice adhesion surfaces, coatings utilising different elastic moduli has been investigated as well. In theory, ice adhesion strength τ depends on the elastic modulus of the surface [35], such that

$$\tau = \sqrt{\frac{E^*G}{\pi a\Lambda}}, \quad (1.1)$$

where E^* is the apparent bulk Young's modulus, G is the surface energy, a is the length of crack and Λ is a nondimensional constant. From equation (1.1), a lower Young's modulus indicates a lower ice adhesion strength. Thus, to tune the elastic modulus has been attempted for more efficient low ice adhesion surfaces. One such

attempt consists of creating sub-structures in a soft polymeric coating, inducing the initiation of macro-cracks and breaking the ice [35, 59, 60]. Similar soft coatings has been prepared by others as well [45], on similar grounds. However, it has also been proposed that hard coatings with high elastic modulus might be better for ice removal, due to a mechanism named low interfacial toughness [61]. Furthermore, a third approach where the surface consists of alternate areas with high and low elastic moduli has been proposed [62], where the soft areas promote low ice adhesion strength while the harder areas increases the durability of the coating.

A fourth strategy for low ice adhesion surfaces consists of dynamic coatings, where the surfaces react actively with the environment or the accreted ice to lower the ice adhesion strength. Two such surfaces are the liquid layer generator [63], which can release ethanol to the ice-solid interface, and metasurfaces with embedded plasmonically enhanced light absorption heating [64], which harness sunlight to increase the temperature of the surface. In addition, a recent paper utilises molecular dynamics simulations to examine the critical ice nucleation and simulate hydrophobic surfaces textured with nanopillars to hinder ice nucleation within the nanostructure and reduce the ice adhesion strength [33].

1.3 Unanswered questions

Research on low ice adhesion surfaces has continuously increased over the past 15 years, as shown in Figure 1.1. However, just as there is no thermodynamic definition of icephobicity [32], the fundamental mechanisms of ice adhesion and ice detachment are largely unknown [8]. There is a great deal of research on the topic of ice adhesion, and older papers generally discussed adhesion on a fundamental level [65]. At the time the technology did not exist to find answers, and authors stopped discussing the fundamental questions. It has since become standard practice to ignore many aspects of testing ice adhesion [65], and many low ice adhesion surfaces are developed with a trial-and-error approach. As a consequence, there are many examples of low ice adhesion surfaces with very good adhesion properties, but with very little discussion on the underlying mechanisms of the ice detachment. Without such fundamental discussions, the way towards the

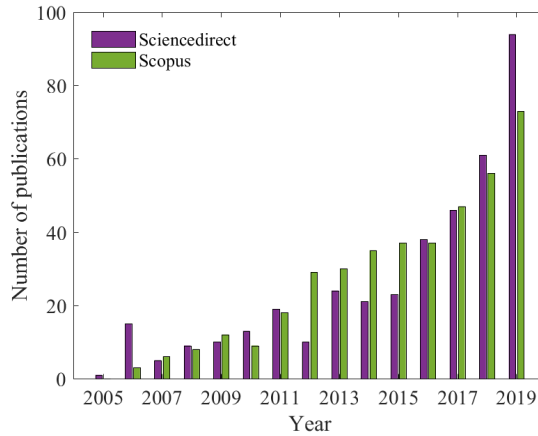


Figure 1.1: Overview of available publications including the phrase "ice adhesion", found with a simple literature search performed at Sciencedirect and Scopus at December 7 2019. No further classification was applied, and no other key words were included.

lowest achievable ice adhesion becomes largely left to chance, as new icephobic surfaces are not developed with an aim to target and increase the most important mechanism in ice detachment.

There are several questions that remain unanswered within ice adhesion research. Some of these unanswered questions can be seen in Table 1.1, organised by topic. The questions show the range of the unknown parameters and mechanisms concerning ice adhesion strength, and describe some of the required discussion to further the understanding of low ice adhesion surfaces.

In this thesis, 5 of the 13 questions will be specifically addressed with suggested answers. These are questions 4., 5., 7., 8., 10. and 13. The answers will be discussed and given in Section 5.1.

This thesis starts with describing the background for the fundamental mechanisms of ice adhesion. This background includes definitions of key terms, forces and interactions, ice adhesion models, ice as a material, and wettability of surfaces. Chapter 3 deals with ice adhesion as reported and measured in publications and studies, and includes measurement techniques of ice adhesion strength, measure-

Table 1.1: Unanswered questions within ice adhesion research.

Theory	
1.	What is the fundamental basis of ice adhesion?
2.	What is the theoretically achievable lowest ice adhesion strength?
3.	What is the bottleneck for decreasing ice adhesion strength?
4.	How do water and ice relate to each other?
Ice detachment	
5.	What is the effect of ice type on ice adhesion strength?
6.	What happens during ice detachment?
7.	What is the most relevant ice adhesion test method?
8.	How does ice adhesion tests impact the results?
Surfaces	
9.	What is the most important surface parameter for lowering ice adhesion strength?
10.	What is the effect of intended application for a low ice adhesion surface?
11.	What is the effect of surface roughness on ice adhesion strength?
12.	What is the effect of the angle of tilt on a tilting surface with respect to ice adhesion strength?
13.	What is the relation between ice adhesion strength and water wettability?

ment of ice adhesion for different ice types, and the status in comparability and standardisation within the ice adhesion research field. Chapter 4 consists of the results and findings from the papers included in this thesis. In the discussion in Chapter 5, the fundamental questions from Table 1.1 are addressed and the future work is discussed. The thesis ends with the concluding remarks.

Chapter 2

Background

Ice is an inherently chaotic substance [66]. When taking into account that there are many differences within the ice itself, as well as many different definitions of icephobicity, it becomes clear that the discussion of the fundamental mechanisms of ice adhesion requires a unified framework to facilitate the discussion. Such a framework will be described in Section 2.1. The following section describes the forces and interactions present in the ice-solid interface, and their believed effect on the ice adhesion strength. The third section describes models developed to predict ice adhesion, while the fourth section concerns ice as a material. The final section describes wettability, and its relation to ice adhesion strength.

2.1 Definitions

Adhesion

Adhesion: The ability of one substance to stick firmly to another [28]. Adhesion describes the strength of the bond between two different materials, and ice adhesion is the strength of the bond between ice and a solid substrate or surface.

Work of adhesion: The reversible thermodynamic work that is needed to separate the interface from the equilibrium state of two phases to a separation distance of infinity [67].

Adhesive failure: A failure between two different substances or materials, where the failure occurs at the interface.

Cohesive failure: A failure within a material. Cohesive failure in ice results in a breaking of the ice sample into two or more separate pieces of ice.

Ice adhesion strength: The adhesion strength between ice and a solid substrate, measured in the unit of pressure, such as kPa or MPa. Ice adhesion strength is normally calculated from the maximum ice detachment force divided by the ice-substrate contact area such that

$$\tau = \frac{F_{max}}{A}, \quad (2.1)$$

where τ is the ice adhesion strength, F_{max} is the maximum detachment force, and A is the ice-substrate contact area. The detachment force might be in either shear or tensile mode, depending on the ice adhesion test and parameters, which induces different fracture modes [32].

Wettability

Contact angle: An angle experimentally observed on the liquid side between the tangent to the solid surface and the tangent to the liquid–fluid interface at the contact line among the three phases [68]. The contact angle is illustrated in Figure 2.1. This definition is general in the sense that it applies to all equilibrium and non-equilibrium situations. Several other and more specific definitions of contact angles exists, among others **Young contact angle**, which is the contact angle calculated from equation (2.4), **apparent contact angle**, which is the contact angle measured experimentally on the macroscopic scale, and the **local contact angle**, which is the contact angle that exists locally at any point along the contact line [68]. The only contact angle that can be routinely measured is the apparent contact angle, and this angle is the one that describes an average contact angle for the entire three-phase contact line [68].

Advancing and receding contact angle: The advancing contact angle is defined as the highest metastable apparent contact angle that can be measured, while the receding contact angle is defined as the lowest metastable contact angle that can be measured [68]. Both the advancing and receding contact angles are often mistakenly called **dynamic contact angles**, which are defined as a contact angle measured under dynamic flow conditions and which are affected by viscous and inertia forces. As such, dynamic contact angles have no thermodynamic properties. However, the mistaken connection between advancing and receding contact angles and dynamic contact angles is commonly applied. The advancing and receding contact angles may depend on the method of measurement and on the parameters of the system [68].

Contact angle hysteresis: The difference between the advancing and receding contact angle [68].

Ideal surfaces and angles: An ideal surface is a smooth surface that is rigid and chemically homogeneous and does not chemically interact with the probe liquid [68]. Analogously, an ideal contact angle is the contact angle on an ideal surface, and for drops with radii of curvature larger than nanoscale, the ideal contact angle equals the Young contact angle and represents the single equilibrium state that a drop may have on an ideal solid [68]. In contrast, a real surface forms the majority of surfaces that are used and tested, and is defined as a solid surface that is not ideal [68].

Hydrophilic surface: A surface characterised by Young contact angle for water that is smaller than 90° [68].

Hydrophobic surface: A surface characterised by Young contact angle for water that is larger than 90° [68].

Superhydrophobic surface: A surface characterised by Young contact angle for water that is larger than 150° , combined with a low contact angle hysteresis [32].

Ice

Grain structure: Grains and grain boundaries in ice crystals comes from the discontinuity present in all matter [30]. The size of the grains in the ice crystal is crucial to distinguish between different types of fracture.

Ice phase: Different ice phases consists of varied crystal structures of ice, determined by the pressure and temperature during ice formation [69]. Only one ice phase is found naturally in the environment, and other ice phases are thus normally not relevant for ice adhesion studies.

Ice type: Different types of ice can be found naturally in the environment. Although all these types of ice consists of the same ice phase, their properties vary due to the changing conditions under which they were frozen.

Quasi-liquid layer: The quasi-liquid layer, also called the **liquid-like layer**, is defined as the outermost layer at the free surface of ice or for ice-water interfaces where the properties of the ice crystal changes and the material is in an intermediate state between the solid and bulk liquid water phases [69]. See Section 2.3 for further discussion of the quasi-liquid layer.

2.2 Forces and interactions

The strong adhesion of ice to other materials is a property of the ice-solid interface [8]. Consequently, the forces and interactions on atomic level largely determine the ice adhesion strength. There are three categories of physical processes that determine adhesion, namely the covalent or chemical bonding, the van der Waals forces or dispersion, and direct electrostatic forces [8].

Chemical bonding involves a chemical reaction directly between the ice and the surface. Consequently, this type of physical process is specific to each surface. For perfect contact, typical chemisorption yields a work of adhesion greater than 0.5 Jm^{-2} which act over a distance of $0.1 - 0.2 \text{ nm}$ [8]. For instance, water molecules are strongly absorbed on the surface for some materials, while there

is no affinity between water molecules and the surface for other materials. This changing affinity is one of the parameters which determines whether a surface is hydrophobic or hydrophilic.

The van der Waals forces, on the other hand, have longer range and act between all kinds of materials [8]. These forces create temporary dipoles in the surfaces which attract regardless of the materials. However, the generalised theory of the van der Waals forces has been applied to interfaces between ice and several different materials and insulators, and was found not to dominate the adhesion process [70].

The third force present at the ice-solid interface is the electrostatic interactions. This force results from non-compensated spatial distributions of charge that exert force on each other [8], and opposite charges attract strongly. The surface of ice consists of such electrostatic charges in the quasi-liquid layer [8, 71]. By investigating the free surface of ice, it has been shown that electrostatic forces could contribute up to 500 mJm^{-2} to the work of adhesion [72]. Based on experiments with changing the electric field at an ice-mercury interface [73], it may be concluded that the electrostatic contribution to the adhesion process in ice is the most important [8]. The presence of hydrogen bonds is included in the electrostatic interactions. The importance of the electrostatic force in ice adhesion is agreed upon by several additional studies [74–78].

To achieve a low ice adhesion strength, the goal is to reduce the ice-solid interactions and forces. Based on the importance of the electrostatic forces, a popular strategy is to utilise an insulator as substrate. As a result, in combination with equation (1.1), several low ice adhesion coatings have been based on PDMS or other polymers [44, 45, 53, 55–57, 59, 62, 79–84]. However, while the forces present at the ice-solid interface and their impact on the adhesion strength are relevant to the energetics of the adhesion process, the actual ice detachment process is much more complicated [8]. Among others, macroscopic experiments are never performed with atomically clean or flat interfaces, which causes the experimental behaviour and results to deviate from the theoretical predictions [8, 29].

2.3 Ice adhesion models

The existing forces at the ice-solid interface create the basis for several models for ice adhesion. Two such general models for predicting ice adhesion strength are further described here. Furthermore, there are several more models available for predicting ice behaviour, both for ice accretion [13, 20–22, 85–90] and ice density [91–99]. In addition to the two general models described here, there are several models describing the adhesion mechanism of ice from specific surfaces [60–62, 100]. However, these specific models only describe ice detachment of one type of ice from one type of surface performed with one type of test, and as a result, are of limited use when discussing the fundamental mechanisms of ice adhesion strength in a broader sense, as in this thesis.

The first general model for ice adhesion strength is based on the electrostatic force, and that this force is the main contribution to ice adhesion strength [101]. The model is based on water behaviour before and after freezing, substrate roughness and includes a porosity fraction to account for ice type. Based on several assumptions, for instance that the water polarisation has time to align to the surface before freezing to create hydrogen bonds and that the water molecules remain polar after freezing, a single predictive equation is proposed for ice adhesion. The equation may be derived from two parts, namely the ice adhesion model which takes into consideration the mechanical force needed to break the molecular adhesion between the ice and the substrate, and the ice strength model which takes into consideration the mechanical force needed to break the ice cohesion. The final equation also takes into account the average molecular distance between ice and aluminium, the ice surface in contact with the substrate, the minimum adhesion shear stress and wettability for a coated substance. Finally, the single model equation becomes

$$\begin{aligned} \tau_{\text{adh}} = & \left\{ \alpha_{\text{ice}} \left(\frac{\chi_{\text{oxygen}} - \chi_{\text{coating}}}{\chi_{\text{oxygen}} - \chi_{\text{substrate}}} \right)^2 \frac{T_f - T}{T_f - T_{\text{ref}}} \frac{4\gamma_{LV}}{\delta_0} \right. \\ & \times \left[f_{\text{RMS}} + \frac{\delta_0}{\kappa} (1 - f_{\text{RMS}}) (1 - f_{\text{cramp}}) \right] + (1 - f_{\text{RMS}}) f_{\text{cramp}} \tau_f \left. \right\} f_{\text{por}}, \end{aligned} \quad (2.2)$$

where the different parameters can be seen in Table 2.1. However, the model

Table 2.1: Parameters from equations (2.2) and (2.3), describing two models for ice adhesion strength. Parameters in alphabetical order, units not included. For more details, see original references.

Electrostatic model [101]		Quasi-liquid layer model [102]	
f_{cramp}	Fraction of mechanical locking	H	Thickness of quasi-liquid layer
f_{por}	Porosity fraction	MVD	Median volume diameter of incoming water droplets
f_{RMS}	Fraction of the ice in contact with the substrate	R_{sm}	Mean spacing of profile irregularities
T	Temperature	R_{α}	Average surface roughness
T_f	Solidification temperature	t_n	Average nucleation time of droplets upon impact
T_{ref}	Reference temperature	U	Droplet impact velocity
α_{ice}	Proportionality constant due to phase change	θ_i	Contact angle between ice crystals and quasi-liquid layer
δ	Distance between charge units	θ_s	Contact angle between the quasi-liquid layer and the substrate
κ	Root mean square roughness height	γ	Surface tension of water
γ_{LV}	Surface tension between liquid and vapour	τ_{ice}	Ice adhesion strength
τ_{adh}	Adhesion shear stress		
τ_f	Ice shear strength		
χ	Electro-negativity		

presented in equation (2.2) cannot predict ice adhesion strength with sufficient accuracy at present [101]. Several of the factors in the model, including the temperature effect, mechanical locking terms and surface roughness parameters, need further validation. Furthermore, the effect of ice type, which is contained in the porosity fraction f_{por} in equation (2.2), does not match the experiments presented in the first paper included in this thesis (Appendix A). However, with further validation of each parameter and the underlying processes, the model could prove useful as a baseline to further develop a more correct prediction of ice adhesion strength for a given material and provide guidelines towards an ideal low ice adhesion surface.

The second analytical model proposed to predict ice adhesion strength is based upon the presence of the quasi-liquid layer at the surface of ice [102]. The quasi-

liquid layer is well documented as part of the regelation phenomena [8, 71, 103–105], and is believed to be present at all ice-solid interfaces in addition to the ice free surface. When assuming that there is a water-like layer between the ice and solid at the interface, the adhesion stress might be calculated based on the surface properties and the thickness of the quasi-liquid layer. The model is based on the assumption that the quasi-liquid layer acts as an adhesive due to capillary forces caused by the result of a pressure difference across a curved liquid-air interface. Furthermore, the viscosity of the quasi-liquid layer is simplified to a friction phenomenon, which depends on the roughness of the solid surface as well as icing parameters. The final model is derived from the definition of the critical shear stress needed to break the interfacial adhesion of accreted ice for different icing conditions and substrates. The model equation is stated as

$$\tau_{ice} = \frac{2R_{sm}R_{\alpha}\gamma(\cos\theta_i + \cos\theta_s)}{MVD \cdot U \cdot H \cdot t_n}, \quad (2.3)$$

where the parameters are given in Table 2.1. The thickness of the quasi-liquid layer, H depends on the icing conditions, more specifically the surface temperature during icing [106]. Equation (2.3) is partly empirical, and has been validated for a specific set of parameters, where the ice adhesion was measured with a centrifugal adhesion test and the ice was created with a freezing drizzle. However, for other types of ice, the model did not match the experimental results (Appendix A).

To date, there exists no unified model to explain ice adhesion strength. The developed models are largely based on empirical investigations, and as a result work for one set of icing conditions and test set-up only. Since such set-ups and conditions vary from research group to research group as seen in Section 3.1.1, a more thorough fundamental study is needed to consolidate the different ice adhesion models.

2.4 Ice as a material

Ice plays a big part in our atmosphere, and for both Arctic and ocean environments. Although the water molecule is one of the simplest in chemistry, the properties of ice are not fully understood [8]. There are more than 15 phases of ice [69],

which differ in their crystal structure and properties. However, only one phase of ice exists in normal conditions on Earth, namely ice Ih. Polycrystalline ice Ih is obtained by freezing water at atmospheric pressure or by direct condensation from water vapour at temperatures above -100°C [8, 30, 69, 107]. Ice Ih crystallises in a hexagonal lattice, where the molecules are linked to each other with hydrogen bonds [8].

Ice that is found naturally in the environment is a stochastic substance. The same applies to ice created in a laboratory setting. Due to several factors, including variable water flow before and during freezing, micro-scale roughness, and varying heat transfer processes, the repetition of an icing experiment does not produce identical ice samples [66]. Furthermore, the properties of ice are highly dependent on the environmental conditions, such as temperature, crystallisation process, grain size, salinity, cooling rate, and the history of the ice [8, 30, 101, 107, 108]. As a result, the mechanical properties differ between various environmental conditions and generation methods. In addition, the mechanical properties of ice are directly related to the micro-structure of the ice. As such, the ice adhesion strength is directly influenced by the formation of the ice, as well as the detachment process.

More information about the impact of mechanical properties of the ice on the ice adhesion, and the different factors, can be found in Paper 1 (Appendix A). A discussion on the density of the ice, and the dividing of ice types based on density, will be given in Section 3.2.1.

2.5 Wettability

Wettability is the description of the behaviour of water on a surface. As such, contact angle is a key factor, defined as a thermodynamic property that characterises the wettability of solid surfaces [68]. Wettability was first discussed by Aristotle, but most credit Thomas Young as the father of the contact angle [109]. A few different contact angles have been defined in Section 2.1.

The most commonly discussed contact angle is the Young contact angle, which is calculated from Young's equation [110] for ideal solid surfaces [111]. Young

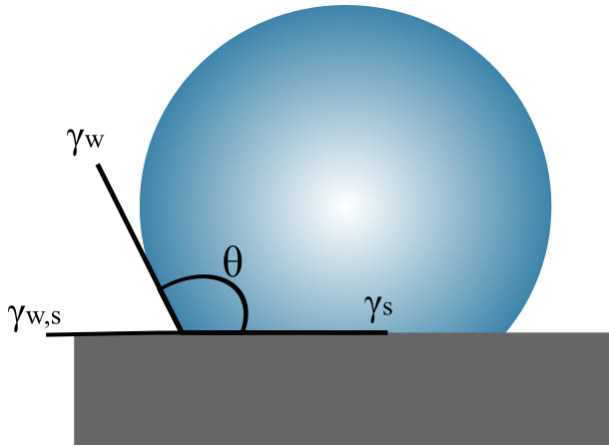


Figure 2.1: Illustration of the most general water contact angle θ . The surface energies γ correspond to the parameters of Young's equation in equation (2.4). Figure also appears in Paper 4 (Appendix D).

contact angle is commonly presented as

$$\gamma_{w,s} + \gamma_w \cos \theta = \gamma_s, \quad (2.4)$$

where θ is the contact angle, γ is the surface tension, and the subscripts w denotes water and s denotes surface. An illustration of the Young contact angle can be seen in Figure 2.1. Equation (2.4) describes the thermodynamic property of a three-phase system, which corresponds to the lowest energy state for the system [68]. For other types of surfaces, other definitions of equilibrium contact angles have been proposed. The Wenzel equation describes contact angle of a droplet on a surface with a given roughness [112], the Cassie equation [113] describes the contact angle of a droplet on a heterogeneous solid surface, and the Cassie-Baxter equation [114] describes the contact angle of a droplet on a textured surface with trapped air underneath the droplet [111]. For information on these definitions of wettability and contact angles, the reader is referred to the review by Drelich [111].

Wettability is a key property of potential low ice adhesion surfaces for many reasons. For instance, Cassie-Baxter ice is applied to describe ice situated on top of air pockets on structured surfaces [25, 41]. A potential connection between

superhydrophobic surfaces as defined previously and low ice adhesion surfaces has been suggested, but was later discounted experimentally, as described in the introduction of this thesis. However, thermodynamic theory predicts a relation between the work of adhesion, denoted as W_a , and the ice adhesion strength of a surface. This relation is defined as [29]

$$W_a = \gamma_s + \gamma_i - \gamma_{i,s}, \quad (2.5)$$

where subscript i denotes ice, and represents the work required to break the bond between the ice and the surface and form two new surfaces. By combining equations (2.4) and (2.5), a direct relation between the ice adhesion strength and the water contact angle θ is found. When the contact angle is substituted with the receding contact angle, the equation relates the practical work of adhesion and the ice adhesion strength. Although these relations have been closely examined experimentally, they are neither agreed nor disagreed upon as experimental results vary. However, in the fourth paper of this thesis, the theoretical relation between ice adhesion strength and water contact angle has been reproduced by utilising atomistic simulations. These results will be further detailed in Appendix D.

Chapter 3

Finding ice adhesion

There are many ways to determine the ice adhesion strength, and many ways to interpret the results. However, the resulting ice adhesion strength depends greatly on both the type of ice tested, and the method of testing. In this chapter, both the different measurement techniques and ice types commonly tested for ice adhesion testing are briefly described. After these descriptions, the current status on comparability between different experimentally obtained ice adhesion values are discussed.

3.1 Measurement techniques

Since there are no standards in the ice adhesion community, there are as many ice adhesion tests as there are research groups investigating low ice adhesion surfaces [34, 62, 115–118]. The definition of ice adhesion strength is largely agreed upon, as defined by equation (2.1), but the calculation of the maximum detachment force F_{max} varies between ice adhesion tests. As a result, each custom-built testing rig might give slightly different ice adhesion values.

Several reviews have collected and discussed different methods for measuring ice adhesion strength [29, 65, 117, 119–122]. An overview of some of these reviews, and the methods included in each review, can be seen in Table 3.1. For more information about the different tests, the reader is referred to Section 3 in Paper 2 (Appendix B).

Table 3.1: Overview of different ice adhesion tests covered by previous reviews, with Paper 2 from this thesis included. Year of publication is included.

Review paper (year) [Ref]	Included ice adhesion tests
Sayward (1975) [119]	Pure tensile test, pure lap shear test, flat plate torsion shear test, cylinder torsion shear test, peel test, blister test, cleavage test, cone test, flexed sheet test, small area tensile test, lap tensile-shear-test, multi flat-plate torsion-shear test, axial cylinder shear test, roll-peel test, and combined mode tests
Kasaai and Farzaneh (2004) [120]	Simple shear test, lap shear test, tensile test, combined shear and tensile test, peel test, impact test, laser spallation test, scratch test, atomic force microscopy test, and electromagnetic tensile test
Makkonen (2012) [29]	U.S. Army Cold Regions Science and Engineering Laboratory (CRREL) test arrangement (torque test), and VTT Technical Research Centre of Finland test arrangement (horizontal shear test)
Schulz and Sinapius (2015) [117]	Tensile test, transverse shear test, bending test, and centrifugal test
CIGRE TB 631 (2015) [16]	Pulling test, centrifugal chamber test, sliding weight test, ice push off test, and conductor ice pull off test
Work and Lian (2018) [65]	Centrifuge adhesion test, calculated centrifuge adhesion test, instrumented centrifuge adhesion test, push test, rotational shear test, 0° cone test, lap shear test, tension test, beam tests, blister test, laser spallation test, and peel test
Rønneberg et al (2019) [2]	Horizontal shear test, vertical shear test, tensile test, centrifuge adhesion test

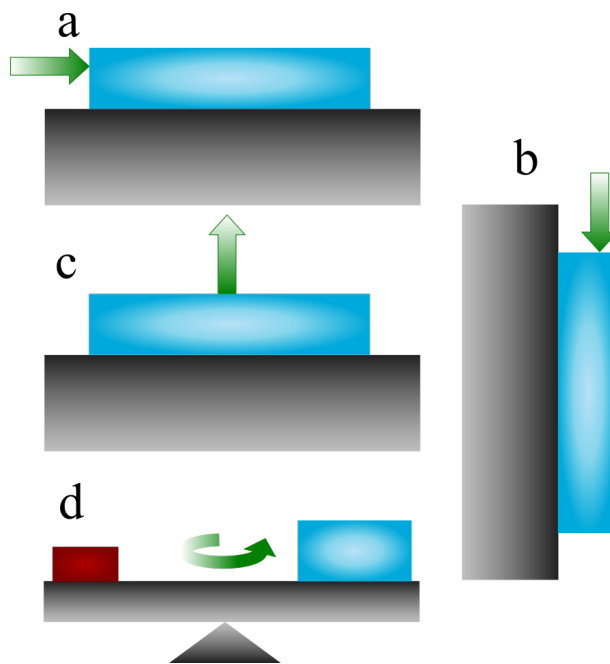


Figure 3.1: Schematic illustration of the four most widely used tests methods for ice adhesion strength measurements: a) Horizontal shear test b) Vertical shear test c) Tensile test d) Centrifugal adhesion test. For all methods, ice is blue and the fixed surface is grey, with the applied force on the ice illustrated by a green arrow. The counterweight in d) is red. Figure from Paper 2 (Appendix B).

3.1.1 Comparisons

The four most applied ice adhesion tests are the four tests covered in Paper 2, namely the horizontal shear test [32, 39, 41, 45, 47, 48, 51, 54, 61, 64, 115, 123], the vertical shear test [35, 46, 55, 57, 59, 80, 116], the tensile test [124–127] and the centrifugal test [102, 128–136]. A schematic overview of these test methods is found in Fig. 3.1, and they are further described in Paper 2 (Appendix B).

Since each research group utilises their own ice adhesion set-up, no comprehensive study has been conducted on the comparability of the different ice adhesion test methods. Several theoretical discussions and reviews have compared the different tests [65, 117, 119, 120], and although they do not include the same tests in

their comparisons the discussions largely agree with each other. However, because their discussions are based upon literature reviews of separate publications, they can only compare the theory behind the different test methods in addition to the reported ice adhesion strengths. And as these reported results often include only the value of ice adhesion strength, and not all the experimental details to enable comparability, the available comparisons are flawed.

In this thesis, two new such comparisons between different ice adhesion have been included. Paper 2 (Appendix B) includes a discussion on the difference between the vertical and horizontal shear test, while Paper 3 (Appendix C) presents the ice adhesion strengths of the same type of ice on the same surfaces performed at two different facilities with a vertical shear test and a centrifugal adhesion test.

The main difference between measured ice adhesion strength with the vertical and horizontal shear test is gravity. Since the vertical shear test pushes the ice sample normal to the ground, the force from gravity is added to the loading of the force probe. Consequently, the ice sample size impacts the ice adhesion strength more when measured with the vertical shear test than the horizontal shear test, assuming that all other parameters are equal. The effect of gravity on the ice sample in the vertical shear test can be found by calculating the ice adhesion strength required to self-remove the ice sample τ' , given by

$$\tau' = \frac{F}{A} = \frac{mg}{A} = \frac{Ah\rho g}{A} = h\rho g, \quad (3.1)$$

where F is the applied force, A is the ice contact area, h is the height of the ice sample, ρ is the density of the ice, and g is the gravitational constant. When this equation is applied to bulk water ice, which has a density of $\rho = 917 \text{ kgm}^{-3}$, and different heights of the ice sample, the self-removal ice adhesion strength is calculated. As can be seen from equation (3.1), τ' is independent of contact area, but depends on the height of the ice sample.

The effect of gravity on an ice sample measured with the vertical shear test can be seen in Figure 3.2, where the amount of measured ice adhesion strength attributed to gravity, given by τ'/τ in percentage is shown for eight different surfaces. It can be seen that the effect of gravity is low even for the largest ice samples when the measured ice adhesion strength is above 10 kPa. However, for

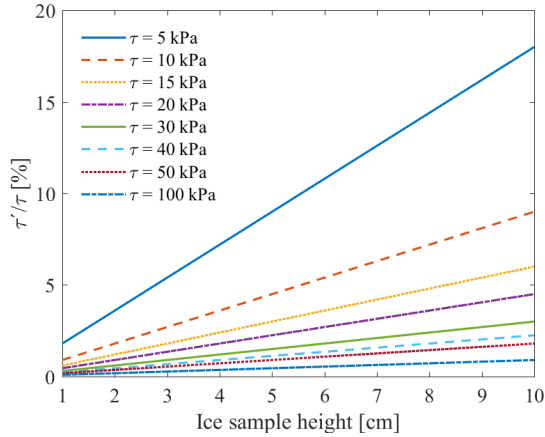


Figure 3.2: Illustration of the effect of gravity on the measured ice adhesion strength, given by the self-removed ice adhesion strength τ' divided by the measured ice adhesion strength τ for several generic low ice adhesion surfaces as a function of the height of the ice sample. The self-removed ice adhesion strength is given in equation (3.1). Figure from Paper 2 (Appendix B).

super-low ice adhesion surfaces the effect of gravity cannot be neglected unless the ice samples are very small.

For the comparison between the vertical shear test and the centrifugal adhesion test, an interlaboratory test was performed in cooperation between NTNU in Trondheim and the Anti-icing Materials International Laboratory (AMIL) in Chicoutimi, Quebec, Canada. The direct comparison between the two test methods can be conducted because the tests were performed with the same type of ice, namely bulk water ice as defined in Section 3.2, and for the exact same surfaces. The surfaces were prepared at AMIL and shipped to NTNU, and were bare aluminium surfaces and commercial icephobic surfaces. The commercial icephobic coating consisted of aluminium covered with EC-3100, a two component, water-based, icephobic, non-stick coating from Ecological Coating, LLC [137]. For full information on the study, see the Paper 3 (Appendix C).

In Figure 3.3, the ice adhesion strength of the two surfaces can be seen for temperatures of both -10°C and -18°C . It can be seen that the vertical shear test systematically results in higher ice adhesion strengths than the centrifugal test.

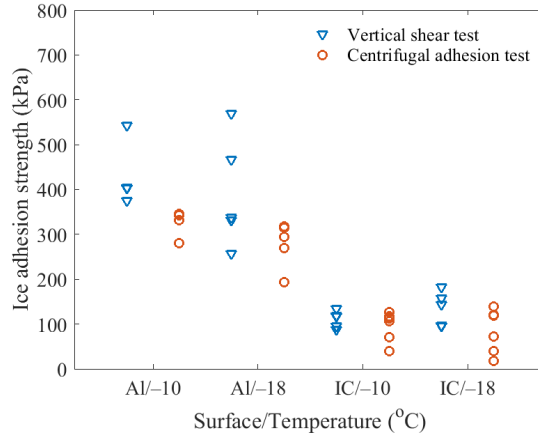


Figure 3.3: Ice adhesion strength of bulk water ice measured with vertical shear test at NTNU and centrifugal adhesion test at AMIL. Al denotes the bare aluminium surface, while IC represents the icephobic coating. Both surfaces were tested at temperatures of both -10°C and -18°C .

This claim is substantiated with a t-test that tests the hypothesis that the vertical shear test yields higher ice adhesion strengths than the centrifugal adhesion test when assuming unequal variances. The t-test rejects the null hypothesis in three of four configurations with a 7% significance level. The configuration that does not reject the null hypothesis is the icephobic coating at temperatures of -10°C , and thus it cannot be concluded that the vertical shear test results higher ice adhesion strengths than the centrifugal test for this specific configuration. However, for both temperatures for bare aluminium surfaces as well as for the icephobic coating at temperatures of -18°C , the vertical shear test yields significantly higher ice adhesion strengths than the centrifugal test.

Furthermore, Figure 3.3 indicates a higher variation for most of the tests performed with the vertical shear test than the centrifugal adhesion test. It also seems that the standard deviation scales with the absolute value of ice adhesion strength. However, the standard deviations depend on the outliers of the experimental results. By investigating the original measurements for the two tests, it was found that when the standard deviation for a configuration was above 30%, there was at least

one significant outlier. It follows that when the ice adhesion strength is higher, the extreme outliers differ more from the mean value, giving higher standard deviations. Based on this reasoning, the most important factor for ice adhesion tests in terms of interlaboratory comparability is the reproducibility of the test. In other words, if two ice adhesion test methods in different facilities are to be compared, it is important to reduce the amount of outliers in the individual ice adhesion tests.

In addition to comparing between different ice adhesion tests, different experimental set-ups of the same type of ice adhesion tests can also be compared. In such comparisons, the effect of changing experimental parameters are important to investigate. One such investigation has been conducted for the vertical shear test, by testing the effect of the distance between the force probe and the surface [116] and the loading rate, or impact speed, of the force probe on the ice [81]. The studies show that the effect of the probe distance is considerable, with a change from 1 mm to 4 mm resulting in a decrease of ice adhesion strength from above 700 kPa to around 200 kPa. Similarly, the effect of the probe impact speed was seen to be significant for some types of polymeric icephobic surfaces, while other surfaces showed no effect. The experimental details and reported ice adhesion strengths of selected low ice adhesion studies utilising similar ice samples and either a horizontal or vertical shear tests are shown in Table 3.2. It can be seen that the studies utilise different parameters during their testing, while some does not include sufficient experimental details.

Lastly, the adhesion reduction factor (ARF) enables comparison of different low ice adhesion surfaces tested with the same experimental set-up. The ARF is equivalent to the adhesion strength of a baseline material, often aluminium, divided by the ice adhesion strength of the surface or substrate of interest [133]. Although the ARF is used more widely to compare different surfaces [15, 50, 65, 117], the ARF only results in qualitative values and thus the reported ice adhesion strengths cannot be compared between different facilities.

3.1.2 Recommendations

Of the reviews describing the ice adhesion test methods as shown in Table 3.1, few make recommendations. Sayward [119] discusses seven fundamental factors to

Table 3.2: Ice adhesion strength and experimental conditions of several studies of low ice adhesion surfaces utilising a shear test and the same type of ice, namely bulk water ice (see Section 3.2).

Shear test	Probe distance	Probe impact speed	Ice adhesion strength	Ref
Vertical	2 mm	0.05 mms ⁻¹	20 – 50 kPa	Wang et al[81]
Vertical	3 mm	0.1 mms ⁻¹	5.7 kPa	He et al[46]
Horizontal	2 mm	0.5 mms ⁻¹	165 – 510 kPa	Meuler et al [115]
Horizontal	1 mm	0.8 mms ⁻¹	5.2 kPa	Beemer et al [45]
Horizontal	3 mm	0.1 mms ⁻¹	1 kPa	Irajizad et al [62]
Horizontal	1 mm	0.001 mms ⁻¹	2.5 kPa	Mitridis et al [64]
Horizontal	1 mm	-	0.15 kPa	Golovin et al[51]
Horizontal	-	0.18 mms ⁻¹	12 kPa	Upadhyay et al [47]
Horizontal	-	-	71 – 252 kPa	Hejazi et al [32]
Horizontal	-	-	27 kPa	Dou et al [54]

lower the ice adhesion of surfaces, and includes fifteen different ice adhesion tests, but does not include which test is deemed most efficient. Kasaai and Farzaneh [120] however, covers nine different tests and recommends a combination of atomic force microscopy or nano-indentation techniques combined with lap-shear and tensile modes for testing ice adhesion strength. Schulz and Sinapius [117] focus on aircraft applications, and recommend a form of de-icing called pneumatic boots. This de-icing technique inflates under the ice and breaks it off both in shear mode and bending mode [29, 117], but pneumatic boots are not recognised as a method for anti-icing. CIGRE released a report about ice mitigation on overhead power lines in 2015 [16], which does not recommend a specific ice adhesion test but organises the described tests into level of commercial maturity. According to this report, only the conductor ice pull off test is defined as more advanced than small scale testing on coated material samples in laboratories. Work and Lian [65] on the other hand, has a clear recommendation among the thirteen tests they discussed. They recommend to either create a new ice adhesion test, or to apply the lap shear test that may be reconfigured into a tension test and apply this test to test a large number of samples. Work et al. [138] have also continued this work by investigating the ice adhesion strength of a large number of ice samples by utilising a modified lap shear test.

The goal of a well-suited ice adhesion test is to measure the ice adhesion strength of any given material with precision and reproducibility. In addition, the method should be able to measure the same ice adhesion strength at a different facilities. Although some reviews recommend ice adhesion tests, none of the reviews recommend the same ice adhesion test. It may be concluded that the an ideal standard ice adhesion test does not yet exist.

In this thesis, no recommendation will be made on the overall best ice adhesion strength test. This choice has been made as each application will require different optimal ice adhesion tests tailored to the application. Instead of suggesting a way of standardisation, the focus is on comparability. This comparability and the ideal future of ice adhesion test strengths will be discussed further in Section 3.3.

3.2 Types of ice

Although all ice investigated in ice adhesion research consists of ice Ih, there are several different types of ice in use. Several different definitions of ice have been collected in Table 3.3, for both power line applications, icing of structures, sea ice, and low ice adhesion surfaces. It can be seen that there are several varying definitions for each type of ice. As each ice type has very different properties, such a lack of consensus might result in misunderstandings and challenge the comparability of research performed at different facilities.

For low ice adhesion research, the biggest effect of different ice types are between impact ice and non-impact ice [65, 117, 122]. While non-impact ice is created from stationary water, impact ice is generated from water with a non-zero impact velocity. Typical impact ice types are the different atmospheric ices, namely precipitation ice types and in-cloud ice types. For unwanted icing of this sort, either the water itself has a non-zero velocity, for instance in case of wind or freezing rain, or the structure or item which experiences the icing is moving with respect to a cloud or similar, such as aircrafts or wind turbine blades. For most of anti-icing applications, and especially those of low ice adhesion surfaces, impact ice is the most realistic type of ice during operation [15, 65, 117]. As a result, low ice adhesion surfaces intended for anti-icing application should be tested with impact ice types to ascertain the functionality.

Table 3.3: Alphabetical selection of definitions of icing and ice types from different references within several applications for anti-icing and ice mitigation.

Ice type	Definition	Reference
Atmospheric icing	Any process of ice build-up and snow accretion on the surface of an object exposed to the atmosphere	CIGRE TB 631 [16]
Bulk water ice	Water frozen in freezer or on a Peltier plate at constant temperature, which may vary from freezer to freezer. Results in a clear and mostly bubble-free ice	Rønneberg et al [1]
Dry snow	A type of precipitation icing that accretes at sub-freezing temperatures. Low density and low adhesion, and appears rarely when wind speed is below 2 ms^{-1}	CIGRE TB 631 [16]
Freezing drizzle	Water droplets that freeze on impact with the ground or with objects on the earth's surface or with aircraft in flight	Armstrong et al [139]
Freezing rain	A type of precipitation icing that falls in liquid form but freezes on impact to form a coating of glaze ice upon the ground and on exposed objects	CIGRE TB 631 [16]
Glaze	A generally homogeneous and transparent deposit of ice formed by the freezing of supercooled drizzle droplets or raindrops on objects the surface temperature of which is below of slightly above 0°C . It may also be produced by the freezing of non-supercooled drizzle droplets or raindrops immediately after impact with surfaces the temperature of which is well below 0°C	Armstrong et al [139]
Glaze ice	Temperatures over -10°C , freeze from water film after droplets have spread out. Has the highest possible ice density	Fortin and Perron [101]
Glaze ice	Hard, bubble-free and clear ice, generated under wet growth conditions and where surface temperature is above 0°C	Makkonen [87]
Glaze ice	Ice frozen in silicone mold at -5°C for 24 hours, resulting in a smooth clear structure. Ice that does not freeze on impact on aircrafts	Janjua et al [136]
Glaze ice	Clear, high density ice	ISO 12494 [17]
Glaze ice	A type of precipitation icing resulting in transparent ice accretion of density $700 - 900 \text{ kgm}^{-3}$, sometimes with the presence of icicles under the conductors. It very strongly adheres to objects, and is difficult to knock off.	CIGRE TB 631 [16]

Table continued on next page.

Table continued from previous page.

Glaze ice	Ice formed under glaze conditions, where the impinging droplets form a liquid film that freezes to form the ice. Latent heat release from formation is not sufficient to completely freeze the water on impact	Work et al [138]
Hoarfrost	A deposit of ice having a crystalline appearance, generally assuming the form of scales, needles, feathers, or fans; produced in a manner similar to dew but at temperatures below 0°C	Armstrong et al [139]
In-cloud icing	Icing due to super-cooled water droplets in a cloud or fog	ISO 12494 [17]
In-cloud ice	Spraying supercooled micro droplets of MVD 27 µm and LWC 2.5 gm ⁻³ in a wind tunnel of wind speed typically 15 ms ⁻¹ at temperatures of -10°C	Rønneberg et al [1]
Precipitation icing	Icing due to either freezing rain or drizzle, or accumulation of wet snow	ISO 12494 [17]
Precipitation icing	A type of atmospheric icing which is caused by rain droplets or snowflakes that freeze or stick to the icing body	CIGRE TB 631 [16]
Precipitation ice	Supercooled droplets of MVD 324 µm as precipitation in a cold room with temperature typically -10°C, impact velocity calculated to 5.6 ms ⁻¹	Rønneberg et al [1]
Rime	A deposit of ice composed of grains more or less separated by trapped air, sometimes adorned with crystalline branches, produced by the rapid freezing of supercooled and very small water droplets	Armstrong et al [139]
Rime ice	White ice with in-trapped air	ISO 12494 [17]
Rime icing / in-cloud icing	A porous, opaque ice deposit which is formed by the impaction and freezing of supercooled water droplets on a substrate. The density of rime can vary from 150 – 700 kgm ⁻³	CIGRE TB 631 [16]
Wet snow	A type of precipitation icing which is observed when the air temperature is just above freezing point, usually between 0.5°C and 2°C	CIGRE TB 631 [16]

Non-impact ice comes in many different forms, but is most often similar to bulk water ice in Table 3.3. This type of ice is the simplest to make, as the only needed infrastructure is a freezer and a syringe to administer water in a mold. Due to this simplicity, non-impact ice is the most frequently used in low ice adhesion research [32, 35, 39, 45–48, 51, 52, 54, 61, 62, 64, 74, 115, 123, 124]. Naming of the non-impact ice applied varies from bulk water ice to static ice, freezer ice, refrigerated ice, and even glaze ice in some publications [15, 47, 122, 136].

3.2.1 Size and density of impact ices

Within impact ice applications, such as overhead power lines or structures, there are several different ways to separate different ice types. The first method is to separate by droplet size, and the second is to separate by the density of the accreted ice. The latter method is the most common, and the one described by the ISO standard of icing on structures (ISO 12949) [17].

To separate by droplet size is more common when investigating anti-ice surfaces focused on the mitigation of ice accretion, often with superhydrophobic surfaces [38, 140]. For atmospheric monitoring, the separation of different types of precipitation and ice is essential, and the types of ice and precipitation typically differentiated between is available in Figure 3.4. From this figure, it can be seen that the different types of precipitation are separated by the droplet sizes, and range over several orders of magnitude. Snow is the largest group, spanning droplet sizes of 2 μm to 10 mm. Ice types included in in-cloud icing, for instance freezing drizzle, are created when the analogous precipitation freezes either directly on impact or afterwards due to low temperatures.

Separating ice types by density creates several different classification schemes as the different definitions often does not match. ISO 12494 [17] includes the most used ice density differentiation scheme, which can be seen in Table 3.4. This table includes both the type of ice with density ranges, the assumed adhesion of the ice type, and the appearance of the ice. Other differentiations of ice types based on densities can be found in Table 3.5 [142] and Table 3.6 [97].

That ice frozen in different conditions have different densities have long been acknowledged, and has been investigated in several publications [91–99, 144, 145].

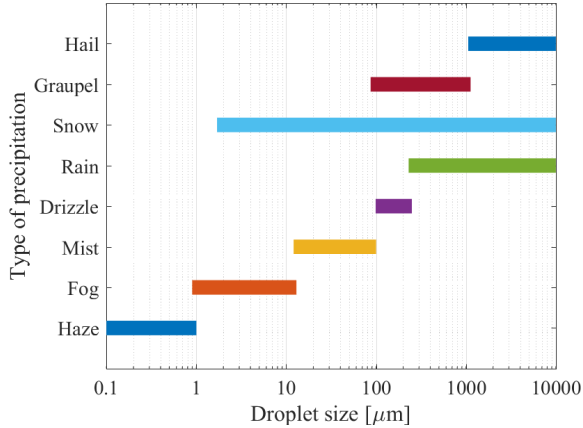


Figure 3.4: Overview of different types of ice and precipitation by droplet size. Overview based on droplet measurement techniques [141].

Table 3.4: Typical properties of accreted atmospheric ice on structures, as defined by ISO 12494 [17].

Type of ice	Density kgm^{-3}	Adhesion and cohesion	General appearance	
			Colour	Shape
Glaze	900	Strong	Transparent	Evenly distributed / icicles
Wet snow	300 – 600	Weak (forming), strong (frozen)	White	Evenly distributed/eccentric
Hard rime	600 – 900	Strong	Opaque	Eccentric, pointing windward
Soft rime	200 – 600	Low to medium	White	Eccentric, pointing windward

Table 3.5: Typical processes of in-cloud icing with densities [142]. Condensation is ice formation by the deposition and freezing of super cooled droplets of vapour, while de-sublimation is the formation of ice crystals bypassing the liquid phase.

Ice type	Density (kgm^{-3})	Process
Glaze ice	700 – 900	Condensation
Hard rime	300 – 700	Condensation
Soft rime	100 – 300	De-sublimation
Hoar frost	< 100	De-sublimation

Table 3.6: Six main classifications of accreted ice by densities and appearance, as described by [97, 143]. The top three ices are in the glaze family, while the bottom three are in the rime family.

Category	Description	Density ρ (average) [gcm^{-3}]
Clear ice	Virtually no air entrapped	> 0.86 (0.906)
Transparent ice	Moderate amounts of air entrapped in fairly large bubbles	> 0.86 (0.906)
Milky ice	Considerable amounts of air enclosed as small bubbles	> 0.80 (0.876)
Opaque rime	Dull and white, crumbles rather than cracks	0.40 – 0.90
Kernel rime	Similar in appearance to kernels of corn on a cob	0.33 – 0.61
Feathery rime	More open and fragile than kernel rime	0.08 – 0.40

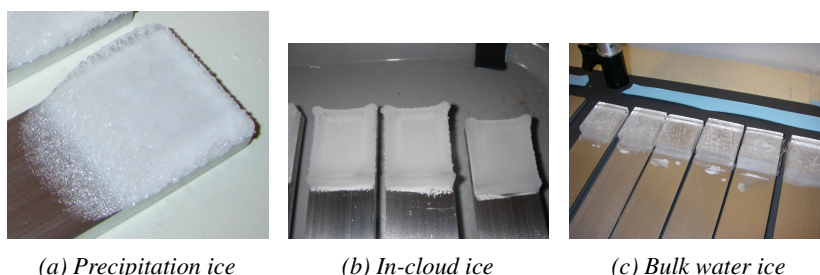
Glaze ice is for instance sometimes defined as the ice type with the theoretically highest density [96, 101, 136]. However, the density of the ice depends on both temperature and droplet impact velocity, and has been found to increase with the increase of impact velocity and droplet size [97]. Since the definition and generation method of glaze ice differs as seen in Table 3.3, it is clear that no ice type can be wholly defined based on density.

3.2.2 Ice type and ice adhesion strength

It has been hypothesised that the type of ice is directly linked to the ice adhesion strength since 1959 [119]. Through the work included in this thesis, this hypothesis has been verified. The work is described by Paper 1 (Appendix A).

In this study, we tested the ice adhesion strength of three different types of ice with the same experimental set-up of a centrifugal adhesion test. The ice types that were tested were bulk water ice, precipitation ice and in-cloud ice as defined in Table 3.3. Images of the ice types investigated can be seen in Figure 3.5. The experiments were performed at the laboratory facilities of AMIL with their standardised ice adhesion test.

The results of the ice adhesion tests are given in Table 3.7. It can be seen that there is a significant difference when comparing the ice adhesion strength of the



(a) Precipitation ice

(b) In-cloud ice

(c) Bulk water ice

Figure 3.5: Images of the different ice types investigated in Paper 1.

Table 3.7: Results of ice adhesion tests for the three different ice types, including the number of samples tested with each ice type. Data taken from Paper 1 (Appendix A).

Ice type	Mean ice adhesion strength [MPa]	Standard deviation [MPa (%)]	# samples
Precipitation ice	0.780	± 0.102 (13.1%)	30
In-cloud ice	0.590	± 0.119 (22.5%)	60
Bulk water ice	0.284	± 0.083 (28.2%)	36

three ice types. Precipitation ice has a higher ice adhesion strength than the other two and bulk water ice is the easiest to remove. Bulk water ice only displays 40% of the ice adhesion of precipitation ice under similar conditions, and the standard deviation is quite high for all three ice types.

The high inherent variation in measured ice adhesion strength found in these experiments, with standard deviations of more than 25% for bulk water ice, are in accordance with other publications. For a study intended to determine the cause of variation in ice adhesion strength measurements utilising a new methodology with a lap joint shear rig, the measured standard deviation remained at 23% and 33% for two different tests campaigns [138]. Similarly, a previous test campaign with more than 200 data points resulted in standard deviations of 13% and 23% for steel and aluminium, respectively [146]. This inherent variation in measured ice adhesion strength for all similar parameters might be a result of the aforementioned stochastic behaviour of ice as a material.

As seen in Section 2.3, several analytical models have been proposed to describe ice adhesion strength on a reference aluminium surface. Both models described in

the previous section include factors accounting for changing ice types, and predict that decreased density of the ice leads to a decreased adhesion force as well. Lower density of ice is directly related to the amount of air bubbles in the ice sample [95], and a higher fraction of micron-size air bubbles results in a more opaque ice [147]. It follows that the more opaque ice types has lower densities, and are expected to display a lower adhesion to a given surface. This expectation is in line with the description of the different ice types from Table 3.4 as well.

From Figure 3.5, it can be seen that precipitation ice has the lowest density according to the optical classification system. According to the ice adhesion models and the ISO 12494 standard, as well as several other publications [50, 136], bulk water ice should thus give the highest ice adhesion value, while precipitation should have the lowest ice adhesion value. However, as can be seen from Table 3.7, the experiments show the opposite relation. The discrepancy between previous assumptions and analytical models and the experimental results in Table 3.7 substantiates the lack of knowledge in ice physics and the fundamental mechanisms of ice adhesion.

3.3 Future comparability and standardisation

The need for comparability and standardisation of the field of low ice adhesion is largely agreed upon. The definition for icephobic surfaces is not uniformly defined, and many different types of accreted ice are utilised which are created in varying ways, which in turn affects the ice adhesion strength. Furthermore, ice adhesion strength is measured with many different set-ups where small changes in experimental parameters can have large consequences for the reported ice adhesion strength.

There is a general agreement that further development of low ice adhesion surfaces needs to include a form of grounds for comparison or standardisation, or a series of standard tests grouped by applications or ice types. Several standardised ice adhesion tests have been proposed the past years, among others a 0° cone test [148], a vertical shear ice adhesion test utilising only commercially available instruments [116], and a horizontal shear test [62]. However, none of these suggestions have been widely accepted as a standard. Furthermore, four out of six

contributions to the low ice adhesion session at the 18th International Workshop on the Atmospheric Icing of Structures (IWAIS), which was held in Reykjavik in June 2019, focused on the issue of comparability [4, 149–151]. As seen in Section 3.1.1, at present a low ice adhesion material developed at one facility cannot be compared to another material developed somewhere else.

The ultimate goal for research into ice adhesion, and to ensure full comparability, must be to understand all underlying mechanisms of the adhering of ice to different surfaces. However, these mechanisms change for different surfaces and under different environmental conditions, and there is not one correct or true value of ice adhesion. To uncover all the theoretical implications of ice-solid adherence is extremely complicated, due to the complex and stochastic behaviour of ice and the many changing parameters. Meanwhile, the ice adhesion research field is result-oriented and moves continually forward, requiring a more empirically based method of comparison between different surfaces and research facilities.

We believe it is unrealistic to aim for a specific standard method for measuring ice adhesion strength. Based on the large amount of research within ice adhesion, and thus the large amount of ice adhesion laboratory set-ups, it is improbable that the research community can agree on a standard method for all applications. However, there is a need for comparison of the reported levels of ice adhesion strength.

A comparison within ice adhesion must be based on real-life experimental set-ups and surfaces to be viable. Ideally, a system for comparison and transferability can be utilised to directly compare two measured ice adhesion strengths when the ice adhesion test and ice type are given, as well as all environmental conditions. As such, a variety of test methods and ice types must be accounted for to generate such a comparability, and multiple research groups must be included.

To be able to compare ice adhesion results from different facilities and set-ups efficiently and with a high degree of repeatability, a basis of reference must be established. If such a reference data bank was agreed upon, all ice adhesion test results could be compared to the common reference and thus be comparable. Ideally, such a basis for comparison would include both ice type and ice adhesion test method, as well as every experimental parameter. When all parameters are individually specified, comparative values will be available for different surfaces

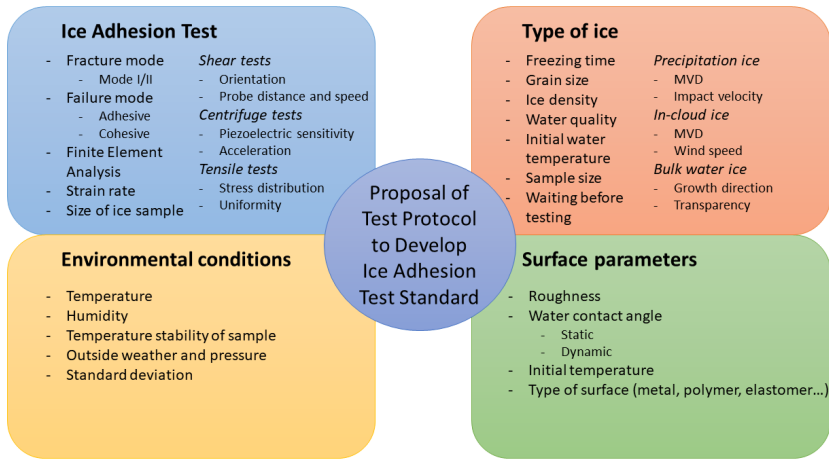


Figure 3.6: Selected elements and parameters of the proposed reference data bank to enable comparison of differently obtained ice adhesion values. Figure from Paper 4 (Appendix D).

and tests.

Such a reference database needs to account for all parameters in ice adhesion measurements. A selection of parameters which need to be included in such a reference is displayed in Figure 3.6. As illustrated, a basis for comparison would need to account for differences in environmental conditions such as temperature, different variations in surface texture and chemistry, the ice adhesion strength test set-up in use at different facilities, and all the different types of ice which are being tested for different applications. As a result, a finished basis for comparison must include large amounts of data, collected from different facilities and compared in a similar manner as the interlaboratory tests from Paper 3 (Appendix C).

As all research groups base their ice adhesion strength data on custom-built ice adhesion tests and ice formation processes, we further recommend a common set of reference ice adhesion data. This reference should not be considered the ideal test set-up or a unanimous solution, but rather as a relatively easy set-up which may be implemented fast. If such a set-up could be utilised as a common reference, all other tests would only need to be compared to the reference instead

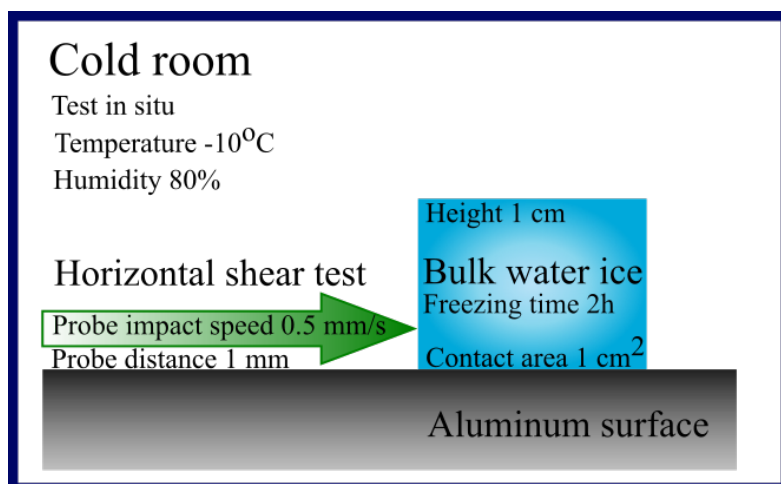


Figure 3.7: Schematic drawing of the proposed reference test for increased comparability within ice adhesion research. Figure from Paper 2 (Appendix B).

of being cross-compared with all other configurations. An example comparison set-up is suggested in Figure 3.7. We propose a horizontal shear test with defined experimental parameters for testing the ice adhesion strength of bulk water ice with specific ice formation properties on a specific type of aluminium surface in constant environmental conditions. The specific experimental parameters have been chosen from the most commonly used configurations in the literature, and the values for probe impact speed and location are well suited to testing on aluminium surfaces. This reference test must be repeated a statistically significant number of times before varying the parameters. Each parameter, such as probe distance or ice sample size, must be tested independently to discover the individual impact of the parameter on the ice adhesion strength. A suggested experimental protocol for such experiments is detailed in Appendix G.

Chapter 4

Results and findings

4.1 The effect of ice type on ice adhesion strength

The type of accreted ice is an important factor in the measurement of ice adhesion strength. In the first paper of this thesis, the aim was to understand the difference in adhesion strength between different types of ice. Precipitation ice from atmospheric precipitation, impact ice from in-cloud icing and bulk water ice were generated on the same substrate at the same air temperature, and were removed by the centrifugal adhesion test. The types of ice were denoted as Ice 1, Ice 2, and Ice 3, respectively, and have been defined in Table 4.1.

The experiments were performed at the AMIL facilities in Chicoutimi, Quebec, Canada. The protocols for generating precipitation ice and in-cloud ice were standardised at AMIL beforehand, while the protocol for bulk water ice was created in connection to this study. Precipitation ice was generated with a freezing drizzle in a cold room, while in-cloud ice was created in a closed-loop icing wind tunnel with wind speed 15 ms^{-1} . The bulk water ice was frozen from water in silicone

Table 4.1: Definition of ice types and ice generation methods.

Ice #	Name	Generation method
Ice 1	Precipitation ice	Super-cooled precipitation in a cold room
Ice 2	In-cloud ice	Super-cooled micro-droplets in a wind tunnel
Ice 3	Bulk water ice	Frozen water in silicon molds in a cold room

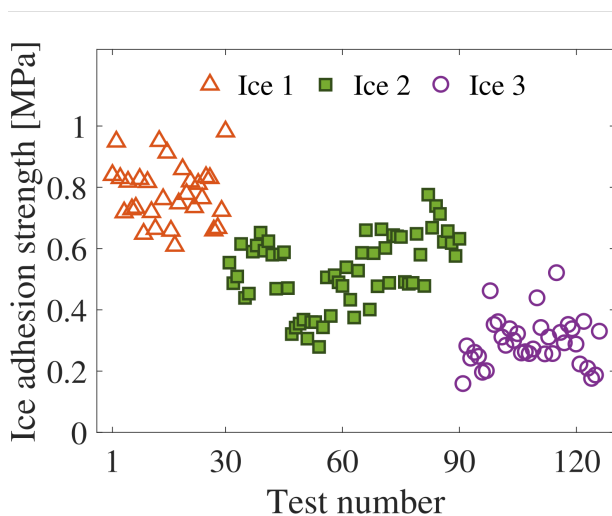


Figure 4.1: Ice adhesion strength obtained with the centrifugal test for the three ice types described in Table 4.1 at temperatures of -10°C on an aluminium surface.

molds in a cold room. All types of ice were created in similar environmental conditions, and temperatures of -10°C .

A total of 126 measurements were performed in this study. The resulting ice adhesion strength for the three ice types can be seen in Figure 4.1. This figure shows significant differences between the three ice types, and considerable variations within each ice type with high standard deviations.

The only relevant parameters differentiating ice adhesion strength between the ice types is found in the ice formation, which means the micro-structures of the ice. An indication of the changes of the micro-structure of the ice can be found in the density of the ice. In this study, the density of the ice types is approximated by the ratio of the mass to the thickness of the ice, and denoted as apparent density.

In Figure 4.2, the mean ice adhesion strength for each ice type is shown as a function of the apparent density. The three ice types are clearly differentiated by this apparent density. However, although there is a significant relationship between apparent density and ice adhesion strength, the number of tests are not sufficiently large to result in a predictive model. To indicate a relation, a linear model is fitted

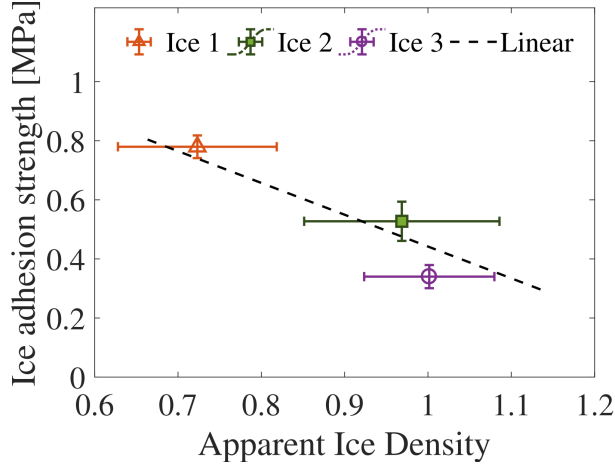


Figure 4.2: Mean ice adhesion strength per ice type as a function of mass per ice thickness, i.e. apparent density, with standard deviations included. The linear fitting is given by equation (4.1), and is calculated from all experimental data.

in Figure 4.2, given by

$$\tau = -0.0015 \cdot 10^{-3} \rho' + 1.7811, \quad (4.1)$$

where τ is the ice adhesion strength in MPa, and ρ' is the ice density in kgm^{-3} .

Although analytical models predict the opposite behaviour of ice adhesion as function of density than observed in these experiments, there are several possible mechanisms to explain the results in Figure 4.1. The stiffness of the ice is likely an important factor, where the stiffness and elastic modulus of ice and the ice porosity have a negative linear relationship for a given grain size. As such, a higher density results in a higher cohesive stiffness of the ice. A consequence is that bulk water ice is stiffer than the other ice types, which might be a factor in the lower ice adhesion strength observed due to higher propagation rate of interfacial cracks.

Further research is required to explore the difference in ice detachment mechanisms for the three ice types. It is especially important to understand the role of grain size on the ice adhesion. Such knowledge may inspire a new strategy in icephobic surfaces, specifically tailored to the ice which is desired removed.

4.2 The need for standards in low ice adhesion surface research

This critical review focused on the urgent needs of applicable standards in the field of ice adhesion research, and includes an overview of widely utilised ice adhesion strength measurement set-ups and methods of ice generation. As there is no available and recognised standard today, all quantitative ice adhesion strength results need to be adjusted in order to be directly comparable. It was shown that the reported ice adhesion strengths are very sensitive to both measurement set-up and ice type.

Based on previously published studies and reviews (see Table 3.1), there exists a sufficient amount of literature comparing different ice adhesion strength test methods. However, there was a need for a review focused on the comparison of low ice adhesion research while not limited to aircraft applications. Furthermore, to our knowledge there existed no publication within ice adhesion strength with a thorough definition concerning ice types for anti-icing applications. This gap in knowledge within the field was filled by this review. The discussion also included specific challenges for low ice adhesion surfaces and tests.

There is a general agreement that the development of low ice adhesion surfaces need to include a form of ground for comparison. This need was also substantiated in this review. However, there are several suggestions as to what this comparison and standardisation should consist of. We proposed here a common reference test which all other tests might be compared to.

Ice adhesion tests and different types of ice were discussed separately. The ice adhesion strength tests discussed were the horizontal shear test, the vertical shear test, the tensile test and the centrifugal adhesion test. The adhesion reduction factor was discussed, and previous attempts at standardisation of ice adhesion tests were included. Then, different types of ice used for ice adhesion research were discussed. Different definitions of glaze ice are shown in Table 4.2 as an example. The inherent variation within values of ice adhesion were discussed based in the stochastic nature of ice. Furthermore, the effect on ice adhesion strength from different parameters were discussed, including temperature differences during ice formation and testing, the ice sample size and gravity, the loading rate and the

Table 4.2: Different definitions of glaze ice as applied to ice adhesion research.

Ice type	Definition	Reference
Glaze	A generally homogeneous and transparent deposit of ice formed by the freezing of supercooled drizzle droplets or raindrops on objects the surface temperature of which is below of slightly above 0°C. It may also be produced by the freezing of non-supercooled drizzle droplets or raindrops immediately after impact with surfaces the temperature of which is well below 0°C	Armstrong et al [139]
Glaze ice	Temperatures over -10°C , freeze from water film after droplets have spread out. Has the highest possible ice density	Fortin and Perron [101]
Glaze ice	Hard, bubble-free and clear ice, generated under wet growth conditions and where surface temperature is above 0°C	Makkonen [87]
Glaze ice	Ice frozen in silicone mold at -5°C for 24 hours, resulting in a smooth clear structure. Ice that does not freeze on impact on aircrafts	Janjua et al [136]
Glaze ice	A type of precipitation icing resulting in transparent ice accretion of density $700 - 900 \text{ kgm}^{-3}$, sometimes with the presence of icicles under the conductors. It very strongly adheres to objects, and is difficult to knock off.	CIGRE TB 631 [16]
Glaze ice	Ice formed under glaze conditions, where the impinging droplets form a liquid film that freezes to form the ice. Latent heat release from formation is not sufficient to completely freeze the water on impact	Work et al [138]

distance between the force probe and the surface, and the stress distribution.

In conclusion, a future standardisation process within ice adhesion research must include several different parameters to successfully compare different reported ice adhesion strengths. To separate the contributions of the different parameters to the final ice adhesion strength, the mechanisms of ice adhesion of different types of accreted ice on different surfaces and different ice adhesion strength measurement methods must be further investigated. Moreover, specific challenges for low ice adhesion surfaces were discussed, including the accuracy and precision of the ice adhesion tests utilised, dynamic ice adhesion tests, the detachment mechanisms of ice from the surface, and the impact of intended application for the developed low ice adhesion surface.

4.3 Interlaboratory study of ice adhesion using different techniques

In this experimental study, the anti-icing research groups at AMIL and NTNU collaborated to compare obtained ice adhesion strength measurements from two commonly available surfaces. The surfaces tested were bare aluminium 6061-T6, and aluminium covered with EC-3100, a two component, water-based, icephobic, non-stick coating from Ecological Coating, LLC [137]. The ice adhesion tests were centrifuge adhesion test at AMIL, and the vertical shear test at NTNU.

As the aim of the study is to examine the comparability of ice adhesion strength measurements, all experimental parameters were kept as constant as possible, and were exactly similar for tests performed at both AMIL and NTNU. This similarity included the icing time, the temperatures, and the surfaces, which were all prepared at AMIL to ensure that systematic errors were avoided. Bulk water ice were tested at both facilities, and precipitation ice was tested additionally at AMIL. The ice adhesion strength was tested at temperatures of both -10°C and -18°C .

The measured ice adhesion strengths are shown in Figure 4.3. It can be seen that all results are comparable to a degree, with the greatest differences for bare aluminium surfaces at -10°C . It can be seen that for bulk water ice and aluminium surfaces, the vertical shear test systematically yields higher ice adhesion strengths than the centrifuge adhesion test as confirmed by a t-test, see Section 3.1.1. For the icephobic coating, the vertical shear tests seems to also give slightly higher ice adhesion strengths than the centrifuge adhesion test, although the trend is not as significant for temperatures of -18°C as for -10°C .

When comparing the two surface types for all ice types, all tests show larger error bars for bare aluminium than for the icephobic coating. The ice adhesion strengths for the icephobic coating from both laboratories are close to each other, but shows larger variations for bulk water ice than for precipitation ice. The fluctuating standard deviations can be partially explained by the original measurements. The instances where the standard deviation is above 30% are bare aluminium surfaces tested at NTNU and the icephobic coating with bulk water ice at AMIL. For all these instances, it can be seen in the original measurements that there were significant outliers.

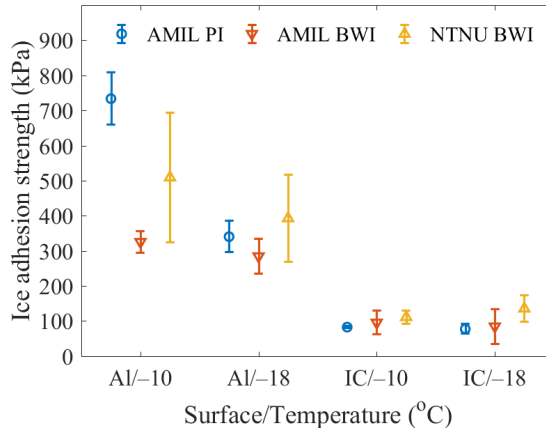


Figure 4.3: Measured ice adhesion strengths. Aluminium surfaces as denoted as Al, while the surfaces with icephobic coating are denoted IC. Precipitation ice is denoted as PI while bulk water ice is denoted BWI. AMIL tests were performed with centrifuge adhesion test, while NTNU tests were performed with vertical shear test. All results for tests on bulk water ice are shown in Figure 3.3.

The test configuration of bulk water ice on aluminium at temperature of -10°C with the vertical shear test performed at NTNU is close to a typical, standard measurement of ice adhesion strength, as the same type of shear tests are commonly applied. However, this configuration results in a high standard deviation and is where the largest differences between the different configurations in this study can be found. When the main outlier from this configuration at NTNU is removed, the mean ice adhesion strength becomes 441 MPa, with a standard deviation of 17%. These values are much closer to what would be expected based on the rest of the tests and configurations. This difference illustrates the significant effect of outliers in the ice adhesion tests, and might indicate why the standard deviation is generally high for ice adhesion tests.

As the amount of samples from each test configuration is so limited, there is no point in testing the significance of the differences between the vertical shear test and centrifugal adhesion test with large outliers removed. For tests performed with the vertical shear test, the removal of an outlier would remove 20% of the data for that configuration, and change the results accordingly. The experiments were

designed to optimise repeatability, and the high standard deviation is as such an integral part of the comparison between the two tests.

In conclusion, more data from several more laboratory facilities are needed, as well as more tests within each laboratory facility. Furthermore, this study provides further evidence that the ice formation is a key parameter in predicting the ice adhesion on different surfaces, as well as for the investigation of the mechanism of the ice detachment from different surfaces and the occurrence of cohesive failures during ice adhesion testing. To determine the ideal ice adhesion strength test, repeatability is a key factor to minimise the number of experimental outliers which greatly impact the standard deviation.

4.4 Nanoscale correlations of ice adhesion strength and water contact angle

The field of low ice adhesion material research has been known to operate by a trial-and-error strategy, where the focus has been on developing new surfaces and coatings without fully understanding the underlying mechanisms. One reason for this haste is the amount of resources required to properly test anti-icing surfaces in realistic conditions. Such resources are for instance the construction of suited laboratory facilities to create realistic ice samples, often including cold-rooms and icing wind tunnels. In order to facilitate the screening of potentially low ice adhesion surfaces, the possible relationships between surface wettability and ice adhesion strength of a given surface has been investigated. Both water contact angle and receding contact angle have been experimentally investigated with respect to a relation with ice adhesion strength, but the experimental results differ greatly.

In this study, the correlation between water contact angle and ice adhesion is investigated by utilising atomistic modelling and molecular dynamics simulations. By simulating the atomistic behaviour of water molecules on an ideal surface, it is possible to investigate the underlying physical mechanisms of ideal water-solid and ice-solid interactions. Surprisingly, the results show a behaviour very close to the theoretical model. This study thus indicates that the experimentally observed difference from the theoretical predictions does not stem from the inherent

behaviour of the water or ice, but rather from other parameters which may be impacted by experimental conditions.

As described in Section 2.5, equations (2.4) and (2.5) describing the Young contact angle and work of adhesion, respectively, may be combined to yield a direct relation between ice adhesion and water contact angle. When assumed that both the surface energies and interfacial energies of water and ice are similar, this equation becomes

$$W_a \approx \gamma_w(1 + \cos \theta), \quad (4.2)$$

where W_a is the work of adhesion, γ_w is the surface tension of water, and θ is the water contact angle. Furthermore, when combining equation (4.2) with the definition of the ice adhesion strength from equation (2.1) and the definitions of the work of adhesion, a direct relation between the ice adhesion strength and water contact angle can be derived. This relation is given by

$$\tau = C_0(1 + \cos \theta), \quad (4.3)$$

where τ is the ice adhesion strength, θ is the water contact angle, and C_0 is a general constant that depends on the surface area of the ice, the water surface tension and other characteristic factors that depends on the specific system under investigation. An illustration of the relation in equation (4.3) is given in Figure 4.4.

The combination of equations (2.1), (2.4) and (2.5) to arrive at equations (4.2) and (4.3) is based on a similar operation as published by Makkonen [29]. However, as equation (2.1) is based on solid-solid interactions while equation (2.4) and its derivatives are related to liquid-solid interfaces. As such, the direct combination of the equations is not straightforward, and requires the assumptions that both surface energies and surface interactions of water and ice are similar. These assumptions are not validated in this work, and the results obtained should be treated with proper care, and not directly applied to situations where the assumptions do not hold.

Our simulation system consists of an ice cube situated on a graphene surface, where the ice melts to water when the temperature is raised. Different contact angles are achieved by changing the energy well depth ε in the Lennard-Jones potential. The simulation details are further detailed in the publication (see Appendix D). Four different system sizes were tested, with details given in Table 4.3. Ice adhesion

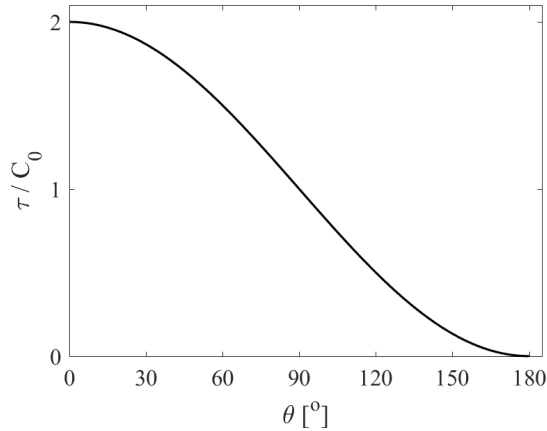


Figure 4.4: Ice adhesion strength as function of the contact angle θ as described by the general relation between ice adhesion strength τ and water contact angle on a generic surface with properties C_0 . The relation is described by equation (4.3).

Table 4.3: Overview of the different simulation systems investigated in this study.

System name	A	B	C	D
Number of atoms	28376	7336	58184	102568

strength is determined by pulling the ice perpendicular to the surface similar to a tensile test as shown in Figure 3.1, while water contact angle is calculated according to the algorithm developed by Khalkhali et al [152].

In Figure 4.5, the correlation between the theoretical relation from equation (4.3) and the simulation results can be seen, with the fitting and level of significance included. It can be seen that the fittings all systems have significances above $R^2 = 0.75$, with significances above $R^2 = 0.95$ for systems A and C. It is the smallest and largest systems which differs the most from the theoretical relation due to the increased amount of outliers in the simulation results.

Although the starting point of the study is a system with ice situated on a graphene surface, the nature of the surface is changed from realistically obtained graphene by changing the energy well depth and thus the water contact angle. Such a change is not experimentally possible, but in computer simulations every parameter of a surface may be changed. As a result, the simulations performed

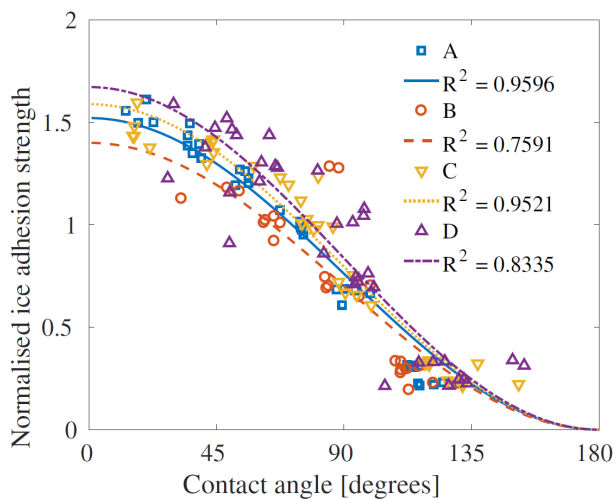


Figure 4.5: Illustration of the normalised ice adhesion strength and water contact angle for all four systems investigated in the simulations, with the theoretical relation from equation (4.3) included together with the significance of the fitting.

can show what happens when water contact angles vary on an otherwise identical surface.

The fact that the theoretical relation between the ice adhesion strength and the water contact angle is found in atomistic simulations indicate that the disagreement from experiments is due to surface properties not included in this study, and not from properties of water molecules in liquid and solid form on the same surface structure. However, it might also be due to the inability of experimental reproductions of different contact angles on the same molecularly structured surface such as performed in this study. The reproduction of the nanoscale theory is interesting and important due to the gap in understanding between experimental observations and theoretical models. The results presented here represents a step towards a more thorough understanding of the fundamental mechanisms of ice adhesion, and its relation to water wettability.

Chapter 5

Discussion and concluding remarks

In this chapter, the most relevant conclusions from the thesis are gathered. First, the 13 unanswered fundamental questions from Table 1.1 are discussed individually. The questions considered fully or partially answered in this thesis are underlined. After the fundamental questions are discussed, the recommended future work is described. Concluding remarks are found in the last section.

5.1 Answers to fundamental questions

Theory

1. What is the fundamental basis of ice adhesion?

Ice adhesion is a measure of the work required to detach a measure of ice from a surface and break the forces and bonds in the ice-solid interface. Ice adhesion strength is most often measured in pressure as the maximum detachment force divided by the ice-solid contact area, and has been described as "a practical engineering metric to quantify the de-icing capabilities of engineered surfaces" [33]. However, as there is no standard ice adhesion measurement technique, and different measurement set-ups utilise slightly different definitions of ice adhesion strength, no unified definition can be applied at present. Furthermore, the fundamental basis of ice adhesion is still unknown, and the mechanisms determining ice adhesion and ice-solid interactions are not unanimously agreed upon.

2. What is the theoretically achievable lowest ice adhesion strength?

The theoretically achievable lowest ice adhesion strength is related to the forces and interactions between the ice and the solid surfaces. To lower the ice adhesion strength, all the forces between the ice and surface must be minimised, so that only the van der Waals forces are present. As water is a polar substance, this strategy is difficult to accomplish experimentally. However, another strategy is to introduce flaws into the ice-solid interface. One way to introduce such flaws is by introducing air by cracking the interface, although this strategy depends on crack propagations along the entire ice sample. Another way is by adding a lubricant, so that detached ice is limited by the cohesive strength of the lubricant instead of the ice-solid adhesion. The disadvantage of this latter strategy is that the durability of the surface declines considerably. It follows therefore that this question cannot be fully answered at present, but is a part of the future work within ice adhesion research.

3. What is the bottleneck for decreasing ice adhesion strength?

The bottleneck for decreasing ice adhesion strength is closely related to the unknown lowest achievable ice adhesion strength as well as the most important surface parameter for lowering ice adhesion strength. However, at the present, the greatest bottleneck for decreasing ice adhesion strength is to relate the experiments to realistic conditions. In controlled environments, ice adhesion strength has been measured to below 1 kPa, which is more than adequate for all anti-icing applications. Unfortunately, the tests have not been performed in realistic conditions, with sufficiently low temperatures or with different types of ice. As seen in this thesis, to simply test surfaces with bulk water ice is not sufficient to ensure required anti-ice behaviour. Furthermore, the durability of most surfaces is insufficient for many applications, some of which require a durability of several decades before passive anti-icing with low ice adhesion surfaces may be attempted.

4. How do water and ice relate to each other?

As both water and ice both consists of water molecules in liquid and solid form, respectively, it is natural that they have several properties in common. Based on thermodynamics, the behaviour of water and ice on a surface is intimately related in

a theoretical relation. In this thesis, ice adhesion strength has been shown to relate to the wettability of water through equation (4.3) by making several assumptions on the similarities of interaction energies and solid-liquid and solid-solid interactions. Thus, ice adhesion strength might be represented by water contact angle, on a fundamental level. By utilising atomistic simulations, the predicted cosine relation was validated, and it is clear that the fundamental properties of water and ice indicate that ice adhesion strength and water wettability should correlate. However, there are several reasons for why this relation is not observed experimentally, and different representations of water wettability have not been investigated yet.

Ice detachment

5. What is the effect of ice type on ice adhesion strength?

This thesis has shown the effect of ice type on ice adhesion to be considerable. Several ice types, represented by precipitation ice, in-cloud ice and bulk water ice, has been shown to result in significantly different ice adhesion strengths when measured with the centrifugal adhesion test. Furthermore, the effect of ice type has been shown to depend on the surface, as bare aluminium had larger differences than a commercial icephobic surface. To examine the full effect of the ice type on ice adhesion strength, a larger range of ice types with different densities should be systematically investigated in a similar matter, for different types of surfaces.

6. What happens during ice detachment?

The detachment process varies for different ice types and ice adhesion measurement techniques. For bulk water ice on a specific type of surface tested with the horizontal shear test, the detachment process has been visualised by Golovin et al [61]. In this instance, the detachment process can be seen as a crack propagating rapidly at the ice-solid interface. For the same set-up of bulk water ice and the horizontal shear test but with an elastomeric surface, however, the ice did not detach but only slid around on the surface [62]. This difference indicates that the detachment mechanism for ice varies between different instances. Furthermore, for many test methods such as several set-ups of the centrifugal adhesion test, it is impossible to observe the actual detachment of the ice due to the large forces

present. In addition, if an ice adhesion test set-up is not fitted with a method to observe the ice detachment, it is not necessarily trivial to install such equipment. In conclusion, the process of ice detachment from a surface is not fully understood and requires systematic investigation.

7. What is the most relevant ice adhesion test method?

The most relevant ice adhesion test depend on the intended application for which the low ice adhesion surface is being developed. To ensure that the surface is sufficiently efficient and mirrors the ice adhesion strength obtained in the laboratory during field conditions, an ideal ice adhesion method must mirror the natural removal method for the given application. For instance, if the application is aircraft icing, and the low ice adhesion surface is to be applied to mitigate icing during take-off, a centrifugal test mimicking the force from the air on the ice sample would be most realistic. As such, there is no one ideal ice adhesion strength test, and the most relevant ice adhesion test will differ with the intended application. This challenge is further explored in question 10.

8. How does ice adhesion tests impact the results?

From interlaboratory research conducted as part of this thesis, it is clear that different ice adhesion tests impact the measured ice adhesion strength. The results indicate that the vertical shear test results in systematic higher ice adhesion strengths than the centrifugal adhesion test. However, the dependence on other types of tests, or other experimental set-ups, is still unknown. At present, there is not enough information to state the systematic impact of a given ice adhesion strength test on the observed ice adhesion strength.

Surfaces

9. What is the most important surface parameter for lowering ice adhesion strength?

The most important surface parameter for lowering ice adhesion strength depends on the type of surface. As there are as many different designs for low ice adhesion surfaces as there are research groups, each type of surface will require a different

ideal set of parameters. However, some key parameters that will most likely impact the ice adhesion strength of multiple surfaces have been determined. These are, among others, a low elastic modulus [59, 60], a nanotexture below the critical size to ensure that interlocked water remain in the liquid state [33], a cross-linked density of polymers to enhance interfacial slippage [52], to increase the hardness and elastic modulus of the surface [61], and to increase the presence of stress-localisation [62]. As can be seen, some of these key parameters are opposites, which underlines the importance of the type of surface under investigation when considering the most important surface parameter.

10. What is the effect of intended application for a low ice adhesion surface?

The intended application of a low ice adhesion surface is important for the type of surface, including the ideal surface for that application. For some surfaces, such as for aircraft application, a super-low ice adhesion strength tailored for impact ice is desired to ensure absolute ice mitigation at take-off and landing but without the need for a durability extending for longer than the longest flight time. For overhead power lines, on the other hand, icing occurs most often during storms, which induces strong winds and does not require as low ice adhesion strengths for the ice to detach. Furthermore, the durability of an anti-ice surface for power line application should be more than five decades to keep operational costs and dangers to a minimum. Other applications, such as wind turbines, require yet another set of ice adhesion strength and durability to achieve optimal application and ice mitigation. As such, different applications require different ice adhesion surface mechanisms, which are not clearly defined at present.

11. What is the effect of surface roughness on ice adhesion strength?

The effect of surface roughness on ice adhesion is considerable and complicated. The three scales of surface roughness, i.e. nanoscale, microscale and macroscale, impact the ice adhesion strength in different ways. As superhydrophobic surfaces has long been investigated for icephobic applications, the interlocking effect of ice and surface roughness on nanoscale and microscale has been examined thoroughly. However, this effect changes with changing ice types, as impact ice types may penetrate further into surface roughness structures. The relations

between surface roughness at different scales and ice adhesion strength are not fundamentally known, and is a topic well suited for future atomistic simulations [33, 103, 153, 154].

12. What is the effect of the angle of tilt on a tilting surface with respect to the ice adhesion strength?

From the definition of ice adhesion strength, a relation between the measured ice adhesion strength and static friction is to be expected, especially when measured with a horizontal shear test or centrifugal adhesion test. Furthermore, a tilted surface induces forces in addition to the applied force, similar to the difference in gravity between the vertical shear test and horizontal shear test. However, studies of dynamic ice adhesion surfaces have already applied tilted surfaces as a function of tilting angle and time until ice detachment as a measure of ice adhesion [155]. This measure of ice adhesion is not directly comparable to traditional ice adhesion strength, due to the effect of the tilted surface and the extra force on the ice. If the definition of ice adhesion strength was expanded to include a tilted surface, super-low ice adhesion surfaces might be more efficiently tested, as the traditional ice adhesion tests might lack the required precision. Ice adhesion on tilted surfaces is an intriguing topic closely related to anti-ice on solar cell panels, as discussed in Section 5.2 and in Appendix G.

13. What is the relation between ice adhesion strength and water wettability?

The relation between ice adhesion strength and water wettability differs between the theoretical and fundamental relations, and the experimental relations. As shown in this thesis, the inherent properties of water in liquid and solid form predict a cosine relation between ice adhesion strength and water contact angle derived from thermodynamic theory. However, this relation is not agreed upon from experiments, which indicates that the experimentally obtained ice adhesion strength depends on experimental parameters, such as material deformation, cohesive fractures, surface irregularities, and other surface parameters not included in the simulations. As a result, more research and experiments are needed to consolidate the fundamental properties with the obtained values of ice adhesion strength and water wettability for both reference surfaces and state-of-the-art low ice adhesion surfaces. These

investigations must also incorporate the effect of the assumptions included when relating ice adhesion strength and water contact angle through thermodynamic relations.

5.2 Future work

Although this thesis has made progress towards fundamental knowledge of the mechanisms of ice adhesion strength on different surfaces, there is still more work to be conducted. The future work indicated in this section have been divided into two categories, namely experimental studies to investigate the nature of the large variations of ice adhesion strength and the different types of ice, and atomistic simulations to investigate the properties of ice on different surfaces to examine the mechanisms of the detachment process and the different surface parameters. The future work is further detailed in Appendix G, with an overview of the suggested future projects in Table G.1.

The future experimental work inspired by this thesis is divided into four separate projects. The first project is a more detailed description of the protocol to establish a database in connection to the reference ice adhesion test described in Figure 3.7 to enhance comparability. A full list of parameters that should be tested and suggested values of the different parameters to be included in the tests can be found in Appendix G.

The second and third experimental projects are closely linked. The second experimental project concerns a more accurate method to determine the density of an ice sample than the measuring of mass and dimensions practised today. The third project is a continuation of the ice density, and concerns the grain structure of different ice types. Grain structure is closely connected to ice density, and may help predict and further understanding of the different detachment mechanisms present in different types of accreted ice. Both the ice density study and the ice grain size study include a suggested cooperation with the sea ice research group situated at the Department of Civil Engineering at NTNU.

The fourth and final suggested future experimental study concerns inclined plane and friction for anti-ice and solar cell applications. This study includes determining the relation between ice adhesion and ice friction, and applying the

knowledge to determine the required ice adhesion strength for passive ice removal on tilted solar cell panels, which may be situated on buildings or similar. Such a study would result in a list of necessary requirements for a low ice adhesion surface intended for photovoltaic applications with a given angle on the surface, and might also investigate whether such surface designs exist today.

The future atomistic studies suggested in this thesis consists of five different projects. The first project is an equilibrium study of water and ice, to determine similarities and differences between water and ice at its simplest state. In this study, both a force interaction study and a phonon vibrational spectra might be included. Furthermore, by changing the systems and conditions as further explained in Appendix G, the properties and characteristics of water and ice may be thoroughly compared. This future project was developed in cooperation with professor Niall English at University College Dublin, and an exchange to his research group is recommended during the work.

The second suggested future work within atomistic simulations is a direct continuation of the fourth paper of this thesis (Appendix D). Where the paper presented here compares the contact angle, and thus the work of adhesion, to the ice adhesion strength, this future study should expand the comparison to other types of contact angles as well, including advancing and receding contact angles, contact angle hysteresis, and a measure of the macroscopic contact angle to investigate the nanoscale size effect. Especially the receding contact angle would be interesting to examine with regards to the ice adhesion, as this comparison would substitute the work of adhesion with the practical work of adhesion, which is theorised to correlate well with the ice adhesion strength experimentally.

The third and fourth proposed future studies utilising atomistic simulations are to investigate ice adhesion strength on different surfaces. The third study aims to examine the impact of surface structure for ice adhesion strength, incorporating both different surface materials and different surface structures. The fourth study aims to determine the theoretical lowest ice adhesion strength for a given surface, based on the presence of only van der Waals forces. These two studies might be combined into one publication.

The final suggested future study is a continuation of the first paper of this thesis which examined the effect of ice type on the ice adhesion strength (Appendix A).

These atomistic simulations should create ice crystals with different grain size distributions and ice densities, and compare the calculated ice adhesion strengths to the published experimental observations and difference between the ice types. The different simulated ice types can either be based on the hypothetical ice structures presented in the published paper and its supplementary materials, or be based on results from the second and third proposed future experimental studies presented here.

5.3 Concluding remarks

The mitigation of unwanted ice by surface design has been investigated for more than half a century. Although we now have several promising options for passive anti-icing surfaces utilising low ice adhesion surfaces, the underlying mechanisms of ice adhesion are still unknown. The goal for the fundamental research of ice adhesion is to understand the theory behind the observed behaviour of ice detachment on different surfaces, and to expand this theory to both varying surfaces and icing conditions, which leads to varying types of ice. However, at present this fundamental research is hindered by the many surfaces and theories available in the research field, which are tailored to the specific cases investigated by the different publications.

This thesis has investigated the fundamental mechanisms of ice adhesion through several approaches. In Chapter 1, unanswered questions within ice adhesion research were presented. Chapter 2 gave an overview of ice and the background of ice adhesion, including a list of definitions to ensure that all concepts were clearly defined. Chapter 3 described the current status of methods applied to determine the ice adhesion strength, and the effect of different ice adhesion test methods and ice types. Chapter 4 summarised the most important points from the four papers included in the thesis, which included the effect of ice type on ice adhesion strength, a critical review on the need for comparability and standardisation in the low ice adhesion research field, an interlaboratory comparative study, and an atomistic simulation study on the relationship between ice adhesion strength and wettability of a surface. In Chapter 5, the fundamental questions from the introduction were reflected upon and partially answered, and suggested future work

was detailed.

It is clear that there is a need for more research on the mechanisms of ice adhesion to be able to design optimised low ice adhesion surfaces for each application or ice type. However, the results from this thesis represent a considerable step forward towards a fundamental understanding of the effect of the experimental facilities utilised. It has been shown that both the type of ice and the measurement of ice adhesion strength greatly impact the ice adhesion values obtained. Furthermore, atomistic simulations indicate that the properties of ice and water might be able to predict the ice adhesion strength on a given surface if the experimental factors and impacts of material deformation could be controlled.

Low ice adhesion strength surfaces are the most promising strategy to achieve passive anti-icing surfaces. To determine the most efficient low ice adhesion surface, all experimental parameters must be published to ensure comparability, and the surface in question must be tested in realistic icing and environmental conditions with a relevant ice adhesion strength test to evaluate its efficacy in ice mitigation.

Bibliography

- [1] S. Rønneberg, C. Laforte, C. Volat, J. He, and Z. Zhang, “The effect of ice type on ice adhesion,” *AIP Advances*, vol. 9, no. 5, p. 055304, 2019.
- [2] S. Rønneberg, J. He, and Z. Zhang, “The need for standards in low ice adhesion surface research: a critical review,” *Journal of Adhesion Science and Technology*, pp. 1–29, 2019.
- [3] S. Rønneberg, Y. Zhuo, C. Laforte, J. He, and Z. Zhang, “Interlaboratory study of ice adhesion using different techniques,” *Coatings*, vol. 9, no. 10, p. 678, 2019.
- [4] S. Rønneberg, J. He, and Z. Zhang, “Standardizing the testing of low ice adhesion surfaces,” in *International Workshops on Atmospheric Icing of Structures (IWAIS), Reykjavik, Iceland, 2019*.
- [5] J. Lv, Y. Song, L. Jiang, and J. Wang, “Bio-inspired strategies for anti-icing,” *ACS Nano*, vol. 8, no. 4, pp. 3152–3169, 2014.
- [6] K. Mittal, “Editorial note,” *Journal of Adhesion Science and Technology*, vol. 26, no. 4-5, pp. 405–406, 2012.
- [7] D. K. Sarkar, “Guest editorial,” *Journal of Adhesion Science and Technology*, vol. 26, no. 4-5, pp. 407–411, 2012.
- [8] V. F. Petrenko and R. W. Whitworth, *Physics of ice*. United Kingdom: Oxford University Press, 2006.
- [9] V. F. Petrenko, “The effect of static electric fields on ice friction,” *Journal of Applied Physics*, vol. 76, no. 2, 1994.
- [10] A. Klein-Paste and J. Wählin, “Wet pavement anti-icing — a physical mechanism,” *Cold Regions Science and Technology*, vol. 96, pp. 1–7, 2013.
- [11] R. W. Gent, N. P. Dart, and J. T. Cansdale, “Aircraft icing,” *Phil. Trans. R. Soc. Lond. A*, vol. 358, pp. 2873–2911, 2000.
- [12] F. T. Lynch and A. Khodadoust, “Effects of ice accretions on aircraft aerodynamics,” *Progress in Aerospace Sciences*, vol. 37, no. 8, pp. 669–767, 2001.
- [13] B. E. K. Nygaard, J. E. Kristjánsson, and L. Makkonen, “Prediction of in-cloud icing conditions at ground level using the wrf model,” *Journal of Applied Meteorology and Climatology*, vol. 50, no. 12, pp. 2445–2459, 2011.

- [14] M.-L. Pervier, *Mechanics of Ice Detachment Applied to Turbomachinery*. Thesis, Cranfield University, United Kingdom, 2012.
- [15] J. Brassard, C. Laforte, F. Guerin, and C. Blackburn, *Icephobicity: Definition and Measurement Regarding Atmospheric Icing*. Germany: Springer, Berlin, Heidelberg, 2017.
- [16] M. Farzaneh, H. Gauthier, G. Castellana, C. Engelbrecht, A. J. Elíasson, S. M. Fikke, C. Greyling, I. Gutmann, T. Hayashi, F. Jakl, Z. Jia, H. Lugschitz, V. Shkaptsov, L. Riera, N. Sugawara, N. Vaga, and B. Wareing, “TB 631 Coatings for protecting overhead power network equipment in winter conditions,” report, CIGRE, 2015.
- [17] ISO, “ISO 12494:2017 Atmospheric icing of structures,” 2017.
- [18] M. C. Homola, T. Wallenius, L. Makkonen, P. J. Nicklasson, and P. A. Sundsbø, “Turbine size and temperature dependence of icing on wind turbine blades,” *Wind Engineering*, vol. 34, no. 6, pp. 615–627, 2010.
- [19] M. C. Homola, T. Wallenius, L. Makkonen, P. J. Nicklasson, and P. A. Sundsbø, “The relationship between chord length and rime icing on wind turbines,” *Wind Energy*, vol. 13, no. 7, pp. 627–632, 2010.
- [20] L. Makkonen, “Modeling power line icing in freezing precipitation,” *Atmospheric Research*, vol. 46, no. 1–2, pp. 131–142, 1998.
- [21] L. Makkonen, “A model of hoarfrost formation on a cable,” *Cold Regions Science and Technology*, vol. 85, pp. 256–260, 2013.
- [22] L. Makkonen, T. Laakso, M. Marjaniemi, and K. J. Finstad, “Modelling and prevention of ice accretion on wind turbines,” *Wind Engineering*, vol. 25, no. 1, pp. 3–21, 2001.
- [23] Y. Liu, W. Cai, S. Gao, T. Yao, D. Huang, Y. Chen, and Z. Xu, “Study of the effect of ice adhesion on electrical power transmission insulator,” *Journal of Adhesion Science and Technology*, vol. 26, no. 4–5, pp. 593–602, 2012.
- [24] C. R. Sullivan, V. F. Petrenko, J. D. McCurdy, and V. Kozliouk, “Breaking the ice: de-icing power transmission lines with high-frequency, high-voltage excitation,” *IEEE Industry Applications Magazine*, vol. 9, no. 5, pp. 49–54, 2003.
- [25] M. J. Kreder, J. Alvarenga, P. Kim, and A. Joanna, “Design of anti-icing surfaces: smooth, textured or slippery?,” *Nature Reviews Materials*, vol. 1, pp. 1–15, 2016.
- [26] L. Makkonen, P. Lehtonen, and M. Hirviniemi, “Determining ice loads for tower structure design,” *Engineering Structures*, vol. 74, pp. 229–232, 2014.
- [27] E. Sundin and L. Makkonen, “Ice loads on a lattice tower estimated by weather station data,” *Journal of Applied Meteorology*, vol. 37, no. 5, pp. 523–529, 1998.
- [28] Collins Dictionary, “<https://www.collinsdictionary.com/dictionary/english/>” 2019.
- [29] L. Makkonen, “Ice adhesion —theory, measurements and countermeasures,” *Journal of Adhesion Science and Technology*, vol. 26, no. 4–5, pp. 413–445, 2012.

- [30] S. Løset, K. N. Shkhinek, O. T. Gudmestad, and K. V. Høyland, *Actions from Ice on Arctic Offshore and Coastal Structures: Student's Book for Institutes of Higher Education*. St. Petersburg: "LAN", 2006.
- [31] I. Gutman, J. Lundengård, V. Naidoo, and B. Adum, "Technologies to reduce and remove ice from phase conductors and shield wires: applicability for norwegian conditions," in *International Workshops on Atmospheric Icing of Structures (IWAIS), Reykjavik, Iceland*, 2019.
- [32] V. Hejazi, K. Sobolev, and M. Nosonovsky, "From superhydrophobicity to icephobicity: forces and interaction analysis," *Scientific Reports*, vol. 3, 2013.
- [33] T. Y. Zhao, P. R. Jones, and N. A. Patankar, "Thermodynamics of sustaining liquid water within rough icephobic surfaces to achieve ultra-low ice adhesion," *Scientific Reports*, vol. 9, no. 1, p. 258, 2019.
- [34] H. Sojoudi, M. Wang, N. D. Boscher, G. H. McKinley, and K. K. Gleason, "Durable and scalable icephobic surfaces: similarities and distinctions from superhydrophobic surfaces," *Soft Matter*, vol. 12, pp. 1938–1963, 2016.
- [35] Z. He, S. Xiao, H. Gao, J. He, and Z. Zhang, "Multiscale crack initiators promoted super-low ice adhesion surfaces," *Soft Matter*, vol. 13, pp. 6562–6568, 2017.
- [36] T. M. Schutzius, S. Jung, T. Maitra, P. Eberle, C. Antonini, C. Stamatopoulos, and D. Poulikakos, "Physics of icing and rational design of surfaces with extraordinary icephobicity," *Langmuir*, vol. 31, no. 17, pp. 4807–4821, 2015.
- [37] T. M. Schutzius, S. Jung, T. Maitra, G. Graeber, M. Köhme, and D. Poulikakos, "Spontaneous droplet trampolining on rigid superhydrophobic surfaces," *Nature*, vol. 527, no. 576, pp. 82–85, 2015.
- [38] S. Jung, M. Dorrestijn, D. Raps, A. Das, C. M. Megaridis, and D. Poulikakos, "Are superhydrophobic surfaces best for icephobicity?," *Langmuir*, vol. 27, no. 6, pp. 3059–3066, 2011.
- [39] J. Chen, J. Liu, M. He, K. Li, D. Cui, Q. Zhang, X. Zeng, Y. Zhang, J. Wang, and Y. Song, "Superhydrophobic surfaces cannot reduce ice adhesion," *Applied Physics Letters*, vol. 101, no. 11, 2012.
- [40] M. Nosonovsky and V. Hejazi, "Why superhydrophobic surfaces are not always icephobic," *ACS Nano*, vol. 6, no. 10, pp. 8488–8491, 2012.
- [41] K. K. Varanasi, T. Deng, J. D. Smith, M. Hsu, and N. Bhate, "Frost formation and ice adhesion on superhydrophobic surfaces," *Appl. Phys. Lett.*, vol. 97, no. 23, pp. 234102–3, 2010.
- [42] S. Jung, M. K. Tiwari, N. V. Doan, and D. Poulikakos, "Mechanism of supercooled droplet freezing on surfaces," *Nature Communications*, vol. 3, p. 615, 2012.
- [43] Z. Zhang and X.-Y. Liu, "Control of ice nucleation: freezing and antifreeze strategies," *Chemical Society Reviews*, vol. 47, no. 18, pp. 7116–7139, 2018.

- [44] D. Chen, M. D. Gelenter, M. Hong, R. E. Cohen, and G. H. McKinley, "Icephobic surfaces induced by interfacial nonfrozen water," *ACS Applied Materials and Interfaces*, vol. 9, no. 4, pp. 4202–4214, 2017.
- [45] D. L. Beemer, W. Wang, and A. K. Kota, "Durable gels with ultra-low adhesion to ice," *Journal of Materials Chemistry A*, vol. 4, pp. 18253–18258, 2016.
- [46] Z. He, E. T. Vågnes, C. Delabahan, J. He, and Z. Zhang, "Room temperature characteristics of polymer-based low ice adhesion surfaces," *Scientific Reports*, vol. 7, p. 42181, 2017.
- [47] V. Upadhyay, T. Galhenage, D. Battocchi, and D. Webster, "Amphiphilic icephobic coatings," *Progress in Organic Coatings*, vol. 112, pp. 191–199, 2017.
- [48] S. Pan, R. Guo, M. Bjornmalm, J. J. Richardson, L. Li, C. Peng, N. Bertleff-Zieschang, W. Xu, J. Jiang, and F. Caruso, "Coatings super-repellent to ultralow surface tension liquids," *Nature Materials*, vol. 17, no. 11, pp. 1040–1047, 2018.
- [49] S. A. Kulinich, S. Farhadi, K. Nose, and X. W. Du, "Superhydrophobic surfaces: Are they really ice-repellent?," *Langmuir*, vol. 27, no. 1, pp. 25–29, 2011.
- [50] H. Niemelä-Anttonen, H. Koivuluoto, M. Tuominen, H. Teisala, P. Juuti, J. Haapanen, J. Harra, C. Stenroos, J. Lahti, J. Kuusipalo, J. M. Mäkelä, and P. Vuoristo, "Icephobicity of slippery liquid infused porous surfaces under multiple freeze–thaw and ice accretion–detachment cycles," *Advanced Materials Interfaces*, vol. 5, no. 20, p. 1800828, 2018.
- [51] K. Golovin, S. P. R. Kobaku, D. H. Lee, E. T. DiLoreto, J. M. Mabry, and A. Tuteja, "Designing durable icephobic surfaces," *Science Advances*, vol. 2, no. 3, 2016.
- [52] K. Golovin and A. Tuteja, "A predictive framework for the design and fabrication of icephobic polymers," *Science Advances*, vol. 3, no. 9, p. e1701617, 2017.
- [53] Y. Wang, X. Yao, J. Chen, Z. He, J. Liu, Q. Li, J. Wang, and L. Jiang, "Organogel as durable anti-icing coatings," *Science China Materials*, vol. 58, pp. 559–565, 2015.
- [54] R. Dou, J. Chen, Y. Zhang, X. Wang, D. Cui, Y. Song, L. Jiang, and J. Wang, "Anti-icing coating with an aqueous lubricating layer," *ACS Applied Materials and Interfaces*, vol. 6, no. 10, pp. 6998–7003, 2014.
- [55] Y. Zhuo, V. Håkonsen, Z. He, S. Xiao, J. He, and Z. Zhang, "Enhancing the mechanical durability of icephobic surfaces by introducing autonomous self-healing function," *ACS Applied Materials and Interfaces*, vol. 10, no. 14, pp. 11972–11978, 2018.
- [56] F. Wang, W. Ding, J. He, and Z. Zhang, "Phase transition enabled durable anti-icing surfaces and its diy design," *Chemical Engineering Journal*, vol. 360, pp. 243–249, 2019.
- [57] Y. Zhuo, F. Wang, S. Xiao, J. He, and Z. Zhang, "One-step fabrication of bioinspired lubricant-regenerable icephobic slippery liquid-infused porous surfaces," *ACS Omega*, vol. 3, no. 8, pp. 10139–10144, 2018.
- [58] T. Li, Y. Zhuo, V. Håkonsen, S. Rønneberg, J. He, and Z. Zhang, "Epidermal gland inspired self-repairing slippery lubricant-infused porous coatings with durable low ice adhesion," *Coatings*, vol. 9, no. 10, p. 602, 2019.

- [59] Z. He, Y. Zhuo, J. He, and Z. Zhang, "Design and preparation of sandwich-like polydimethylsiloxane (pdms) sponges with super-low ice adhesion," *Soft Matter*, vol. 14, pp. 4846–4851, 2018.
- [60] Z. He, Y. Zhuo, F. Wang, J. He, and Z. Zhang, "Understanding the role of hollow sub-surface structures in reducing ice adhesion strength," *Soft Matter*, vol. 15, no. 13, pp. 2905–2910, 2019.
- [61] K. Golovin, A. Dhyani, M. D. Thouless, and A. Tuteja, "Low–interfacial toughness materials for effective large-scale deicing," *Science*, vol. 364, no. 6438, p. 371, 2019.
- [62] P. Irajizad, A. Al-Bayati, B. Eslami, T. Shafquat, M. Nazari, P. Jafari, V. Kashyap, A. Masoudi, D. Araya, and H. Ghasemi, "Stress-localized durable icephobic surfaces," *Materials Horizons*, vol. 6, pp. 758–766, 2019.
- [63] F. Wang, S. Xiao, Y. Zhuo, W. Ding, J. He, and Z. Zhang, "Liquid layer generator for excellent icephobicity at extremely low temperature," *Materials Horizons*, vol. 6, pp. 2063–2072, 2019.
- [64] E. Mitridis, T. M. Schutzius, A. Sicher, C. U. Hail, H. Eghlidi, and D. Poulikakos, "Metasurfaces leveraging solar energy for icephobicity," *ACS Nano*, vol. 12, no. 7, pp. 7009–7017, 2018.
- [65] A. Work and Y. Lian, "A critical review of the measurement of ice adhesion to solid substrates," *Progress in Aerospace Sciences*, vol. 98, pp. 1–26, 2018.
- [66] T. Cebeci and F. Kafyeke, "Aircraft icing," *Annual Review of Fluid Mechanics*, vol. 35, no. 1, pp. 11–21, 2003.
- [67] S. Ebnesajjad, *Surface Tension and Its Measurement*, book section 3, pp. 21–30. Oxford: William Andrew Publishing, NY, United States, 2011.
- [68] A. Marmur, C. Della Volpe, S. Siboni, A. Amirfazli, and J. W. Drelich, "Contact angles and wettability: towards common and accurate terminology," *Surface Innovations*, vol. 5, no. 1, pp. 3–8, 2017.
- [69] T. Bartels-Rausch, V. Bergeron, J. H. E. Cartwright, R. Escibano, J. L. Finney, H. Grothe, P. J. Gutierrez, J. Haapala, W. F. Kuhs, J. B. C. Pettersson, S. D. Price, C. I. Sainz-Díaz, D. Stokes, G. Strazzulla, E. S. Thomson, H. Trinks, and N. Uras-Aytemiz, "Ice structures, patterns, and processes: A view across the ice-fields," *Rev. Mod. Phys.*, vol. 84, pp. 885–944, 2012.
- [70] L. A. Wilen, J. S. Wettlaufer, M. Elbaum, and M. Schick, "Dispersion-force effects in interfacial premelting of ice," *Physical Review B*, vol. 52, no. 16, pp. 12426–12433, 1995.
- [71] I. A. Ryzhkin and V. F. Petrenko, "Violation of ice rules near the surface: A theory for the quasiliquid layer," *Physical Review B*, vol. 65, no. 1, p. 012205, 2001.
- [72] I. A. Ryzhkin and V. F. Petrenko, "Physical mechanisms responsible for ice adhesion," *The Journal of Physical Chemistry B*, vol. 101, no. 32, pp. 6267–6270, 1997.

- [73] V. F. Petrenko, "Effect of electric fields on adhesion of ice to mercury," *Journal of Applied Physics*, vol. 84, no. 1, pp. 261–267, 1998.
- [74] K. Matsumoto, D. Tsubaki, K. Sekine, H. Kubota, K. Minamiya, and S. Yamanaka, "Influences of number of hydroxyl groups and cooling solid surface temperature on ice adhesion force," *International Journal of Refrigeration*, vol. 75, no. Supplement C, pp. 322–330, 2017.
- [75] V. F. Petrenko, "Study of the surface of ice, ice/solid and ice/liquid interfaces with scanning force microscopy," *The Journal of Physical Chemistry B*, vol. 101, no. 32, pp. 6276–6281, 1997.
- [76] K. Matsumoto and Y. Daikoku, "Fundamental study on adhesion of ice to solid surface: Discussion on coupling of nano-scale field with macro-scale field," *International Journal of Refrigeration*, vol. 32, no. 3, pp. 444–453, 2009.
- [77] H. Jiang, F. Müller-Plathe, and A. Z. Panagiotopoulos, "Contact angles from young's equation in molecular dynamics simulations," *The Journal of Chemical Physics*, vol. 147, no. 8, p. 084708, 2017.
- [78] V. F. Petrenko and S. Peng, "Reduction of ice adhesion to metal by using self-assembling monolayers (sams)," *Canadian Journal of Physics*, vol. 81, no. 1-2, pp. 387–393, 2003.
- [79] J. Li, Y. Zhao, J. Hu, L. Shu, and X. Shi, "Anti-icing performance of a superhydrophobic pdms/modified nano-silica hybrid coating for insulators," *Journal of Adhesion Science and Technology*, vol. 26, no. 4-5, pp. 665–679, 2012.
- [80] C. Wang, T. Fuller, W. Zhang, and K. J. Wynne, "Thickness dependence of ice removal stress for a polydimethylsiloxane nanocomposite: Sylgard 184," *Langmuir*, vol. 30, no. 43, pp. 12819–12826, 2014.
- [81] C. Wang, M. C. Gupta, Y. H. Yeong, and K. J. Wynne, "Factors affecting the adhesion of ice to polymer substrates," *Journal of Applied Polymer Science*, vol. 135, no. 24, 2017.
- [82] L. Wang, Q. Gong, S. Zhan, L. Jiang, and Y. Zheng, "Robust anti-icing performance of a flexible superhydrophobic surface," *Advanced Materials*, vol. 28, no. 35, pp. 7729–7735, 2016.
- [83] C. Yang, F. Wang, W. Li, J. Ou, C. Li, and A. Amirfazli, "Anti-icing properties of superhydrophobic zno/pdms composite coating," *Applied Physics A*, vol. 122, no. 1, p. 1, 2015.
- [84] E. M. Yorkgitis, K. C. Melancon, A. M. Hine, and S. M. Giaquinto, "Glaciphobic polymeric materials," *Journal of Adhesion Science and Technology*, vol. 26, no. 4-5, pp. 681–699, 2012.
- [85] W. C. Macklin and G. S. Payne, "A theoretical study of the ice accretion process," *Quarterly Journal of the Royal Meteorological Society*, vol. 93, no. 396, pp. 195–213, 1967.
- [86] L. Makkonen, "Estimating intensity of atmospheric ice accretion on stationary structures," *Journal of Applied Meteorology*, vol. 20, no. 5, pp. 595–600, 1981.

- [87] L. Makkonen, "Atmospheric icing on sea structures," report, Cold Regions Research and Engineering Lab, Hanover, NH, United States, 1984.
- [88] L. Makkonen, "Modeling of ice accretion on wires," *Journal of Climate and Applied Meteorology*, vol. 23, no. 6, pp. 929–939, 1984.
- [89] G. Thompson, B. E. Nygaard, L. Makkonen, and S. Dierer, "Using the weather research and forecasting (wrf) model to predict ground/structural icing," in *IWAIS XIII*, Andermatt, Switzerland, 2009.
- [90] L. Wenjuan, F. Zhang, C. Yong, W. Qiang, X. Haiwei, and H. Mingfeng, "Remote icing monitoring and prediction model for icing accretion on power lines," in *International Workshop on Atmospheric Icing of Structures (IWAIS)*, Reyjavik, Iceland, 2019.
- [91] K. F. Jones, "The density of natural ice accretions related to nondimensional icing parameters," *Quarterly Journal of the Royal Meteorological Society*, vol. 116, no. 492, pp. 477–496, 1990.
- [92] P. L. I. Skelton and G. Poots, "The effect of density variations during rime growth on overhead transmission line conductors," *Cold Regions Science and Technology*, vol. 22, no. 4, pp. 311–317, 1994.
- [93] K. Szilder, "The density and structure of ice accretion predicted by a random-walk model," *Quarterly Journal of the Royal Meteorological Society*, vol. 119, no. 513, pp. 907–924, 1993.
- [94] K. Szilder and E. P. Lozowski, "Three-dimensional modelling of ice accretion density," *Quarterly Journal of the Royal Meteorological Society*, vol. 126, no. 568, pp. 2395–2404, 2000.
- [95] M. Vargas, H. Broughton, J. J. Sims, B. Bleeze, and V. Gaines, "Local and total density measurements in ice shapes," *Journal of Aircraft*, vol. 44, no. 3, pp. 780–789, 2007.
- [96] G.-L. Lei, W. Dong, M. Zheng, Z.-Q. Guo, and Y.-Z. Liu, "Numerical investigation on heat transfer and melting process of ice with different porosities," *International Journal of Heat and Mass Transfer*, vol. 107, pp. 934–944, 2017.
- [97] W. C. Macklin, "The density and structure of ice formed by accretion," *Quarterly Journal of the Royal Meteorological Society*, vol. 88, no. 375, pp. 30–50, 1962.
- [98] F. Prodi, L. Levi, and P. Pederzoli, "The density of accreted ice," *Quarterly Journal of the Royal Meteorological Society*, vol. 112, no. 474, pp. 1081–1090, 1986.
- [99] G. W. Timco and R. M. W. Frederking, "A review of sea ice density," *Cold Regions Science and Technology*, vol. 24, no. 1, pp. 1–6, 1996.
- [100] D. S. Thompson, D. Meng, A. Afshar, R. Bassou, J. Zong, E. Bonaccorso, A. Laroche, and V. Vercillo, "Initial development of a model to predict impact ice adhesion stress," in *Atmospheric and Space Environments Conference*, Atlanta, Georgia, United States, 2018.
- [101] G. Fortin and J. Perron, "Ice adhesion models to predict shear stress at shedding," *Journal of Adhesion Science and Technology*, vol. 26, no. 4-5, pp. 523–553, 2012.

- [102] F. Guerin, C. Laforte, M.-I. Farinas, and J. Perron, "Analytical model based on experimental data of centrifuge ice adhesion tests with different substrates," *Cold Regions Science and Technology*, vol. 121, pp. 93–99, 2016.
- [103] S. Xiao, J. He, and Z. Zhang, "Nanoscale deicing by molecular dynamics simulation," *Nanoscale*, vol. 8, p. 14625, 2016.
- [104] X. Zhang, Y. Huang, P. Sun, X. Liu, Z. Ma, Y. Zhou, J. Zhou, W. Zheng, and C. Q. Sun, "Ice regelation: Hydrogen-bond extraordinary recoverability and water quasisolid-phase-boundary dispersivity," *Scientific Reports*, vol. 5, p. 13655, 2015.
- [105] H. H. G. Jellinek, "Ice adhesion," *Canadian Journal of Physics*, vol. 40, no. 10, pp. 1294–1309, 1962.
- [106] A. Döppenschmidt and H.-J. Butt, "Measuring the thickness of the liquid-like layer on ice surfaces with atomic force microscopy," *Langmuir*, vol. 16, no. 16, pp. 6709–6714, 2000.
- [107] E. M. Schulson, "The structure and mechanical behavior of ice," *JOM*, vol. 51, no. 2, pp. 21–27, 1999.
- [108] G. F. N. Cox and W. F. Weeks, "Changes in the salinity and porosity of sea-ice samples during shipping and storage," *Journal of Glaciology*, vol. 32, no. 112, pp. 371–375, 1986.
- [109] R. J. Good, "Contact angle, wetting, and adhesion: a critical review," *Journal of Adhesion Science and Technology*, vol. 6, no. 12, pp. 1269–1302, 1992.
- [110] T. Young, "Iii. an essay on the cohesion of fluids," *Philosophical Transactions of the Royal Society of London*, vol. 95, pp. 65–87, 1805.
- [111] J. W. Drelich, "Contact angles: From past mistakes to new developments through liquid-solid adhesion measurements," *Advances in Colloid and Interface Science*, vol. 267, pp. 1–14, 2019.
- [112] R. N. Wenzel, "Resistance of solid surfaces to wetting by water," *Industrial and Engineering Chemistry*, vol. 28, no. 8, pp. 988–994, 1936.
- [113] A. B. D. Cassie, "Contact angles," *Discussions of the Faraday Society*, vol. 3, pp. 11–16, 1948.
- [114] A. B. D. Cassie and S. Baxter, "Wettability of porous surfaces," *Transactions of the Faraday Society*, vol. 40, pp. 546–551, 1944.
- [115] A. J. Meuler, J. D. Smith, K. K. Varanasi, J. M. Mabry, G. H. McKinley, and R. E. Cohen, "Relationships between water wettability and ice adhesion," *ACS Applied Materials and Interfaces*, vol. 2, no. 11, pp. 3100–3110, 2010.
- [116] C. Wang, W. Zhang, A. Siva, D. Tiew, and K. J. Wynne, "Laboratory test for ice adhesion strength using commercial instrumentation," *Langmuir*, vol. 30, no. 2, pp. 540–547, 2014.
- [117] M. Schulz and M. Sinapius, "Evaluation of different ice adhesion tests for mechanical deicing systems," in *SAE International*, 2015.

- [118] N. Cohen, A. Dotan, H. Dodiuk, and S. Kenig, "Thermomechanical mechanisms of reducing ice adhesion on superhydrophobic surfaces," *Langmuir*, vol. 32, no. 37, pp. 9664–9675, 2016.
- [119] J. M. Sayward, "Seeking low ice adhesion," report, U.S. Army Cold Regions Research and Engineering Laboratory, 72 Lyme Road, Hanover, NH USA 03755-1290, 1979.
- [120] M. R. Kasaai and M. Farzaneh, "A critical review of evaluation methods of ice adhesion," in *23rd International Conference on Offshore Mechanics and Arctic Engineering, Vancouver, British Columbia, Canada*, vol. 3, pp. 919–926, June 20–25 2004.
- [121] V. F. Petrenko, "Study of the physical mechanisms of ice adhesion," report number ADA422288, Thayer School of Engineering, Hanover, NH, USA, 2003.
- [122] D. N. Anderson and A. D. Reich, "Tests of the performance of coatings for low ice adhesion," *Technical Memorandum 107399*, p. 14, 1997.
- [123] L. E. Raraty and D. Tabor, "The adhesion and strength properties of ice," *Proceedings The Royal Society A: Mathematical Physical and Engineering Sciences*, vol. 245, pp. 184–201, 1958.
- [124] D. K. Sarkar and M. Farzaneh, "Superhydrophobic coatings with reduced ice adhesion," *Journal of Adhesion Science and Technology*, vol. 23, no. 9, pp. 1215–1237, 2009.
- [125] H. H. G. Jellinek, "Adhesive properties of ice," *Journal of Colloid Science*, vol. 14, no. 3, pp. 268–280, 1959.
- [126] Y. Yeong, J. Sokhey, and E. Loth, *Ice Adhesion on Superhydrophobic Coatings in an Icing Wind Tunnel*. Germany: Berlin, Heidelberg, Springer, 2017.
- [127] J. Schaaf and M. Kauffeld, "Ice aluminum debonding with induction heating," *Journal of Adhesion Science and Technology*, vol. 32, no. 19, pp. 2111–2127, 2018.
- [128] A. Dotan, H. Dodiuk, C. Laforte, and S. Kenig, "The relationship between water wetting and ice adhesion," *Journal of Adhesion Science and Technology*, vol. 23, no. 15, pp. 1907–1915, 2009.
- [129] S. A. Kulinich and M. Farzaneh, "Ice adhesion on super-hydrophobic surfaces," *Applied Surface Science*, vol. 255, no. 18, pp. 8153–8157, 2009.
- [130] S. A. Kulinich and M. Farzaneh, "How wetting hysteresis influences ice adhesion strength on superhydrophobic surfaces," *Langmuir*, vol. 25, no. 16, pp. 8854–8856, 2009.
- [131] R. Menini and M. Farzaneh, "Elaboration of Al₂O₃/PTFE icephobic coatings for protecting aluminum surfaces," *Surface and Coatings Technology*, vol. 203, no. 14, pp. 1941–1946, 2009.
- [132] S. A. Kulinich and M. Farzaneh, "On ice-releasing properties of rough hydrophobic coatings," *Cold Regions Science and Technology*, vol. 65, no. 1, pp. 60–64, 2011.
- [133] C. Laforte and A. Beisswenger, "Icephobic material centrifuge adhesion test," in *11th International Workshop on Atmospheric Icing on Structures (IWAIS)*, pp. 1–5, 2005.

- [134] R. G. Douglas, J. Palacios, and G. Schneeberger, "Design, fabrication, calibration, and testing of a centrifugal ice adhesion test rig with strain rate control capability," in *2018 Atmospheric and Space Environments Conference*, 2018.
- [135] Z. A. Janjua, "The influence of freezing and ambient temperature on the adhesion strength of ice," *Cold Regions Science and Technology*, vol. 140, pp. 14–19, 2017.
- [136] Z. A. Janjua, B. Turnbull, K.-L. Choy, C. Pandis, J. Liu, X. Hou, and K.-S. Choi, "Performance and durability tests of smart icephobic coatings to reduce ice adhesion," *Applied Surface Science*, vol. 407, pp. 555–564, 2017.
- [137] Ecological Coatings, LLC, "Icephobic coatings | anti-ice. available online: <http://www.ecologicalcoatings.com/icephobic.html> (accessed on 01.10.2019)," 2019.
- [138] J. Work, Andrew H., A. L. Gyekenyesi, R. E. Kreeger, J. A. Salem, M. M. Vargas, and D. R. Drabiak, "The adhesion strength of impact ice measured using a modified lap joint test," in *AIAA Aviation Forum*, p. 23, 25 June, 2018.
- [139] T. Armstrong, B. Roberts, and C. Swithinbank, *Illustrated Glossary of Snow and Ice*. Cambridge, United Kingdom: Scott Polar Research Institute, 1973.
- [140] Y. Wang, M. Li, T. Lv, Q. Wang, Q. Chen, and J. Ding, "Influence of different chemical modifications on the icephobic properties of superhydrophobic surfaces in a condensate environment," *Journal of Materials Chemistry A*, vol. 3, no. 9, pp. 4967–4975, 2015.
- [141] Droplet Measurement Techniques, "Products. available online: <http://www.dropletmeasurement.com/products> (accessed on 04.11.2019)."
- [142] D. Titov, K. Volkhov, N. Ivanov, A. Melnikov, and P. Vorobev, "Experimental study of resistance of aerial bundled cables with different hydrophobic coatings to hoar frost and soft rime," in *International Workshop on Atmospheric Icing of Structures (IWAIS) 2019*, 2019.
- [143] V. Clark, "Icing nomenclature," technical report 5676, U. S. Air Material Command, 1948.
- [144] Y. Zhu, X. Huang, J. Jia, Y. Tian, L. Zhao, Y. Zhang, Y. Cui, and X. Li, "Experimental study on the thermal conductivity for transmission line icing," *Cold Regions Science and Technology*, vol. 129, pp. 96–103, 2016.
- [145] M. Rios, *Icing simulations using Jones' density formula for accreted ice and LEWICE*. Aerospace Sciences Meetings, American Institute of Aeronautics and Astronautics, 1991.
- [146] R. J. Scavuzzo and M. L. Chu, "Structural properties of impact ices accreted on aircraft structures," report, NASA, 1987.
- [147] A. E. Carte, "Air bubbles in ice," *Proceedings of the Physical Society*, vol. 77, no. 3, p. 757, 1961.
- [148] N. D. Mulherin, R. B. Haehnel, and K. F. Jones, "Toward developing a standard shear test for ice adhesion," in *8th International Workshop on Atmospheric Icing of Structures (IWAIS), Reykjavik, Iceland*, pp. 73–79, 1998.

- [149] C. Laforte, J. D. Brassard, and C. Volat, “Extended evaluation of icephobic coating regarding their field of application,” in *International Workshops on Atmospheric Icing of Structures (IWAIS), Reykjavik, Iceland*, 2019.
- [150] H. Niemelä-Anttonen, J. Kiilakoski, P. Vuoristo, and H. Koivuluoto, “Icephobic performance of different surface designs and materials,” in *International Workshop on Atmospheric Icing of Structures (IWAIS), Reykjavik, Iceland*, 2019.
- [151] N. Rehfeld, B. Speckmann, and S. Grünke, “Durability of icephobic materials,” in *International Workshop on Atmospheric Icing of Structures (IWAIS), Reykjavik, Iceland*, 2019.
- [152] M. Khalkhali, N. Kazemi, H. Zhang, and Q. Liu, “Wetting at the nanoscale: A molecular dynamics study,” *The Journal of Chemical Physics*, vol. 146, no. 11, p. 114704, 2017.
- [153] S. Xiao, Z. Zhang, and J. He, “Atomistic dewetting mechanics at wenzel and monostable cassie-baxter states,” *Physical Chemistry Chemical Physics*, vol. 20, pp. 24759–24767, 2018.
- [154] S. Xiao, B. H. Skallerud, F. Wang, Z. Zhang, and J. He, “Enabling sequential rupture for lowering atomistic ice adhesion,” *Nanoscale*, vol. 11, no. 35, pp. 16262–16269, 2019.
- [155] T. Li, P. Ibáñez, J. Wu, V. Håkonsen, Y. Zhuo, S. Luo, J. He, and Z. Zhang, “Anti-icing ionic hydrogel with ignorable ice adhesion and anti-freezing/frost properties,” *In preparation*.
- [156] S. Maus, “The skeletal layer of sea ice: X-ray microtomography and modeling,” in *14th International Conference on the Physics and Chemistry of Ice, Zürich, Switzerland*, 2019.
- [157] P.-O. Borrebæk, B. P. Jelle, A. Klein-Paste, and Z. Zhang, “A gravity based method for measuring snow adhesion,” *Submitted*, 2019.
- [158] B. P. Jelle, “The challenge of removing snow downfall on photovoltaic solar cell roofs in order to maximize solar energy efficiency—research opportunities for the future,” *Energy and Buildings*, vol. 67, pp. 334–351, 2013.
- [159] F. Leroy and F. Müller-Plathe, “Dry-surface simulation method for the determination of the work of adhesion of solid–liquid interfaces,” *Langmuir*, vol. 31, no. 30, pp. 8335–8345, 2015.

Part I
Included papers

Appendix A

Paper 1

The Effect of Ice Type on Ice Adhesion Strength

Rønneberg, Sigrid, Caroline Laforte, Christophe Volat, Jianying He,
and Zhiliang Zhang. 2019. AIP Advances, 9: 055304.

The effect of ice type on ice adhesion

Cite as: AIP Advances 9, 055304 (2019); doi: 10.1063/1.5086242

Submitted: 19 December 2018 • Accepted: 26 April 2019 •

Published Online: 7 May 2019



Sigrud Rønneberg,¹ Caroline Laforte,²  Christophe Volat,² Jianying He,¹  and Zhiliang Zhang^{1,a} 

AFFILIATIONS

¹Department of Structural Engineering, Norwegian University for Science and Technology (NTNU), NO-7491 Trondheim, Norway

²Anti-Icing Materials International Laboratory (AMIL), Université du Québec à Chicoutimi, 555 Blvd. de l'Université, Chicoutimi, Québec G7H 2B1, Canada

^aCorresponding author. E-mail: zhiliang.zhang@ntnu.no. Telephone: +4773592530 / +4793001979

ABSTRACT

To lower the ice adhesion strength is the most efficient technique for passive ice removal for several applications. In this paper, the effect of different types of ice on the ice adhesion strength was investigated. The ice types precipitation ice, in-cloud ice and bulk water ice on the same aluminum substrate and under similar environmental conditions were investigated. The ice adhesion strength was measured with a centrifugal adhesion test and varied from 0.78 ± 0.10 MPa for precipitation ice, 0.53 ± 0.12 MPa for in-cloud ice to 0.28 ± 0.08 MPa for bulk water ice. The results indicate that the ice adhesion strength inversely correlates with the density of ice. The results inspire a new strategy in icephobic surface development, specifically tailored to the relevant ice type.

© 2019 Author(s). All article content, except where otherwise noted, is licensed under a Creative Commons Attribution (CC BY) license (<http://creativecommons.org/licenses/by/4.0/>). <https://doi.org/10.1063/1.5086242>

I. INTRODUCTION

Ice removal is necessary to avoid both dangerous situations^{1–5} and the unwanted icing of infrastructure^{6–10} and aircrafts.^{11,12} The most promising strategy for creating anti-icing surfaces^{1,9,13–15} are the lowering of ice adhesion strength.^{16–18} With a low ice adhesion strength, the ice formed on a surface might be shed off merely due to natural vibrations, its own weight or naturally occurring wind.^{18,19} Such a reduction requires a thorough understanding of the mechanisms of ice-solid adhesion. However, the fundamental physics of ice adhesion are not yet well understood.⁴

When measuring ice adhesion strength, there are several available methods.^{10,20–22} As of today, there is no testing standard, and each research group often develops its own testing techniques.^{20,23,24} Ice adhesion strength data measured at different laboratories can therefore not be easily compared.^{20,25,26} The choice of an efficient testing method depends on both the ice sample, and the type of surface to be tested. Different surfaces have different adhesion mechanisms to ice, which closely link with the ice removal process.²⁷ The size, chemical and mechanical properties, and the realistic icing conditions prevailing in the targeted application of the anti-icing surface are also important to determine the most efficient testing method.

The adhesion strength of ice Ih, which is the relevant ice phase for anti-icing applications, depends on many factors. These factors include the surface chemistry, the surface roughness profile, the elastic modulus, the temperature, and the ice micro-structure.^{5,27} The type of accreted ice is an important factor in the measurement of ice adhesion strength.²⁵ When water freezes in various atmospheric conditions, different types of ice are generated.^{4,5,10,14,20} These different types of ice vary in micro-structures and densities,²⁸ and behave in different manners when adhering to any given surface.^{22,25} Among the applications of anti-icing, there is a need to remove several different types of ice depending on icing conditions. For example, the ice that is accreted on aircrafts during flight, on roads, and on power transmission lines are different, with different accretion mechanisms. As a result, it is a limitation of most laboratory work that only one type of ice is tested for anti-icing surfaces in each laboratory with the same measurement techniques.

The present investigation aims to understand the difference in adhesion strength between different types of ice. Precipitation ice from a simulation of atmospheric precipitation, impact ice from in-cloud icing and bulk water ice were generated on the same substrate at the same air temperature and removed by the same ice adhesion strength test method. The results indicate that the ice type has

TABLE I. Definition of ice types and ice generation methods.

Ice #	Name	Type of ice	Generation method
Ice 1	Precipitation ice	Hard rime ice	Super-cooled precipitation in a cold room
Ice 2	In-cloud ice	Impact ice	Super-cooled micro-droplets in a wind tunnel
Ice 3	Bulk water ice	Clear ice	Frozen water in silicon molds in a cold room

a clear effect on adhesion strength. This difference of ice adhesion strength is attributed to the density. The findings from this study inspire a new strategy in icephobic surface design and development. For instance, a future surface might be tailored to repel a certain type of ice, depending on the application.

II. EXPERIMENTAL METHODS

The experimental work was performed at the Anti-icing Materials International Laboratory (AMIL) in Chicoutimi, Canada, which is the only laboratory in the world approved by ISO 9001:2015, PRI AC3001 and PRI AC3002 to qualify de-icing and anti-icing products for aircraft applications.²⁹ The experiments conducted here consist of more than 120 measurements of ice adhesion strength with a centrifugal adhesion test (CAT) and three types of ice at the same temperature. The generation of ice will be detailed first, before the CAT procedure is explained.

A. Generation of ice samples

The three types of ice generated in this study were precipitation ice from simulated atmospheric precipitation, impact ice from in-cloud icing and bulk water ice. These are denoted as ice type 1, 2 and 3, respectively, as defined in Table I. All ice was generated with demineralized water of resistivity 18 Ω . The air temperature T_{air} was kept constant at -10°C similar to other studies,^{17,23,30–32} while the sample surface temperature was recorded during icing for ice type 1 and 2. Other environmental conditions, such as humidity, were kept constant. An overview of both environmental and icing conditions are found in the [supplementary material](#).

All tests were conducted on bare aluminum 6061-T6 bars polished with Walter BLENDEX Drum fine 0724 M4. The bars had length 340 mm, width 31.8 mm and thickness 6.3 mm, and icing occurred over an area of 1100 mm^2 independent of the ice type. The accreted ice had a thickness of 7.5 ± 0.8 mm and a mass of 7 ± 2 g, depending on the type of ice. Before icing, the bars were stored in a cold room so the icing would start with a surface temperature of -10°C .

The experimental protocols for Ice 1 and Ice 2 were standardized at AMIL,^{30,33} while the protocol for generating Ice 3 was developed for this study. Ice 1 was created from a freezing drizzle and is denoted as precipitation ice. This ice was generated in a cold room with an air temperature of $-10.0 \pm 0.2^{\circ}\text{C}$ and a relative humidity of $80\% \pm 2\%$ as described elsewhere.³³ Six beams were iced simultaneously with water with a median volume drop diameter (MVD) of 324 μm and at an initial temperature of 4°C . As the water hit the beams, however, it had become super-cooled due to the low ambient temperature. Water impact speed was the free fall value of the droplets in the vertical airflow from an overhead nozzle, which was calculated to be 5.6 ms^{-1} . The bars were subjected to the precipitation for 33 minutes, and kept in the cold room for 1 hour between the icing and the centrifuge test to allow the ice to thermally stabilize. The surface temperature of the aluminum during icing was measured to be $-6.8 \pm 0.1^{\circ}\text{C}$. A typical sample of Ice 1 is shown in Fig. 1a. Ice 1 is similar to ice studied in several other publications,^{17,33,34} and is typically found in nature after instances of super-cooled rain.

Ice 2, impact ice created from in-cloud icing, was generated by spraying supercooled micro-droplets of water in a closed-loop icing wind tunnel at air temperature -10°C with a wind speed of 15 ms^{-1} , liquid water content (LWC) of 2.5 gm^{-3} and MVD of $27 \pm 3 \mu\text{m}$. The choice of these parameters was elaborated elsewhere,³³ as part of the standardized procedures at AMIL. The aluminum bars were placed upright in the wind tunnel, with seven to nine bars in each test. Everything except the icing area was shielded by a screen during icing. The icing time was 8 minutes and 15 seconds for all ice generated in the wind tunnel. The surface temperature of the aluminum during icing was measured to be $-9.1 \pm 0.3^{\circ}\text{C}$. The bars were kept in the cold room for 1 hour of waiting time between the icing and the centrifuge test. The resulting ice can be seen in Fig. 1b. Ice 2 is similar to other ice generated in a wind tunnel.^{20,30,35–37} Such ice is typically found after super-cooled rain coupled with high wind speeds, such as on ships and large structures after storms.

Ice 3, or bulk water ice, was assumed similar to clear ice such as found in ice cubes, and was generated by freezing water with a starting temperature of 4°C in silicon molds. The silicon molds

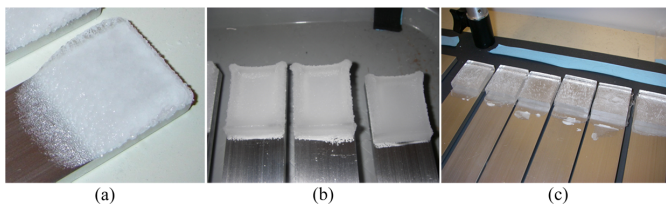


FIG. 1. Images of the different types of ice used in this investigation. (a) Ice 1. (b) Ice 2. (c) Ice 3.

were created from MoldMax30 by Smooth-On,³⁸ and the conditions in the cold room were the same as for Ice 1. The aluminum bars were placed at the water interface of the silicon molds at the same time as the water insertion, and the bars had an initial temperature of -10°C . To investigate the effect of the initial temperature difference between the inserted water and the aluminum bars, two measurement series were performed, where both the water and the bars had the initial temperature of 4°C at start of freezing. Each silicon mold contained 10 ml of water, and had the same dimensions as the iced area of the bars. The icing time varied from 2 hours to 3 hours and 15 minutes. The bars were spun in the centrifuge immediately after the mold was removed. Due to the inability to distinguish between the samples with different initial water temperatures and icing time, it can be concluded that these parameters do not impact the ice adhesion strength. Six bars were iced simultaneously for each measurement series. Typical samples of Ice 3 are found in Fig. 1c. Ice cubes similar to Ice 3 have been studied in several other investigations.^{13,15,18,19,23,31,32,39–41} This type of ice is often found when the temperature has dropped rapidly in an available body of water.

Before the centrifuge test, the mass and thickness of the accreted ice were measured. Each sample was spun individually in the centrifuge. The mass and dimensions of each aluminum bar were known, which made it possible to find the exact mass and thickness of the accreted ice. The total mass of the accreted ice and aluminum bar was measured both immediately before and after the centrifuge test, to calculate the mass of the detached ice. The mass was measured in grams on a digital scale. The thickness of the accreted ice was measured with a vernier caliper right before spinning. Because the thickness of the ice samples varies from one end to the other as seen in Fig. 1, especially for Ice 1 in Fig. 1a, all the thickness measurements were conducted on the thickest part of the ice samples. This protocol gives a higher experimental uncertainty for Ice 1 than Ice 2 and Ice 3. The uncertainties of the mass and thickness measurements are further discussed in Section IV A.

As the centrifuge was placed inside the cold room at -10°C , there was no thermal variation associated with the centrifuge test. The specimen was kept in -10°C for at least one hour prior to spinning, which was sufficient for the sample temperature to stabilize. Consequently, it is reasonable to assume that there was no difference in the temperature of the ice-solid interface between the different samples. Moreover, the temperature of a control sample was monitored with a thermocouple during the waiting time before spinning to ensure that all latent heat from the solidification of water had left the ice samples.

All measurements of the mass and thickness of the ice samples were taken right before the centrifuge adhesion test. The short amount of time between the measurements of the ice samples and the ice adhesion test lessens the effect of sublimation, which might otherwise have resulted in a substantial error in the measurements of the ice samples compared to the measured ice adhesion strength.

B. Centrifugal adhesion test

The ice adhesion strength is measured with centrifugal force in a CAT apparatus, which consists of a centrifuge, the placed sample beam, and a cover as seen in Fig. 2.³³ A counterweight was applied



FIG. 2. The centrifuge adhesion test set-up with the centrifuge at position a, the iced beam at position b and the cover with the piezoelectric cells at position c.

to the opposite end to balance the beam during spinning. The balanced and iced bars were spun in the centrifuge at an accelerating speed of 300 rpm s^{-1} between 0 and 30 seconds until the ice was detached by the centrifugal force. At this strain rate, calculated to be about $\dot{\epsilon} = 10^{-6}$, polycrystalline ice displays brittle behavior.³³ Piezoelectric cells situated around the centrifuge cover instantly detected the detachment of the ice. The rotation speed at the time of the ice detachment was recorded. The ice adhesion strength corresponds to the centrifugal shear stress at the position of the ice sample at the moment of detachment. The ice adhesion strength τ is thus given by

$$\tau = \frac{F}{A} = \frac{m_{ice}\omega^2 r}{A}, \quad (1)$$

where F is the centrifugal force, m_{ice} is the mass of the detached ice, ω is the angular velocity at the time of detachment, r is the radius of the beam at the center of mass for the accreted ice and A is the surface area of the detached ice.

The test was discarded if a cohesive break occurs. Such a cohesive break is not frequent with the CAT apparatus, but can occur under certain circumstances.³³ All the samples included in this study showed full adhesive failure, with no ice left on the bars after removal.

The accuracy of the CAT apparatus in terms of correctly determining the ice adhesion strength is among the most accurate in the field.⁴² The piezoelectric cells ensure determination of the exact detachment speed, which uniquely calculates the ice adhesion strength. The error from the piezoelectric cells is negligible, and is not separated out in the final error analysis but rather incorporated in the standard deviation of the measurements.

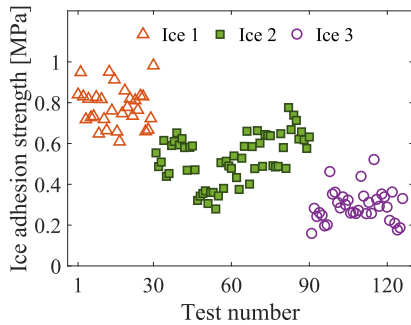


FIG. 3. Ice adhesion strength for the three ice types.

III. RESULTS

A total of 126 measurements are included in this analysis. See [supplementary material](#) for more information on the individual tests. The number of measurements per ice type were 30 for Ice 1, 60 for Ice 2 and 36 for ice type 3.

The ice adhesion strength is displayed in [Fig. 3](#) for all tests. This figure shows a significant difference in ice adhesion strength for the three ice types. It can also be seen that the ice adhesion strength varies considerably within all three ice types, with large standard deviations (see [supplementary material](#)). Such variations are to be expected, as the ice will crystallize in a random manner for each sample. The variation is larger for Ice 2, which was generated in a wind tunnel, indicating that this ice generation method has a larger inherent variance than other types of ice.

The mean ice adhesion strength for the three ice types is shown in [Table II](#) together with the standard deviation. [Table II](#) also shows the ice adhesion strength relative to Ice 1, and it can be seen that the ice adhesion strength for Ice 3 is less than 40% of that for Ice 1. Although the standard deviation is up to 30%, the trend of decrease in ice adhesion strength from Ice 1 to Ice 3 is clear.

IV. DISCUSSION

A. Effect of experimental parameters and ice density

The only relevant parameters differentiating ice adhesion strengths between ice types is the ice formation process, i.e. the corresponding ice types and their micro-structure.

TABLE II. Mean ice adhesion strength for the three types of ice, including the standard deviation. The percentage of ice adhesion strength relative to Ice 1 are also shown, with τ and $\tau_{Ice 1}$ as the ice adhesion strength of the ice type and Ice 1.

Ice type	Mean ice adhesion strength [MPa]	Standard deviation [MPa (%)]	$\tau/\tau_{Ice 1}$
Ice 1	0.780	± 0.102 (13.1%)	100%
Ice 2	0.529	± 0.119 (22.5%)	68%
Ice 3	0.284	± 0.083 (28.2%)	36%

Under different icing conditions, the micro-structure and density of the accreted ice change. The importance of changing density for accreted ice and ice properties has been investigated in several publications.^{28,43-51} In this study, the density of the ice is approximated by the ratio of the mass to the thickness of the ice, as the area of the aluminum bars exposed to icing is the same for all ice types resulting in an approximately equal icing area. This approximation of the density is denoted as apparent density.

Uncertainties in the apparent density are a combination of the uncertainty in the mass of the detached ice and the maximum thickness of the ice samples. However, neither the uncertainty from the digital weight, the uncertainty from the vernier caliper, nor the uncertainty from the varying thickness of the ice samples are included in the error analysis of the apparent density. As the use of the apparent density is an approximated parameter to discuss the actual density of the ice, the added uncertainty of the apparent density calculations has been omitted for simplicity. When these observations are repeated or expanded in a later study, these uncertainties must be accounted for in a systematic fashion to ensure that the discussion includes the actual density of the different ice types.

In [Fig. 4](#), the mean ice adhesion strength for each ice type is shown as a function of the mass divided by the thickness. In this figure, the three ice types are clearly differentiated by their apparent density. This observation is in accordance with other studies.^{28,44-46,48,51} It can be seen from [Fig. 4](#) that a higher apparent density indicates a lower ice adhesion strength.

Although the results from the large number of tests indicate a relation between density and ice adhesion strength, the number of tests are not sufficiently large to result in a predictive model. When a best fit function is forced, it becomes overfitted and thus non-predictive. However, there is a significant relationship between the apparent density and the ice adhesion strength as shown by *P*-values in [supplementary material](#). To indicate the relation, a best-fit linear model for the adhesion strength as function of density based on all performed experiments became

$$\tau = -0.0015 \times 10^{-3} \rho' + 1.7811, \tag{2}$$

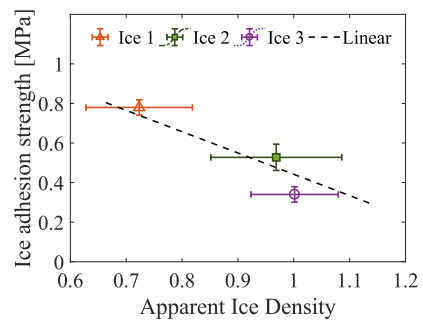


FIG. 4. Mean ice adhesion strength per ice type as a function of mass per ice thickness, i.e. apparent density, with standard deviations included. The linear fitting is given by equation (2), and is calculated from all experimental data (see [supplementary material](#)).

where τ is the ice adhesion strength in MPa, and ρ' is the ice density in kgm^{-3} . The ice density ρ' is calculated as the ratio of apparent density in gmm^{-3} to the icing area $A = 1100 \text{ mm}^2$, which is constant for all ice types. The linear relation for ice adhesion strength in equation (2) is given as a function of the ice density ρ' instead of apparent density to make the relation applicable for testing by other research groups in SI-units.

The significance of the linear relation decreases when subsets of the experimental data points are considered compared to the linear relation in equation (2) where all observations are included (see [supplementary material](#)). Both quadratic and exponential models show similar or less correlation than linear models, but as the exact relation is unknown at this time the simplest linear relation is shown. Further research is needed to establish the exact correlation between ice adhesion strength and density of different ice types and more variables, such as icing conditions. It is important to remember that such an improved relation might not be linear.

The results in this study are preliminary, and only deal with apparent density as compared to actual density. The authors plan to conduct further studies, which will increase the insight into the relation between the ice density and ice adhesion strength for all three types of accreted ice.

B. Properties of the ice

The three ice types included in this study are all composed of ice Ih, as they are all obtained by freezing water at atmospheric pressure in a temperature above -100°C .⁴ Ice Ih crystallizes in a hexagonal lattice, where the molecules are linked to each other with hydrogen bonds.

The porosity of sea ice is a function of density, temperature and salinity.⁵² For zero salinity, as in de-mineralized water, and at constant temperature, the porosity of ice will depend on density alone. For the rest of this paper, the term porosity will therefore be inversely equivalent to the ice density.

The density of the three types of ice are all dependent on the fraction of air volume. From [Fig. 4](#), it is seen that Ice 1 has the lowest density, followed by Ice 2 and then Ice 3. The opacity of the ice is also a measure of the density of the ice, as a higher fraction of air bubbles in the ice results in a more opaque ice.⁵³ From [Fig. 1a](#), it is clear that Ice 1 has a much higher degree of air bubbles present than the other types of ice, and that Ice 3 in [Fig. 1c](#) is almost completely free of air bubbles. The different transparencies of the ices substantiates the different densities of the ice types as seen in [Fig. 4](#).

The ice type with the highest theoretical density is often denoted as glaze ice, due to the lack of air bubbles in the ice^{25,45} compared to other ice types such as for instance freezing drizzle, hail, hoarfrost, rime, and others.⁵⁴ The exact definition of glaze ice varies,^{25,42,54} but it can be assumed that Ice 3 displays a structure similar to that of theoretical glaze ice due to the high transparency and the lack of air bubbles.⁵³ Micro-structures of the ice types might be proposed based on the densities, and such proposed structures can be found in the [supplementary material](#).

The density of accreted ice depends on both temperature and the droplet impact velocity, and has been found to increase with the increase of impact velocity and droplet size.²⁸ For low impact velocity the droplets retain their spherical shapes and form an open ice structure of low densities when freezing. At -10°C , droplets

start merging together, but are still individually discernible.²⁸ For higher impact velocity, the droplets start fusing together, mostly by a spreading in liquid state over the underlying ice. Such a process increases the density of the ice. At similar temperatures, the only difference in density will be due to the impact velocity. With respect to the processes described, the micro-structure of Ice 1 and Ice 2 should be similar to the proposed micro-structures.

It is worth mentioning that when the iced surface area is assumed constant and equal to the surface area of the detached ice, the density of the ice types fits well with the predictions of previous studies on density of ice types,²⁸ although slightly elevated compared to what is expected (see [supplementary material](#)).

C. Comparison with analytical models

The ice adhesion results obtained in this investigation match previous experiments.^{22,55} Several analytical models have tried to explain the mechanisms of ice adhesion. One model explains ice adhesion through electrostatic interactions,²⁵ while another explains ice adhesion through the existence of a liquid-like layer at the ice-solid interface.³⁴ These models are further described in [supplementary material](#).

Both analytical models include different ice types in their equations, but when the parameters from this study are tested, the models give predictions that are in direct contrast with the experimental results. The electrostatic model gives a lower ice adhesion strength for lower densities,²⁵ which would mean that Ice 1 should have a lower ice adhesion strength than Ice 3. For the model based on the liquid-like layer in the ice-solid interface,³⁴ the calculations predict that the ice adhesion strength of Ice 2 should be higher than the ice adhesion strength of Ice 1. It is clear from [Fig. 3](#) that neither trend is observed. It can be concluded that the existing models do not take different ice types sufficiently into account. To increase the predictability of models, new models of ice adhesion strength should be tested with several different types of ice to be as general as possible.

D. Possible mechanisms

So far, there is no clear explanation as to why the different ice types behave as observed in the experiments performed in this study. In addition, the mechanisms governing the ice detachment during ice adhesion tests are strongly coupled. The mechanical properties of ice are directly related to their micro-structure. In this section, some of the factors which might influence the ice detachment of the three different ices are described and briefly discussed. These factors should be included in further studies to predict the ice adhesion strength of different ice types and explain their detachment mechanisms.

The micro-structure of ice is determined during the crystallization process. Icing can generally be divided into wet icing and dry icing,^{5,56} which are separated by the amount of available water during freezing. For dry icing, such as Ice 1 and Ice 2, the density is lower than for wet icing,⁵ such as Ice 3. In addition, the crystallization process is influenced by the heat balance of the icing,⁵⁷ which varies for different icing conditions.

The stiffness and elastic modulus of ice and the ice porosity have a negative linear relationship for a given grain size,^{58,59} such that a higher density results in a higher cohesive stiffness of the ice.

It has been suggested that hydrogen bonds greatly influence the ice adhesion strength,⁴⁰ which is consistent with the stiffening of the ice at higher densities due to a shortening hydrogen bond.^{50,61} A consequence of this stiffening is that Ice 3 is stiffer than the other ice types, due to a higher density. The higher stiffness might be a factor for the lower ice adhesion strength observed, similar to that found in the adhesion of geckos.⁶²

There are two relevant length scales in freshwater ice which affects the fracture behavior, namely the grain size and the ice thickness.^{63,64} As such, the most important factor for the detachment behavior is likely the grain size distribution. An increase of grain size reduces the strength of the ice.⁵ There are larger stress concentrations in front of larger crystal grains, and grain sizes influence whether the failure of ice is brittle or ductile at a given strain rate $\dot{\epsilon}$.^{65–67} Furthermore, the density of micro-cracks is proportional to the grain size,⁶⁸ giving more faults in ices with larger grain sizes.

Another important factor which influences the ice adhesion strength is the temperature at the ice and surface interface. However, in this study, this factor can be excluded due to the same air temperature for all tests and the inability to distinguish the instances of Ice 3 where a different initial water temperature was utilized.

Further research is required to explore the difference in ice detachment mechanisms for the three ice types. As several of the potential influencing factors depend on the grain sizes, it is important to understand the role of grain size on the ice adhesion. The relevant detachment processes could also be investigated computationally, similarly to previous simulations of ice adhesion.^{69–71} Such knowledge could lead to the improvement of anti-icing surfaces by specializing the detachment process of ice.

V. CONCLUDING REMARKS

Ice and frost cause inconvenience for daily life, and can have potentially catastrophic consequences. One of the promising anti-icing strategies is the reduction of ice adhesion. Unlike previous studies focusing on the development of icephobic surfaces, this investigation is an attempt on the impact of different types of ice on the ice adhesion properties for the same substrate and environmental conditions. The ice types included in the investigation were precipitation ice created in a cold room with water droplets raining, in-cloud ice generated in a wind tunnel, and bulk water ice frozen directly onto the bars with silicon molds. The ice was frozen on identical aluminum 6061-T6 bars, and ice adhesion strength was measured with the centrifuge adhesion test. A relation was found between the mass per thickness of the generated ice and the ice adhesion strength. From this relation, it is seen that the ice adhesion strength decreases for an increasing density of the generated ice. Ice 3, which was the ice type with the highest density, was found to have an ice adhesion strength of less than 40% of that of Ice 1, which was hardest to remove. It appears that ice stiffness or porosity plays an unexpected role in ice adhesion strength and more studies are definitely needed to depict the effect of icing process on the resulting adhesion mechanisms. If correct, these observations may inspire a new strategy in icephobic surfaces, specifically tailored to the ice which is desired removed.

SUPPLEMENTARY MATERIAL

Supplementary material available, including full experimental results, information about statistical analysis, proposed microstructures for the ice types, and comparison of results with analytical models.

ACKNOWLEDGMENTS

The authors gratefully acknowledge the financial support from the Norwegian Research Council FRINATEK project Towards Design of Super-Low Ice Adhesion Surfaces (SLICE, 250990). The work was supported by the Anti-icing Materials International Laboratory (AMIL) by use of laboratory time. The experiments were performed by Caroline Blackburn and Caroline Laforte at AMIL, with the help of Sigrid Rønneberg. The manuscript was written by Sigrid Rønneberg and revised by the other authors. The funding sources had no involvement in designing the study or the publication.

The authors declare no conflicts of interest.

REFERENCES

1. J. Lv, Y. Song, L. Jiang, and J. Wang, "Bio-inspired strategies for anti-icing," *ACS Nano* **8**, 3152–3169 (2014).
2. K. Mittal, "Editorial note," *Journal of Adhesion Science and Technology* **26**, 405–406 (2012).
3. D. K. Sarkar, "Guest editorial," *Journal of Adhesion Science and Technology* **26**, 407–411 (2012).
4. V. F. Petrenko and R. W. Whitworth, *Physics of ice* (Oxford University Press, Great Britain, 2006).
5. S. Løset, K. N. Shkhinek, O. T. Gudmestad, and K. V. Hoyland, *Actions from Ice on Arctic Offshore and Coastal Structures: Student's Book for Institutes of Higher Education* (LAN, St. Petersburg, 2006), p. 277.
6. V. F. Petrenko, "The effect of static electric fields on ice friction," *Journal of Applied Physics* **76** (1994).
7. L. Makkonen, "Modeling power line icing in freezing precipitation," *Atmospheric Research* **46**, 131–142 (1998).
8. L. Makkonen, T. Laakso, M. Marjanemi, and K. J. Finstad, "Modelling and prevention of ice accretion on wind turbines," *Wind Engineering* **25**, 3–21 (2001).
9. M. J. Kreder, J. Alvarenga, P. Kim, and J. Aizenberg, "Design of anti-icing surfaces: Smooth, textured or slippery?," *Nature Reviews Materials* **1**, 1–15 (2016).
10. L. Makkonen, "Ice adhesion—Theory, measurements and countermeasures," *Journal of Adhesion Science and Technology* **26**, 413–445 (2012).
11. R. W. Gent, N. P. Dart, and J. T. Cansdale, "Aircraft icing," *Phil. Trans. R. Soc. Lond. A* **358**, 2873–2911 (2000).
12. F. T. Lynch and A. Khodadoust, "Effects of ice accretions on aircraft aerodynamics," *Progress in Aerospace Sciences* **37**, 669–767 (2001).
13. V. Hejazi, K. Sobolev, and M. Nosonovsky, "From superhydrophobicity to icephobicity: Forces and interaction analysis," *Scientific Reports* **3**, 2194 (2013).
14. H. Sojoudi, M. Wang, N. D. Boscher, G. H. McKinley, and K. K. Gleason, "Durable and scalable icephobic surfaces: Similarities and distinctions from superhydrophobic surfaces," *Soft Matter* **12**, 1938–1963 (2016).
15. Z. He, S. Xiao, H. Gao, J. He, and Z. Zhang, "Multiscale crack initiators promoted super-low ice adhesion surfaces," *Soft Matter* (2017).
16. K. K. Varanasi, T. Deng, J. D. Smith, M. Hsu, and N. Bhate, "Frost formation and ice adhesion on superhydrophobic surfaces," *Appl. Phys. Lett.* **97**, 234102–234103 (2010).
17. A. Dotan, H. Dodiuk, C. Laforte, and S. Kenig, "The relationship between water wetting and ice adhesion," *Journal of Adhesion Science and Technology* **23**, 1907–1915 (2009).

- ¹⁸J. Chen, J. Liu, M. He, K. Li, D. Cui, Q. Zhang, X. Zeng, Y. Zhang, J. Wang, and Y. Song, "Superhydrophobic surfaces cannot reduce ice adhesion," *Applied Physics Letters* **101**, 111603 (2012).
- ¹⁹D. L. Beemer, W. Wang, and A. K. Kota, "Durable gels with ultra-low adhesion to ice," *Journal of Materials Chemistry A* **4**, 18253 (2016).
- ²⁰M. Schulz and M. Sinapius, "Evaluation of different ice adhesion tests for mechanical deicing systems" (2015).
- ²¹M. R. Kasaii and M. Farzaneh, "A critical review of evaluation methods of ice adhesion," 23rd International Conference on Offshore Mechanics and Arctic Engineering **3**, 919–926 (2004).
- ²²D. N. Anderson and A. D. Reich, "Tests of the performance of coatings for low ice adhesion," Technical Memorandum 107399, 14 (1997).
- ²³A. J. Meuler, J. D. Smith, K. K. Varanasi, J. M. Mabry, G. H. McKinley, and R. E. Cohen, "Relationships between water wettability and ice adhesion," *ACS Applied Materials & Interfaces* **2**, 3100–3110 (2010).
- ²⁴C. Wang, W. Zhang, A. Siva, D. Tiew, and K. J. Wynne, "Laboratory test for ice adhesion strength using commercial instrumentation," *Langmuir* **30**, 540–547 (2014).
- ²⁵G. Fortin and J. Perron, "Ice adhesion models to predict shear stress at shedding," *Journal of Adhesion Science and Technology* **26**, 523–553 (2012).
- ²⁶M. Javan-Mashmool, C. Volat, and M. Farzaneh, "A new method for measuring ice adhesion strength at an ice–substrate interface," *Hydrological Processes* **20**, 645–655 (2006).
- ²⁷J. M. Sayward, "Seeking low ice adhesion," Report (U.S. Army Cold Regions Research and Engineering Laboratory, 72 Lyme Road, Hanover, NH, USA, 03755-1290, 1979).
- ²⁸W. C. Macklin, "The density and structure of ice formed by accretion," *Quarterly Journal of the Royal Meteorological Society* **88**, 30–50 (1962).
- ²⁹A. Icing, Materials International Laboratory (AMIL), Available from <http://amilaboratory.ca/about-us/> and <http://amilaboratory.ca/about-us/accreditations/> [Accessed January 29 2019].
- ³⁰S. A. Kulinich and M. Farzaneh, "Ice adhesion on super-hydrophobic surfaces," *Applied Surface Science* **255**, 8153–8157 (2009).
- ³¹K. Golovin, S. P. R. Kobaku, D. H. Lee, E. T. DiLoreto, J. M. Mabry, and A. Tuteja, "Designing durable icephobic surfaces," *Science Advances* **2** (2016).
- ³²K. Golovin and A. Tuteja, "A predictive framework for the design and fabrication of icephobic polymers," *Science Advances* **3** (2017).
- ³³C. Laforte and A. Beisswenger, "Icephobic material centrifuge adhesion test," in *11th International Workshop on Atmospheric Icing on Structures (IWAIS)* (2005), pp. 1–5.
- ³⁴F. Guerin, C. Laforte, M.-I. Farinas, and J. Perron, "Analytical model based on experimental data of centrifuge ice adhesion tests with different substrates," *Cold Regions Science and Technology* **121**, 93–99 (2016).
- ³⁵S. A. Kulinich, S. Farhadi, K. Nose, and X. W. Du, "Superhydrophobic surfaces: Are they really ice-repellent?," *Langmuir* **27**, 25–29 (2011).
- ³⁶S. A. Kulinich and M. Farzaneh, "How wetting hysteresis influences ice adhesion strength on superhydrophobic surfaces," *Langmuir* **25**, 8854–8856 (2009).
- ³⁷S. A. Kulinich and M. Farzaneh, "On ice-releasing properties of rough hydrophobic coatings," *Cold Regions Science and Technology* **65**, 60–64 (2011).
- ³⁸Smooth-On, Inc., 5600 Lower Macungie Road, Macungie, PA 18062, USA, "Mold max™ series tin cure silicone mold making rubber," Available from <https://www.smooth-on.com/product-line/mold-max/> [Accessed February 08 2018] (2018).
- ³⁹Z. He, E. T. Vágenes, C. Delabahan, J. He, and Z. Zhang, "Room temperature characteristics of polymer-based low ice adhesion surfaces," *Scientific Reports* **7**, 42181 (2017).
- ⁴⁰K. Matsumoto, D. Tsubaki, K. Sekine, H. Kubota, K. Minamiya, and S. Yamanaka, "Influences of number of hydroxyl groups and cooling solid surface temperature on ice adhesion force," *International Journal of Refrigeration* **75**, 322–330 (2017).
- ⁴¹L. E. Rataty and D. Tabor, "The adhesion and strength properties of ice," *Proceedings the Royal Society A: Mathematical Physical & Engineering Sciences* **245**, 184–201 (1958).
- ⁴²A. Work and Y. Lian, "A critical review of the measurement of ice adhesion to solid substrates," *Progress in Aerospace Sciences* **98**, 1–26 (2018).
- ⁴³G. W. Timco and R. M. W. Frederking, "A review of sea ice density," *Cold Regions Science and Technology* **24**, 1–6 (1996).
- ⁴⁴K. F. Jones, "The density of natural ice accretions related to nondimensional icing parameters," *Quarterly Journal of the Royal Meteorological Society* **116**, 477–496 (1990).
- ⁴⁵G.-L. Lei, W. Dong, M. Zheng, Z.-Q. Guo, and Y.-Z. Liu, "Numerical investigation on heat transfer and melting process of ice with different porosities," *International Journal of Heat and Mass Transfer* **107**, 934–944 (2017).
- ⁴⁶F. Prodi, L. Levi, and P. Pederzoli, "The density of accreted ice," *Quarterly Journal of the Royal Meteorological Society* **112**, 1081–1090 (1986).
- ⁴⁷M. Rios, "Icing simulations using Jones' density formula for accreted ice and LEWICE," in *29th Aerospace Sciences Meeting*, Aerospace Sciences Meetings (American Institute of Aeronautics and Astronautics, 1991).
- ⁴⁸P. L. I. Skelton and G. Poots, "The effect of density variations during rime growth on overhead transmission line conductors," *Cold Regions Science and Technology* **22**, 311–317 (1994).
- ⁴⁹K. Szilder, "The density and structure of ice accretion predicted by a random-walk model," *Quarterly Journal of the Royal Meteorological Society* **119**, 907–924 (1993).
- ⁵⁰K. Szilder and E. P. Lozowski, "Three-dimensional modelling of ice accretion density," *Quarterly Journal of the Royal Meteorological Society* **126**, 2395–2404 (2000).
- ⁵¹M. Vargas, H. Broughton, J. J. Sims, B. Bleeze, and V. Gaines, "Local and total density measurements in ice shapes," *Journal of Aircraft* **44**, 780–789 (2007).
- ⁵²G. F. N. Cox and W. F. Weeks, "Changes in the salinity and porosity of sea-ice samples during shipping and storage," *Journal of Glaciology* **32**, 371–375 (1986).
- ⁵³A. E. Carte, "Air bubbles in ice," *Proceedings of the Physical Society* **77**, 757 (1961).
- ⁵⁴T. Armstrong, B. Roberts, and C. Swinbank, *Illustrated Glossary of Snow and Ice* (Scott Polar Research Institute, Cambridge, 1973).
- ⁵⁵A. Reich, "Interface influences upon ice adhesion to airfoil materials," in *32nd Aerospace Sciences Meeting and Exhibit*, Aerospace Sciences Meetings (American Institute of Aeronautics and Astronautics, 1994).
- ⁵⁶G. S. H. Lock, *The Growth and Decay of Ice*, Studies in Polar Research (Cambridge University Press, Great Britain, 1990).
- ⁵⁷L. Yanan, G. Xiaosong, and H. Yecong, "Experimental study on criteria correlation of heat convection between air and wires in icing conditions," in *2013 Fourth International Conference on Digital Manufacturing and Automation*, pp. 591–594.
- ⁵⁸B. Michel, *Ice Mechanics* (Les Presses De L'Université Laval, Canada, 1978).
- ⁵⁹D. M. Cole, "Modeling the cyclic loading response of sea ice," *International Journal of Solids and Structures* **35**, 4067–4075 (1998).
- ⁶⁰C. Q. Sun, X. Zhang, and W. Zheng, "The hidden force opposing ice compression," *Chemical Science* **3**, 1455–1460 (2012).
- ⁶¹C. Q. Sun, X. Zhang, X. Fu, W. Zheng, J.-I. Kuo, Y. Zhou, Z. Shen, and J. Zhou, "Density and phonon-stiffness anomalies of water and ice in the full temperature range," *The Journal of Physical Chemistry Letters* **4**, 3238–3244 (2013).
- ⁶²B. I. N. Chen and H. Gao, "An alternative explanation of the effect of humidity in gecko adhesion: Stiffness reduction enhances adhesion on a rough surface," *International Journal of Applied Mechanics* **02**, 1–9 (2010).
- ⁶³J. P. Dempsey, S. J. Defranco, R. M. Adamson, and S. V. Mulmule, "Scale effects on the in-situ tensile strength and fracture of ice. Part I: Large grained freshwater ice at spray lakes reservoir, Alberta," *International Journal of Fracture* **95**, 325 (1999).
- ⁶⁴C. Bu, C. A. Duker, and R. A. Baragiola, "Spontaneous cracking of amorphous solid water films and the dependence on microporous structure," *Applied Physics Letters* **109**, 201902 (2016).
- ⁶⁵R. W. Lee and E. M. Schulson, "The strength and ductility of ice under tension," *Journal of Offshore Mechanics and Arctic Engineering* **110**, 187–191 (1988).
- ⁶⁶E. M. Schulson, "The structure and mechanical behavior of ice," *JOM* **51**, 21–27 (1999).

⁶⁷E. M. Schulson, P. N. Lim, and R. W. Lee, "A brittle to ductile transition in ice under tension," *Philosophical Magazine A* **49**, 353–363 (1984).

⁶⁸D. M. Cole, "Effect of grain size on the internal fracturing of polycrystalline ice," Report (Cold Region Research and Engineering Lab, Hanover, NH, 1986).

⁶⁹S. Xiao, J. He, and Z. Zhang, "Nanoscale deicing by molecular dynamics simulation," *Nanoscale* **8**, 14625 (2016).

⁷⁰T. Hynninen, V. Heinonen, C. L. Dias, M. Karttunen, A. S. Foster, and T. Ala-Nissila, "Cutting ice: Nanowire regelation," *Physical Review Letters* **105** (2010).

⁷¹C. J. Burnham, J.-C. Li, and M. Leslie, "Molecular dynamics calculations for ice Ih," *The Journal of Physical Chemistry B* **101**, 6192–6195 (1997).

The Effect of Ice Type on Ice Adhesion: Supplementary materials

Sigrid Rønneberg,¹ Caroline Laforte,² Christophe Volat,² Jianying He,¹ and Zhiliang Zhang^{1, a)}

¹⁾Department of Structural Engineering, Norwegian University for Science and Technology (NTNU), NO-7491 Trondheim, Norway

²⁾Anti-icing Materials International Laboratory (AMIL), Université du Québec à Chicoutimi, 555 blvd. de l'Université, Chicoutimi, Québec, Canada, G7H 2B1

S1. ENVIRONMENTAL AND ICING CONDITIONS

The environmental conditions for the icing is apparent in Tab. S1. The icing conditions are apparent in Tab. S2. Another version of Fig. 3 is shown in Fig. S1, where the number of samples in each measurement series are included. The measurements are in the same order as in Tab. S1 and S2.

All experimental data, observations and results are available on request.

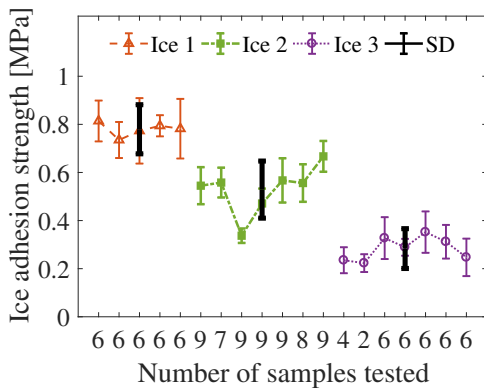


FIG. S1: Values of the ice adhesion strength for the three ice types with total standard deviation for each ice type. The number of samples tested in each measurement series is included for comparison.

S2. EXPERIMENTAL PARAMETERS

A. Temperature

In Fig. S2, the variations in air temperature during the icing processes for the different measurement series can be seen. It is apparent that the air temperature was more variable for Ice 2 generated in the wind tunnel than for the icing processes performed in the cold room. However, there is no apparent relation between the ice adhesion strength and the air temperature for any of the icing processes. Even though the Ice 3 air

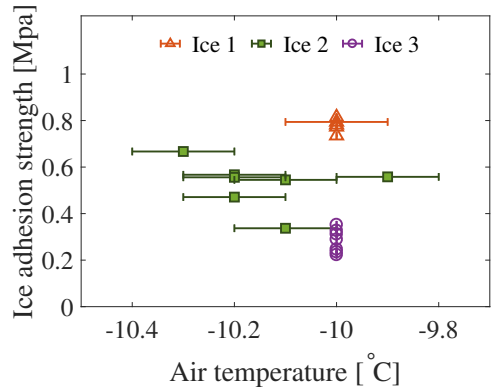


FIG. S2: Ice adhesion strength as function of variations in air temperature during the icing processes for the different measurement series.

temperature is included in this overview, the air temperature in the cold room was not actively recorded during this icing, as the icing time was so long and variable.

The variations in the surface temperature of the aluminum bars during icing are seen in Fig. S3. This Fig. shows that there is a much greater variation in the temperature of the bars subjected to freezing drizzle than the two other icing processes. For Ice 3, the surface temperature was not measured beyond the initial temperature, and there is therefore no record of the temperature surface variation.

Ice 1 has an icing time of 33 minutes, with only 8 minutes and 15 seconds for Ice 2. Comparing these two ice types, it seems that a higher icing time is related to an increase in both the temperature of the surface and the temperature variation. This increase might be a result of more latent heat released during icing for a longer icing time. However, the release of latent heat is dependent on the amount of ice accreted, which might be measured in the mass of ice on the sample.

In Fig. S4, the surface temperature is given as a function of the mass of the ice. From this Fig., it can be seen that the three types of ice has a different ice mass. The smallest mass of ice is found in Ice 1, which also have the largest increase and variation in surface temperature. From the small mass, it would seem that the latent heat released would be smaller than for heavier ice. It therefore seems that the release of latent heat is not the main mechanisms behind the differing surface temperatures of the ice types. The difference will most likely be in the crystallization process itself.

^{a)}Corresponding author. E-mail: zhiliang.zhang@ntnu.no. Telephone: +4773592530 / +4793001979

Type of ice	T_{air} (°C)	Wind speed (m/s)	Number of samples	Test series number
In-cloud icing	-10.1 ± 0.1	15	9	1
In-cloud icing	-9.9 ± 0.1	15	7	2
In-cloud icing	-10.1 ± 0.1	15	9	3
In-cloud icing	-10.2 ± 0.1	15	9	4
In-cloud icing	-10.2 ± 0.1	15	9	5
In-cloud icing	-10.2 ± 0.1	15	8	6
In-cloud icing	-10.3 ± 0.1	15	9	7
Freezing drizzle	-10.0 ± 0.0	0	6	1
Freezing drizzle	-10.0 ± 0.0	0	6	2
Freezing drizzle	-10.0 ± 0.0	0	6	3
Freezing drizzle	-10.0 ± 0.1	0	6	4
Freezing drizzle	-10.0 ± 0.0	0	6	5
Mold ice*	-10	0	4	1
Mold ice*	-10	0	2	2
Mold ice	-10	0	6	3
Mold ice	-10	0	6	4
Mold ice	-10	0	6	5
Mold ice	-10	0	6	6
Mold ice	-10	0	6	7

TABLE S1: Overview of the environmental conditions for the different measurement series. The amount of samples in each measurement series is also included. For measurement series marked with *, the thickness of ice was not measured. Their results are not included in the density calculations.

Type of icing	$T_{surface}$ (°C)	Icing time	Waiting time before testing	Number of samples
In-cloud icing	-9.4 ± 0.2	8min15sec	1h	9
In-cloud icing	-9.3 ± 0.2	8min15sec	1h	7
In-cloud icing	-8.8 ± 0.4	8min15sec	1h	9
In-cloud icing	-9.2 ± 0.2	8min15sec	1h	9
In-cloud icing	-9.3 ± 0.2	8min15sec	1h	9
In-cloud icing	-8.8 ± 0.3	8min15sec	1h	8
In-cloud icing	-8.8 ± 0.4	8min15sec	1h	9
Freezing drizzle	-6.8 ± 1.6	33min	1h	6
Freezing drizzle	-6.8 ± 1.6	33min	1h	6
Freezing drizzle	-6.7 ± 1.5	33min	1h	6
Freezing drizzle	-6.7 ± 1.5	33min	1h	6
Freezing drizzle	-6.9 ± 1.5	33min	1h	6
Mold ice*	-10	2h30min	–	4
Mold ice*	-10	2h15min	–	2
Mold ice	-10	2h	–	6
Mold ice	-10	3h15min	–	6
Mold ice	-10	2h	–	6
Mold ice	4	3h	–	6
Mold ice	4	2h	–	6

TABLE S2: Overview of the icing conditions for the different measurement series, including the amount of samples tested in each series. For measurement series marked with *, the thickness of ice was not measured. Their results are not included in the density calculations.

B. Icing time

The generation of Ice 3 was not standardized at the time of testing, and several different icing times were utilized. In Fig. S5, the icing time is displayed as a function of the ice adhesion strength. The initial temperature of the aluminum bars were either -10° or 4° , and the tests performed with the

higher initial temperature are marked with a frame in Fig. S5. It can be assumed from the lack of order in Fig. S5 that the initial temperature of the aluminum bars does not impact the ice adhesion strength for an icing time of two hours or more, and that there was no relation between the icing time and ice adhesion strength for Ice 3.

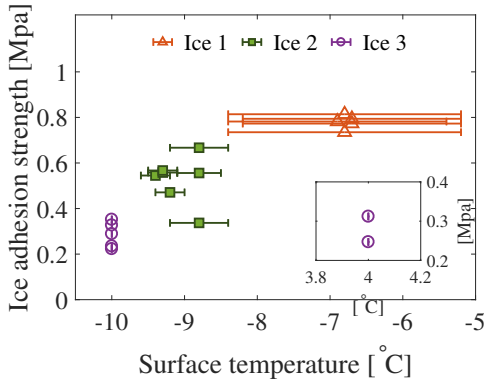


FIG. S3: Ice adhesion strength as function of variations in surface temperature during the icing process for the different measurement series. For the Ice 3, only the initial temperature was measured due to the long icing time. The inset shows Ice 3 with initial temperature 4°C.

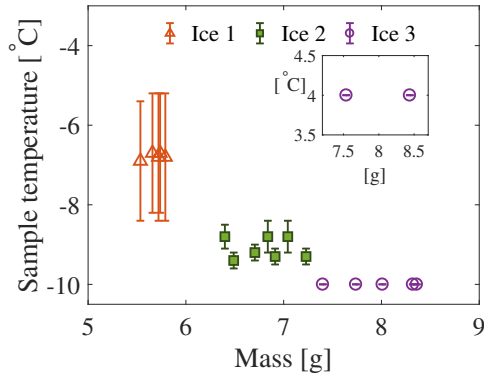


FIG. S4: Variations in surface temperature during the icing process as function of the mass for the different measurement series. For the Ice 3, only the initial temperature was measured due to the long icing time. The inset shows Ice 3 with initial temperature 4°C.

S3. STATISTICS

A. Standard deviation

The standard deviation of the ice adhesion strengths were calculated both for all experiments as seen in Fig. 4, and for each measurement series as given in Fig. S1. Standard deviations are calculated by the formula

$$S = \sqrt{\frac{\sum (x - \bar{x})^2}{(n-1)}}, \quad (\text{S1})$$

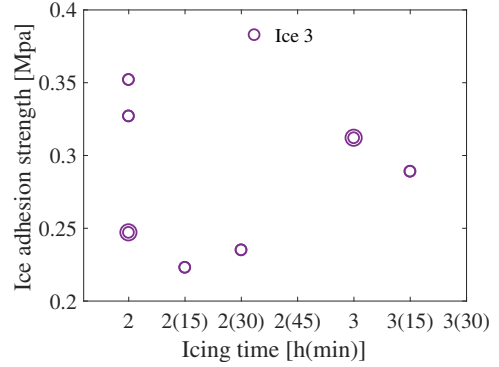


FIG. S5: Ice adhesion strength as function of icing time of Ice 3 for the different measurement series. The series with surface temperature 4°C are marked with an extra circle.

where S is the standard deviation, x is the ice adhesion strength from each test, \bar{x} is the mean ice adhesion strength per measurement series and n is the number of tests per measurement series.

Additionally, when calculating the total standard deviation of the ice adhesion strengths for each ice types, as shown in Fig. S1, the calculation was given by [S1,S2,S3]

$$S_{total}^2 = \frac{\sum_{i=1}^g n_i (s_i^2 + (\bar{x}_i - \bar{x}_{tot})^2)}{\sum_{i=1}^g n_i}, \quad (\text{S2})$$

where S_{total} is the total standard deviation, g is the number of measurement series, n_i is the amount of tests in measurement series i , s_i is the standard deviation of measurement series i , \bar{x}_i is the mean ice adhesion strength of measurement series i and \bar{x}_{total} is the mean ice adhesion strength for all measurement series for that ice type.

B. Probability distribution

In Fig. S6, the probability distribution based on the collected data of the ice adhesion strength for the different ice types is shown. The probability is normalized, and the height of each bar is equal to the probability of selecting an observation within that bin interval [S4].

C. Regression analysis

In total, the regression analysis included 120 measurements of ice adhesion strengths for the three different ice types. For five tests with Ice 3, bulk water ice, the thickness of the ice was not measured before the ice adhesion strength was tested due to experimental issues. These samples do not therefore have a measure of apparent density. The five tests were from two different measurement series, and these measurement series were not included in the regression analysis.

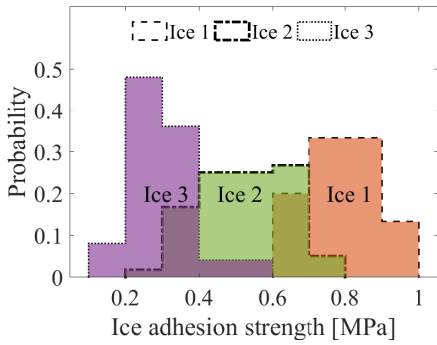


FIG. S6: Probability distribution for ice adhesion strength of the three ice types. The ice types according to Tab. 1 are marked for each section, and the overlap between the ice types are darker than the surrounding sections. The different sections are boarded with differing line styles for easier differentiation in the overlap.

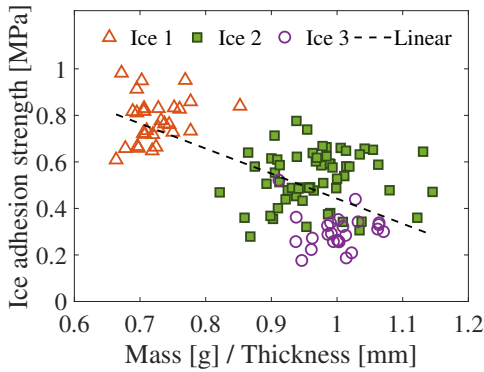


FIG. S7: Ice adhesion strength as a function of mass per ice thickness for all ice types with all measurements included, with a best-fit linear model.

The regression analysis used in this study was performed in Matlab [S4]. A linear model was obtained with the function *fitglm.m*, which created a generalized linear model with the ice adhesion strength as response variable fitted to the apparent density. In Fig. S7 the generalized linear model is shown for all the data points of the ice adhesion strength. In addition, both a quadratic fitting with the function *polyfit.m* and an exponential fitting of the form $a - b \exp(cx)$ with the function *fit.m* were performed for all the data points. The results of these models can be seen in Fig. S8 and Fig. S9.

A measure of the goodness of fit between the ice adhesion strength and the apparent density is found in the goodness-of-fit parameter R^2 from models, as well as in the results R and P from the *corrcoef.m*-function, which was also included [S4].

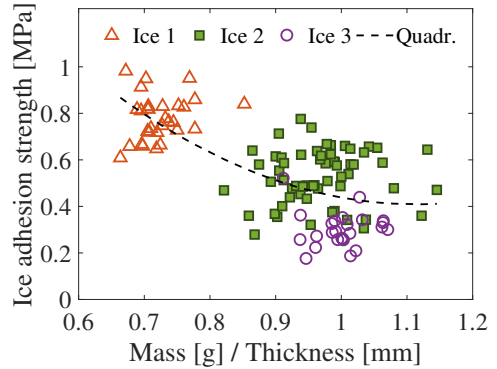


FIG. S8: Ice adhesion strength as a function of mass per ice thickness for all ice types with all measurements included, with a best-fit quadratic model.

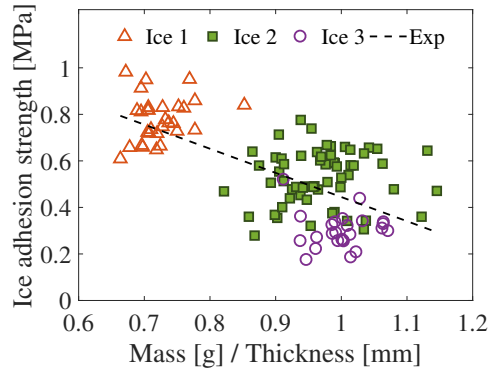


FIG. S9: Ice adhesion strength as a function of mass per ice thickness for all ice types with all measurements included, with a best-fit exponential model.

The results of the goodness-of-fit parameters associated with the regression models are found in Tab. S3, while the correlation in the raw data are found in Tab. S4. The acceptable value of R^2 for the fit of data to a model varies for different applications [S2], but a value between 0.7 and 0.95 is considered "satisfactory to good" [S3]. When R^2 is in this range, the data fits well with the predicted model. When R^2 is above 0.95 it is an indication of over fitting, which decreases the models ability to predict other results [S2].

The P -values are computed from the *corrcoef.m*-function. These P -values are designed for testing the hypothesis that there is no relationship between the observed phenomena [S4]. If P is smaller than the significance level, then the corresponding correlation is considered significant. The default significance level is 0.05, and it can be seen from Tab. S4 that the P -values obtained for the relation between apparent

density and ice adhesion strength are well below this significance level when all experimental observations are included. As expected, the correlation decreases when fewer data points are included. The significant correlation of all experimental observations clearly indicates a relation between the apparent density of the bulk ice and the ice adhesion strength.

S4. PROPOSED MICRO-STRUCTURE

In Fig. S10, the proposed micro-structures of the three types of ice can be seen. These three structures are based on assumptions found in section IV B.

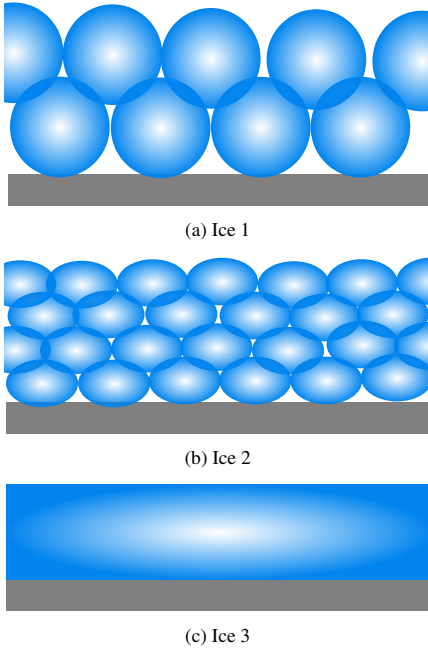


FIG. S10: Sketch of the proposed micro-structure of the three types of ice included in this investigation. The three types of ice are described in Tab. I.

S5. ANALYTICAL MODELS

A. Ice adhesion based on electrostatic interactions

A theoretical model of ice adhesion has been developed based on the electrostatic interaction as the main contribution to the adhesive force [S5]. The model presented is based on water behavior, substrate roughness and ice type [S5]. The ice adheres to the surface as an effect of electrostatic attraction, which is due to the polarization of the water molecules.

The model differentiates between different types of ice by introducing a porosity fraction, given by

$$f_{por} = \rho_{ice} / \rho_{glaze},$$

where $\rho_{glaze} = 917 \text{ kg m}^{-3}$ is the theoretical highest density for ice. For different types of ice with a lower density than the theoretical maximum, the porosity fraction is less than 1. According to the model [S5], the porosity fraction is multiplied with the ice adhesion strength, meaning that a lowering of the density lowers the ice adhesion strength. This trend predicted by the model is not in accordance with our observations, where the ice adhesion strength increased for less dense ice types.

B. Ice adhesion based on the liquid-like layer

The liquid-like layer is a layer of water situated at the surface of ice. The liquid-like layer is well documented as part of regelation phenomena [S6], and is believed to be present at all ice-solid interfaces as well as free ice surfaces. The thickness of the liquid-like layer depends on the icing conditions, more specifically the surface temperature during icing. The liquid-like layer is given by [S7]

$$H = a - b \log_{10}(T_f - T_a), \quad (\text{S3})$$

where $a = 32 \text{ nm}$ and $b = 21 \text{ nm}$ are constants, T_f is the fusion temperature of ice, T_a is the ambient temperature during icing and H is the thickness of the liquid-like layer measured in nm. In this study, the surface temperature of the aluminum is applied instead of the air temperature, as the surface temperature will be determinative for the icing conditions and varies between the different ice types to a greater degree than the air temperature. The thickness of the liquid-like layer increases for higher surface temperatures [S7]. As the surface temperature of the aluminum bars during generation of Ice 1 was higher than the surface temperature of the aluminum bars during generation of Ice 2, the liquid-like layer is assumed to be higher for Ice 1 than for Ice 2.

A model has been developed which bases an analytical approach to ice adhesion on the assumption of a liquid-like layer [S8]. This model is given by

$$\tau_{ice} = \frac{2R_{sm}R_{\alpha}\gamma(\cos\theta_i + \cos\theta_s)}{MVD \cdot U \cdot H \cdot t_n}, \quad (\text{S4})$$

where τ_{ice} is the ice adhesion strength, R_{sm} is the mean spacing of profile irregularities, R_{α} is the average roughness, γ is the surface tension of water, $\cos\theta_i$ is the contact angle between ice crystals and the liquid-like layer, $\cos\theta_s$ is the contact angle between the liquid-like layer and the substrate, MVD is the median volume diameter of incoming droplets, U is the droplet impact velocity, H is the thickness of the liquid-like layer and t_n is the average nucleation time of droplets upon impact with the substrate.

When applying this model to explain the differences of ice adhesion strength seen in this investigation for different types

Type of fit	Data included	Model equation	R^2	Fig.
Linear	All data points	$\tau = -1.0764\rho' + 1.5184$	0.453	S7
Quadratic	All data points	$\tau = 2.2567\rho'^2 - 5.0289\rho' + 3.2107$	-	S8
Exponential	All data points	$\tau = 220.9 - 219.4 \exp(0.005\rho')$	0.453	S9

TABLE S3: Table of obtained model parameters through regression analysis in Matlab for the relation of ice adhesion strength, τ , and apparent density, ρ' .

Data included	R	P
All data points	-0.6733	$2.65 \cdot 10^{-17}$
Mean per measurement series	-0.8478	$1.72 \cdot 10^{-5}$
Mean per ice type	-0.9460	0.210

TABLE S4: Table of obtained correlation coefficients from the correlation analysis of the raw data in Matlab in *corrcoef.m*.

of ice, the only relevant parameters are the parameters connected to the icing as the surface remains constant. It is further assumed that, as the same type of water and the same environmental conditions are applied, the nucleation time t_n remain constant. The only parameters we need to check are therefore the median volume diameter of the incoming droplets MVD the droplet impact velocity U and the thickness of the liquid-like layer. To compare the effect of these two parameters we introduce the constant C given by

$$C = MVD \cdot U \cdot H. \quad (S5)$$

This constant can be calculated for both Ice 1 and Ice 2, and is displayed in Tab. S5. As the generation of Ice 3 does not involve a drop impact, the ice adhesion strength for Ice 3 cannot be modelled by this analytical model. The value of this constant may enable us to approximately compare the ice adhesion strength Ice 1 and Ice 2.

Ice 2 is investigated first. The wind speed is constant, and set to 15 ms^{-1} , giving this value for the droplet impact velocity U_2 . The value of the median droplet volume diameter is $MVD_2 = 27 \mu\text{m}$. From equation (S3), the liquid-like layer is calculated to $H_2 = 11.9 \text{ nm}$. These values gives the constant

$$C_{Ice2} = 4.80 \times 10^{-3} \text{ m}^2 \text{ s}^{-1}. \quad (S6)$$

For the calculation of C for Ice 1, the median droplet volume diameter is $MVD_{Ice1} = 324 \mu\text{m}$. From equation (S3), the liquid-like layer is calculated to $H_2 = 14.5 \text{ nm}$. The droplet impact velocity U_{Ice1} needs to be calculated separately. This calculation is performed by using an equation of motion

$$v_1^2 - v_0^2 = 2a_g s,$$

where v_0 and v_1 are the initial and final velocities respectively, a_g is the acceleration due to gravity, and s is the distance travelled by the droplet. The acceleration is given by gravity, and the distance travelled by the droplet is measured to $s = 1.6 \text{ m}$ with a tape measure. It is assumed zero initial velocity when the droplet is released from the nozzle. The droplet impact

velocity U is given by v_1 , and becomes

$$U_{Ice1} = \sqrt{2a_g s - v_0^2} = 5.60 \text{ ms}^{-1}. \quad (S7)$$

When this value is included in equation (S5), the constant becomes

$$C_{Ice1} = 2.64 \times 10^{-2} \text{ m}^2 \text{ s}^{-1}. \quad (S8)$$

These results show that $C_{Ice1} > C_{Ice2}$.

As can be seen in equation (S4), the constant C of equation (S5) is situated in the denominator of the fraction. This position means that a larger value of C gives a smaller value of the ice adhesion strength τ . According to this analysis, the value of ice adhesion strength for Ice 1 should therefore be lower than the ice adhesion strength for Ice 2. As can be seen from Fig. 3 and S1, the experiments do not agree with this reasoning and gives the opposite result. However, the parameters in equation (S4) which have been assumed constant are possible sources of error.

For Ice 3, the model described by Guerin *et al* [S8] cannot be directly appropriated. The model requires an impact velocity, which is not present in the generation of Ice 3 by use of silicon molds.

The difference in ice types is not included in the analytical model [S8]. If an additional factor of density or porosity was included in the model, the results might be in better agreement with our observations. There are still aspects of the liquid-like layer and its distribution which are unknown, and this uncertainty might also impact the model. In addition, the nucleation time t_n has been assumed constant in the calculation of C , and this constancy is most likely not correct. Furthermore, neither the droplet size nor the effect of air circulation has been included in the model.

C. Ice density models

As different types of ice has different densities, an effort has been made to predict the density of accreted ice under various conditions. One such model [S9] states that the ice density is a function of the droplet size $r_d = \frac{1}{2}MVD$, the impact speed

Ice type	\bar{T}_s [°C]	MVD [μm]	U [ms^{-1}]	H [nm]	C [$\text{m}^2\text{nms}^{-1}$]	ρ_c [gcm^{-3}]	$\bar{\rho}$ [gcm^{-3}]
Ice 1	-6.8	324	5.60	14.5	$2.64 \cdot 10^{-2}$	4.55	0.66
Ice 2	-9.1	27	15	11.9	$4.80 \cdot 10^{-3}$	1.16	0.88
Ice 3	—	—	—	—	—	—	0.94

TABLE S5: Parameters for calculating the model density together with the calculated and approximated actual density of the ice types. \bar{T}_s is the average measured surface temperature for the icing process, MVD is the median volume diameter of incoming water droplets, U is the droplet impact velocity, H is the thickness of the liquid-like layer calculated by equation (S3), $C = U(MVD)H$ is a non-physical constant, ρ_c is the ice density calculated from equation (S9) and $\bar{\rho}$ is an approximation of the density of the ice types, which is the mass of the ice divided by the thickness and the constant surface area $A = 1100\text{mm}^2$.

Category	Description	Density ρ (average) [gcm^{-3}]
Clear ice	Virtually no air entrapped	> 0.86 (0.906)
Transparent ice	Moderate amounts of air entrapped in fairly large bubbles	> 0.86 (0.906)
Milky ice	Considerable amounts of air enclosed as small bubbles	> 0.80 (0.876)
Opaque rime	Dull and white, crumbles rather than cracks	0.40 – 0.90
Kernel rime	Similar in appearance to kernels of corn on a cob	0.33 – 0.61
Feathery rime	More open and fragile than kernel rime	0.08 – 0.40

TABLE S6: Six main classifications of accreted ice, as described by [S9,S10]. The top three ices are in the glaze family, while the bottom three are in the rime family.

and the surface temperature, such that

$$\rho_c = 0.110 \left(-\frac{r_d U}{\bar{T}_s} \right)^{0.76}. \quad (\text{S9})$$

To check whether this model holds for the ice generated in this study, the density of the ice types is approximated by dividing the apparent density on a constant surface area of $A = 1100\text{mm}^2$. These densities are shown in Tab. S5, together with the calculated densities from equation (S9).

As can be seen from Tab. S5, the measured densities $\bar{\rho}$ of the ices are within a reasonable range of the expected densities of ice. In contrast, the densities predicted by equation (S9) are much higher than anticipated, with higher densities than water. However, the model in question was created with respect to cloud droplets [S9], and the values of the impact velocity and droplet radius are higher than the model accounts for.

In Tab. S6, an overview of different ice types is shown [S9,S10]. When compared to the descriptions of the ice types, Ice 1 might be described as kernel rime, Ice 2 might be described as opaque rime and Ice 3 might be described as clear ice. When comparing the measured ice densities $\bar{\rho}$ with the densities in Tab. S6, it is clear that the values are within the predicted range for the three ice types.

A comparison of ice types similar to the one in this investigation, between glaze ice, hard rime and soft rime, have been performed by other authors as well [S11,S12]. Their definitions of the three ice types are similar to those outlined in Tab. S6, and therefore also substantiates the densities and classifications of the three ice types in the present study. However, in this previous comparison [S11], glaze ice is described as highly adhesive while rime ice is described as less adhesive. These descriptions are not consistent with the findings of this

investigation, and indicates that more research is needed.

It is worth noting that the densities reported in Tab. S6 was calculated by dividing the mass by the measured volume of the accreted ice [S9], which is the same method used in this study. The slightly elevated densities might be a result of the assumed constant surface area of icing.

Neither of the models for predicting ice adhesion strength have been in accordance with the observations in this study. Different classifications of ice types and their densities are more in accordance with the ices generated here, but the prediction by models is still not correct. It may therefore be concluded that new models should be based on more than one type of ice to be fully predictive.

REFERENCES

- [S1] S. Løset, K. N. Shkhinek, O. T. Gudmestad, and K. V. Høyland, *Actions from Ice on Arctic Offshore and Coastal Structures: Student's Book for Institutes of Higher Education*. St. Petersburg: "LAN", 2006.
- [S2] R. E. Walpole, R. H. Myers, S. L. Myers, and K. Ye, *Probability and Statistics for Engineers and Scientists*. Unites States of America: Pearson Education, Inc., 2012.
- [S3] M. Sarstedt, C. M. Ringle, D. Smith, R. Reams, and J. F. j. Hair, "Partial least squares structural equation modeling (pls-sem): A useful tool for family business researchers," *Journal of Family Business Strategy*, vol. 5, no. 1, pp. 105–115, 2014.
- [S4] MATLAB, *version R2017a*. Natick, Massachusetts: The MathWorks Inc., 2017.

[S5] G. Fortin and J. Perron, "Ice adhesion models to predict shear stress at shedding," *Journal of Adhesion Science and Technology*, vol. 26, no. 4-5, pp. 523-553, 2012.

[S6] V. F. Petrenko and R. W. Whitworth, *Physics of ice*. Great Britain: Oxford University Press, 2006.

[S7] A. Döppenschmidt and H.-J. Butt, "Measuring the thickness of the liquid-like layer on ice surfaces with atomic force microscopy," *Langmuir*, vol. 16, no. 16, pp. 6709-6714, 2000.

[S8] F. Guerin, C. Laforte, M.-I. Farinas, and J. Perron, "Analytical model based on experimental data of centrifuge ice adhesion tests with different

substrates," *Cold Regions Science and Technology*, vol. 121, pp. 93-99, 2016.

[S9] W. C. Macklin, "The density and structure of ice formed by accretion," *Quarterly Journal of the Royal Meteorological Society*, vol. 88, no. 375, pp. 30-50, 1962.

[S10] V. Clark, "Icing nomenclature," report, Harvard-Mt. Washington Icing Research Report 1946-1947, U.S. Air Material Command, Tech. Rapt. 5676, 1948.

[S11] G. S. H. Lock, *The Growth and Decay of Ice*. *Studies in Polar Research*, Great Britain: Cambridge University Press, 1990.

[S12] D. Kuroiwa, "Icing and snow accretion on electric wires," report, *Cold Region Research and Engineering Lab Hanover NH*, 1965.

Appendix B

Paper 2

The Need for Standards in Ice Adhesion Research: A
Critical Review

Rønneberg, Sigrid, Jianying He, and Zhiliang Zhang. 2019. Journal
of Adhesion Science and Technology: 1-29.

This paper is not included due to copyright
available at <https://doi.org/10.1080/01694243.2019.1679523>

Appendix C




Paper 3

Interlaboratory study of ice adhesion using different techniques

Rønneberg, Sigrid, Yizhi Zhuo, Caroline Laforte, Jianying He, and Zhiliang Zhang. 2019. *Coatings*, 9: 678.

Article

Interlaboratory Study of Ice Adhesion Using Different Techniques

Sigrid Rønneberg ¹, Yizhi Zhuo ¹, Caroline Laforte ², Jianying He ¹ and Zhiliang Zhang ^{1,*}

¹ Department of Structural Engineering, Norwegian University for Science and Technology (NTNU), NO-7491 Trondheim, Norway; sigrid.ronneberg@ntnu.no (S.R.); yizhi.zhuo@ntnu.no (Y.Z.); jianying.he@ntnu.no (J.H.)

² Anti-Icing Materials International Laboratory (AMIL), Université du Québec à Chicoutimi, 555 Blvd. de l'Université, Chicoutimi, QC G7H 2B1, Canada; Caroline_Laforte@uqac.ca

* Correspondence: zhiliang.zhang@ntnu.no; Tel.: +47-73592530 & +47-93001979

Received: 13 September 2019; Accepted: 16 October 2019; Published: 18 October 2019



Abstract: Low ice adhesion surfaces are a promising anti-icing strategy. However, reported ice adhesion strengths cannot be directly compared between research groups. This study compares results obtained from testing the ice adhesion strength on two types of surfaces at two different laboratories, testing two different types of ice with different ice adhesion test methods at temperatures of -10 and -18 °C. One laboratory used the centrifuge adhesion test and tested precipitation ice and bulk water ice, while the other laboratory used a vertical shear test and tested only bulk water ice. The surfaces tested were bare aluminum and a commercial icephobic coating, with all samples prepared in the same manner. The results showed comparability in the general trends, surprisingly, with the greatest differences for bare aluminum surfaces at -10 °C. For bulk water ice, the vertical shear test resulted in systematically higher ice adhesion strength than the centrifugal adhesion test. The standard deviation depends on the surface type and seems to scale with the absolute value of the ice adhesion strength. The experiments capture the overall trends in which the ice adhesion strength surprisingly decreases from -10 to -18 °C for aluminum and is almost independent of temperature for a commercial icephobic coating. In addition, the study captures similar trends in the effect of ice type on ice adhesion strength as previously reported and substantiates that ice formation is a key parameter for ice adhesion mechanisms. Repeatability should be considered a key parameter in determining the ideal ice adhesion test method.

Keywords: ice adhesion; interlaboratory; ice removal; ice type; anti-icing; icephobic

1. Introduction

Anti-icing surfaces, or icephobic surfaces, are a promising technique for passive ice removal and may help mitigate and avoid dangerous situations and unwanted icing in our daily life [1–4]. The most promising strategy for anti-icing surfaces is low ice adhesion surfaces, where the ice automatically detaches from the surface by its own weight or natural forces [5–7]. However, although the amount of research on low ice adhesion surfaces has steadily increased over the past few years [8] and record low ice adhesion strengths of below 1 kPa have been reported [9–11], each research group develops its own custom-built set-up for measuring ice adhesion strength [9,12–15]. As a result, reported ice adhesion strength measurements cannot be directly compared [7,8,16,17].

In this experimental study, the research groups at the Anti-icing International Materials Laboratory (AMIL) at the University of Québec in Chicoutimi and the Nanomechanical Lab at the Norwegian University of Science and Technology (NTNU) collaborated to compare obtained ice adhesion strength measurements from two commonly available surfaces. Both have custom-built laboratory facilities able

to measure internally comparable ice adhesion strength in controlled environments. The ice adhesion strength was measured with a centrifuge adhesion test (CAT) at AMIL, and with a vertical shear test (VST) at NTNU. The centrifuge test is one of the most repeatable ice adhesion tests, although it cannot produce stress–strain curves [8,17,18]. For larger facilities, the CAT is a common way to measure ice adhesion strength, often for impact ice types produced with a freezing drizzle or in-flight icing simulation [19–31]. The VST is very common due to its simple and economical set-up and performance, although the location of the force probe impacts the ice adhesion strength greatly [32], and the stress distribution may not be completely uniform [8,17,18]. The VST is commonly in use by several research groups [7,11,32–39], and has been suggested as a standard for ice adhesion measurement utilizing only commercially available instruments [14].

When comparing reported ice adhesion strengths, it is also necessary to include the type of ice tested. Measured ice adhesion strength is highly dependent on the ice tested [40], and it is essential to test ice adhesion strength with a realistic ice type for low ice adhesion surfaces with a specific application in mind. In this study, both ice from freezing precipitation and ice from bulk water samples were tested (see Figure 1). These ice types are analogous to those presented elsewhere [40], and while precipitation ice (PI) is a form of ice from impacting freezing supercooled droplets (Figure 1a), bulk water ice (BWI) is a static, non-impact type of ice (Figure 1b,c). BWI is the most common ice for testing of ice adhesion strength [5,9,10,12,33,34,41–50], although PI has also been studied [19,24,51,52]. For most practical applications, PI is more realistic than BWI [8,17].

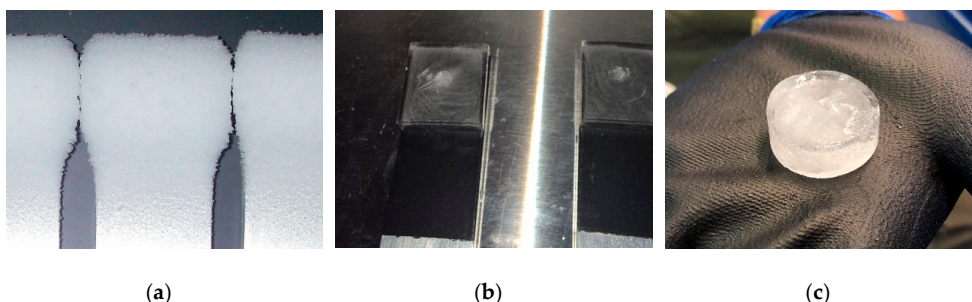


Figure 1. Pictures of the ice types tested in the study. (a) Illustration of precipitation ice (PI) created at the Anti-icing International Materials Laboratory (AMIL) ($T_{air} = -18\text{ }^{\circ}\text{C}$); (b) illustration of bulk water ice (BWI) created at AMIL ($T_{air} = -18\text{ }^{\circ}\text{C}$); (c) illustration of bulk water ice created at the Nanomechanical Lab at the Norwegian University of Science and Technology (NTNU) ($T_{air} = -18\text{ }^{\circ}\text{C}$).

The comparison of ice adhesion strength measured at the AMIL and NTNU for the two types of ice showed that all results are comparable within the general trends between the NTNU and AMIL, with the greatest differences for bare aluminum surfaces at $-10\text{ }^{\circ}\text{C}$. However, there are considerable differences between different laboratories. The study provides further evidence that ice formation is a key parameter in predicting the ice adhesion on different surfaces.

2. Materials and Methods

The ice adhesion strength of two surfaces were tested by both the AMIL and NTNU in their respective facilities. The surfaces tested were bare aluminum 6061-T6, and aluminum covered with EC-3100, a two component, water-based, icephobic, non-stick coating from Ecological Coating, LLC (New York, NY, USA) [53]. The testing of this icephobic coating has been reported previously [52,54]. The bare aluminum samples were polished with Walter BLENDEX Drum fine 0724 M4 (Windsor, CT, USA). To ensure similar surfaces, all the tested surfaces were prepared at AMIL facilities and transported to NTNU for testing. Each surface was tested only once to discount the durability aspect of the surfaces. All ice was generated with demineralized water of resistivity $18\text{ M}\Omega\text{ cm}$. Both

temperatures of $-10\text{ }^{\circ}\text{C}$ and $-18\text{ }^{\circ}\text{C}$ were tested with six different samples from each configuration to generate average ice adhesion strength. Full experimental protocol is available as part of the Supplementary Materials.

2.1. AMIL Facility

The samples tested at AMIL were in the form of bars fit to the CAT apparatus, with the iced area on one side and a counterweight on the other. The bars had a length of 340 mm and thickness of 6.3 mm, with icing occurring over an area of about 1100 mm^2 . This area was measured more precisely after the ice adhesion test in order to have the exact ice-surface detached surfaces.

PI was created through a freezing drizzle in a cold room of constant temperature and a relative humidity of $80\% \pm 2\%$. Six samples were iced simultaneously, with water of a median volume drop diameter (MVD) of $324\text{ }\mu\text{m}$ and an initial temperature of $4\text{ }^{\circ}\text{C}$ at the exit of the sprayer nozzle. The surfaces had initial temperatures of the testing temperature, meaning either $-10\text{ }^{\circ}\text{C}$ or $-18\text{ }^{\circ}\text{C}$. As the water hit the sample surface, it supercooled and froze on contact. Water impact speed is due to gravity as the water droplets fall from the nozzle; it is estimated to about 5 ms^{-1} . The samples were iced for 33 min and kept in a cold room for 1 h between icing and the ice adhesion test to allow the ice to thermally stabilize.

BWI was created in the same cold room by freezing water in silicon molds from MoldMax30 by Smooth-On (Macungie, PA, USA) [55]. The silicon molds had the same dimensions as the area iced during the freezing drizzle to generate ice samples as similar as possible to the PI. The molds were filled full of water, with the samples placed on top of the molds in contact with the water for freezing to occur. The surfaces and water were at room temperature at the start of the icing. Freezing time was 3 h, after which the molds were removed. The ice adhesion test was conducted after 15 min, in which the samples were weighed and measured.

The ice adhesion strength was measured with the CAT apparatus developed at AMIL [52] (see Figure 2). The CAT apparatus consists of a centrifuge, a placed sample beam, a counterweight to stabilize the bar with the ice sample, and a cover. The apparatus was placed within a cold room, ensuring in situ measurements of the ice adhesion strength for PI and BWI. The balanced and iced sample bars were spun in the centrifuge at an accelerating speed of 300 rpms^{-1} until the ice was detached by the centrifugal force. Piezoelectric cells situated around the cover instantly detected the detachment of the ice, giving a detachment angular velocity. The ice adhesion strength was calculated as the centrifugal shear stress at the position of the center of mass of the ice sample at detachment divided by the ice-solid contact area [52].

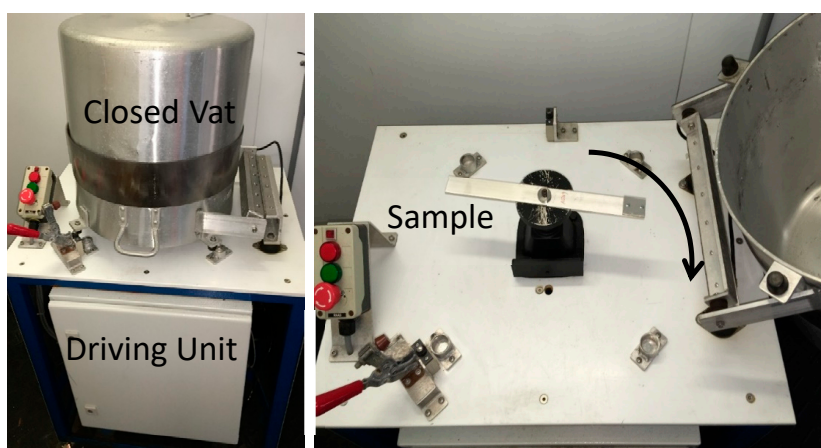


Figure 2. AMIL centrifuge adhesion test (CAT) apparatus.

2.2. NTNU Facility

The surfaces tested at NTNU were approximately square surfaces with a width of 7.3 cm, height of 7.2 cm, and thickness of 25 mm. The ice sample was frozen in the middle of the surface for testing. Both water and surfaces were initially at room temperature for the testing at NTNU.

The ice tested at NTNU was BWI. For the temperature of $-18\text{ }^{\circ}\text{C}$, the ice samples were frozen in a freezer, while for the temperature of $-10\text{ }^{\circ}\text{C}$, the ice was frozen in a cold room situated at a slight distance from the ice adhesion test. For both temperatures, the ice was frozen *ex situ*, and required transportation through room temperature to the testing rig where the samples were again placed in the original temperature for ice adhesion tests. For $-18\text{ }^{\circ}\text{C}$, the transport time was about one min and 30 s, while for $-10\text{ }^{\circ}\text{C}$, the transport time was about three min. To account for the transport from the cold room, the samples were transported in a box made of expanded polystyrene with freezer elements. Both the box and freezer elements were placed in the cold room for thermal equilibration before and after the transportation. After the transportation, the ice samples were placed in the ice adhesion test chamber for 15 min before testing to achieve thermal stability.

The BWI samples were frozen on the tested surfaces in a polypropylene centrifuge tube mold with a wall thickness of 1 mm and inner diameter of 27.5 mm. Silicone grease [56] was used to fasten the tube mold to the tested surface to avoid leakage during water insertion. Then, 5 mL of deionized water was inserted into the mold with a syringe to avoid air at the ice-solid interface, and pressure from a 200 g metal cylinder was placed on top of the tube to avoid water leakage during freezing. The water was frozen for 3 h before it was moved to the testing apparatus.

The ice adhesion test was performed with a VST and a custom-built set-up as modeled from other facilities [14] (see Figure 3). The detachment force was measured with an Instron machine (model 5944, Norwood, MA, USA) with load cell capacity of 2 kN (2530 Series static load cells), equipped with a home-built cooling system and chamber. The force probe fixed to the load cell was 5 mm in diameter and imposed an increasing force on the tube-encased ice samples with an impact velocity of 0.01 mms^{-1} . The placement of the probe was at the same point on the sample each test, situated 3 mm away from the tested surface during loading. The loading curve was recorded, and the peak value of the shear force was divided by the contact area to obtain the ice adhesion strength. As the probe distance is small and the measured ice adhesion strength is above 10 kPa for all tests, gravity can be discarded as negligible [8].

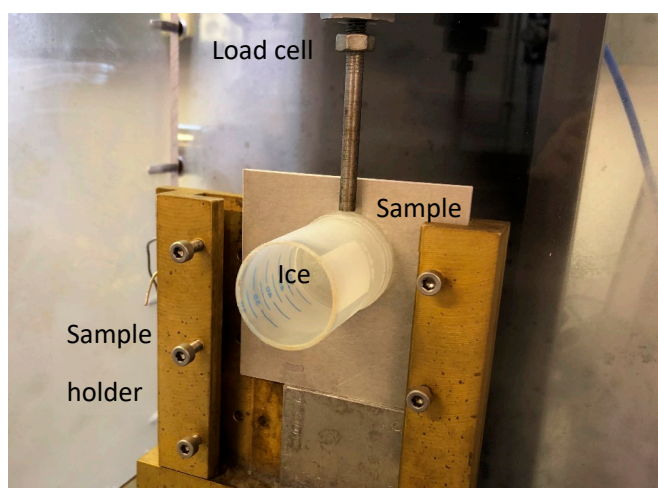


Figure 3. Vertical shear test (VST) as utilized at NTNU to measure ice adhesion strength.

3. Results

The measured ice adhesion strengths are shown in Figure 4. It can be seen that all results are comparable to a degree, with the greatest differences for bare aluminum surfaces at $-10\text{ }^{\circ}\text{C}$. Table 1 presents an overview of all the ice adhesion strengths obtained from both laboratories. To obtain an average value, six different samples were tested at AMIL, except for BWI on bare aluminum at $-10\text{ }^{\circ}\text{C}$ where only four samples could be tested. At NTNU, averages were created from five samples. All the data are given in the supplementary materials.

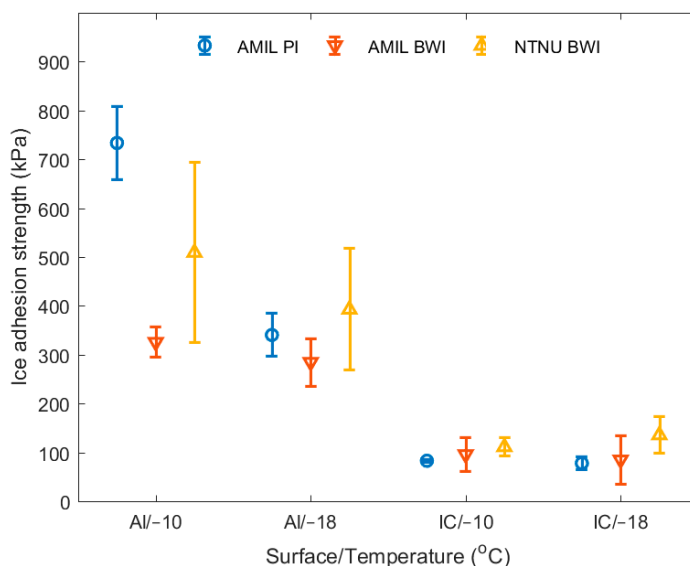


Figure 4. Measured ice adhesion strengths. Aluminum surfaces are denoted as Al, while the surfaces with icephobic coating are denoted as IC. All three ice types created are shown for each surface-temperature combination. Data displayed in Table 1.

Table 1. Overview of mean values and standard deviations of ice adhesion strength. Data illustrated in Figure 4, with all data available in the supplementary information.

Surface/Temperature	Ice Adhesion Strength (kPa \pm SD (%))		
	AMIL PI	AMIL BWI	NTNU BWI
Aluminum/ $-10\text{ }^{\circ}\text{C}$	734 \pm 75 (10%)	326 \pm 30 (9%)	509 \pm 185 (36%)
Aluminum/ $-18\text{ }^{\circ}\text{C}$	340 \pm 44 (13%)	285 \pm 49 (17%)	393 \pm 124 (32%)
Coating/ $-10\text{ }^{\circ}\text{C}$	83 \pm 3 (4%)	96 \pm 34 (35%)	111 \pm 19 (17%)
Coating/ $-18\text{ }^{\circ}\text{C}$	78 \pm 14 (18%)	85 \pm 49 (58%)	135 \pm 38 (28%)

From Figure 4, it can be seen that for BWI, the NTNU VST method systematically yields higher ice adhesion strength than the AMIL CAT method for both aluminum surfaces and the icephobic coating. However, the standard deviation depends on the surface type. For bare aluminum, the deviation for VST is higher than CAT, while for the icephobic coating, the opposite trend is observed.

The original measurements for the ice adhesion tests are displayed in Figure 5 for the CAT and Figure 6 for the VST. For CAT at AMIL, the original measurements consisted of rounds per minute (RPM) vs. time, including the constantly increasing RPM in the centrifuge combined with the piezoelectric signal indicating the RPM at ice detachment. For VST at NTNU, the original measurements were of force per time.

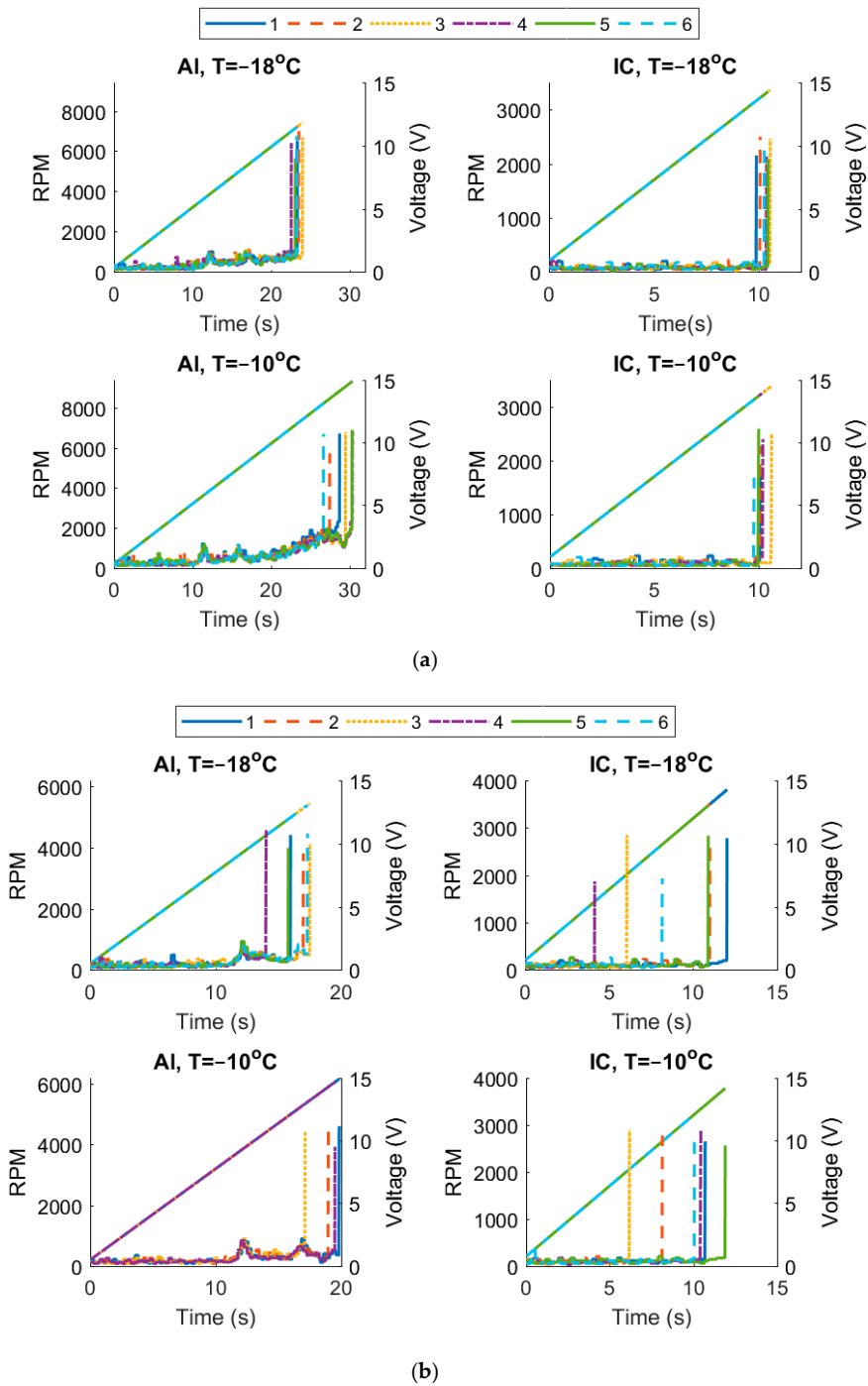


Figure 5. Rounds per minute (RPM)-time curves for CAT measured at AMIL for both ice types. The left axis denotes the RPM, which increases with constant acceleration, and the right axis displays the voltage measured by the piezoelectric cells. The end RPM was utilized to calculate the ice adhesion strength as described elsewhere [52], and can be deduced by the placement of the piezoelectric signal for each sample. All six samples for each surface and temperature are indicated, for (a) PI and (b) BWI.

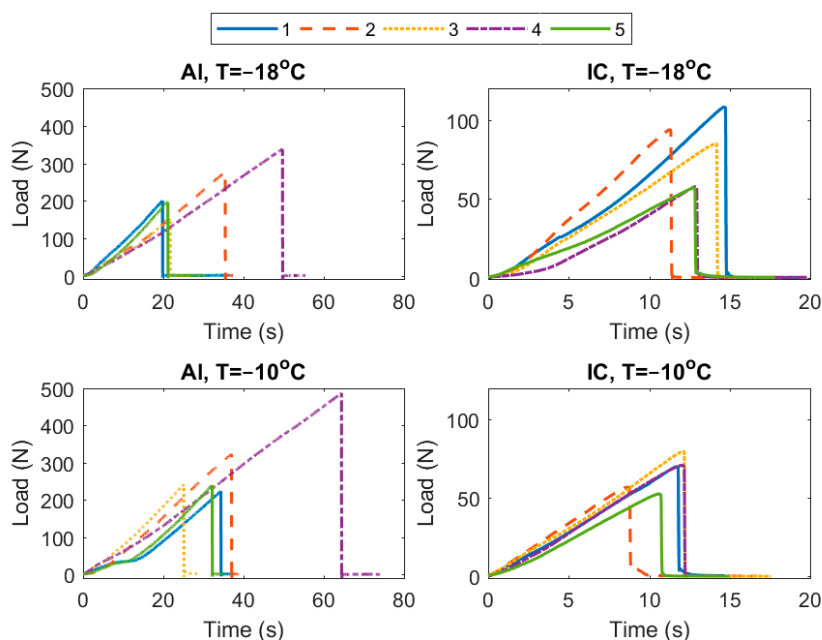


Figure 6. Force–time curves for VST ice adhesion measurements performed at NTNU. The maximum force was divided by the contact area of the ice sample to calculate the ice adhesion strength. All five samples for each surface and temperature are indicated.

4. Discussion

When comparing the two surface types for all ice types, all tests showed larger error bars for aluminum than for the icephobic coating. This high standard deviation is in accordance with other studies of ice adhesion strength and may be an inherent property of the ice removal mechanisms [8,56]. The ice adhesion strengths for the icephobic coating from both laboratories are close to each other, but show larger variations for BWI up to 58%, compared to only 18% for PI.

The fluctuating standard deviations can be partially explained by the original measurements in Figures 5 and 6. In Table 1, the instances with a standard deviation above 30% are bare aluminum surfaces tested at NTNU and the icephobic coating with bulk water ice at AMIL. For all these instances, it can be seen in the original measurements that there are significant outliers. In other words, some samples for these cases display significantly changing behavior concerning ice adhesion strength, which greatly impacts the mean value and standard deviation. The standard deviation for the icephobic coating is generally lower than for bare aluminum, because there are fewer outliers in these measurements, with the exception of bulk water ice on icephobic coating tested at AMIL in Figure 5b. The standard deviations should be investigated further by expanding on this interlaboratory study with more samples and more tests, in addition to including more laboratory facilities.

The most commonly utilized configuration when testing ice adhesion strength is a shear test analogous to VST with bulk water ice at $-10\text{ }^{\circ}\text{C}$ [8]. As seen in Figure 6, this configuration includes a high standard deviation for bare aluminum and is where the greatest difference between the two laboratories and ice types are found. However, when the outlier from NTNU is removed, the mean ice adhesion strength becomes 441 MPa, with a standard deviation of 17%. These values are much closer to what would be expected based on the rest of the tests and configurations. However, a goal of this interlaboratory study was to perform the tests in the default manner of the two laboratories. Although the outlier for bare aluminum at $-10\text{ }^{\circ}\text{C}$ at NTNU displayed partly cohesive failure, as seen when comparing Figures S10 and S12 in the supplementary materials, the failure was not clearly cohesive

and as such would not have been excluded from the study. If it is assumed that the tendency for outliers is possible for all ice adhesion tests, it might indicate why the standard deviation is generally high for ice adhesion measurements for all test methods.

The effect of decreasing temperature varied for the tested surfaces. At AMIL, there was a marked decrease of ice adhesion strength for PI on bare aluminum, and a lesser decrease for the icephobic coating as well. This decrease is due to the increased occurrence of cohesive failures. Between -10 and -18 °C, there is a transition from adhesive failures to more cohesive failures for aluminum and PI, as shown previously [24]. The same transition can be seen for the icephobic coating (see supplementary materials). At NTNU on the other hand, there was only one occurrence of partial cohesive failure for bare aluminum surfaces, which occurred at -10 °C when using the VST. These observations indicate that the transition to cohesive failures and the occurrence and impact of non-adhesive failures depends on the ice adhesion test method and ice type. Furthermore, the occurrence of cohesive failure displays no relation to the standard deviations in Table 1 and outliers in Figures 5 and 6. For the BWI on the icephobic coating tested at NTNU, there is a slight increase of ice adhesion strength with temperature. The varying effect of temperature on the ice adhesion strength for the different configurations substantiate the difficulty in predicting the dependence of ice adhesion strength on temperature, as reported previously [17].

In general terms, this study shows that there are large differences between different laboratories, and that the differences do not seem to be systematic. It seems that for higher ice adhesion strengths, the difference between different ice adhesion tests and ice types increases. It follows that more tests with a larger range of ice adhesion values are needed to explore this relation more fully.

As two different ice types were tested at AMIL, a similar trend from Rønneberg et al. [40] can be seen in that BWI has a lower ice adhesion strength than PI for bare aluminum. However, for the icephobic coating, the ice adhesion strength for both ice types is very similar. As a result, it may be that the difference in ice adhesion strength between different types of ice depends on whether the tested surface is defined as a low adhesion surface.

When comparing the results from AMIL and NTNU, some general comments about different ice adhesion measurement set-ups can be made. At low ice adhesion, the two test methods gave similar results, while the VST seemed to give larger deviations than the CAT methodology. However, the VST was easier to implement, and had a slightly lower standard deviation for low ice adhesion surfaces with BWI. An alternative might be the lap shear test, as studied recently [57], although no comparison can be made between this new test method and the ones presented in this study. As the outliers that differed in ice adhesion strength from their peers greatly impacted the standard deviation for the ice adhesion strength tests, repeatability should be a key factor in determining the ideal ice adhesion test.

Lastly, some additional sources of error present in the experiments reported here must be mentioned. For the tests performed at NTNU, the ice adhesion tests were performed *ex situ* and the ice samples and tested surfaces were moved between the freezer to the testing apparatus. Especially the tests performed at -10 °C were subject to a long transport between two different laboratories, and to account for this thermal variation, a polystyrene container was used. The effect of this container compared to the shorter transport at room temperature for the tests performed at -18 °C cannot be determined exactly. However, despite the transport which was assumed detrimental for ice adhesion, the NTNU VST method yielded higher ice adhesion for both coatings, compared to AMIL results where the experiments were performed *in situ*. This observation may indicate that the transportation did not significantly affect the ice adhesion.

The ice sample size differed between AMIL and NTNU, with an iced area of about 1100 mm² at AMIL and only 594 mm² at NTNU. While at AMIL, the ice samples covered the entire tested surface as seen in Figure 1a,b; at NTNU the ice sample was situated at a part of the tested surface only, as seen in Figure 3. The fact that the ice sample at NTNU was smaller compared to the surface structure, especially for aluminum, may be a factor in the much higher standard deviation seen for the aluminum samples from NTNU than the icephobic coating.

5. Conclusions

In this study, the ice adhesion strength of two different surfaces were tested at two laboratories with different ice adhesion test methods and two types of accreted ice. Despite the differences between the laboratories, the experiments capture the overall trends in which the ice adhesion strength surprisingly decreased from $-10\text{ }^{\circ}\text{C}$ to $-18\text{ }^{\circ}\text{C}$ for bare aluminum and was almost independent of temperature for a commercial icephobic coating. For BWI, the NTNU VST method systematically yielded higher ice adhesion strength than the AMIL CAT method. The standard deviations were approximately constant when testing PI at AMIL and seem to scale with the absolute value of ice adhesion at NTNU. The VST had higher deviations than CAT methodology for high ice adhesion values but were more similar when testing low ice adhesion surfaces. For configurations with standard deviation above 30%, the ice adhesion tests showed more significant outliers that differed from the other tests for that configuration than those with a smaller standard deviation.

The experiments in this study were performed with a focus on keeping the conditions similar, both within each lab and between AMIL and NTNU. However, the results still show significant differences and variations for all configurations. As a result, more data from several more laboratory facilities are needed, as well as more tests within each laboratory facility. Furthermore, the study provides further evidence that the ice formation is a key parameter in predicting the ice adhesion on different surfaces, as well as for the investigation of the mechanism of the ice detachment from different surfaces and the occurrence of cohesive failures during ice adhesion testing. To determine the ideal ice adhesion strength test, repeatability is a key factor to minimize the number of experimental outliers which greatly impact the standard deviation.

Supplementary Materials: The following are available online at <http://www.mdpi.com/2079-6412/9/10/678/s1>: Table S1: Experimental protocol, Table S2: All experimental results, Figure S1: Formation BWI at AMIL, Figure S2 and S3: Formation BWI at NTNU, Figure S4 and S5: Typical adhesive failure at AMIL, Figure S6–S9: Typical cohesive failure at AMIL, Figure S10 and S11: Typical adhesive failure at NTNU, Figure S12: Cohesive failure at NTNU, Figure S13: Adhesion reduction factor (ARF).

Author Contributions: All authors contributed in conceptualization, methodology and writing—review and editing; investigation S.R., Y.Z., and C.L.; visualization, formal analysis, and writing—original draft, S.R.; supervision and project administration, C.L., J.H., and Z.Z.; funding acquisition, J.H. and Z.Z.

Funding: The authors gratefully acknowledge the financial support from the Norwegian Research Council FRINATEK project Towards Design of Super-Low Ice Adhesion Surfaces (SLICE, 250990) and from the PETROMAKS2 project Durable Arctic Icephobic Materials (AIM, 255507).

Conflicts of Interest: The authors declare no conflicts of interest.

Nomenclature

AMIL	Anti-icing Materials International Laboratory
ARF	Adhesion reduction factor
BWI	Bulk water ice
CAT	Centrifuge adhesion test
F	Centrifugal force
IC	Icephobic coating
MVD	Median volume drop diameter
NTNU	Norwegian University of Science and Technology
PI	Precipitation ice
RPM	Rounds per minute
VST	Vertical shear test

References

1. Brassard, J.; Laforte, C.; Guerin, F.; Blackburn, C. Icephobicity: Definition and Measurement Regarding Atmospheric Icing. In *Advances in Polymer Science*; Springer: Berlin/Heidelberg, Germany, 2017. [CrossRef]

2. Lv, J.; Song, Y.; Jiang, L.; Wang, J. Bio-inspired strategies for anti-icing. *ACS Nano* **2014**, *8*, 3152–3169. [[CrossRef](#)] [[PubMed](#)]
3. Kreder, M.J.; Alvarenga, J.; Kim, P.; Aizenberg, J. Design of anti-icing surfaces: Smooth, textured or slippery? *Nat. Rev. Mater.* **2016**, *1*, 15003. [[CrossRef](#)]
4. Makkonen, L. Ice Adhesion—Theory, Measurements and Countermeasures. *J. Adhes. Sci. Technol.* **2012**, *26*, 413–445. [[CrossRef](#)]
5. Chen, J.; Liu, J.; He, M.; Li, K.; Cui, D.; Zhang, Q.; Zeng, X.; Zhang, Y.; Wang, J.; Song, Y. Superhydrophobic surfaces cannot reduce ice adhesion. *Appl. Phys. Lett.* **2012**, *101*. [[CrossRef](#)]
6. Varanasi, K.K.; Deng, T.; Smith, J.D.; Hsu, M.; Bhate, N. Frost formation and ice adhesion on superhydrophobic surfaces. *Appl. Phys. Lett.* **2010**, *97*, 234102–234103. [[CrossRef](#)]
7. Wang, F.; Ding, W.; He, J.; Zhang, Z. Phase transition enabled durable anti-icing surfaces and its DIY design. *Chem. Eng. J.* **2019**, *360*, 243–249. [[CrossRef](#)]
8. Rønneberg, S.; He, J.; Zhang, Z. The Need for Standards in Ice Adhesion Research: A Critical Review. *J. Adhes. Sci. Technol.* **2019**. [[CrossRef](#)]
9. Irajizad, P.; Al-Bayati, A.; Eslami, B.; Shafquat, T.; Nazari, M.; Jafari, P.; Kashyap, V.; Masoudi, A.; Araya, D.; Ghasemi, H. Stress-Localized Durable Icephobic Surfaces. *Mater. Horiz.* **2019**, *6*, 758–766. [[CrossRef](#)]
10. Golovin, K.; Dhyani, A.; Thouless, M.D.; Tuteja, A. Low-interfacial toughness materials for effective large-scale deicing. *Science* **2019**, *364*, 371. [[CrossRef](#)]
11. He, Z.; Zhuo, Y.; He, J.; Zhang, Z. Design and Preparation of Sandwich-Like Polydimethylsiloxane (PDMS) Sponges with Super-Low Ice Adhesion. *Soft Matter* **2018**, *14*, 4846–4851. [[CrossRef](#)]
12. Meuler, A.J.; Smith, J.D.; Varanasi, K.K.; Mabry, J.M.; McKinley, G.H.; Cohen, R.E. Relationships between Water Wettability and Ice Adhesion. *ACS Appl. Mater. Interfaces* **2010**, *2*, 3100–3110. [[CrossRef](#)] [[PubMed](#)]
13. Schulz, M.; Sinapius, M. *Evaluation of Different Ice Adhesion Tests for Mechanical Deicing Systems*; SAE International: Warrendale, PA, USA, 2015.
14. Wang, C.; Zhang, W.; Siva, A.; Tiew, D.; Wynne, K.J. Laboratory test for ice adhesion strength using commercial instrumentation. *Langmuir* **2014**, *30*, 540–547. [[CrossRef](#)] [[PubMed](#)]
15. Sojoudi, H.; Wang, M.; Boscher, N.D.; McKinley, G.H.; Gleason, K.K. Durable and scalable icephobic surfaces: Similarities and distinctions from superhydrophobic surfaces. *Soft Matter* **2016**, *12*, 1938–1963. [[CrossRef](#)]
16. Rønneberg, S.; He, J.; Zhang, Z. Standardizing the testing of low ice adhesion surfaces. In Proceedings of the International Workshops on Atmospheric Icing of Structures (IWAIS) 2019, Reykjavik, Iceland, 23–28 June 2019.
17. Work, A.; Lian, Y. A critical review of the measurement of ice adhesion to solid substrates. *Prog. Aerosp. Sci.* **2018**, *98*, 1–26. [[CrossRef](#)]
18. Kasaai, M.R.; Farzaneh, M. A critical review of evaluation methods of ice adhesion. In Proceedings of the 23rd International Conference on Offshore Mechanics and Arctic Engineering, Vancouver, BC, Canada, 20–25 June 2004; Volume 3, pp. 919–926.
19. Dotan, A.; Dodiuk, H.; Laforte, C.; Kenig, S. The Relationship between Water Wetting and Ice Adhesion. *J. Adhes. Sci. Technol.* **2009**, *23*, 1907–1915. [[CrossRef](#)]
20. Kulinich, S.A.; Farhadi, S.; Nose, K.; Du, X.W. Superhydrophobic Surfaces: Are They Really Ice-Repellent? *Langmuir* **2011**, *27*, 25–29. [[CrossRef](#)] [[PubMed](#)]
21. Kulinich, S.A.; Farzaneh, M. Ice adhesion on super-hydrophobic surfaces. *Appl. Surf. Sci.* **2009**, *255*, 8153–8157. [[CrossRef](#)]
22. Kulinich, S.A.; Farzaneh, M. How wetting hysteresis influences ice adhesion strength on superhydrophobic surfaces. *Langmuir* **2009**, *25*, 8854–8856. [[CrossRef](#)]
23. Kulinich, S.A.; Farzaneh, M. On ice-releasing properties of rough hydrophobic coatings. *Cold Reg. Sci. Technol.* **2011**, *65*, 60–64. [[CrossRef](#)]
24. Guerin, F.; Laforte, C.; Farinas, M.-I.; Perron, J. Analytical model based on experimental data of centrifuge ice adhesion tests with different substrates. *Cold Reg. Sci. Technol.* **2016**, *121*, 93–99. [[CrossRef](#)]
25. Douglas, R.G.; Palacios, J.; Schneeberger, G. Design, Fabrication, Calibration, and Testing of a Centrifugal Ice Adhesion Test Rig with Strain Rate Control Capability. In Proceedings of the 2018 Atmospheric and Space Environments Conference, Atlanta, GA, USA, 25–29 June 2018.
26. Janjua, Z.A. The influence of freezing and ambient temperature on the adhesion strength of ice. *Cold Reg. Sci. Technol.* **2017**, *140*, 14–19. [[CrossRef](#)]

27. Janjua, Z.A.; Turnbull, B.; Choy, K.-L.; Pandis, C.; Liu, J.; Hou, X.; Choi, K.-S. Performance and durability tests of smart icephobic coatings to reduce ice adhesion. *Appl. Surf. Sci.* **2017**, *407*, 555–564. [[CrossRef](#)]
28. Menini, R.; Farzaneh, M. Elaboration of Al₂O₃/PTFE icephobic coatings for protecting aluminum surfaces. *Surf. Coat. Technol.* **2009**, *203*, 1941–1946. [[CrossRef](#)]
29. Niemelä-Anttonen, H.; Koivuluoto, H.; Tuominen, M.; Teisala, H.; Juuti, P.; Haapanen, J.; Harra, J.; Stenroos, C.; Lahti, J.; Kuusipalo, J.; et al. Icephobicity of Slippery Liquid Infused Porous Surfaces under Multiple Freeze–Thaw and Ice Accretion–Detachment Cycles. *Adv. Mater. Interfaces* **2018**, *5*, 1800828. [[CrossRef](#)]
30. Koivuluoto, H.; Stenroos, C.; Ruohomaa, R.; Bolelli, G.; Lusvarghi, L.; Vuoristo, P. Research on icing behavior and ice adhesion testing of icephobic surfaces. In Proceedings of the International Workshop on Atmospheric Icing of Structures (IWAIS) 2015, Uppsala, Sweden, 28 June–3 July 2015.
31. Niemelä-Anttonen, H.; Kiilakoski, J.; Vuoristo, P.; Koivuluoto, H. Icephobic Performance of Different Surface Designs and Materials. In Proceedings of the International Workshop on Atmospheric Icing of Structures (IWAIS) 2019, Reykjavik, Iceland, 23–28 June 2019.
32. Wang, C.; Fuller, T.; Zhang, W.; Wynne, K.J. Thickness Dependence of Ice Removal Stress for a Polydimethylsiloxane Nanocomposite: Sylgard 184. *Langmuir* **2014**, *30*, 12819–12826. [[CrossRef](#)]
33. He, Z.; Vågenes, E.T.; Delabahan, C.; He, J.; Zhang, Z. Room Temperature Characteristics of Polymer-Based Low Ice Adhesion Surfaces. *Sci. Rep.* **2017**, *7*, 42181. [[CrossRef](#)]
34. He, Z.; Xiao, S.; Gao, H.; He, J.; Zhang, Z. Multiscale Crack Initiators Promoted Super-Low Ice Adhesion Surfaces. *Soft Matter* **2017**, *13*, 6562–6568. [[CrossRef](#)]
35. He, Z.; Zhuo, Y.; Wang, F.; He, J.; Zhang, Z. Understanding the role of hollow sub-surface structures in reducing ice adhesion strength. *Soft Matter* **2019**, *15*, 2905–2910. [[CrossRef](#)]
36. Zhuo, Y.; Håkonsen, V.; He, Z.; Xiao, S.; He, J.; Zhang, Z. Enhancing the Mechanical Durability of Icephobic Surfaces by Introducing Autonomous Self-Healing Function. *ACS Appl. Mater. Interfaces* **2018**, *10*, 11972–11978. [[CrossRef](#)]
37. Zhuo, Y.; Wang, F.; Xiao, S.; He, J.; Zhang, Z. One-Step Fabrication of Bioinspired Lubricant-Regenerable Icephobic Slippery Liquid-Infused Porous Surfaces. *ACS Omega* **2018**, *3*, 10139–10144. [[CrossRef](#)]
38. Wang, F.; Xiao, S.; Zhuo, Y.; Ding, W.; He, J.; Zhang, Z. Liquid layer generator for excellent icephobicity at extremely low temperature. *Mater. Horiz.* **2019**. [[CrossRef](#)]
39. Wang, Y.; Yao, X.; Chen, J.; He, Z.; Liu, J.; Li, Q.; Wang, J.; Jiang, L. Organogel as durable anti-icing coatings. *Sci. China Mater.* **2015**, *58*, 559–565. [[CrossRef](#)]
40. Ronneberg, S.; Laforte, C.; Volat, C.; He, J.; Zhang, Z. The effect of ice type on ice adhesion. *AIP Adv.* **2019**, *9*, 055304. [[CrossRef](#)]
41. Matsumoto, K.; Tsubaki, D.; Sekine, K.; Kubota, H.; Minamiya, K.; Yamanaka, S. Influences of number of hydroxyl groups and cooling solid surface temperature on ice adhesion force. *Int. J. Refrig.* **2017**, *75*, 322–330. [[CrossRef](#)]
42. Beemer, D.L.; Wang, W.; Kota, A.K. Durable gels with ultra-low adhesion to ice. *J. Mater. Chem. A* **2016**, *4*, 18253–18258. [[CrossRef](#)]
43. Golovin, K.; Kobaku, S.P.R.; Lee, D.H.; DiLoreto, E.T.; Mabry, J.M.; Tuteja, A. Designing durable icephobic surfaces. *Sci. Adv.* **2016**, *2*. [[CrossRef](#)] [[PubMed](#)]
44. Golovin, K.; Tuteja, A. A predictive framework for the design and fabrication of icephobic polymers. *Sci. Adv.* **2017**, *3*, e1701617. [[CrossRef](#)]
45. Hejazi, V.; Sobolev, K.; Nosonovsky, M. From superhydrophobicity to icephobicity: Forces and interaction analysis. *Sci. Rep.* **2013**, *3*. [[CrossRef](#)]
46. Dou, R.; Chen, J.; Zhang, Y.; Wang, X.; Cui, D.; Song, Y.; Jiang, L.; Wang, J. Anti-icing Coating with an Aqueous Lubricating Layer. *ACS Appl. Mater. Interfaces* **2014**, *6*, 6998–7003. [[CrossRef](#)]
47. Sarkar, D.K.; Farzaneh, M. Superhydrophobic Coatings with Reduced Ice Adhesion. *J. Adhes. Sci. Technol.* **2009**, *23*, 1215–1237. [[CrossRef](#)]
48. Upadhyay, V.; Galhenage, T.; Battocchi, D.; Webster, D. Amphiphilic icephobic coatings. *Prog. Org. Coat.* **2017**, *112*, 191–199. [[CrossRef](#)]
49. Mitridis, E.; Schutzius, T.M.; Sicher, A.; Hail, C.U.; Eghlidi, H.; Poulidakos, D. Metasurfaces Leveraging Solar Energy for Icephobicity. *ACS Nano* **2018**, *12*, 7009–7017. [[CrossRef](#)] [[PubMed](#)]

50. Pan, S.; Guo, R.; Björnalm, M.; Richardson, J.J.; Li, L.; Peng, C.; Bertleff-Zieschang, N.; Xu, W.; Jiang, J.; Caruso, F. Coatings super-repellent to ultralow surface tension liquids. *Nat. Mater.* **2018**, *17*, 1040–1047. [[CrossRef](#)] [[PubMed](#)]
51. Laforte, C.; Beisswenger, A. Icephobic Material Centrifuge Adhesion Test. In Proceedings of the 11th International Workshop on Atmospheric Icing on Structures (IWAIS), Montréal, QC, Canada, 16 June 2005; pp. 1–5.
52. Laforte, C.; Blackburn, C.; Perron, J.; Aubert, R. Icephobic Coating Evaluation for Aerospace Application. In Proceedings of the 55th AIAA/ASME/ASCE/AHS/ASC Structures, Structural Dynamics, and Materials Conference, National Harbor, MD, USA, 13–17 January 2014. [[CrossRef](#)]
53. Ecological Coatings. Icephobic Coatings Anti-Ice. Available online: <http://www.ecologicalcoatings.com/icephobic.html> (accessed on 1 October 2019).
54. Susoff, M.; Siegmann, K.; Pfaffenroth, C.; Hirayama, M. Evaluation of icephobic coatings—Screening of different coatings and influence of roughness. *Appl. Surf. Sci.* **2013**, *282*, 870–879. [[CrossRef](#)]
55. Mold Max TM Series Tin Cure Silicone Mold Rubber. Available online: <https://www.smooth-on.com/product-line/mold-max/> (accessed on 8 July 2019).
56. Dow Corning High-Vacuum Silicone Grease. Available online: <https://www.sigmaaldrich.com/catalog/product/aldrich/z273554> (accessed on 22 July 2019).
57. Work, A.H., Jr.; Gyekenyesi, A.L.; Kreeger, R.E.; Salem, J.A.; Vargas, M.M.; Drabiak, D.R. The Adhesion Strength of Impact Ice Measured Using a Modified Lap Joint Test. In Proceedings of the AIAA Aviation Forum, Atlanta, GA, USA, 25–28 June 2018; p. 23.



© 2019 by the authors. Licensee MDPI, Basel, Switzerland. This article is an open access article distributed under the terms and conditions of the Creative Commons Attribution (CC BY) license (<http://creativecommons.org/licenses/by/4.0/>).

Interlaboratory study of ice adhesion using different techniques

Supplementary materials

Sigrid Rønneberg, Yizhi Zhuo, Caroline Laforte, Jianying He, Zhiliang Zhang

Contents

S1. Experimental protocol.....	1
S2. All experimental results	2
S3. Ice formation.....	3
S4. Typical failure modes	5
S5. Adhesion reduction factor (ARF).....	10
References	10

S1. Experimental protocol

Table S1 Experimental protocol used for the interlaboratory study. See Experimental section for more info on procedures.

Facility	Ice type	Surface #	Temperature	Repetitions	Icing time	Waiting time
AMIL	Precipitation ice	Aluminum	-10	6	33min	1h
AMIL	Precipitation ice	Coating	-10	6	33min	1h
AMIL	Precipitation ice	Aluminum	-18	6	33min	1h
AMIL	Precipitation ice	Coating	-18	6	33min	1h
AMIL	Bulk water ice	Aluminum	-10	6	3h	15min
AMIL	Bulk water ice	Coating	-10	6	3h	15min
AMIL	Bulk water ice	Aluminum	-18	6	3h	15min
AMIL	Bulk water ice	Coating	-18	6	3h	15min
NTNU	Bulk water ice	Aluminum	-10	5	3h	15min
NTNU	Bulk water ice	Coating	-10	5	3h	15min
NTNU	Bulk water ice	Aluminum	-18	5	3h	15min
NTNU	Bulk water ice	Coating	-18	5	3h	15min

Notes

- Temperature relates to both freezing temperature and testing temperature
- Initial temperature of both surfaces and water was room temperature for bulk water ice
- All surfaces were only tested once

S2. All experimental results

Table S2 Experimental results from the ice adhesion tests for all 66 samples.

Surface		Aluminum	Aluminum	Coating	Coating
Temperature		T _{air} = -10°C	T _{air} = -18°C	T _{air} = -10°C	T _{air} = -18°C
AMIL, precipitation ice	1	727	265	81	62
	2	741	320	79	81
	3	782	387	84	90
	4	788	346	85	59
	5	774	344	81	83
	6	589	380	86	90
	Mean	734	340	83	78
	SD	75	44	3	14
		10 %	13 %	4 %	18 %
AMIL, bulk water ice	1	343	269	118	139
	2	346	315	70	119
	3	281	318	39	39
	4	332	193	113	17
	5		294	127	121
	6		318	106	72
	Mean	326	285	96	85
	SD	30	49	34	49
		9 %	17 %	36 %	58 %
NTNU, bulk water ice	1	375	338	118	182
	2	543	467	96	158
	3	405	257	134	143
	4	819	569	119	97
	5	402	332	88	96
	Mean	509	393	111	135
	SD	185	124	19	38
		36 %	32 %	17 %	28 %

S3. Ice formation

The formation of bulk water ice is illustrated in Figures 1, 2 and 3 for AMIL and NTNU, respectively. For the generation of precipitation ice, we refer to other publications [1, 2].



Figure S1 Formation of bulk water ice at AMIL, same procedure for both temperatures.

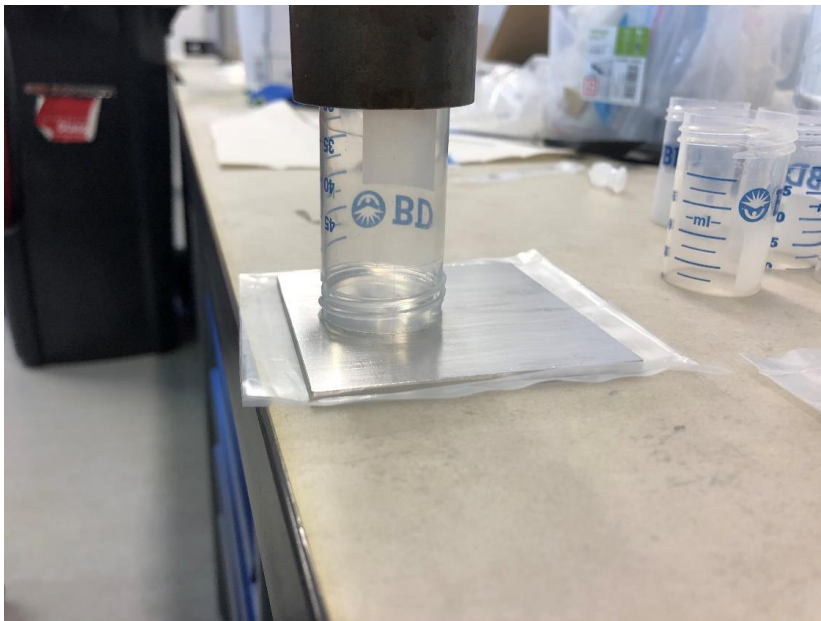


Figure S2 Formation of bulk water ice on aluminum surface at NTNU. For $T_{air} = -18^{\circ}\text{C}$, the water was added in room temperature and moved to the freezer. For -10°C , the water insertion was performed in a cold room, otherwise with the same procedure.

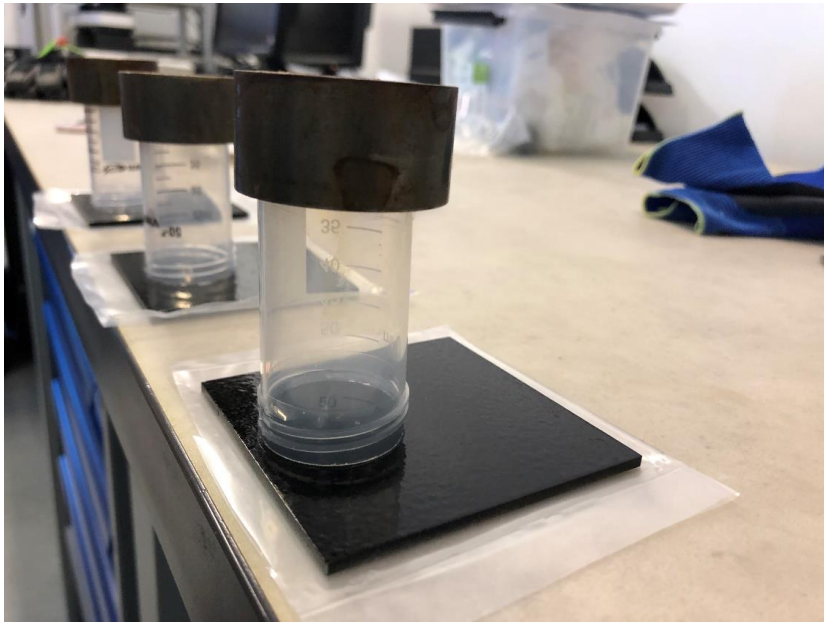


Figure S3 Formation of bulk water ice on icephobic coating at NTNU, similar to Figure 2.

S4. Typical failure modes

Typical failure modes when testing ice adhesion strength can be seen in Figures 4-12. For bulk water ice, the failures were adhesive. For precipitation ice at AMIL, the failures were mostly adhesive at $T_{\text{air}} = -10^{\circ}\text{C}$ and cohesive at $T_{\text{air}} = -18^{\circ}\text{C}$.

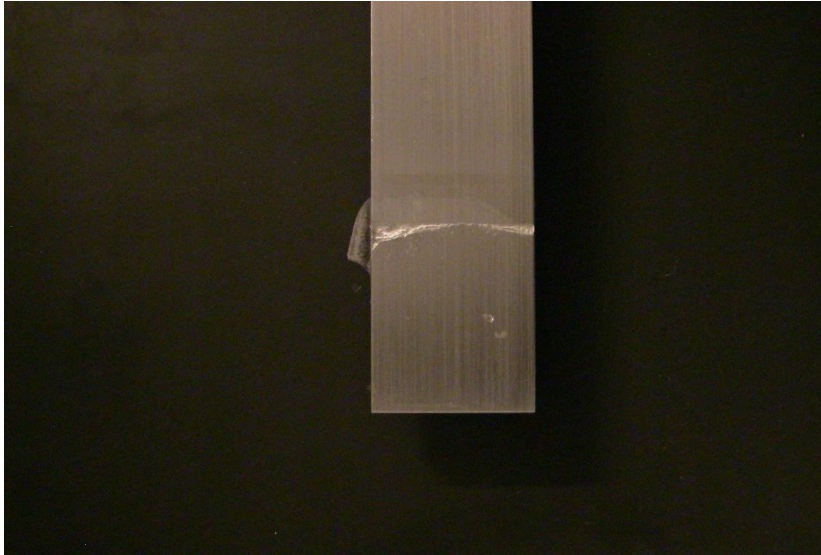


Figure S4 Typical adhesive failure observed at AMIL for bulk water ice at both temperatures, here for aluminum surface.

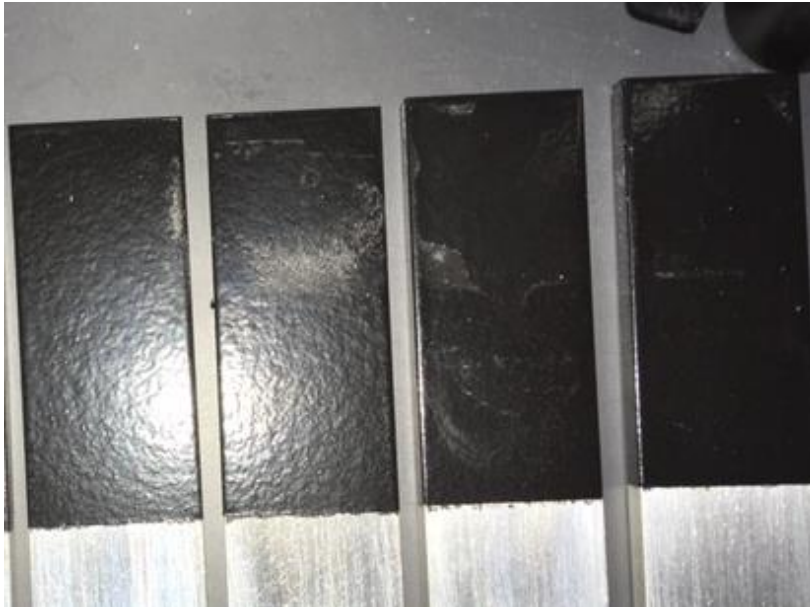


Figure S5 Typical adhesive failure observed at AMIL for bulk water ice at both temperatures, here for the icephobic coating.

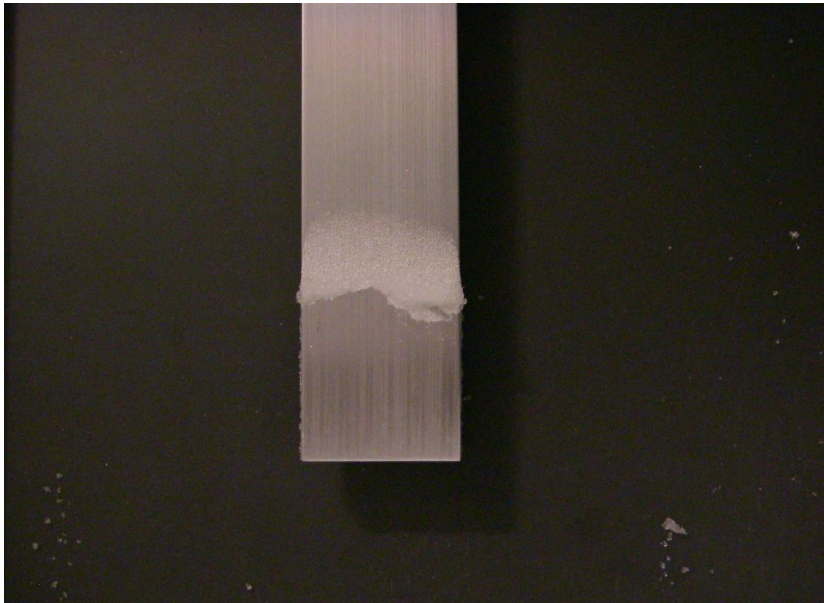


Figure S6 Adhesive failure observed at AMIL for precipitation ice at $T_{air} = -10^{\circ}\text{C}$, here for aluminum surface.

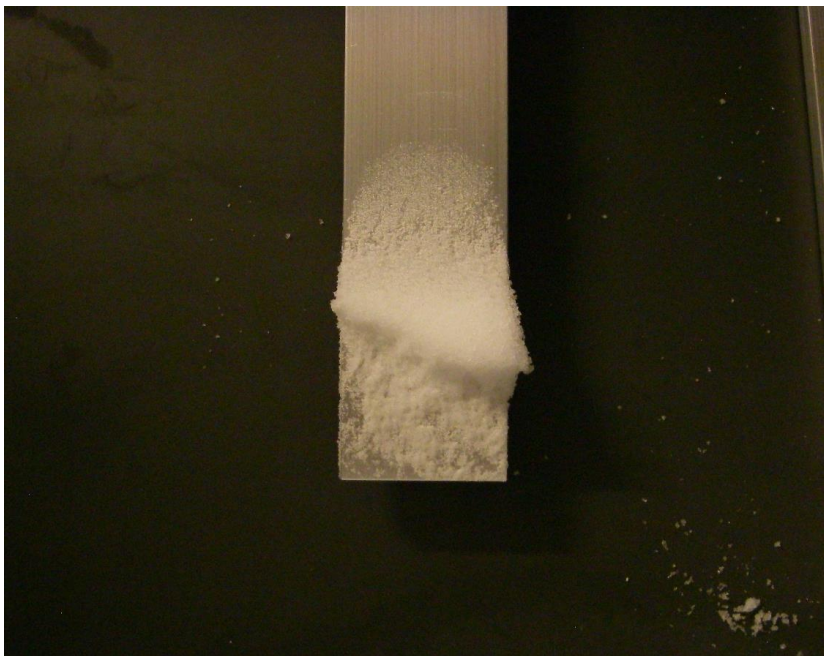


Figure S7 Cohesive failure observed at AMIL for precipitation ice at $T_{air} = -18^{\circ}\text{C}$, here for aluminum surface.

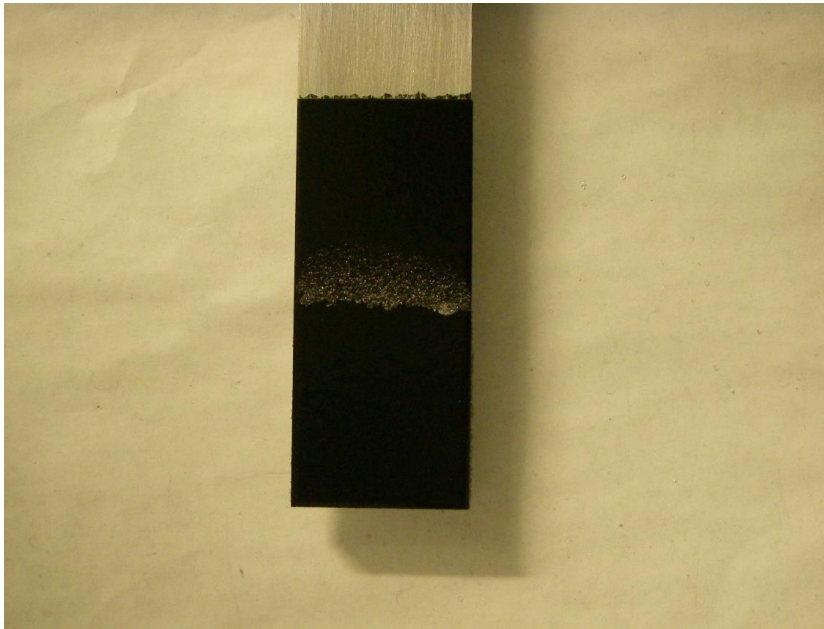


Figure S8 Adhesive failure observed at AMIL for precipitation ice at $T_{air} = -10^{\circ}\text{C}$, here for icephobic coating.

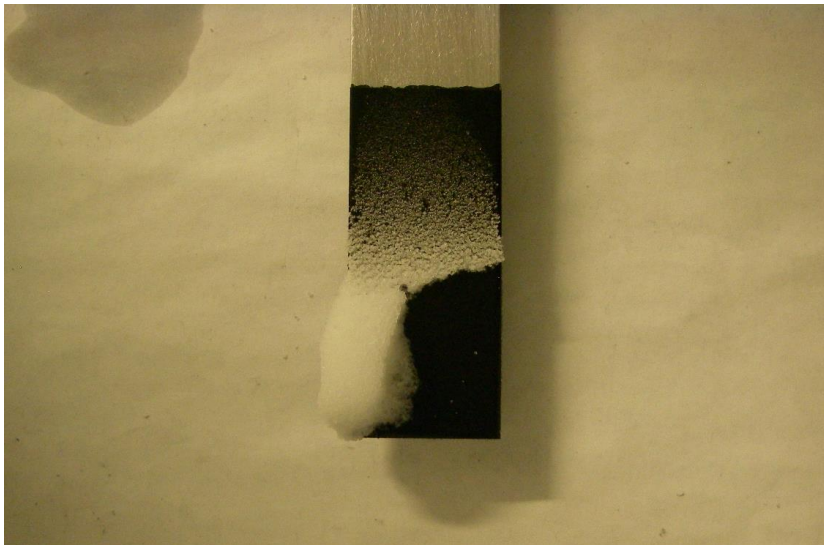


Figure S9 Cohesive failure observed at AMIL for precipitation ice at $T_{air} = -18^{\circ}\text{C}$, here for icephobic coating.

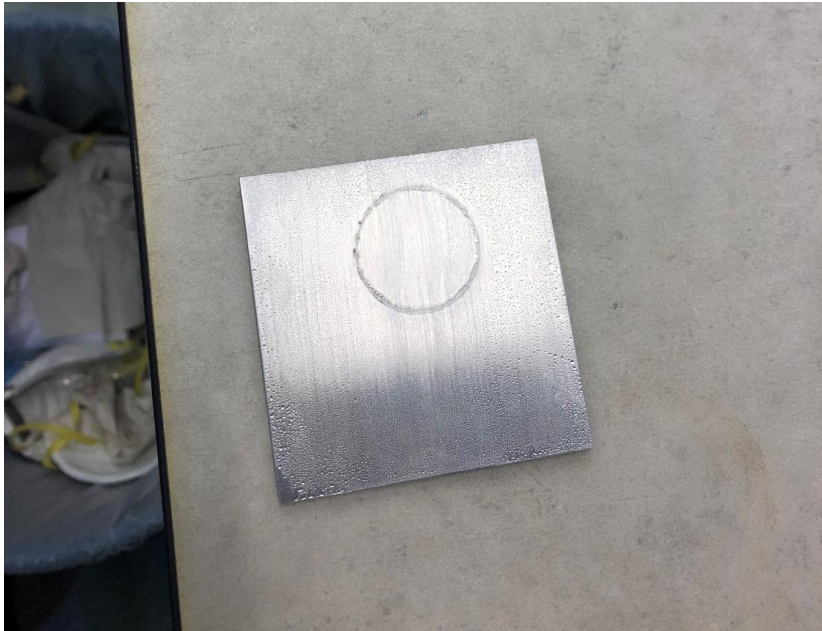


Figure S10 Typical adhesive failure at ice detachment for tests performed at NTNU. Here for aluminum surface tested at $T_{air} = -18^{\circ}\text{C}$.

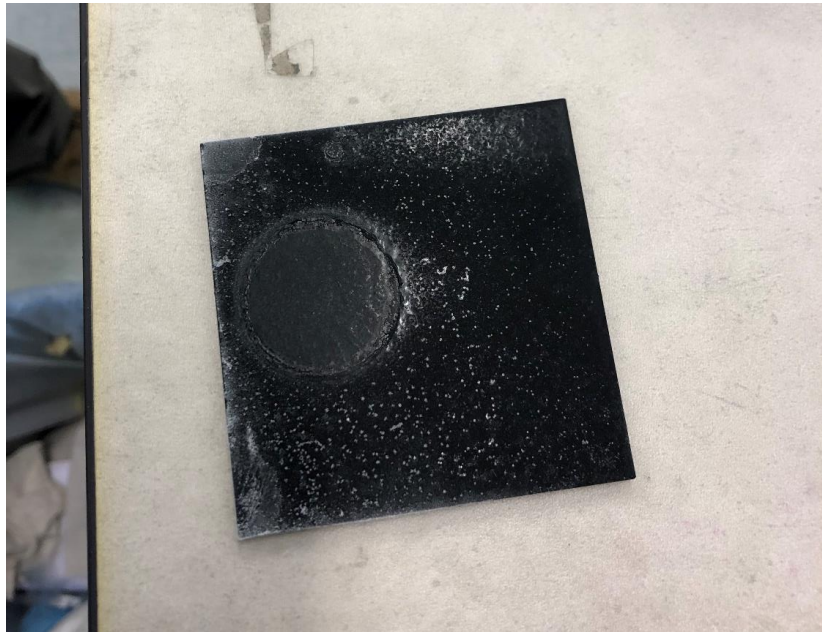


Figure S11 Typical adhesive failure at ice detachment for tests performed at NTNU. Here for icephobic surface tested at $T_{air} = -18^{\circ}\text{C}$.

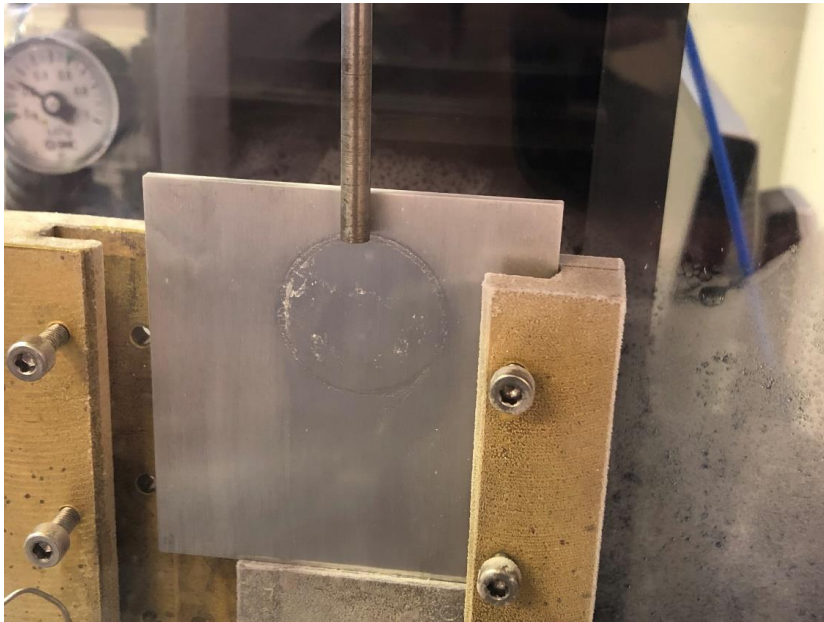


Figure S12 Picture of the only cohesive failure observed for tests at NTNU. This failure occurred for aluminum surface at $T_{air} = -10^{\circ}C$.

S5. Adhesion reduction factor (ARF)

The Adhesion reduction factor (ARF) is defined as the ratio of the ice adhesion strength of a reference material, often aluminum, to the ice adhesion strength of the coating being tested [3]. If the ARF is above 1, the coating has an improved anti-icing behavior. The ARF for the coating tested in this study is shown in Figure 13 for all configurations of ice type and laboratory. The discussion of the ARF is left for a later publication.

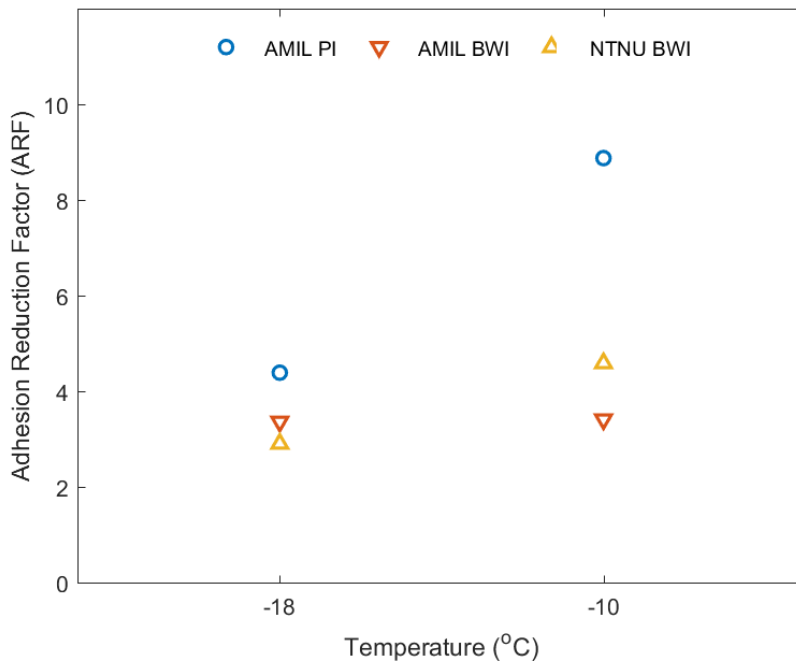


Figure S13 Overview of ARF for the three ice types for both temperatures.

References

1. Laforte, C. and A. Beisswenger. *Icephobic Material Centrifuge Adhesion Test*. in *11th International Workshop on Atmospheric Icing on Structures (IWAIS)*. 2005. Montral, Canada.
2. Guerin, F., et al., *Analytical model based on experimental data of centrifuge ice adhesion tests with different substrates*. *Cold Regions Science and Technology*, 2016. **121**: p. 93-99.
3. Brassard, J., et al., *Icephobicity: Definition and Measurement Regarding Atmospheric Icing*, in *Advances in Polymer Science*. 2017, Springer: Berlin, Heidelberg.

Appendix D

Paper 4

Nanoscale Correlations of Ice Adhesion Strength and Water Contact Angle

Rønneberg, Sigrid, Senbo Xiao, Jianying He, and Zhiliang Zhang. 2020. Submitted.

Nanoscale Correlations of Ice Adhesion Strength and Water Contact Angle

Sigrid Rønneberg¹, Senbo Xiao¹, Jianying He¹, and Zhiliang Zhang^{*1}

¹NTNU Nanomechanical Lab, Department of Structural Engineering, Norwegian University of Science and Technology (NTNU), Richard Birkelandsvei 1A, NO-7491, Trondheim, Norway

Abstract

Surfaces with low ice adhesion represent a promising strategy to achieve passive anti-icing performance. However, as a successful and robust low ice adhesion surface must be tested under realistic conditions at low temperatures and for several types of ice, the initial screening of potential low ice adhesion surfaces requires large resources. A theoretical relation between ice adhesion and water wettability in the form of water contact angle exists, but there is disagreement on whether this relation holds for experiments. In this study, we utilise molecular dynamics simulations to examine the fundamental relations between ice adhesion and water contact angle on an ideal graphene surface. The results show a significant correlation according to the theoretic predictions, indicating that the theoretical relation holds for the ice and water when discarding surface material deformations and other experimental factors. The reproduction of the thermodynamic theory at the nanoscale is important due to the gap between experimental observations and theoretical models. The results in this study represent a step forward towards understanding the fundamental mechanisms of water-solid and ice-solid interactions, and the relationship between them.

1 Introduction

Unwanted icing and ice accretion are potentially hazardous and can impact daily life [1].

Dangerous situations occur for instance within wind energy, aircrafts, power lines, and

*Corresponding author. E-mail: zhiliang.zhang@ntnu.no. Telephone: +4773592530 / +4793001979

industries in Arctic environments [2]. Passive anti-icing surfaces where the accreted ice is automatically removed is a possible solution [3]. There are three main pathways to such passive anti-icing, or icephobic surfaces, namely 1) the removal of water before it is allowed to freeze, 2) the delay of ice nucleation, and 3) the lowering of ice adhesion so that formed ice does not stick to the surface [1, 3–6]. Due to the nature of icing, and that it is impossible to fully avoid icing, the lowering of ice adhesion strength is considered as the most promising strategy for anti-icing surfaces [7–10].

The development of low ice adhesion surfaces has been in focus for several years. The aim for these surfaces are to reach ice adhesion strength below 20 kPa [9, 11], which is considered as the limit to remove accreted ice naturally by wind or gravity due to its own weight. Surfaces with ice adhesion strength below 10 kPa are often denoted as super-low, or ultra-low, ice adhesion surfaces (SLIAS) [6]. In the past years, examples of surfaces reaching below 1 kPa have also been reported [12–14]. However, the field of low ice adhesion materials research has been known to operate by continuum theory or a trial-and-error strategy, where the focus has been on developing new surfaces and coatings without fully understanding the underlying mechanisms [15–17]. One reason for this lack of understanding is the amount of resources required to properly test anti-icing surfaces in realistic conditions. It is important to use realistic ice samples and temperatures to test ice adhesion surfaces for a given application [16]. However, to test surfaces in cold rooms of temperatures below -20°C , or the construction of realistic ice types for surface testing, which may need icing wind tunnels, require both energy and infrastructure. As a result, an ideal solution would be to screen a potential low ice adhesion surface with water at room temperature before testing the ice adhesion strength.

In order to facilitate the screening of potentially low ice adhesion surfaces, the possible relationships between room temperature characteristics related to surface wettability and ice adhesion strength of a given surface has been investigated [18]. Several studies showed a correlation between water contact angle and ice adhesion, both for the static contact angle [7, 8, 19, 20] and for the receding contact angle [20–26], while other studies discard such correlations [18, 27–30]. In short, the experimental results differ greatly, and there is little agreement on whether there exist experimental correlations between the ice adhesion

and wettability of a surface.

In this study, the correlation between water contact angle and ice adhesion is investigated by utilising atomistic modelling and molecular dynamics simulations. By simulating the atomistic behaviour of water molecules on an ideal surface, it is possible to investigate the underlying physical mechanisms of water-solid and ice-solid interactions. By addressing the thermodynamic models governing water behaviour, which are not reproduced clearly through experiments, the hypothesis of this study is that the simulations will show a trend between the experimental results and the predictions made by pure theoretical relations. Surprisingly, the results show a behaviour very close to the theoretical model. This study thus indicates that the difference from the theoretical predictions stems from experimental factors, and not the inherent behaviour of the water or ice. The reproduction of the theoretic relation between wettability and ice adhesion at the nanoscale is important as it helps to bridge the understanding between experimental observations and theoretical models. Other measured of wettability should be similarly investigated to fully examine simulation results compared with the experimental studies on low ice adhesion surfaces. The application of atomistic simulations to investigate the underlying characteristics of materials provide new insights to the fundamental mechanisms of ice adhesion strength and ice detachment, extending the experimental limits of resolution.

2 Theoretical aspects

The contact angle is the most common measure of the wettability of a surface. The contact angle is defined as the experimentally observed angle of a liquid droplet, as seen in Figure 1. The general definition applies to all equilibrium and non-equilibrium situations [31]. In this study, the ideal contact angle is studied. The ideal contact angle is the contact angle on an ideal surface, which is a smooth surface that is rigid and chemically homogeneous, and does not chemically bond with the liquid [31]. Such a surface is typically not experimentally viable, due to the difficulties associated with preparing and maintaining an ideal surface. In experimental studies, the most common measured contact angle is the apparent contact angle [31], although so-called static and dynamic contact angles are often discussed as well.

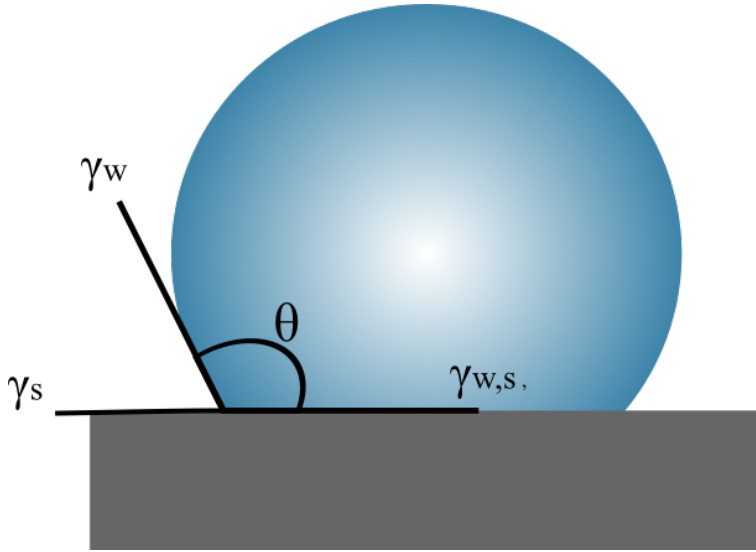


Figure 1: Illustration of the most general water contact angle θ . The surface energies γ correspond to the parameters of Young's equation in equation (1), where $\gamma_{w,s}$, γ_s and γ_w refer to the specific energies of the solid/water, solid/vapour and water/vapour interfaces, respectively.

The most widely referred contact angle is the Young contact angle, which is calculated from Young's equation [32], as stated in equation (1), for ideal solid surfaces [28]. Young contact angle is a thermodynamic property of a three-phase system, which corresponds to the lowest energy state for the system [31]. For other types of surfaces, other definitions of equilibrium contact angles have been proposed. The Wenzel equation describes contact angle of a droplet on a surface with a given roughness [33], the Cassie equation [34] describes the contact angle of a droplet on a heterogeneous solid surface, and the Cassie-Baxter equation [35] describes the contact angle of a droplet on a textured surface with trapped air underneath the droplet [28].

The theoretical relation between the water contact angle θ and ice adhesion is based purely on thermodynamic relations. These relations are described by Makkonen [36], and briefly reiterated here. We consider a drop of water (w) on a solid (s) with an interface (w,s) and the corresponding surface energies γ and droplet contact angle θ . The situation is schematically illustrated in Figure 1. We assume the Young contact angle, described by the equation

$$\gamma_{w,s} + \gamma_w \cos \theta = \gamma_s, \quad (1)$$

where the subscripts w denotes water and s denotes surface, respectively. It is further

assumed that the water droplet freezes to ice on the surface. The work that is required to remove the ice is defined as the thermodynamic work of adhesion, W_a [36]. This work of adhesion is defined as

$$W_a = \gamma_s + \gamma_i - \gamma_{i,s}, \quad (2)$$

where subscript i denotes ice, and represents the work required to break the bond between the ice and the surface and form two new surfaces. Combining equations (1) and (2) shows that

$$W_a = \gamma_i + \gamma_w \cos \theta + (\gamma_{w,s} - \gamma_{i,s}).$$

When considering the commonly accepted assumption that the surface energies of water and ice are similar [37], and thus also the interfacial energies are similar [36], equation (2) can be reduced to

$$W_a \approx \gamma_w(1 + \cos \theta). \quad (3)$$

The ice adhesion strength τ is commonly defined as the maximum force required to detach the ice from the surface divided by the contact area of the ice solid surface, given by

$$\tau = \frac{F_{max}}{A}. \quad (4)$$

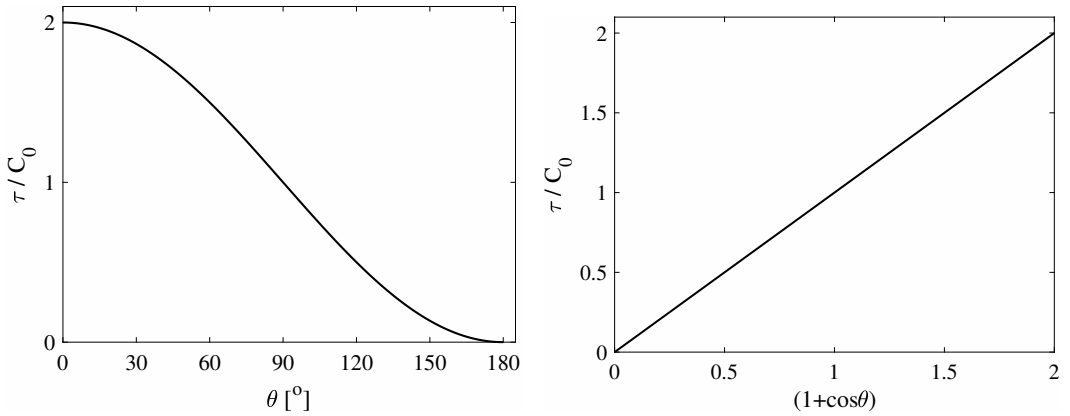
The ice adhesion strength is thus a measure of pressure, and when considering that the work of adhesion is a measure of energy, it can be assumed in general that the relation between the ice adhesion strength and the work of adhesion is given by

$$W_a = \tau A \delta, \quad (5)$$

where A is the surface area of the ice and δ is a characteristic measure of the removal distance between the ice and surface. Combining equations (3) and (5) thus gives

$$\tau \approx \frac{\gamma_w}{A \delta} (1 + \cos \theta).$$

Both the surface area of the ice A , the distance δ , and the water surface tension γ_w are constants, and can be combined to a general constant C_0 and neglected when the general



(a) Normalised ice adhesion strength as function of the contact angle θ .

(b) Normalised ice adhesion strength as function of the cosine of the contact angle $(1 + \cos \theta)$.

Figure 2: Two forms of the general relation between ice adhesion strength τ and water contact angle θ on a generic surface with properties C_0 . The relation is described by equation (6).

trend is of interest. The theoretical relation between the ice adhesion strength and the water contact angle thus becomes

$$\tau = C_0(1 + \cos \theta). \quad (6)$$

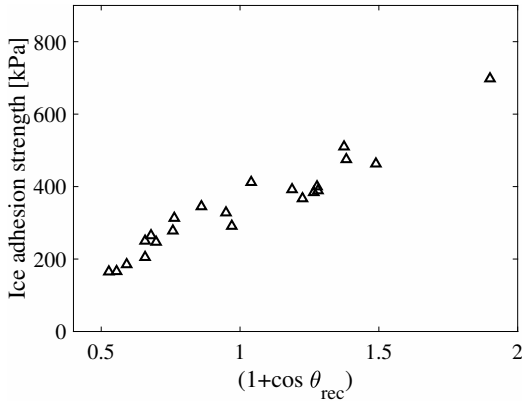
This relation is illustrated in Figure 2.

The relation from equation (6) and Figure 2 has been extensively studied for experimental screening of low ice adhesion surfaces. When the contact angle in equation (3) is substituted with the receding contact angle θ_{rec} , which is defined as the lowest metastable contact angle that can be measured [31], the work of adhesion is replaced with the practical work of adhesion W_p such that [21, 22]

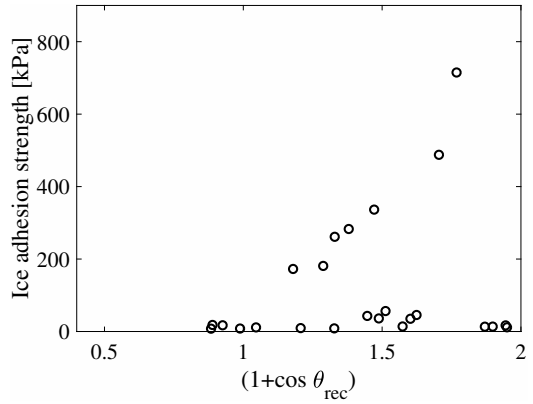
$$W_p \approx \gamma_w(1 + \cos \theta_{rec}). \quad (7)$$

The same reasoning may be applied to equation (7) as applied to equation (3) to derive equation (6), with an analogous result. As such, both the contact angle and receding contact angle may correlate with the ice adhesion strength.

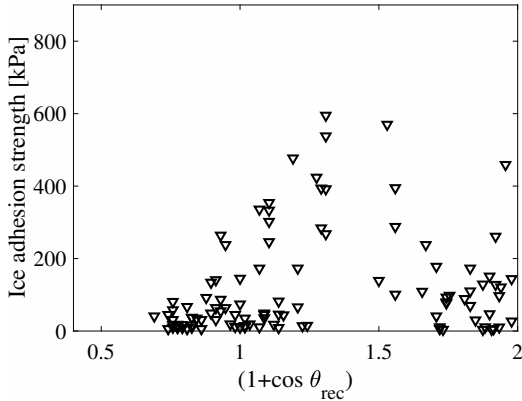
Meuler et al [22] investigated the receding contact angle and its relation to the ice adhesion strength for commercially available icephobic surfaces. Analogous experiments were performed by He et al [18] and Golovin et al [38]. Their experimental results are



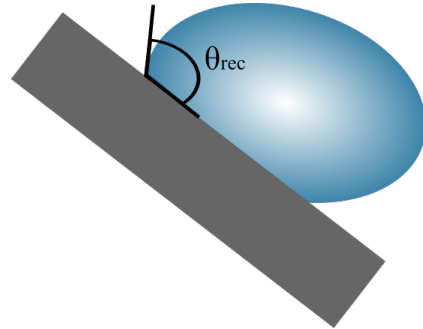
(a) Results from Meuler et al [22], with 22 samples.



(b) Results from He et al [18], with 24 samples.



(c) Results from Golovin et al [38], with 108 samples. Ice adhesion is average value.



(d) Illustration of receding contact angle compared to the equilibrium contact angle in Figure 1.

Figure 3: Experimental results on the relation between receding contact angle and ice adhesion strength for a collection of surfaces. The relation from (6) and Figure 2b is clearest for 3a, and can be seen for higher ice adhesion strengths in 3b. The relation cannot be seen in 3c. The definition of the receding contact angle is shown in 3d.

shown in Figure 3. It can be seen that the relation from equation (6) agrees with the results from Meuler et al in Figure 3a, but only for surfaces with ice adhesion strengths above about 160 kPa as shown by He et al in Figure 3b. The same relation is not apparent for the large number of samples tested by Golovin et al [38], as seen in Figure 3c.

Ideally, the relation from equation (6) and Figure 2a should predict the ice adhesion strength of a given surface based on the water contact angle, or similarly for the receding contact angle. However, the experimental studies vary considerably, and ice adhesion strength depends on more parameters than just wettability, such as for instance softness of the surface, and elastic incompatibility between ice and the surface. The discrepancy between theory and macroscale experiments with ice adhesion and wettability is well

known, and might be due to mechanical deformation or the varying structure of ice, among others. So far, the only investigations have been performed either at macroscale or by theoretical analyses. In this study, molecular dynamics simulations were applied to breach this gap and investigate the relation in equation (6) at the nanoscale.

The use of molecular dynamics enables the system to be controlled precisely, and to investigate the underlying mechanisms of the ice adhesion related to water contact angle. The water itself, and the water-solid and ice-solid interactions which govern the behaviour, can be controlled and observed while changing the parameters of the water/ice interaction with the surface. Consequently, it is possible to investigate different water contact angles for the same water-surface system, and the associated ice adhesion strength.

In this study, only the water contact angle is investigated, and not the receding contact angle. To perform similar investigations as presented in this study with the receding contact angle to determine the practical work of adhesion will be part of a future project.

3 Methods

Our simulation system consisted of an ice cube situated on a graphene surface, which melts to water when the temperature is raised. The system is similar to a previously published system [39]. The aim of the study was to determine the relation between the ideal water contact angle and the ice adhesion strength on an ideal graphene surface.

3.1 Atomistic modelling

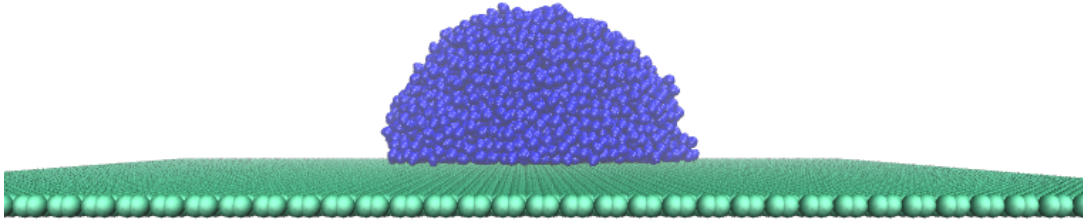
The chosen water model was the all-atom TIP4P/ICE [40], both for the ice cube during ice adhesion simulations and for the water droplet contact angle calculations. Compared to other widely applied water models, such as SPC [41], SPC/E [42], TIP3P and TIP4P [43], this water model was reported to reproduce appropriate properties for both ice and water, in addition to a more correct phase transition [40]. TIP4P/ICE has a higher transition temperature of 272.2 K, and is suitable for investigating the detachment of ice from a solid substrate as is the aim of this study. For the graphene surface, parameters from the OPLS force field [44, 45] were applied, as discussed later.

The ice modelled in this study was ice Ih. This ice phase was chosen because it is the only phase of ice occurring naturally during normal conditions [46], and this ice phase is thus the only ice phase of interest to the ice adhesion research. The ice cubes were modelled with a hexagonal molecular arrangement. The basal face of the ice cube, (0 0 0 1), was the face used to adhere to the surface. The ice cube had surface area $A = 8.0 \times 7.6 \text{ nm}^2$, and thickness 2 nm. The size of the ice cube was thus on nanometre scale, and might be considered as a nanoscale location of a realistic sample at microscale and macroscale.

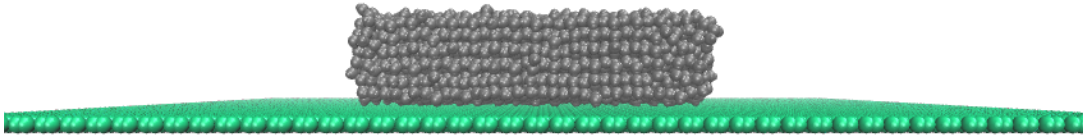
Both electrostatic interactions and van der Waals forces are important for ice adhesion [47, 48]. However, due to the highly complex situation of coulombic interactions and the possible surface oxidation by the water molecules [39], we chose graphene that interact with water through van der Waals forces via Lennard-Jones potential.

Graphene was chosen as the surface in study for the sake of simplicity and because the surface can be considered atomically flat and thus an ideal surface [31] when comparing to water. The graphene surface consisted of electrically neutral carbon atoms, with a surface area of $19.9 \text{ nm} \times 20.3 \text{ nm}$. This surface area was more than four times larger than the contact area of the ice cube and the associated water droplet, which assured enough space for the water molecules to migrate during the simulation. The system is illustrated in Figure 4. The system had periodic boundary conditions in all directions, and thus the surfaces expand to infinite surfaces during simulations.

The van der Waals parameters for the simulated graphene surface were a van der Waals radius of $\sigma = 0.355 \text{ nm}$ and an energy well depth $\varepsilon = 0.29288 \text{ kJmol}^{-1}\text{nm}^{-2}$. These parameters were borrowed from naphthalene fusion carbon number 9 in the OPLS force field [44, 45], as this atom only connects to other carbon atoms [39]. The carbon atoms were situated in aromatic ring structures and bonded to their closest neighbours by harmonic potentials with an equilibrium bond length and force constant of 0.14 nm and $3.924592 \times 10^5 \text{ kJmol}^{-1}\text{nm}^{-2}$, respectively. More information about the graphene surface has been published previously [39]. To simulate different water contact angles with the same system, the energy well depth ε was changed manually. This energy well depth determined the interaction potential between the water molecules and the surface, and is a



(a) Water drop at $T = 275$ K.



(b) Ice cube at $T = 180$ K.

Figure 4: Illustrations of the simulation system in this study of water molecules on a graphene surface, here represented by system A. This system had interaction potential $\varepsilon_0 = 2.9288 \times 10^{-1} \text{ kJmol}^{-1}\text{nm}^{-2}$.

common method to investigate wettability through changing contact angles [17, 49–51].

The energy well depth, or interaction energy, was changed as seen in Table 1.

In addition to the simulation system described so far, three additional simulation systems were tested. These systems were similar to the one already described, denoted as system A, except that they had different sizes. The changes in size refer both to the size of the graphene surface, and the size of the original ice cube. All the simulation systems are detailed further in Table 2, and range from roughly 7000 atoms to 100 000 atoms. All four systems are displayed in Figure S1 and Figure S2.

ε	Value [$\text{kJmol}^{-1}\text{nm}^{-2}$]
$0.05\varepsilon_0$	1.4644×10^{-2}
$0.1\varepsilon_0$	2.9288×10^{-2}
$0.5\varepsilon_0$	1.4644×10^{-1}
ε_0	2.9288×10^{-1}
$1.5\varepsilon_0$	4.3932×10^{-1}
$2\varepsilon_0$	5.8576×10^{-1}
$2.5\varepsilon_0$	7.3220×10^{-1}

Table 1: Overview of the energy well depths, or interaction energies, ε applied in the seven different simulation systems to change the water contact angle. All systems was simulated five times to obtain averages.

System	Number of atoms	Area of graphene sheet	Area of ice-solid contact
A	28376	19.9 nm \times 20.3 nm	8.0 nm \times 7.6 nm
B	7336	8.0 nm \times 8.1 nm	4.9 nm \times 4.6 nm
C	58184	19.9 nm \times 19.9 nm	14.7 nm \times 13.8 nm
D	102568	26.3 nm \times 26.1 nm	19.6 nm \times 18.5 nm

Table 2: Overview of the differently sized simulation systems. The different interaction energies ε from Table 1 are applied to all four systems to investigate water contact angles.

3.2 Simulation details

Three different types of subsequent molecular dynamics (MD) simulations were performed on the atomistic models for accessing the ice adhesion strength. These were structural energy minimisation, ice adhesion equilibration and force-probe MD simulations. For determining the water contact angle, the structural energy minimisation and equilibration were applied. The MD simulation package GROMACS 5.1.2 [52] was employed to carry out the simulations. The substrates were placed in the XY-plane of the simulation boxes, and the Z-dimension of the simulation boxes was large enough to ensure that the atoms did not interact with their periodic images at any time. The particle-Ewald method was applied to account for the long-range electrostatic interactions [53] for the water and ice molecules, and the LINCS algorithm was applied to constrain bond vibration in order to use a longer time step of 0.002 ps [54]. The simulation system was set in a NVT ensemble at varied temperatures depending on whether ice or water was investigated, and use the Nosé-Hoover coupling method to maintain the simulation temperature [55, 56], with a coupling time constant $\tau_T = 0.4$ ps.

First, the steepest descent algorithm was applied to relax the atomistic structures in the simulation system by energy minimisation. The aim of this energy minimisation was to remove any possible close atom contacts. Then, system equilibration was performed. With experience from a similar ice cube system on silicon and graphene [39], temperatures of 180 K were applied to test ice adhesion strength, while temperatures of 275 K were applied to investigate the water contact angle. For the larger systems (denoted C and D in Table 2), the temperature to test the water contact angle was increased to 300 K in order to decrease the remnants of ice crystal in the system after equilibration.

The graphene surface was fixed during simulations, such that it represented an inert wall. This fixing does not affect the contact angle, and reduces the computation time [57].

For the ice adhesion simulations, the systems were equilibrated for 20 ns. The final equilibrated structures were used for force-probe MD simulations to determine ice adhesion strength. The ice adhesion strength is, as mentioned, defined by equation (4), and is calculated by the simulation system as pulling the ice cube perpendicular to the surface, similar to an experimental tensile test [16]. To detach the ice, the center of mass (COM) of the ice cube was linked to a moving virtual harmonic spring with a spring constant of $5000 \text{ kJmol}^{-1}\text{nm}^{-2}$. The spring starts at the COM of the ice cube and moved with a constant speed of 0.5 nmns^{-1} perpendicular to the graphene surface. At the same time, a counter force acted on the COM of the graphene surface. The pulling force generated by the displacement between the spring and the ice cube COM is collected every 5 ps. The ice adhesion strength is determined by collecting the force peak value (F_{max}) from each independent simulations, and normalising by the contact area of the ice cube. For the larger systems, denoted C and D in Table 2, the spring constant was increased to $10\,000 \text{ kJmol}^{-1}\text{nm}^{-2}$ to ensure ice detachment for the highest values of interaction energies.

The water contact angle was calculated by applying the algorithm presented by Khalkhali et al. [58]. This algorithm calculates the contact angle along the contact line and provides an angular distribution, which is useful for a more thorough analysis of the droplet. Furthermore, the algorithm does not assume a spherical droplet. Therefore, the algorithm can be applied to droplets with less regular shapes, as is the case for several of the water droplets in this study.

Snapshots of the analysis of the water contact angles and distributions, and maximum detachment force for ice adhesion strength calculations can be found in Figures S3, S4 and S5, respectively. The effect of changing the box size in the z-dimension and the spring constant in the determination of the ice adhesion strength is also shown in Figure S7. It can be seen that neither the spring constant nor the box size has significant impact on the calculated ice adhesion strength in the simulations.

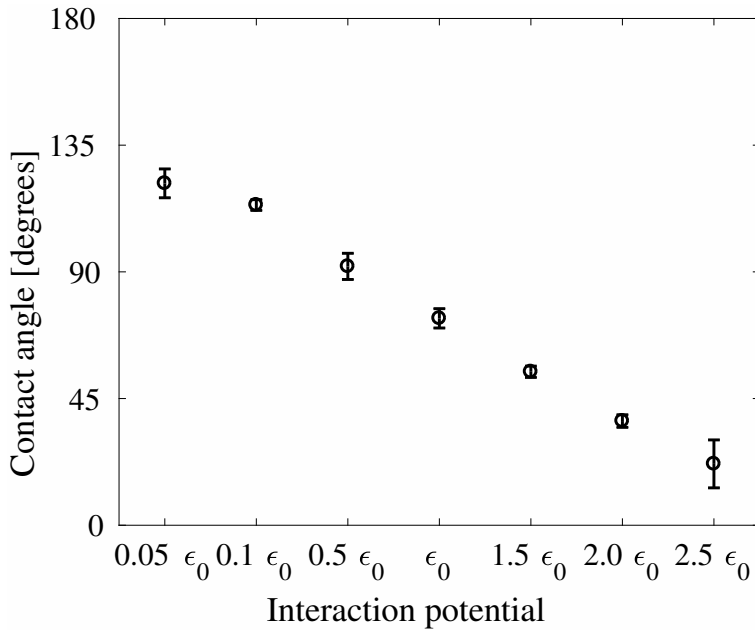


Figure 5: Water contact angle θ as function of the interaction potential ϵ for the system A. The values of ϵ can be found in Table 1.

4 Results

Figure 5 shows the average water contact angle as function of the changing interaction potential ϵ for system A. It can be seen that the contact angle scales almost linearly with the chosen values of the energy well depth. For the system with the original energy well depth ϵ_0 , the water contact angle is calculated to be $73.49 \pm 3.44^\circ$. The contact angle of graphite and graphene has been studied by atomistic simulations previously, with reported contact angles ranging from 83° for graphite [58] to a predicted $90 - 95^\circ$ for graphene [59]. Although the contact angles obtained in this study are below these values, the studies in literature used the SPC/E forcefield, which may give different contact angle values. Furthermore, the present system has a fixed ideal surface, and contact angle is impacted by surface roughness and impurities. As such, the contact angles in this study are within the range to be expected for water wettability on graphene.

The ice adhesion strength of system A is displayed in Figure 6, also as a function of the interaction potential ϵ . It can be seen that the trend of the ice adhesion strength is similar to that seen for the ideal relation between ice adhesion strength and contact angle shown in Figure 2a. For the system with the original interaction energy ϵ_0 , the ice adhesion strength

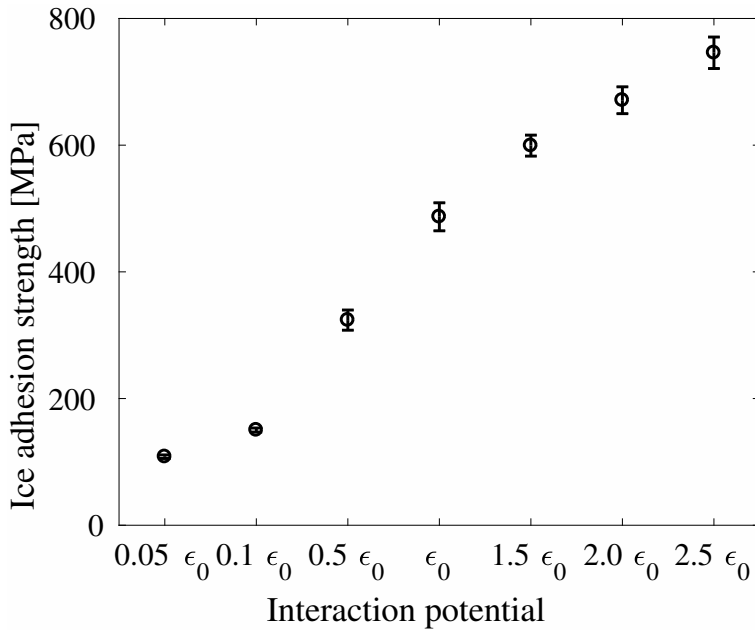


Figure 6: Ice adhesion strength τ as function of interaction potential ϵ for system A. The values of ϵ can be found in Table 1.

was found to be 487 ± 22 MPa. This ice adhesion strength is significantly higher than previously found for this type of system, which was 259 ± 21 MPa [39]. However, the previous study allowed flexible graphene sheets, while the present study has fixed the graphene sheet. It is likely this difference which have caused the disagreement in reported ice adhesion strengths. Furthermore, the ice adhesion strength of different system sizes and spring constants are all consistent in value, as seen in Table S1.

In Figure 7, the results of the ice adhesion strength as function of the water contact angles are displayed. This figure displays all data points from the combination of Figures 5 and 6, and includes a fitting of the theoretical relation from equation (6). As can be seen from Figure 7, the theoretical relation matches the simulation results with a high significance. This similarity between simulation results and theoretical relation is in contrast with the absence of similar trends in Figure 3.

In Figure 8, the contact angle for all system sizes can be seen for the seven different interaction energies. It can be seen that the contact angles are relatively constant, although there are large outliers in the extreme cases and for the largest systems tested. For system B, which is the smallest system, the water droplets deplete to a water layer already

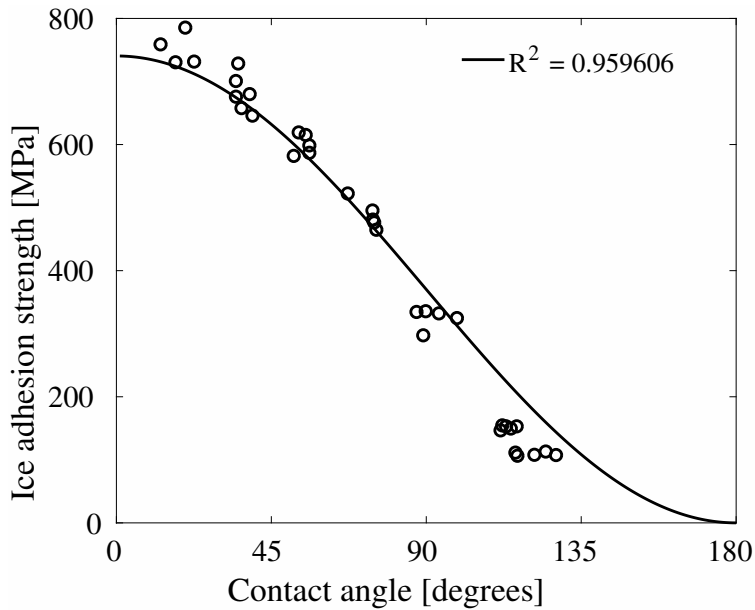


Figure 7: Ice adhesion strength as function of contact angle, with the relation from equation (6) fitted to the data. It can be seen that the fit of the general relation shows a very high level of significance.

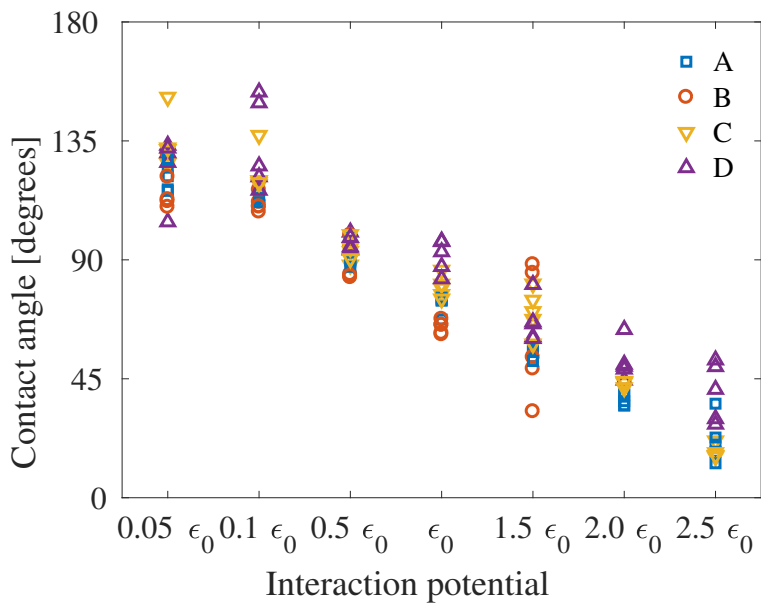


Figure 8: Contact angle as function of interaction energy ϵ for all system sizes. Separate figures can be seen in Figure S8.

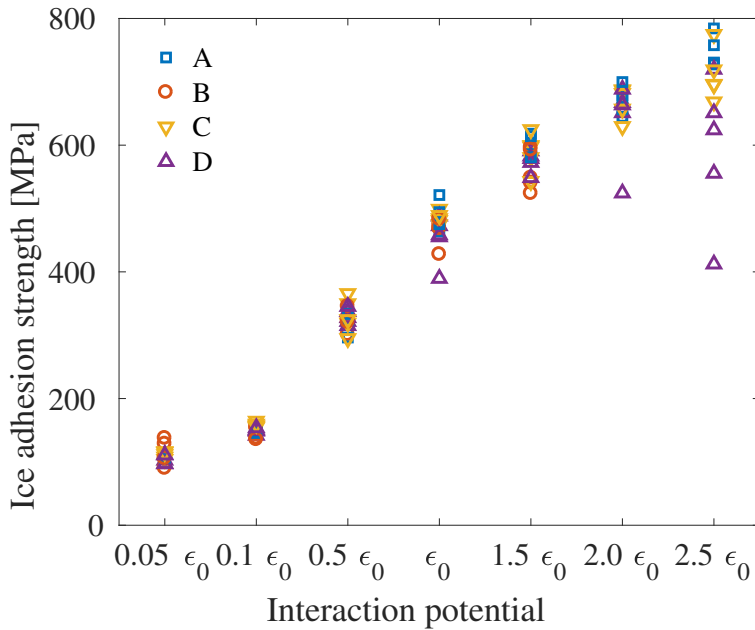


Figure 9: Ice adhesion strength as function of interaction energy ϵ for all system sizes. Separate figures can be seen in Figure S9.

at interaction energy of $1.5\epsilon_0$, and the higher interactions energies are therefore not investigated for this system. For system D, it can be seen that the contact angles are fairly large relative to the other systems, especially for the highest interaction energies.

The ice adhesion strength as function of the interaction energies is shown in Figure 9. It can be seen that the ice adhesion strength is very similar for all systems, with the greatest variance at the highest interaction energy. Furthermore, system D displays larger differences of measured ice adhesion strength than for each interaction energy than the other systems.

When combining the contact angles and ice adhesion strengths displayed in Figures 8 and 9, the ice adhesion strength as function of the contact angle can be viewed and compared to Figure 2 and equation (6). In Figure 10, the correlation between this theoretical relation and the simulation results can be seen, with the fitting and level of significance included. All systems have significances above $R^2 = 0.75$, with significances above $R^2 = 0.95$ for systems A and C. Hence, it is the smallest and largest systems which differs the most from the theoretical relation due to the increase of outliers in the results.

Separated results from the four different systems can be found in supplementary

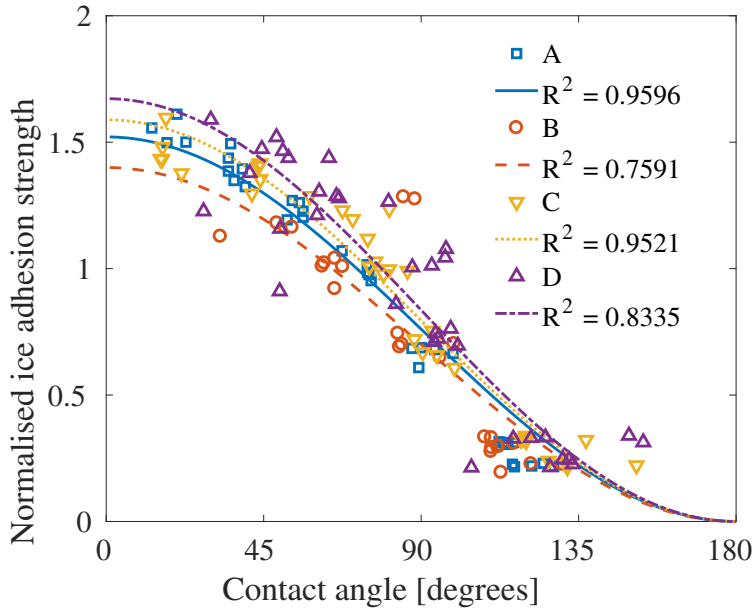


Figure 10: Overview of the correlation with equation (6) for the four systems investigated in this study. The ice adhesion strength has been normalised with respect to the mean value from the interaction energy ε_0 .

materials.

5 Discussion

From the high level of significance seen in Figure 10, it is clear that the theoretical relation from equation (6) holds for simulations at the nanoscale for water molecules situated on an ideal surface and for adhesive perpendicular detachment of a perfect ice crystal. The same relation is, however, not agreed upon from an experimental point of view.

The fact that the theoretical relation between the ice adhesion strength and the water contact angle is found in atomistic simulations indicate that the disagreement from experiments, as seen in Figure 2 and 3, comes from experimental factors and not from properties of water molecules in liquid and solid form on the same surface. Such an experimental disagreement might stem from material or substrate deformations during detachment, an incomplete ice-solid contact [36] or the so-called nanoscale crack initiators [6], or the difference in other surface parameters for the real surfaces during experiments compared to the ideal surface investigated in this study. Several surface parameters which are known

to impact the ice adhesion strength, such as material softness and elastic modulus [14], have not been included in this study. Furthermore, real materials are often deformed upon detachment, and work may be done in forming micro-cracks within the ice. While a perfectly smooth and ideal surface has been studied here, a real surface will contain defects, interlocking and other irregularities. As a result, we cannot expect to match experimental observations with the current simulations. The work spent to detach ice from a surface is typically much more than the work of adhesion, due to experimental deformations and mechanisms [36]. It follows that the work of adhesion W_a might be considered a theoretical minimal adhesion strength for a given material.

The ice adhesion strength obtained through the simulations in this study are higher than experimental values for similar systems, as well as previously performed simulations [39]. As stated earlier, the difference from previous simulations likely results in the fixing of the graphene surface. For the difference to experimental results, this fixing of the graphene surface is probably also an impacting factor. Furthermore, in contrast to most experimental ice adhesion tests which utilises shear force [16], the ice adhesion strength in this study was determined through tensile ice detachment. It has been shown previously that tensile failure results in much higher ice adhesion strengths than shear failures [60], and more often results in a cohesive fracture [16]. However, as the simulation system is ideal and ice is detached through COM movement of the ice sample, an adhesive failure is assured. Furthermore, as the ice adhesion strength values obtained in this study are consistent for the different systems and configurations included, it may be concluded that the ice adhesion strengths represent a realistic trend although the values are higher than expected experimentally.

Out of interest, several different forms of a relation between ice adhesion and wettability were tested on the simulation data obtained in this study. In addition to the theoretical relation from equation (6), a linear relation, a polynomial relation and a power law relation were tested. All these relationships showed less significance than equation (6). Lastly, a more complicated cosine relation were tested, where the coefficient C_0 from equation (6) were assumed as a function of cosine, such that

$$\tau = A \cos(B\theta)(1 + \cos \theta). \quad (8)$$

The result of this fitting can be seen in Figure S11. Although equation (8) is more complicated than equation (6), the significance between the ice adhesion strength and water contact angle improved only marginally. As such, the theoretical relation from equation (6) is still considered the optimal relationship for the fundamental correlation between ice adhesion strength and water wettability.

By testing several different system sizes, as described in Table 2, the size effect of water contact angle and ice adhesion strength may be investigated. It has been stated previously that the droplet size impacts the contact angle [61]. For systems similar to the one investigated here, it has been found that increasing droplet sizes results in narrower contact angle distributions [58]. Furthermore, fluctuations in the droplet shape decreases for larger droplets. Both of these effects are proposed to originate from higher sphericity in larger droplets. For the simulations performed in this study, the probability distributions of one simulation for each system size can be seen in Figure S12. This figure shows very similar probability distributions, except for system D. However, the higher contact angle and non-uniform probability distribution of this system is likely caused by an unmelted remnant of the original ice crystal.

As seen in Figure 10, the amplitude of the fitting of equation (6) seems to scale with the size of the system. This scaling indicates that there is a size effect present. In Figure 8 and Table S2, it can be seen that the contact angle increases with increases of system sizes. Overall however, it is thought that the contact angle decreases as the droplet size increases [57, 58, 62, 63]. The reason for this disagreement is unclear, but as the different contact angles obtained in this study are relatively similar and often within the range of deviation, the size effect may be less than previously thought, and the effect of the fitting amplitude might be due to the combined size effect of the water droplets and ice adhesion strength.

In this study, the contact angles investigated have been the so-called static contact angle as described with Young's equation from equation (1) and Figure 1. However, as can be seen in the literature [22–25, 64] and Figure 3, wettability is most often referred to as the receding contact angle, or contact angle hysteresis, when compared with the ice adhesion strength. Due to resources and because the dynamic contact angles are more computationally demanding than the static contact angles, only the static contact angle

was investigated here. The next step will be to include the dynamic contact angles, such as the advancing and receding contact angle as well as the contact angle hysteresis, and see if equation (6) holds for these measures of the wettability as well.

Future work for continuing to probe the relation between the ice adhesion strength and wettability of a surface thus includes investigating the dynamic contact angles, in addition to testing other surfaces. This study tests only one type of ideal surface, and to change to a metallic surface might change the simulation results. Furthermore, surfaces with texture and nanostructures must be investigated for ice adhesion strength and wettability. In addition, only contact angles obtained at the nanoscale can be investigated in atomic simulations. Due to size-effects for nanoscale systems, the contact angles obtained in molecular dynamics simulations are not necessarily transferable to macroscopic contact angles [59, 61]. Further work should thus also include a comparison between wettability measured obtained at the nanoscale and experimental results on macroscopic scale. Such a comparison may be carried out for instance by the dry surface simulation approach [65].

An effect of probing the relation between ice adhesion strength and water contact angle in atomistic simulations is that the system created is idealistic. In experimental situations, the contact angle of a smooth surface, such as the surface simulated in this study, cannot surpass 120° . However, by tuning the interaction potential directly in the atomistic simulations, the graphene surface can attain contact angles of more than 150° , as seen in Figure 8. As a result of the artificiality of the surface, the results of the molecular dynamics simulations presented in this study cannot be directly transferred to real systems. Nonetheless, the results here shed light on the fundamental relation between water and ice situated on a surface, and brings us one step closer to the fundamental relation between ice adhesion and wettability.

6 Conclusion

In this study, the correlation between water contact angle and ice adhesion was investigated by utilising atomistic modelling and molecular dynamics simulations. By comparing the results from ice adhesion calculations by detaching an ice sample normal to a graphene surface and water contact angle on the same surface, the relation from thermodynamic

theory is reproduced. This correlation indicates that the discrepancy in experimental results stems from experimental parameters and not the properties of the ice-solid or water-solid interactions. The reproduction of the theoretical relation between wettability and ice adhesion at the nanoscale is important due to the gap in understanding between experimental observations and theoretical models. The results presented here represent a step towards a more thorough understanding of the fundamental mechanisms of ice adhesion, and its relation to water wettability.

Acknowledgements

The authors gratefully acknowledge the financial support from the Norwegian Research Council FRINATEK project Towards Design of Super-Low Ice Adhesion Surfaces (SLICE, 250990). The funding sources had no involvement in designing the study or the publication.

The authors declare no conflicts of interest.

Supplementary material

Supplementary materials are available, including mean values of ice adhesion strength and contact angles for all systems, illustrations of the systems, and comparable simulation results for each simulation system.

References

- [1] J. Lv, Y. Song, L. Jiang, and J. Wang, “Bio-inspired strategies for anti-icing,” *ACS Nano*, vol. 8, no. 4, pp. 3152–3169, 2014.
- [2] J. Brassard, C. Laforte, F. Guerin, and C. Blackburn, *Icephobicity: Definition and Measurement Regarding Atmospheric Icing*. Berlin, Heidelberg: Springer, 2017.
- [3] M. J. Kreder, J. Alvarenga, P. Kim, and J. Aizenberg, “Design of anti-icing surfaces: smooth, textured or slippery?,” *Nature Reviews Materials*, vol. 1, pp. 1–15, 2016.

- [4] V. Hejazi, K. Sobolev, and M. Nosonovsky, "From superhydrophobicity to icephobicity: forces and interaction analysis," *Scientific Reports*, vol. 3, 2013.
- [5] H. Sojoudi, M. Wang, N. D. Boscher, G. H. McKinley, and K. K. Gleason, "Durable and scalable icephobic surfaces: similarities and distinctions from superhydrophobic surfaces," *Soft Matter*, vol. 12, pp. 1938–1963, 2016.
- [6] Z. He, S. Xiao, H. Gao, J. He, and Z. Zhang, "Multiscale crack initiators promoted super-low ice adhesion surfaces," *Soft Matter*, vol. 13, pp. 6562–6568, 2017.
- [7] K. K. Varanasi, T. Deng, J. D. Smith, M. Hsu, and N. Bhate, "Frost formation and ice adhesion on superhydrophobic surfaces," *Appl. Phys. Lett.*, vol. 97, no. 23, pp. 234102–3, 2010.
- [8] A. Dotan, H. Dodiuk, C. Laforte, and S. Kenig, "The relationship between water wetting and ice adhesion," *Journal of Adhesion Science and Technology*, vol. 23, no. 15, pp. 1907–1915, 2009.
- [9] J. Chen, J. Liu, M. He, K. Li, D. Cui, Q. Zhang, X. Zeng, Y. Zhang, J. Wang, and Y. Song, "Superhydrophobic surfaces cannot reduce ice adhesion," *Applied Physics Letters*, vol. 101, no. 11, 2012.
- [10] F. Wang, W. Ding, J. He, and Z. Zhang, "Phase transition enabled durable anti-icing surfaces and its diy design," *Chemical Engineering Journal*, vol. 360, pp. 243–249, 2019.
- [11] D. L. Beemer, W. Wang, and A. K. Kota, "Durable gels with ultra-low adhesion to ice," *Journal of Materials Chemistry A*, vol. 4, pp. 18253–18258, 2016.
- [12] P. Irajizad, A. Al-Bayati, B. Eslami, T. Shafquat, M. Nazari, P. Jafari, V. Kashyap, A. Masoudi, D. Araya, and H. Ghasemi, "Stress-localized durable icephobic surfaces," *Materials Horizons*, vol. 6, pp. 758–766, 2019.
- [13] K. Golovin, A. Dhyani, M. D. Thouless, and A. Tuteja, "Low–interfacial toughness materials for effective large-scale deicing," *Science*, vol. 364, no. 6438, p. 371, 2019.

- [14] Z. He, Y. Zhuo, J. He, and Z. Zhang, "Design and preparation of sandwich-like polydimethylsiloxane (pdms) sponges with super-low ice adhesion," *Soft Matter*, vol. 14, pp. 4846–4851, 2018.
- [15] A. Work and Y. Lian, "A critical review of the measurement of ice adhesion to solid substrates," *Progress in Aerospace Sciences*, vol. 98, pp. 1–26, 2018.
- [16] S. Rønneberg, J. He, and Z. Zhang, "The need for standards in low ice adhesion surface research: a critical review," *Journal of Adhesion Science and Technology*, pp. 1–29, 2019.
- [17] T. Y. Zhao, P. R. Jones, and N. A. Patankar, "Thermodynamics of sustaining liquid water within rough icephobic surfaces to achieve ultra-low ice adhesion," *Scientific Reports*, vol. 9, no. 1, p. 258, 2019.
- [18] Z. He, E. T. Vågenes, C. Delabahan, J. He, and Z. Zhang, "Room temperature characteristics of polymer-based low ice adhesion surfaces," *Scientific Reports*, vol. 7, p. 42181, 2017.
- [19] V. F. Petrenko and S. Peng, "Reduction of ice adhesion to metal by using self-assembling monolayers (sams)," *Canadian Journal of Physics*, vol. 81, no. 1-2, pp. 387–393, 2003.
- [20] M. Sarshar, C. Swartz, S. Hunter, J. Simpson, and C.-H. Choi, "Effects of contact angle hysteresis on ice adhesion and growth on superhydrophobic surfaces under dynamic flow conditions," *Colloid and Polymer Science*, vol. 291, no. 2, pp. 427–435, 2013.
- [21] D. Chen, M. D. Gelenter, M. Hong, R. E. Cohen, and G. H. McKinley, "Icephobic surfaces induced by interfacial nonfrozen water," *ACS Applied Materials & Interfaces*, vol. 9, no. 4, pp. 4202–4214, 2017.
- [22] A. J. Meuler, J. D. Smith, K. K. Varanasi, J. M. Mabry, G. H. McKinley, and R. E. Cohen, "Relationships between water wettability and ice adhesion," *ACS Applied Materials and Interfaces*, vol. 2, no. 11, pp. 3100–3110, 2010.

- [23] R. M. Fillion, A. R. Riahi, and A. Edrissy, "Design factors for reducing ice adhesion," *Journal of Adhesion Science and Technology*, vol. 31, no. 21, pp. 2271–2284, 2017.
- [24] Z. A. Janjua, B. Turnbull, K.-L. Choy, C. Pandis, J. Liu, X. Hou, and K.-S. Choi, "Performance and durability tests of smart icephobic coatings to reduce ice adhesion," *Applied Surface Science*, vol. 407, pp. 555–564, 2017.
- [25] S. A. Kulinich and M. Farzaneh, "How wetting hysteresis influences ice adhesion strength on superhydrophobic surfaces," *Langmuir*, vol. 25, no. 16, pp. 8854–8856, 2009.
- [26] R. Karmouch and G. G. Ross, "Experimental study on the evolution of contact angles with temperature near the freezing point," *The Journal of Physical Chemistry C*, vol. 114, no. 9, pp. 4063–4066, 2010.
- [27] W. D. Bascom, R. L. Cottingham, and C. R. Singleterry, "Ice adhesion to hydrophilic and hydrophobic surfaces," *The Journal of Adhesion*, vol. 1, no. 4, pp. 246–263, 1969.
- [28] J. W. Drelich, "Contact angles: From past mistakes to new developments through liquid-solid adhesion measurements," *Advances in Colloid and Interface Science*, vol. 267, pp. 1–14, 2019.
- [29] H. Koivuluoto, C. Stenroos, R. Ruohomaa, G. Bolelli, L. Lusvarghi, and P. Vuoristo, "Research on icing behavior and ice adhesion testing of icephobic surfaces," in *International Workshop on Atmospheric Icing of Structures (IWAIS)*, 2015.
- [30] J. Liu, C. Zhu, K. Liu, Y. Jiang, Y. Song, J. S. Francisco, X. C. Zeng, and J. Wang, "Distinct ice patterns on solid surfaces with various wettabilities," *Proceedings of the National Academy of Sciences*, vol. 114, no. 43, pp. 11285–11290, 2017.
- [31] A. Marmur, C. Della Volpe, S. Siboni, A. Amirfazli, and J. W. Drelich, "Contact angles and wettability: towards common and accurate terminology," *Surface Innovations*, vol. 5, no. 1, pp. 3–8, 2017.

- [32] T. Young, “Iii. an essay on the cohesion of fluids,” *Philosophical Transactions of the Royal Society of London*, vol. 95, pp. 65–87, 1805.
- [33] R. N. Wenzel, “Resistance of solid surfaces to wetting by water,” *Industrial and Engineering Chemistry*, vol. 28, no. 8, pp. 988–994, 1936.
- [34] A. B. D. Cassie, “Contact angles,” *Discussions of the Faraday Society*, vol. 3, pp. 11–16, 1948.
- [35] A. B. D. Cassie and S. Baxter, “Wettability of porous surfaces,” *Transactions of the Faraday Society*, vol. 40, no. 0, pp. 546–551, 1944.
- [36] L. Makkonen, “Ice adhesion —theory, measurements and countermeasures,” *Journal of Adhesion Science and Technology*, vol. 26, no. 4-5, pp. 413–445, 2012.
- [37] L. Makkonen, “Surface melting of ice,” *The Journal of Physical Chemistry B*, vol. 101, no. 32, pp. 6196–6200, 1997.
- [38] K. Golovin, S. P. R. Kobaku, D. H. Lee, E. T. DiLoreto, J. M. Mabry, and A. Tuteja, “Designing durable icephobic surfaces,” *Science Advances*, vol. 2, no. 3, 2016.
- [39] S. Xiao, J. He, and Z. Zhang, “Nanoscale deicing by molecular dynamics simulation,” *Nanoscale*, vol. 8, p. 14625, 2016.
- [40] J. L. F. Abascal, E. Sanz, R. García Fernández, and C. Vega, “A potential model for the study of ices and amorphous water: Tip4p/ice,” *The Journal of Chemical Physics*, vol. 122, no. 23, p. 234511, 2005.
- [41] H. J. C. Berendsen, J. P. M. Postma, W. F. v. Gunsteren, and J. Hermans, *Interaction Models for Water in Relation to Protein Hydration*, vol. 14, pp. 331–342. The Jerusalem Symposia on Quantum Chemistry and Biochemistry: Springer, Dordrecht, 1981.
- [42] H. J. C. Berendsen, J. R. Grigera, and T. P. Straatsma, “The missing term in effective pair potentials,” *The Journal of Physical Chemistry*, vol. 91, no. 24, pp. 6269–6271, 1987.

- [43] W. L. Jorgensen, J. Chandrasekhar, J. D. Madura, R. W. Impey, and M. L. Klein, "Comparison of simple potential functions for simulation liquid water," *The Journal of Chemical Physics*, vol. 79, no. 2, pp. 926–935, 1983.
- [44] W. L. Jorgensen and J. Tirado-Rives, "The opls [optimized potentials for liquid simulations] potential functions for proteins, energy minimizations for crystals of cyclic peptides and crambin," *Journal of the American Chemical Society*, vol. 110, no. 6, pp. 1657–1666, 1988.
- [45] W. L. Jorgensen, D. S. Maxwell, and J. Tirado-Rives, "Development and testing of the opls all-atom force field on conformational energetics and properties of organic liquids," *Journal of the American Chemical Society*, vol. 118, no. 45, pp. 11225–11236, 1996.
- [46] T. Bartels-Rausch, V. Bergeron, J. H. E. Cartwright, R. Escibano, J. L. Finney, H. Grothe, P. J. Gutierrez, J. Haapala, W. F. Kuhs, J. B. C. Pettersson, S. D. Price, C. I. Sainz-Díaz, D. Stokes, G. Strazzulla, E. S. Thomson, H. Trinks, and N. Uras-Aytemiz, "Ice structures, patterns, and processes: A view across the ice-fields," *Rev. Mod. Phys.*, vol. 84, pp. 885–944, 2012.
- [47] L. A. Wilen, J. S. Wettlaufer, M. Elbaum, and M. Schick, "Dispersion-force effects in interfacial premelting of ice," *Physical Review B*, vol. 52, no. 16, pp. 12426–12433, 1995.
- [48] I. A. Ryzhkin and V. F. Petrenko, "Physical mechanisms responsible for ice adhesion," *The Journal of Physical Chemistry B*, vol. 101, no. 32, pp. 6267–6270, 1997.
- [49] M. J. de Ruijter, T. D. Blake, and J. De Coninck, "Dynamic wetting studied by molecular modeling simulations of droplet spreading," *Langmuir*, vol. 15, no. 22, pp. 7836–7847, 1999.
- [50] E. B. Moore, J. T. Allen, and V. Molinero, "Liquid-ice coexistence below the melting temperature for water confined in hydrophilic and hydrophobic nanopores," *The Journal of Physical Chemistry C*, vol. 116, no. 13, pp. 7507–7514, 2012.

- [51] J. K. Singh and F. Müller-Plathe, “On the characterization of crystallization and ice adhesion on smooth and rough surfaces using molecular dynamics,” *Applied Physics Letters*, vol. 104, no. 2, p. 021603, 2014.
- [52] M. Abraham, D. v. d. Spoel, E. Lindahl, B. Hess, and G. d. team, *GROMACS User Manual version 5.1.2*. 2016.
- [53] T. Darden, D. York, and L. Pedersen, “Particle mesh ewald: An nlog(n) method for ewald sums in large systems,” *The Journal of Chemical Physics*, vol. 98, no. 12, pp. 10089–10092, 1993.
- [54] B. Hess, H. Bekker, H. J. C. Berendsen, and J. G. E. M. Fraaije, “Lincs: A linear constraint solver for molecular simulations,” *Journal of Computational Chemistry*, vol. 18, no. 12, pp. 1463–1472, 1997.
- [55] S. Nosé, “A molecular dynamics method for simulations in the canonical ensemble,” *Molecular Physics*, vol. 52, no. 2, pp. 255–268, 1984.
- [56] W. G. Hoover, “Canonical dynamics: Equilibrium phase-space distributions,” *Physical Review A*, vol. 31, no. 3, pp. 1695–1697, 1985.
- [57] T. Werder, J. H. Walther, R. L. Jaffe, T. Halicioglu, and P. Koumoutsakos, “On the water-carbon interaction for use in molecular dynamics simulations of graphite and carbon nanotubes,” *The Journal of Physical Chemistry B*, vol. 107, no. 6, pp. 1345–1352, 2003.
- [58] M. Khalkhali, N. Kazemi, H. Zhang, and Q. Liu, “Wetting at the nanoscale: A molecular dynamics study,” *The Journal of Chemical Physics*, vol. 146, no. 11, p. 114704, 2017.
- [59] F. Taherian, V. Marcon, N. F. A. van der Vegt, and F. Leroy, “What is the contact angle of water on graphene?,” *Langmuir*, vol. 29, no. 5, pp. 1457–1465, 2013.
- [60] H. H. G. Jellinek, “Adhesive properties of ice,” *Journal of Colloid Science*, vol. 14, no. 3, pp. 268–280, 1959.

- [61] R. J. Good, "Contact angle, wetting, and adhesion: a critical review," *Journal of Adhesion Science and Technology*, vol. 6, no. 12, pp. 1269–1302, 1992.
- [62] R. Ramírez, J. K. Singh, F. Müller-Plathe, and M. C. Böhm, "Ice and water droplets on graphite: A comparison of quantum and classical simulations," *The Journal of Chemical Physics*, vol. 141, no. 20, p. 204701, 2014.
- [63] R. C. Dutta, S. Khan, and J. K. Singh, "Wetting transition of water on graphite and boron-nitride surfaces: A molecular dynamics study," *Fluid Phase Equilibria*, vol. 302, no. 1, pp. 310–315, 2011.
- [64] L. Makkonen, "Back to the basics: Wettability, icing and ice adhesion," in *International Workshop on Atmospheric Icing of Structures (IWAIS)*, 2015.
- [65] F. Leroy and F. Müller-Plathe, "Dry-surface simulation method for the determination of the work of adhesion of solid-liquid interfaces," *Langmuir*, vol. 31, no. 30, pp. 8335–8345, 2015.

Supplementary materials

- Table S1** Mean value and standard deviation for ice adhesion strength of simulation systems with different sizes and spring constants.
- Table S2** Mean contact angles and standard deviations for the four different systems and the different interaction energies.
- Figure S1** The four simulation systems from Table 2 with equilibrated water droplets.
- Figure S2** The four simulation systems from Table 2 with ice samples before detachment.
- Figure S3** Illustration of the quickhull-algorithm for mapping the droplet [S1].
- Figure S4** Illustration of the contact angle probability distribution [S1].
- Figure S5** The resulting force-time curve when detaching an ice cube from the graphene surface.
- Figure S6** Root mean square deviation of ice for the ice detachment process
- Figure S7** Effect of changing simulation parameters on the recorded ice adhesion strength.
- Figure S8** Contact angle as function of interaction potential for the four different system sizes.
- Figure S9** Ice adhesion strength as function of interaction potential for the four different system sizes.
- Figure S10** Ice adhesion strength as function of contact angle with fitting from equation (6) for the four different system sizes.
- Figure S11** Overview of the fitting of the correlation from equation (8).
- Figure S12** Contact angle distributions for the first simulations performed with interaction energy for the four different system sizes.

References

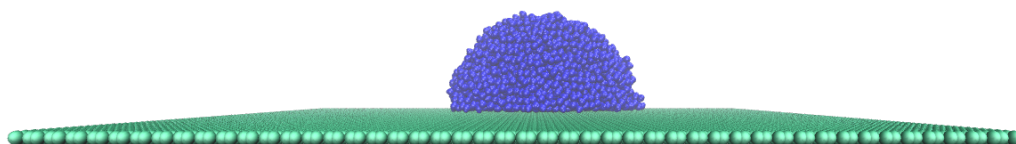
- [S1] M. Khalkhali, N. Kazemi, H. Zhang, and Q. Liu, "Wetting at the nanoscale: A molecular dynamics study," *The Journal of Chemical Physics*, vol. 146m no. 11, p. 114704, 2017.
- [S2] S. Xiao, J. He, and Z. Zhang. "Nanoscale deicing by molecular dynamics simulation," *Nanoscale*, vol. 8, p. 14625, 2016.

Type of system	Mean value for ε_0 [MPa]	SD
System A	486.92	22.106
System B	464.78	21.529
System C	485.532	9.159
System D	452.774	37.642
$k_B = 500 \text{ kJmol}^{-1}\text{nm}^{-2}$	406.61	—
$k_B = 3000 \text{ kJmol}^{-1}\text{nm}^{-2}$	489.20	15.136
$k_B = 4000 \text{ kJmol}^{-1}\text{nm}^{-2}$	470.38	23.967
$k_B = 5000 \text{ kJmol}^{-1}\text{nm}^{-2}$	482.66	13.908
$k_B = 6000 \text{ kJmol}^{-1}\text{nm}^{-2}$	477.82	36.421
$k_B = 7000 \text{ kJmol}^{-1}\text{nm}^{-2}$	468.13	13.004
Xiao et al [S2]	259	21

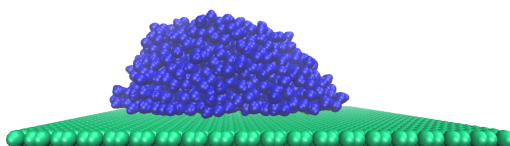
Table S1: Mean value and standard deviation for ice adhesion strength of simulation systems with different sizes and spring constants, all reported for original interaction energy ε . Systems A and B were run with spring constants $k_B = 5000 \text{ kJmol}^{-1}\text{nm}^{-2}$, while systems C and D were run with spring constants $10\,000 \text{ kJmol}^{-1}\text{nm}^{-2}$. The different spring constants were tested with simulation system A.

ε	System A	System B	System C	System D
$0.05\varepsilon_0$	$121.44^\circ \pm 5.12^\circ$	$117.38^\circ \pm 8.50^\circ$	$134.76^\circ \pm 9.68^\circ$	$125.46^\circ \pm 12.05^\circ$
$0.1\varepsilon_0$	$113.74^\circ \pm 1.91^\circ$	$111.37^\circ \pm 3.13^\circ$	$122.95^\circ \pm 7.94^\circ$	$133.22^\circ \pm 17.00^\circ$
$0.5\varepsilon_0$	$91.94^\circ \pm 4.65^\circ$	$89.33^\circ \pm 7.53^\circ$	$93.15^\circ \pm 4.36^\circ$	$96.33^\circ \pm 2.98^\circ$
ε_0	$73.49^\circ \pm 3.44^\circ$	$64.49^\circ \pm 2.42^\circ$	$79.65^\circ \pm 4.19^\circ$	$91.46^\circ \pm 6.21^\circ$
$1.5\varepsilon_0$	$54.51^\circ \pm 2.01^\circ$	$61.58^\circ \pm 24.15^\circ$	$70.34^\circ \pm 8.47^\circ$	$66.81^\circ \pm 8.25^\circ$
$2\varepsilon_0$	$37.00^\circ \pm 2.23^\circ$	—	$43.39^\circ \pm 1.01^\circ$	$51.39^\circ \pm 7.22^\circ$
$2.5\varepsilon_0$	$21.79^\circ \pm 8.51^\circ$	—	$17.23^\circ \pm 2.47^\circ$	$40.07^\circ \pm 11.07^\circ$

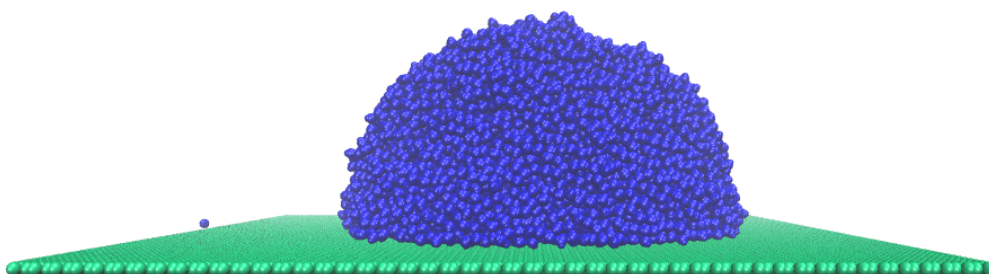
Table S2: Mean contact angles and standard deviations for the four different systems and the different interaction energies, as defined in Table 1.



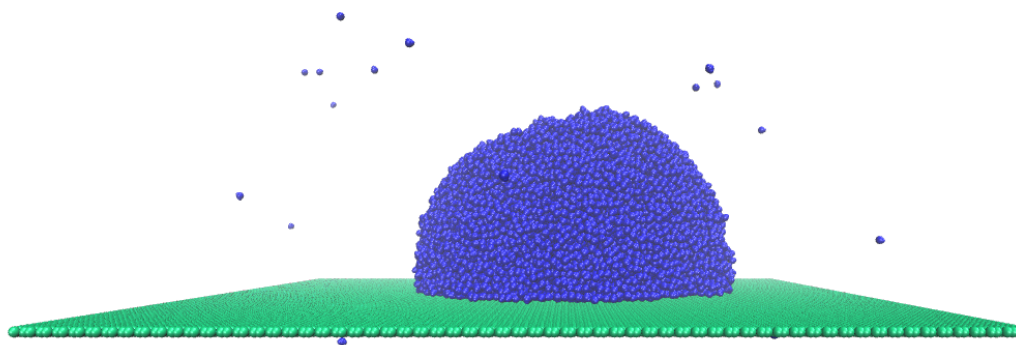
(a) System A.



(b) System B.

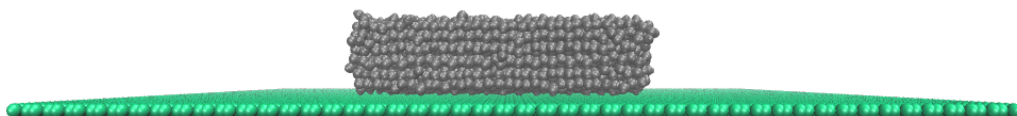


(c) System C.

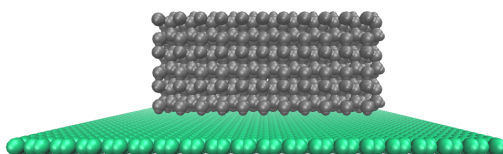


(d) System D.

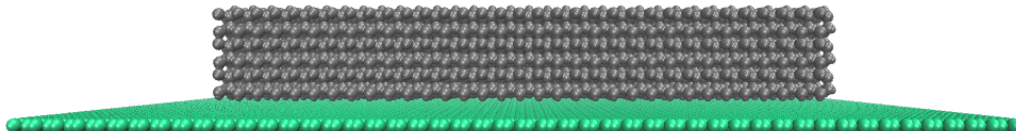
Figure S1: The four simulation systems from Table 2 with equilibrated water droplets.



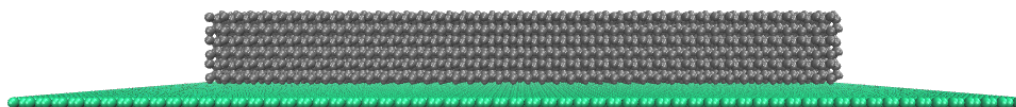
(a) System A.



(b) System B.



(c) System C.



(d) System D.

Figure S2: The four simulation systems from Table 2 with ice samples before detachment.

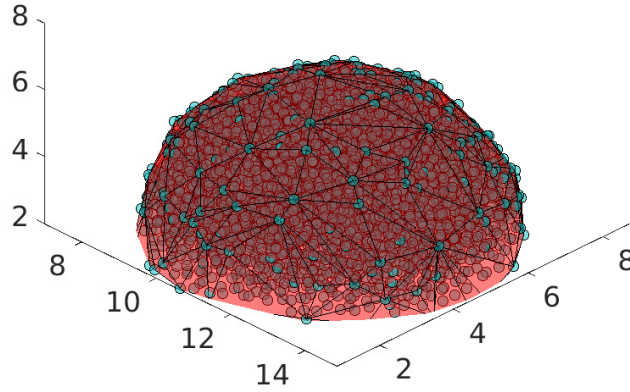


Figure S3: Illustration of the quickhull-algorithm for mapping the droplet, as developed by Khalkhali et al [S1]. The imaged droplet is for the normal sized system and original energy well depth ε_0 in Table 1.

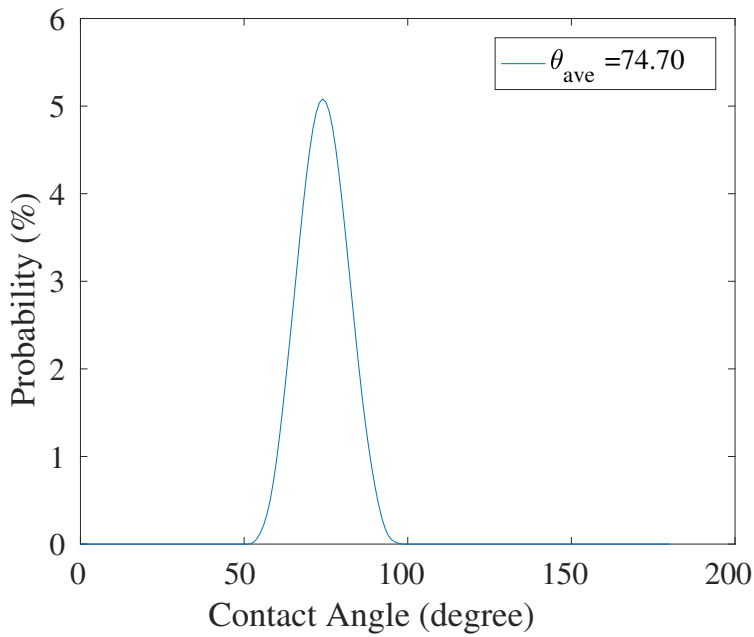


Figure S4: Illustration of the contact angle probability distribution, as developed by Khalkhali et al [S1], with the average value indicated. The contact angle distribution is for the droplet imaged in Figure S3, for system A and energy well depth ε_0 in Table 1.

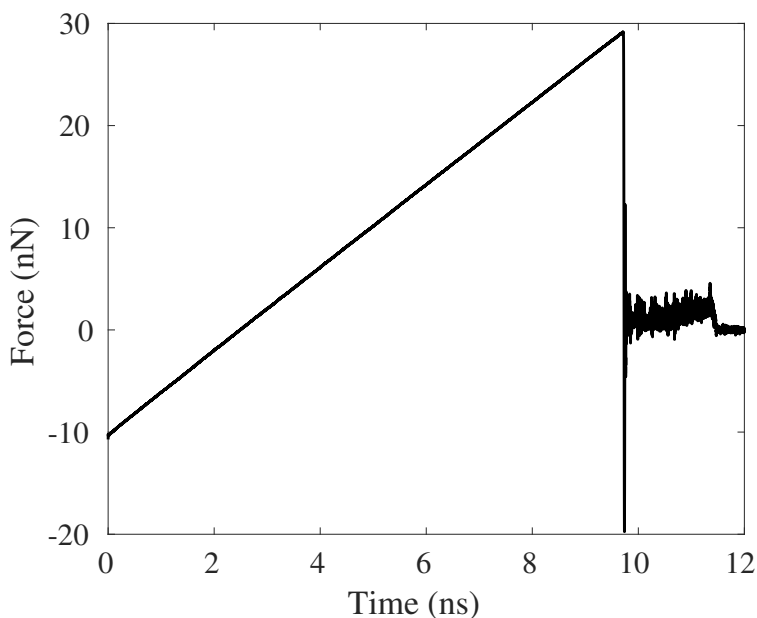


Figure S5: The resulting force-time curve when detaching an ice cube from the graphene surface to calculate the ice detachment stress, which is given by the first force maxima and dividing by the ice-solid area. The curve is for the ice cube analogous to the water droplet imaged in Figure S3, for the normal sized system and original energy well depth ε_0 in Table 1.

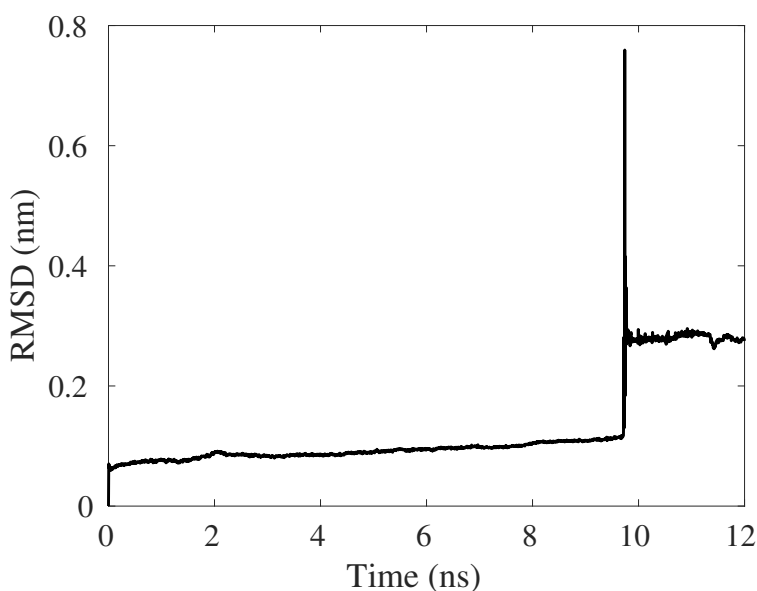


Figure S6: Root mean square deviation (RMSD) of ice for the ice detachment process with force curve in Figure S5. Even though the force from the harmonic oscillator presses the ice into the graphene surface at the start of the simulation, as seen by the negative force, the RMSD shows that the ice is not impacted by this pressing movement before it is pulled away from the graphene surface.

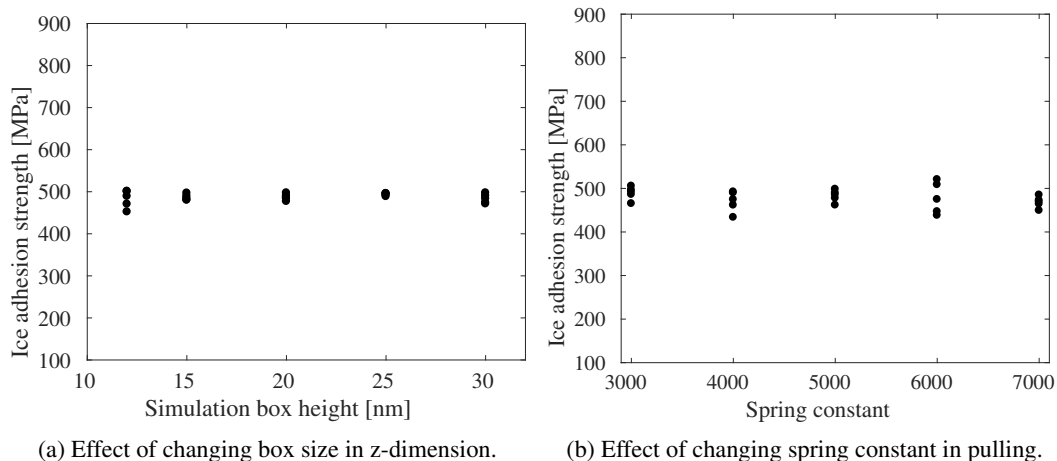


Figure S7: Effect of changing simulation parameters on the recorded ice adhesion strength. Simulations performed for normal system. Parameters utilized in the simulations otherwise were spring constant $k_B = 5000 \text{ kJmol}^{-1}\text{nm}^{-2}$ and box size 12 nm.

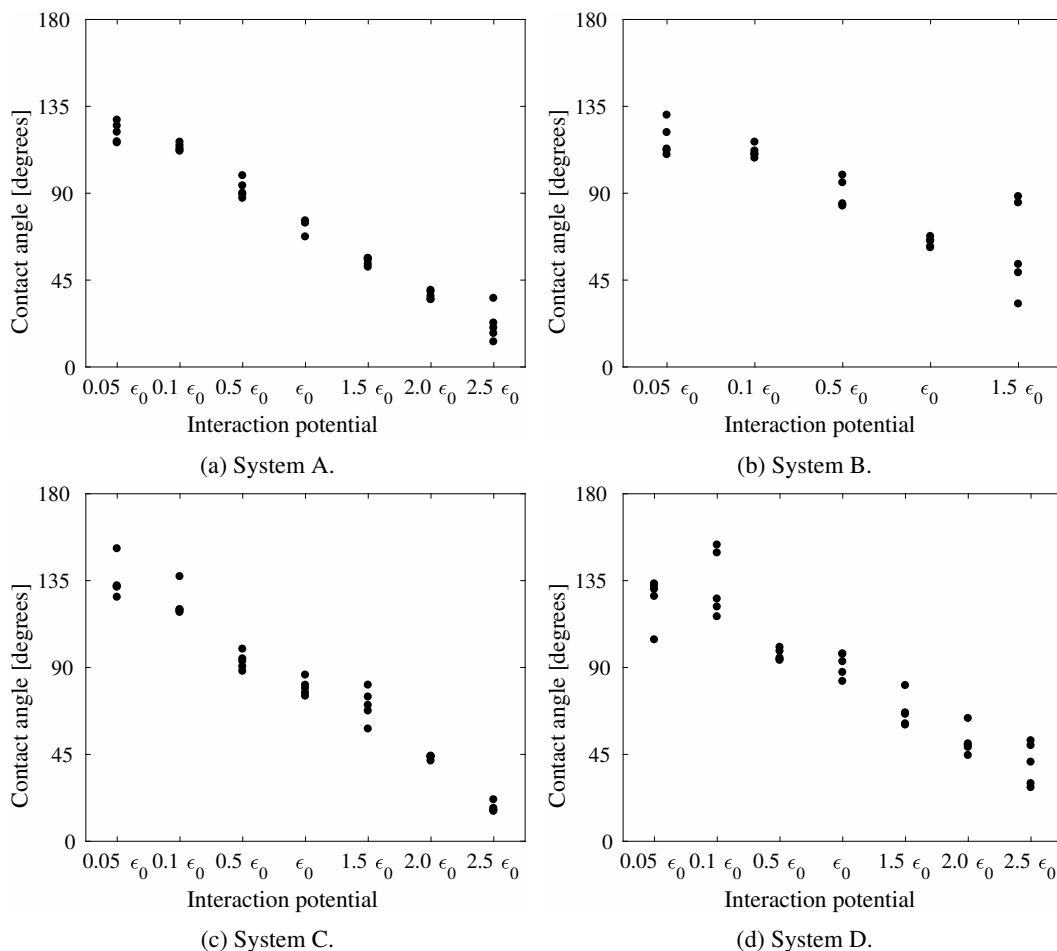


Figure S8: Contact angle as function of interaction potential ε for the four different system sizes.

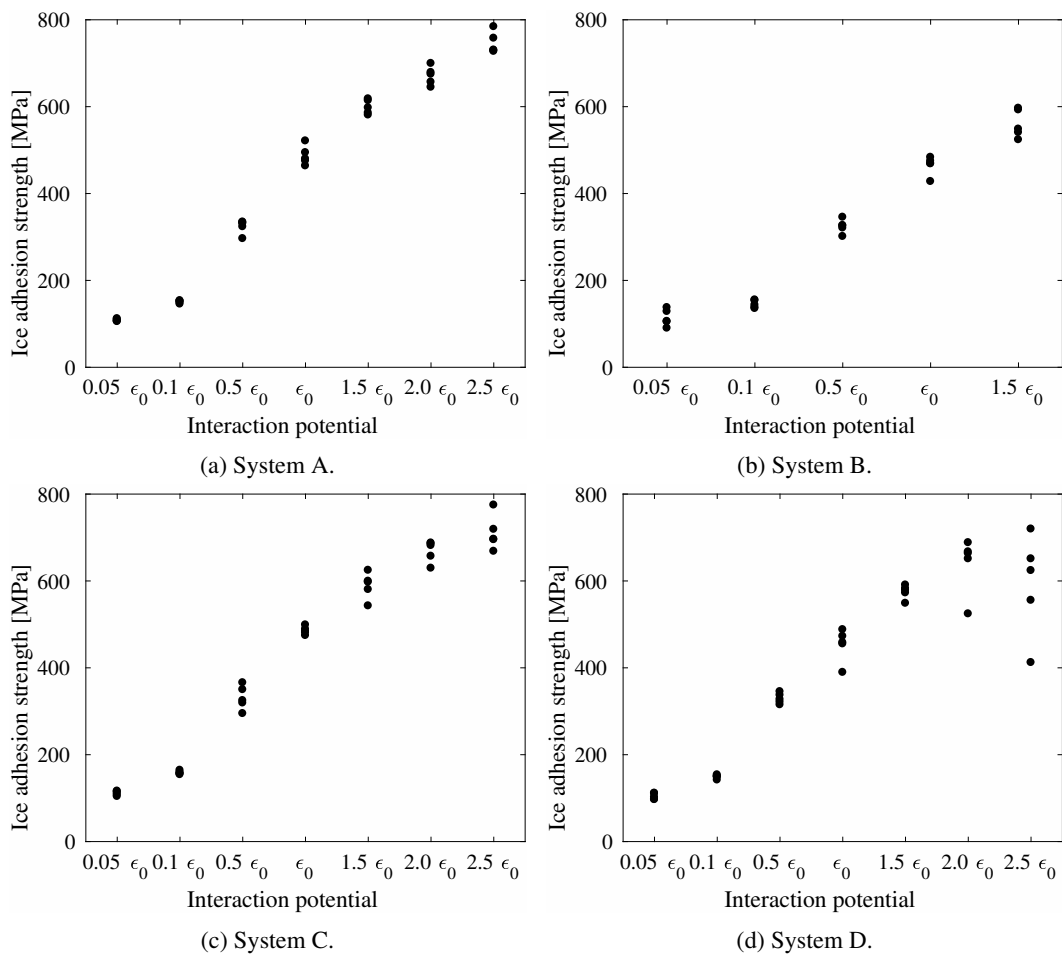
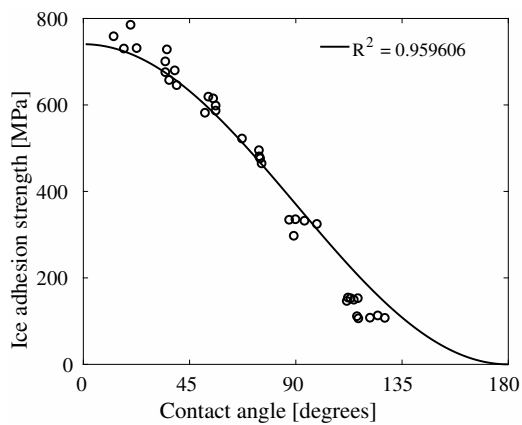
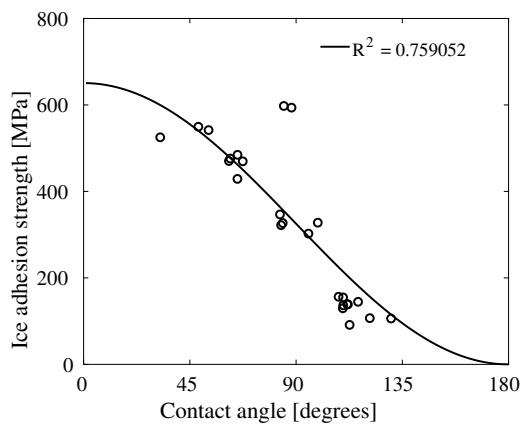


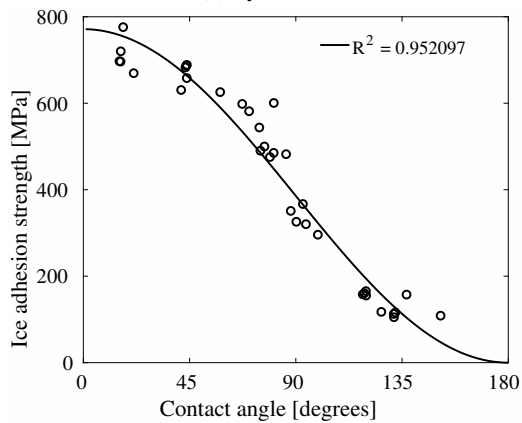
Figure S9: Ice adhesion strength as function of interaction potential ε for the four different system sizes.



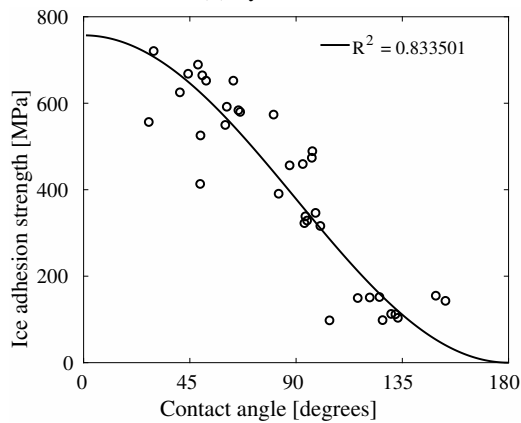
(a) System A.



(b) System B.



(c) System C.



(d) System D.

Figure S10: Ice adhesion strength as function of contact angle with fitting from equation (6) for the four different system sizes.

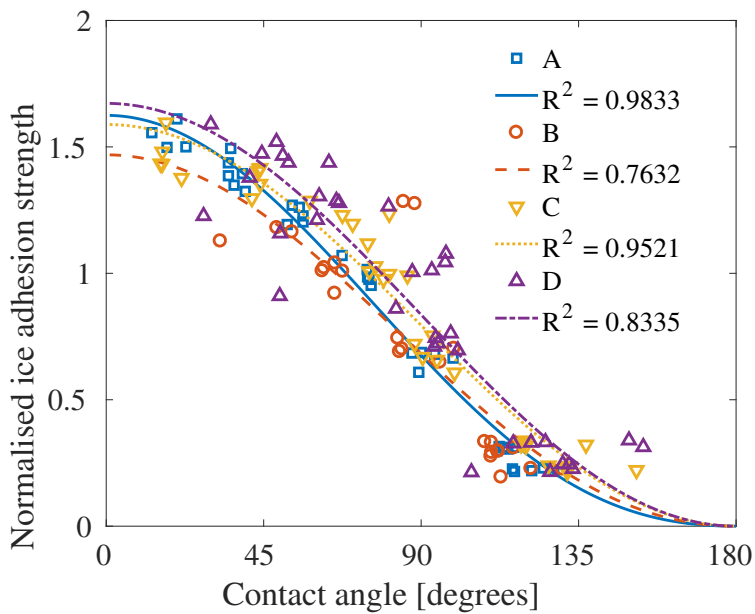
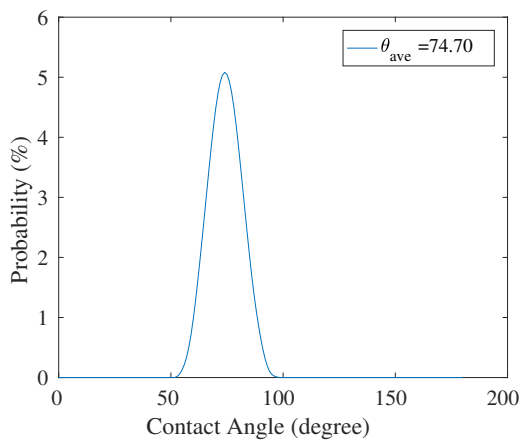
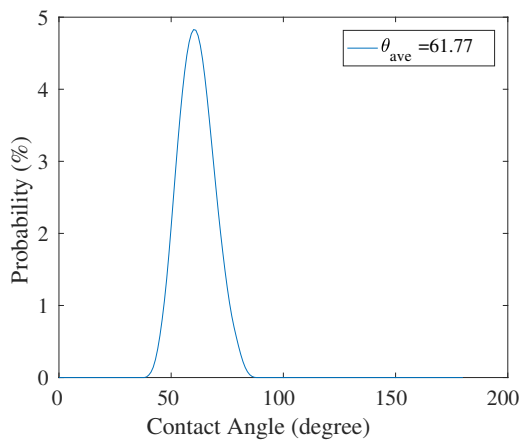


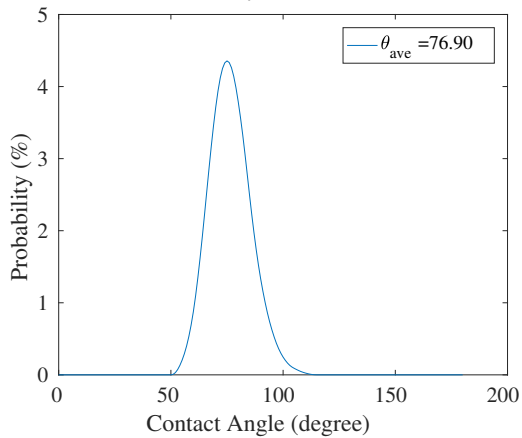
Figure S11: Overview of the fitting of the correlation from equation (8) of a cosine dependence added to the amplitude of the theoretical relation from equation (6) between the ice adhesion strength and water contact angle. Compared with the levels of significance of equation (6) from Figure 10, it can be seen that equation (8) does not offer sufficient improvement to warrant the more complicated relation.



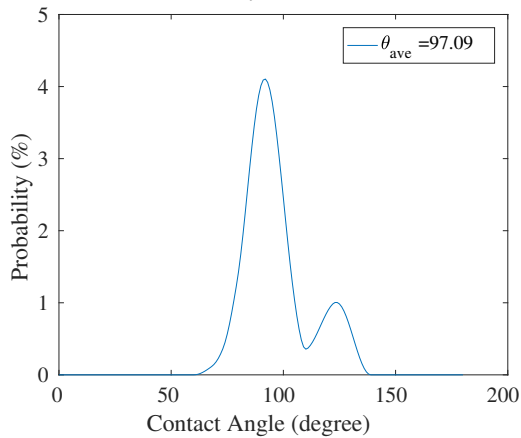
(a) System A.



(b) System B.



(c) System C.



(d) System D.

Figure S12: Contact angle distributions for the first simulations performed with interaction energy ε_0 for the four different system sizes.

Part II

Other publications

Appendix E

Book chapter

Comparison of icephobic materials through interlaboratory studies

Rønneberg, Sigrid, Caroline Laforte, Jianying He, and Zhiliang Zhang. 2020. In Kash Mittal and Chang-Hwan Choi (eds.), *Ice Adhesion: Mechanism, Measurement and Mitigation* (Wiley).

Comparison of icephobic materials through interlaboratory studies

Sigrid Rønneberg¹, Caroline Laforte^{2*}, Jianying He¹ and Zhiliang Zhang^{1*}

¹ Department of Structural Engineering, Norwegian University for Science and Technology (NTNU), NO-7491 Trondheim, Norway

² Anti-Icing Materials International Laboratory (AMIL), Université du Québec à Chicoutimi, 555 Blvd. de l'Université, Chicoutimi, Québec G7H 2B1, Canada

*corresponding author, Caroline.Laforte@uqac.ca; zhiliang.zhang@ntnu.no

Abstract

Unwanted icing can lead to dangerous situations for both daily life and infrastructure, and deicing methods in use today are either inefficient or expensive. Passive anti-icing surfaces, or icephobic surfaces, ensure that no ice is formed on the surface or structure, without the need to add external energy to the system. The most promising pathway towards icephobic surfaces is the lowering of ice adhesion strength, so that the ice is self-removed from the surface due to natural wind or its own weight. However, the physics of ice adhesion is not fully understood yet and developed low ice adhesion surfaces cannot be directly compared, both due to the formation of the ice and the measurement of the ice adhesion strength, which are not standardized. This chapter presents the results of an interlaboratory study where the ice adhesion strengths of two surfaces were tested in two different laboratory facilities with two types of ice, ensuring comparability between analogous ice types. The results display the same trends with some significant differences and indicate that the type of ice accretion is less important when the ice adhesion is low. Similarly, the difference between ice adhesion tests is smaller for low ice adhesion strengths. The standard deviations seem to scale with the absolute value of the ice adhesion strength. To fully compare different ice adhesion measurements and advance the scope of low ice adhesion surfaces, a reference test basis should be agreed upon, and more comparative experiments should be performed.

Keywords: ice adhesion, icephobic surfaces, adhesion tests, standard test, transferability

1. Introduction

Unwanted icing and ice accretion can lead to hazardous situations for both daily life and infrastructure [1]. Atmospheric icing may especially lead to numerous problems in telecommunications, road, marine, electrical distribution, and aviation transport networks [2]. It is well known that ice accumulation on aircraft causes loss of lift, increase in drag, faults in gauge readings, and great risk of stalling and potentially fatal crashes. Icing on structures can cause failure from static ice loads, dynamic effects, wind action, and damage caused by falling ice [3]. Icing on overhead power lines causes outages with serious socioeconomic impacts, as well as major damage to the power lines and infrastructure [4]. Examples of such aircraft accidents can be found in Table 1 [2].

Table 1 Selected fatal aircraft crashes caused by icing over the past five decades. Table from [2], references in original table.

Flight name	Date	Fatalities / Survivors	Causes
Surugut Aeroflot Antonov	Jan 22 nd , 1971	14/0	Icing due to bleed air valves being closed
Turkish Airlines Flight 301	Jan 26 th , 1974	66/7	Atmospheric icing, loss of control
Air Florida Flight 90	Jan 13 th , 1982	78/5	Faulty engine gauge readings caused by atmospheric icing and pilot error
Arrow Air Flight 1285	Dec 12 th , 1985	256/0	Icing conditions, weight and reference speed miscalculation
Air Ontario Flight 1363	Mar 10 th , 1989	24/45	Icing, improper de-icing procedures, pilot error
USAir Flight 405	Mar 22 nd , 1992	27/24	Icing, improper de-icing procedures, pilot error
American Eagle Flight 4184	Oct 31 st , 1994	68/0	Freezing rain
China Eastern Airlines Flight 5210	Nov 21 st , 2004	55/0	Ice accumulation, no de-icing done before take-off
Colgan Air Flight 3407	Feb 9 th , 2009	50/4	Inadequate procedures for airspeed selection and management during approaches in icing conditions.
Air France Flight 447	Jun 1 st , 2009	228/0	Obstruction of Pitot probes by ice crystals during flight

Currently, various methods are in use to remove or prevent the formation of unwanted icing. These techniques are categorized as thermal, mechanical or chemical methods. Thermal methods are the most used in both automotive and aerospace applications, where the iced elements cover relatively small areas [2]. The most common thermal methods apply thermal heating elements and fluids at high temperature. For marine applications, heating of the vessel and the application of hot water are commonly used methods for avoiding icing [5, 6]. The most common chemical methods utilize commercial fluids or salts that lower the freezing point of water, thereby reducing the icing [2, 7]. These methods are important for both aircraft and other transportation. Mechanical methods using pneumatic deicers, often called boots, piezoelectric cells and manual deicing are also widely in use [5].

Although the traditional methods for ice removal are functioning, they are either inefficient or expensive, in addition to often being environmentally hazardous. Due to the high amount of heat required to melt ice, thermal ice removal requires large amount of energy and effective strategies for removing the resulting water. Mechanical ice removal may cause damage to the structure as well as pose a hazard by itself, for instance when icing on power lines are removed with helicopters. Chemical methods often cause risks to the environment, such as around airports or increased amount of salt around roads.

The traditional ice removal methods are defined as de-icing methods, where the ice is removed after accretion. Anti-icing, on the other hand, is defined as ensuring that no ice accretion will take place. Passive anti-icing methods do not require external input of energy to induce early ice detachment or

to mitigate ice formation. By employing the natural forces, such as gravity, natural wind, or surface tension, the accreted ice never forms on the exposed surface or structure.

This chapter aims to give an overview of the status of comparison between icephobic materials to date, and to outline the possibility for direct comparison of low ice adhesion surfaces at present. We start with defining icephobic materials in section 2 and discussing the potential of low ice adhesion surfaces. Then, in section 3, we discuss different types of ice and the impact of different ice formation processes on the ice adhesion strength. In section 4, we discuss different ways of measuring ice adhesion strength and the effect of changing experimental parameters. The focus of the discussion is in section 5, where the results of recently conducted interlaboratory ice adhesion experiments are detailed and discussed with respect to the possibility of direct comparison between low ice adhesion surfaces and materials. Finally, the main points of the chapter are summarized in the concluding remarks.

2. Icephobicity and anti-icing surfaces

Passive anti-icing surfaces are specially developed to decrease the accretion and formation of ice on surfaces or structures. Ideally, such anti-icing surfaces would be solid, durable, easy to apply, inexpensive, efficient over a wide range of icing conditions, and applicable for several anti-icing applications [2]. To date, no material has been identified that is efficient enough to ensure adequate protection against ice accumulation, nor durable enough to be economically viable.

The term icephobic has been chosen analogously to hydrophobicity, which was introduced in the 17th century [2]. As expected from the word *phobia*, Latin for fear of a specific substance, hydrophobic surfaces have little or no interaction with water. Analogously, icephobic surfaces have little or no interaction with ice by definition. However, the exact thermodynamic definition of icephobicity is missing in the literature [8].

There are three different properties that are often associated with icephobic properties of a surface. These are 1) the prevention of water accumulation on the surface, 2) the delay in freezing of accumulated water, and 3) the lowering of the ice-solid adhesion so that ice can be easily removed [1, 8-11]. Any icephobic surface must display at least one of these properties to successfully mitigate hazardous icing. This chapter will focus on materials displaying the third property, called low ice adhesion surfaces.

The first property, the prevention of water accumulation on the surface, is often achieved by the use of superhydrophobic surfaces. Such surfaces display very high water contact angles, and facilitate the bouncing of incoming water droplets [11, 12]. It follows that if there is no water on the surface, there will be no ice formation. However, although superhydrophobic surfaces and icephobic surfaces have several important characteristics in common, it has been concluded that they are not directly correlated [8, 13-15]. Furthermore, superhydrophobic surfaces for icephobic applications have been found to degrade in high humidity environments and at low temperatures due to mechanical interlocking and frost formation [16, 17].

The second property, the delay in freezing of accumulated water, has been almost equally investigated as the removal of water from the surfaces. With a delay in nucleation of incoming water, the water may be removed with other means prior to freezing [10, 18]. This nucleation delay

may be achieved with superhydrophobic surfaces or other methods of surface texturing [10], or by the use of ice-binding molecules, which are also called anti-freeze proteins [19].

The third property is the lowering of the ice-solid adhesion, such that the ice is removed easily from the surface after formation. At sufficiently low temperatures, the formation of ice is inevitable [17]. As a result, it might be unreliable to base an anti-icing strategy on the avoidance of ice. Following this uncertainty, the reduction of ice adhesion strength might therefore be the most promising anti-icing strategy. With a sufficiently low ice adhesion, the ice accreted on a surface might shed merely due to its own weight or a natural wind action [14, 20].

As previously stated, the perfect icephobic material has not been discovered yet [2]. Consequently, the efficiency and viability of icephobic materials must be determined with the target application in mind, and suitable environmental conditions. In addition, the realistic types of ice must be identified, and the ideal ice adhesion test set-up must be decided and built. Furthermore, economic demands and durability must be investigated and discussed.

3. Ice formation and properties

Ice plays a large part in our atmosphere, as well as for both arctic and ocean environments. Although the water molecule is one of the simplest in chemistry, the properties of ice are not fully understood [21]. There are more than 15 forms of ice [22], which differ in their crystal structure and properties. However, only one form of ice exists in normal conditions on Earth, namely ice Ih. Polycrystalline ice Ih is obtained by freezing water at atmospheric pressure or by direct condensation from water vapor at temperatures above -100°C [21]. For the rest of this chapter, ice will refer to polycrystalline ice Ih.

Ice that is found naturally in the environment is a stochastic substance. The same applies to ice created in a laboratory setting. Due to several factors, including variable water flow before and during freezing, micro-scale roughness, and varying heat transfer processes, the repetition of an icing experiment does not produce identical ice samples [23]. Furthermore, the properties of ice are highly dependent on the environmental conditions, such as temperature, crystallization process, grain size, and cooling rate. As a result, the mechanical properties differ between various environmental conditions and generation methods.

3.1 Definitions of ice

There are many different definitions of ice. A selection of different definitions of ice has been collected in Table 2 which presents an overview of ice types for different application organized by field of application. As can be seen, there are several differing definitions for each type of ice, both between the application areas and even within one field of application. As each ice type has very different properties, such a lack of consensus might result in misunderstandings and challenge the comparability of research performed at different facilities.

Table 2 presents ice type definition from different publications and fields of application. From the overview of ice type definitions, it appears that there is a certain level of discrepancy between authors. An accurate description of ice types seems to be a first key point in an ice adhesion research project.

Table 2 Overview of ice types for different applications

Ice type	Definition	Field of application [ref]
Atmospheric icing	A general expression for any process of ice build-up and snow accretion on the surface of an object exposed to the atmosphere	Powerline icing [4]
Freezing rain	A type of precipitation icing that falls in liquid form but freezes on impact to form a coating of glaze ice upon the ground and exposed objects.	Powerline icing [4]
Glaze ice	A type of precipitation icing resulting in transparent ice accretion of density 700-900 kg/m ³ , sometimes with the presence of icicles underneath the iced structure or power line.	Powerline icing [4]
Precipitation icing	A type of atmospheric icing which is caused by rain droplets or snowflakes that freeze or stick to the exposed surface or structure.	Powerline icing [4]
Rime icing (in-cloud icing)	A porous, opaque ice deposit which is formed by the impaction and freezing of supercooled water droplets on a substrate. Density from 150-700 kg/m ³ .	Powerline icing [4]
Glaze ice	Clear, high density ice	Icing on structures [3]
In-cloud icing	Icing due to super-cooled water droplets in a cloud or fog	Icing on structures [3]
Precipitation icing	Icing due to either freezing rain or drizzle, or accumulation of wet snow	Icing on structures [3]
Rime ice	White ice with trapped air	Icing on structures [3]
Freezing drizzle	Water droplets that freeze on impact with the ground or with objects on the earth's surface or with aircraft in flight	Sea-ice [24]
Glaze ice	A generally homogeneous and transparent deposit of ice formed by the freezing of supercooled drizzle droplets or raindrops on objects the surface temperature of which is below, or slightly above, 0°C. It may also be produced by the freezing of non-supercooled drizzle droplets or raindrops immediately after impact with surfaces the temperature of which is well below 0°C.	Sea-ice [24]
Hoarfrost	A deposit of ice having a crystalline appearance, generally assuming the form of scales, needles, feathers, or fans; produced in a manner similar to dew but at temperatures below 0°C.	Sea-ice [24]
Rime ice	A deposit of ice composed of grains more or less separated by trapped air, sometimes adorned with crystalline branches, produced by the rapid freezing of supercooled and very small water droplets.	Sea-ice [24]
Glaze ice	Hard, bubble-free and clear ice, generated under wet growth conditions and where surface temperature is above 0°C	Sea-ice [25]

Bulk water ice	Water frozen in freezer or on a Peltier plate at constant temperature, which may vary from freezer to freezer. Results in a clear and mostly bubble-free ice.	Low ice adhesion surfaces [26]
Glaze ice	Temperatures above -10°C, freezes from water film after droplets have spread out. Has the highest possible ice density	Low ice adhesion surfaces [27]
Glaze ice	Ice frozen on silicone mold at -5°C for 24 hours, resulting in a smooth clear structure. Ice that does not freeze on impact on aircraft.	Low ice adhesion surfaces [28]
Glaze ice	Ice formed under glaze conditions, where the impinging droplets form a liquid film that freezes to form the ice. Latent heat release from formation is not sufficient to completely freeze the water on impact.	Low ice adhesion surfaces [29]
In-cloud ice	Spraying supercooled micro-droplets of median volume diameter 27 μm and liquid water content 2.5 g/m^3 in a wind tunnel of wind speed typically 15 m/s at temperatures of -10°C.	Low ice adhesion surfaces [26]
Precipitation ice	Supercooled droplets of median volume diameter 324 μm as precipitation in a cold room with temperature typically -10°C, impact velocity calculated to be 5.6 m/s .	Low ice adhesion surfaces [26]

For ice adhesion research, the biggest difference between ice types is between impact ice and non-impact ice [30-32]. While non-impact ice is created from stationary water, impact ice is generated from water with a non-zero impact velocity. Typical impact ice types are atmospheric ice, precipitation ice and in-cloud ice. For unwanted icing of this sort, either the water itself has a non-zero velocity, for instance in case of wind or freezing rain, or the structure or item which experiences the icing is moving with respect to a cloud or similar, such as aircraft or wind turbine blades. For most of anti-icing applications, and especially those of low ice adhesion surfaces, impact ice is the most realistic type of ice during operation. As a result, low ice adhesion surfaces intended for anti-icing application should be tested with impact ice types to ascertain the functionality.

Non-impact ice comes in many different forms, but is most often similar to bulk water ice in Table 2. This type of ice is the simplest to make, as the only needed equipment is a freezer and a syringe to administer water in a mold. As a result, this ice type is the most frequently used in low ice adhesion research. Naming of this ice varies from bulk water ice to static ice, freezer ice, refrigerated ice, and even glaze ice in some publications [2, 28, 32, 33].

3.2 The effect of ice type on ice adhesion strength

That bulk water ice is most frequently used in low ice adhesion research raises the question whether the reported ice adhesion strengths are realistic when applied to industrial applications. Impact ice types react differently from non-impact ice types, as impacting water easily experiences a Cassie-to-Wenzel transition on impact [34]. Following this transition, the droplet spreads out over the surface and penetrates the surface texture. As a result, the extent of mechanical interlocking increases dramatically, which also increases the measured ice adhesion strength. As the bulk water ice has a zero water impact velocity and thus does not experience the Cassie-to-Wenzel transition as easily as

impact ice types, it is not unlikely that the reported ice adhesion strengths are unnaturally low when tested with bulk water ice in laboratories.

It has been hypothesized that the type of ice is directly linked to the ice adhesion strength since 1979 [35]. This hypothesis has been strengthened recently by testing the ice adhesion strength of the three most common ice types with the same ice adhesion test set-up [26]. The tests were performed in the facilities of the Anti-icing Materials International Laboratory (AMIL), Canada, which is the only laboratory in the world approved by ISO 9001:2015, PRI AC3001 and PRI AC3002 to qualify de-icing and anti-icing fluids for aircraft applications [36]. All tests and results were further described in the relevant publication [26].

The three ice types tested correspond to bulk water ice, in-cloud ice and precipitation ice in Table 2. All ice types were formed on bare aluminum 6061-T6 bars polished with Walter BLENDEX Drum fine 0724 M4. Icing occurred over an area of 1100 mm² for all ice types. The environmental conditions were constant for all tests, and the temperature was -10°C. All surfaces had reached the test temperature before icing, and all water was deionized with resistivity 18 MΩ.cm and had initial temperature of 4±1°C at the beginning of icing. All ice adhesion tests were performed with the centrifuge adhesion test (see section 4.1, section 5.2 and Figure 13).

Precipitation ice was created in a cold room by freezing drizzle from an overhead nozzle. The water droplets had median volume drop diameter of 324 μm and impact speed estimated to 6 m/s due to gravity alone. The surfaces were subjected to icing for 33 minutes and kept in a cold room for 1 hour after icing for the ice to become thermally stable. The ice adhesion test was performed in the same cold room. Precipitation ice is illustrated in Figure 1.

In-cloud ice was created in a closed-loop icing wind tunnel. Here, super-cooled microdroplets of water with median volume drop diameter of 27 ± 3 μm were sprayed with a wind speed of 15m/s and liquid water content of 2.5 g/m³. The icing time was 8 minutes and 15 seconds, and the surfaces and ice were transferred immediately to the cold room after icing. Consequently, a systematic error of ex situ icing exists for this ice type. Similar to precipitation ice, the in-cloud ice samples were kept in the cold room for 1 hour to ensure thermal stability before ice adhesion tests were performed. In-cloud ice is illustrated in Figure 2.

Bulk water ice was created by freezing water in silicone molds in the cold room. The silicone molds were created from Smooth-On [37], under similar conditions as for precipitation ice. The molds were crafted to give the same icing area as the other ice types. 10 mL of water were inserted into the molds, and the aluminum surfaces were placed on top at the water-air interface. The icing time was at least 2 hours. The ice adhesion tests were performed immediately after the removal of the molds from the ice sample, and the test was performed in situ in the same cold room. Bulk water ice is illustrated in Figure 3.



Figure 1 Example of precipitation ice. Picture also published in [26].



Figure 2 Example of in-cloud ice. Picture also published in [26].



Figure 3 Example of bulk water ice. Picture also published in [26].

Ideally, the ice adhesion strength should be similar for all three ice types tested. If that were the case, there would not be any difference in testing low ice adhesion surfaces with ice created in different facilities, even if the ice type varied. However, this is not the cause the results show.

In Figure 4, the ice adhesion strengths are shown for all three types of ice. The mean values are given in Table 3, together with the standard deviation and the number of samples. It can be seen that there is a significant difference when comparing the ice adhesion strengths of the three ice types, where precipitation ice has a higher ice adhesion strength than the other two and bulk water ice is the easiest to remove. Bulk water ice only displays 40 % of the adhesion of precipitation ice under similar conditions, and the standard deviation is quite high for all three ice types.

The high inherent variation in measured ice adhesion strengths shown in Table 3 are in accord with other publication [38]. For a study intended to determine the cause of variation in ice adhesion strength measurements utilizing a new methodology with a lap joint shear rig, the measured standard deviation remained at 23 % and 33 % for two different test campaigns [29]. Similarly, a previous test campaign with more than 200 data points resulted in standard deviations of 13 % and 23 % for steel and aluminum, respectively [39]. This inherent variation in measured ice adhesion strengths for all similar parameters might be a result of the aforementioned stochastic behavior of ice as a material.

Several analytical models have been proposed to describe ice adhesion strength on a reference aluminum surface, among these are the one based on electrostatic interactions at the interface [27] and the one based on the presence of a liquid-like layer at the ice-solid interface [40]. Both models include factors accounting for changing ice type and predicting that an increased porosity of the ice leads to a decreased adhesion force as well. An increased porosity of ice is directly related to the amount of air bubbles in the ice sample [41], and a higher fraction of micrometer-size air bubbles results in a more opaque ice [42]. Therefore, the opaquer ice types have a higher porosity, and is expected to have a lower adhesion to a given surface.

However, as seen from Figure 4, the ice type with the highest porosity, which is precipitation ice, displays the highest ice adhesion strength. This result is in opposition to the analytical models, as well as previously assumed relations between the different types of ice in other publications [28, 43]. The discrepancy between previous assumptions and analytical models, and the experimental results in Figure 4 substantiate the lack of knowledge about ice physics as well as about the fundamental mechanisms of ice adhesion.

Table 3 Results of ice adhesion tests for the three different ice types, including the number of samples tested with each ice type. Data taken from [26].

Ice type	Mean ice adhesion strength [MPa]	Standard deviation [MPa (%)]	# samples
Precipitation ice	0.780	± 0.102 (13.1 %)	30
In-cloud ice	0.590	± 0.119 (22.5 %)	60
Bulk water ice	0.284	± 0.083 (28.2 %)	36

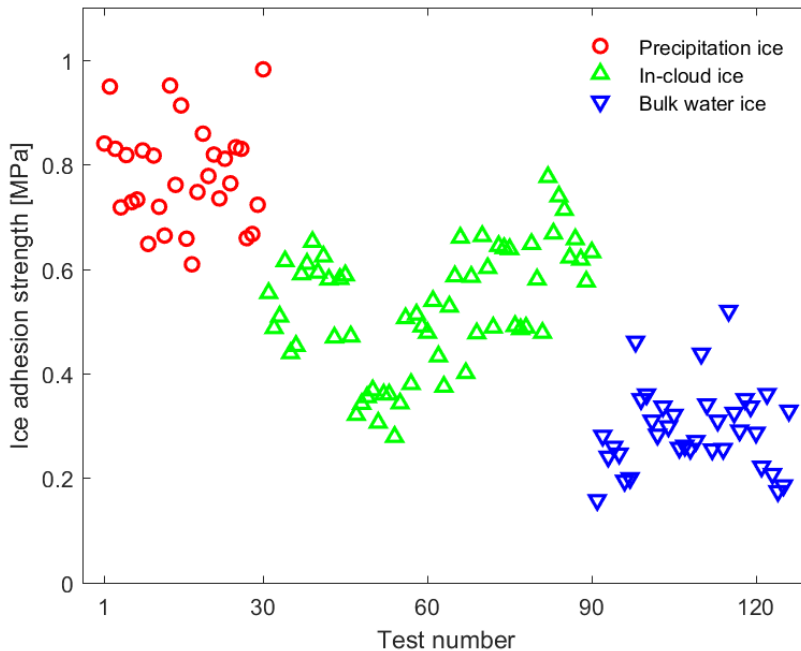


Figure 4 Measured ice adhesion strength for each performed test for the three ice types. Adapted from [26].

4. Testing ice adhesion

Ice adhesion strength is measured by detaching an ice sample from a given surface. The most common definition of ice adhesion strength is the maximum detachment force divided by the contact area of the ice, i. e.,

$$\tau = \frac{F}{A} \quad (1)$$

However, although the basic definition of ice adhesion strength is agreed upon, the testing of ice adhesion strength varies from facility to facility. At present, there are no applicable standards for the testing of ice adhesion strength. As a result, each research group develops its own custom-built testing rig [11, 31, 44-47]. In Table 4, the different ice adhesion tests that have been included and

discussed in some recent reviews can be seen. This overview illustrates the multitude of different available ice adhesion tests, and the many variations of each test.

Table 4 Overview of ice adhesion tests included in recent reviews. From [38].

Review paper (year) [Ref]	Included ice adhesion tests
Sayward (1979) [35]	Pure tensile test, pure lap shear test, flat plate torsion shear test, cylinder torsion shear test, peel test, blister test, cleavage test, cone test, flexed sheet test, small area tensile test, lap tensile-shear-test, multi flat-plate torsion-shear test, axial cylinder shear test, roll-peel test, and combined mode tests
Kasaai and Farzaneh (2004) [48]	Simple shear test, lap shear test, tensile test, combined shear and tensile test, peel test, impact test, laser spallation test, scratch test, atomic force microscopy (AFM) test, and electromagnetic tensile test
Makkonen (2012) [5]	U.S. Army Cold Regions Science and Engineering Laboratory (CRREL) test arrangement (torque test), and VTT Technical Research Centre of Finland test arrangement (horizontal shear test)
Schulz and Sinapius (2015) [31]	Tensile test, transverse shear test, bending test, and centrifugal test
CIGRE TB631 (2015) [4]	Pull test, centrifugal chamber test, sliding weight test, ice push off test, and conductor ice pull-off test
Work and Lian (2018) [30]	Centrifuge adhesion test, calculated centrifuge adhesion test, instrumented centrifuge adhesion test, push test, rotational shear test, 0° cone test, lap shear test, tension test, beam tests, blister test, laser spallation test, and peel test

4.1 Description of selected common ice adhesion tests

Two of the most common tests to measure ice adhesion strength are the centrifugal adhesion test and the shear test [38]. Both test methods utilize the basic equation of ice adhesion strength, but they measure the peak detachment force in different manners.

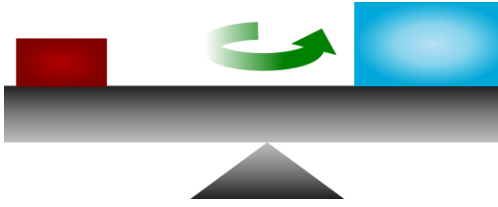


Figure 5 Schematic overview of centrifugal adhesion test.



Figure 6 Schematic overview of the horizontal shear test, also called push test.

A schematic overview of the centrifugal adhesion test can be seen in Figure 5. This test utilizes the centrifugal acceleration to apply the detachment force by rotating a small ice sample with a constant acceleration rate. By recording the moment of detachment with piezoelectric cells, the instant angular velocity at detachment can be found. This angular velocity is then used to calculate the detachment force through the equation

$$\tau = \frac{F}{A} = \frac{m_{ice}\omega^2 r}{A} \quad (2)$$

where F is the centrifugal force, A is the ice-solid contact area of the detached ice, m_{ice} is the mass of the detached ice, ω is the angular velocity at the time of detachment, and r is the radius of the beam at the center of mass for the ice sample. Centrifugal adhesion test is simple and inexpensive but requires a more complex set-up than other tests. Furthermore, the centrifugal test is only compatible with one beam shape and may be damaging to the surface coatings as well as the ice sample itself [48], and the stress distribution is not uniform over the interface during testing [31]. On the other hand, the centrifugal adhesion test results in more repeatable measurements than many other methods, and has a very high probability of adhesive failure [49].

To account for some of the disadvantages of the centrifugal adhesion test, several adaptations of the test method have been developed recently [30]. The calculated centrifuge adhesion test determines the adhesion strength based on the length of a shed piece of ice from a rotor, and is considered an improvement because it enables testing in situ, without handling or moving the ice sample after freezing. The instrumented centrifuge adhesion test is another adaptation and enables changing of rotors for ice detachment. With this set-up, the impact velocity can be varied by varying the speed of the rotor. The rotors spin at a constant velocity and impact ice grows on the spinning rotors until the ice is shed due to its weight. Although no centrifuge adhesion test can provide stress-strain curves from the ice detachment, the instrumented centrifuge adhesion test can record total interfacial stress as a function of time. However, the change in the stress distribution is higher for this type of centrifuge adhesion test, as the ice grows on the rotors while they are rotating [30].

Shear tests constitute the most diverse group of ice adhesion tests. A shear test is defined as a test in which the load is distributed over the ice sample in an apparently uniform manner, meant to distribute the force evenly at the interface with the direction of motion parallel to the surface [30]. The simplest and most common shear test is the horizontal shear test, also called the push test, which can be seen in Figure 6. The horizontal shear test utilizes a force probe to detach the ice from the surface, which records the moment of ice detachment as a sudden decrease in registered force.

Simple shear tests utilizing a force probe to either pull or push the ice sample can be found in many configurations. The vertical shear test, for instance, is nearly identical to the horizontal shear test in

Figure 6, except that the vertical shear test is oriented 90° so that the ice is pushed downwards and falls at the moment of detachment.

There are several different set-ups of these types of shear tests or push tests available, and they are both simple and economical to perform. However, due to the effect from the force probe, the tests do not induce a uniform stress distribution at the ice-solid interface. As a result, finite element analysis should be performed to correct the measured ice adhesion strength against the stress distribution [31]. Furthermore, due to the set-up of the simple shear tests utilizing force probes, it is difficult to apply them to impact ice type [30].

Other types of shear tests are also in common use, such as the rotational shear test, the lap shear test, the pull test and the 0° cone test. One example of such shear tests is the modified lap joint test set-up, utilized to determine the cause of the high variation in ice adhesion for impact ice [29]. In such a shear test, the ice sample is frozen on the surface and placed in a sandwich configuration with teeth fastened at the free ice surface by slight heating of Peltier elements. To detach the ice, the teeth are gradually displaced upwards, parallel to the surface, giving a mode II-failure of the ice at detachment. Other shear tests use similar principles, exemplified by the hollow cylinder and rod with ice in between such as in the 0° cone test.

There are many different ice adhesion test set-ups in use daily. The centrifugal adhesion test is utilized by AMIL, while the 0° cone test is utilized by the Cold Regions Research and Engineering Lab (CRREL) [50]. A more standard horizontal shear test is used by both VTT [5] and Meuler et al. [44], of which the latter set-up has been used as an inspiration for several other low ice adhesion test facilities [38]. Furthermore, there have been several attempts to standardize the measurement of ice adhesion strength. Mulherin et al. [51] proposed a standard shear test in 1998, utilizing the 0° cone test. In 2014, Wang et al. [45] proposed a vertical shear ice adhesion test utilizing only commercially available instruments. A similar attempt was made in 2019 by Irajizad et al. [47], using a horizontal shear test.

4.2 Adhesion reduction factor

It is a challenge to obtain ice adhesion values that are both reliable and precise. As seen in section 3.2, the variation is often high, and it is difficult to compare different existing icephobic materials and candidates for future development. Two strategies for comparison are to compare potential icephobic surfaces in a single laboratory facility, or to compare icephobic surfaces tested at different laboratory facilities with each other. The first strategy for comparison is possible at present with the Adhesion Reduction Factor (ARF) which will be discussed in this section. The second strategy for comparison will be dealt with in section 5.

The ARF was first introduced by AMIL in 2003, with the aim to normalize ice adhesion strength values between different materials and methods. The ARF is calculated as the ratio of the ice adhesion measured for a reference surface, often aluminum, to the ice adhesion of the icephobic surface. Following the tests, the icephobic performance in terms of reduced ice adhesion strength is evaluated such that:

- ARF > 1: Reduction of ice adhesion strength, higher numbers indicate more icephobic
- ARF < 1: Increased ice adhesion strength when compared to aluminum

Since 2003, 345 different coatings have been tested and evaluated at AMIL under similar conditions. In the context of this manuscript, the ice type tested has been precipitation ice as described in Table 2 with temperature at -8°C , and the test method was the CAT from Figure 5 at temperatures of -10°C . The range of ARF results is displayed in Figure 7, which includes freshly applied solid coatings, embedded polymeric coupons, viscous greases, and surface treatments. The tests have been classified by the year of the test. Every coating tested has been compared to an aluminum 6061 T6 reference surface, with an average roughness of $0.8\ \mu\text{m}$ and a water contact angle of approximately 75° . The average bulk shear stress measured is about $0.51\ \text{MPa} \pm 7\%$ [52]. The standard deviation of ARFs is $\pm 15\%$, based on 6 icing repeats.

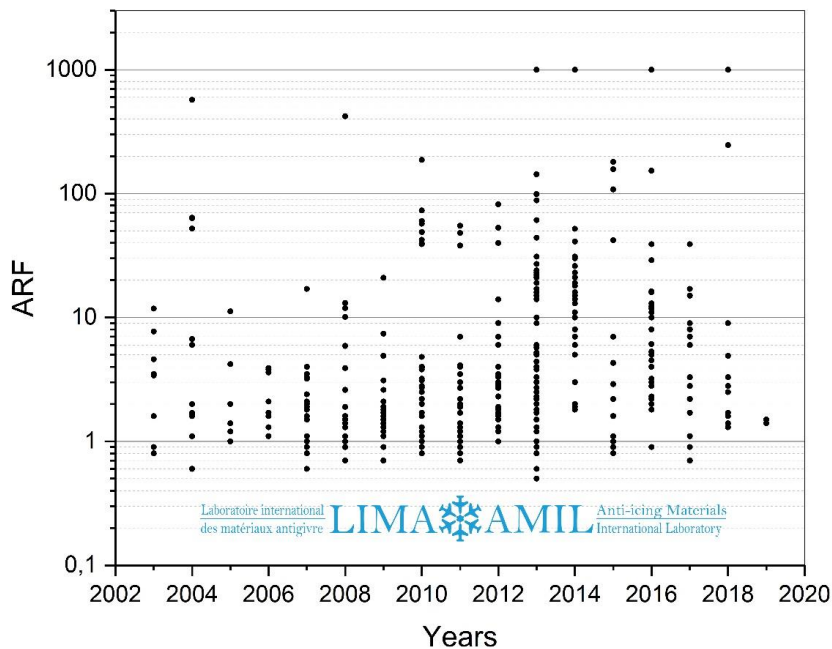


Figure 7 Adhesion Reduction Factors (ARFs) from AMIL CAT tests, where icephobic coatings were compared to aluminum surfaces, tested at a temperature of -10°C with precipitation ice generated at temperature of -8°C .

Overall, the coatings tested over the years display similar performance within a wide range of ARF values, ranging from 0.5 to 1000. This range corresponds to stresses from about 0.8 to 0.0005 MPa. Most of the candidates reduce ice adhesion by a factor between 1 and 5 compared to bare aluminum. Only 23% of the solid coatings demonstrate significant reductions of ice adhesion strength with ARFs above 10. Grease-based materials have been found to be the most efficient because the mechanical anchorage of ice was inhibited by the viscous nature of the coatings. However, their use is limited because they are non-permanent, and their efficiency has been shown to be affected by wear. This effect of wear on the icephobic performance needs to be assessed before use.

Since 2005, many other laboratories and research groups have also expressed their results in terms of ARFs [2]. However, nearly every group uses different definitions or experimental protocols. Therefore, ARF should only be used within a specific number of criteria. ARF should be applied only to compare an icephobic material to its reference substrate iced under the same icing conditions, or to repeat the measurement with the reference substrate at each test and specify the frequency of reference measurements during the test campaign. The soundness of ARF results is based on that intrinsic experimental variations are attenuated using reference controls.

4.3 Effect of experimental parameters

Most publications do not include all their experimental data and details. As a result, it is difficult to compare reported ice adhesion strengths. Ice adhesion strengths in the literature vary with up to three orders of magnitude, and even ice adhesion strengths for the same surface, for instance aluminum or steel, vary within more than one order of magnitude [30, 38].

In Table 5, an overview of available experimental parameters from a selection of publications can be seen. All these publications focus on low ice adhesion studies, testing different surfaces with the aim to achieve ice adhesion strength as low as possible. All the ice adhesion tests were performed with the simple shear test, and all ice types tested were equivalent to bulk water ice in Table 2. This table clearly shows how much the experimental conditions vary within the ice adhesion research community for one common type of ice adhesion test.

*Table 5 Overview of experimental conditions for a selection of different ice adhesion studies with bulk water ice. All studies utilized a shear test to measure the ice adhesion strength. Temperature and time refer to the freezing temperature and freezing time of the bulk water ice, respectively. Probe distance and impact speed have been included where given. *denotes where the icing time was unspecified. As the studies tested different low ice adhesion surfaces, the reported ice adhesion strengths are not directly comparable. Table from [38].*

Shear test	Temperature	Freezing time	Probe distance	Probe loading rate	Ice adhesion strength	Ref.
Vertical	-15°C	3 h	2 mm	0.05 mm/s	50 kPa	Wang et al. [53]
Vertical	-15°C	24 h	3 mm	0.1 mm/s	5-7 kPa	He et al. [54]
Horizontal	-10°C	15 h	2 mm	0.5 mm/s	165-510 kPa	Meuler et al. [44]
Horizontal	-20°C	1 h	1 mm	0.8 mm/s	5-2 kPa	Beemer et al. [20]
Horizontal	-25°C	1 h	3 mm	0.1 mm/s	1 kPa	Irajizad et al. [47]
Horizontal	-4°C	-	1 mm	0.001 mm/s	2.5 kPa	Mitridis et al. [55]
Horizontal	-10°C	*	1 mm	-	0.15 kPa	Golovin et al. [56]
Horizontal	-12°C	12-14 min	-	0.18 mm/s	12 kPa	Upadhyay et al. [33]
Horizontal	-20°C	*	-	-	252 kPa	Hejazi et al. [8]

Horizontal	-15°C	5 h	-	-	27 kPa	Dou et al. [57]
------------	-------	-----	---	---	--------	-----------------

4.3.1 Temperature

There is a general trend of increasing ice adhesion strength with decreasing temperature during ice adhesion testing and ice formation [30, 58]. However, there are not enough data for a specific relation to be settled. The effect of temperature on ice adhesion strength is partly due to the effect of temperature on the properties of the ice itself [6], and partly due to the changing interaction mechanisms at the interface [5]. For instance, temperature has a direct impact on the behavior of the liquid-like layer at the ice-solid interface [40]. For the ice itself, the temperature is a factor when determining what sort of icing occurs, for instance in the division between different types of impact ice [3]. Another important aspect of the temperature is whether the tested ice has been allowed to reach thermal equilibrium before testing [7], and whether the samples are created in situ, or handled in some way between ice formation and ice adhesion testing. For ice adhesion tests performed in the same cold room or in the same set-up throughout both ice formation and ice adhesion testing [56], the thermal conditions remain similar for the entire process. However, when the ice is moved between facilities, rooms or set-ups, changing thermal conditions might induce systematic errors. For instance, ice adhesion strength might be highly dependent on the thermal mismatch between the adhering surface and the ice, especially for ice samples with less than 1 hour freezing time [46].

4.3.2 Ice sample size

The effect on ice adhesion strength of ice sample size has not been systematically investigated. Consequently, the sample size of ice for ice adhesion testing varies from nanoscale droplets to large scale applications [5]. Fracture behavior of ice, and thus the ice adhesion strength as well, is determined largely by the grain size and thickness of the ice [59]. However, whether the measured ice adhesion strength depends on the ice sample size during ice adhesion testing is not agreed upon [20, 31, 60]. Furthermore, not all ice adhesion publications disclose the dimensions of the ice samples.

There are several ways that changes in ice sample size might impact the ice adhesion strength. In Figure 8, four different realistic ice samples tested in a horizontal shear test are shown together with a possible probe placement. The four cases illustrate different probe placements, different ice-solid interface areas and different ice sample heights. The effect of probe distance will be dealt with in section 4.3.3.

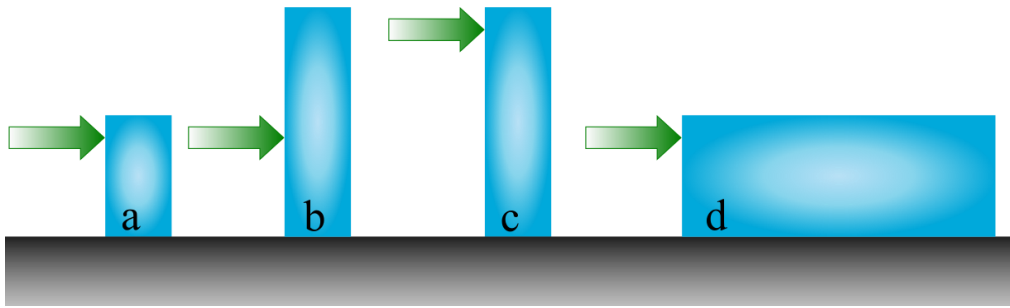


Figure 8 Illustrations of different realistic ice sample sizes in a horizontal shear ice adhesion test. The four examples are: a) typical ice sample, b) ice sample with a larger height, c) ice sample with larger height, and a greater distance between the force probe and surface, and d) ice sample with a longer length dimension.

A recent study [56] tested the effect of changing the ice-solid surface contact area on the ice sample in the length direction, as illustrated in the difference between a) and d) in Figure 8. The study tested lengths from 0.5 cm up to 1 m, with the same height and width of the samples. It was found that the required detachment force for the ice sample increased with the length of the sample as predicted by equation (1), up to a critical value which depended on the surface. Above this critical value, the maximum detachment force remained constant even for longer ice samples.

Although this study seems to confirm the impact of ice-solid contact area, and partly ice sample size, on the measured ice adhesion strength, the study has some weaknesses. It only investigates one type of ice with one type of ice adhesion test and does not investigate any other changing ice sample dimensions. As such, the dependence of ice adhesion strength on the length of the sample does not necessarily describe the dependence of ice adhesion strength on the ice sample size in its entirety. To fully ascertain the effect of ice-solid contact area on the ice adhesion strength, systematic testing is required, which needs to include different types of grain sizes together with different ice types and ice morphologies.

Another aspect of the ice sample size is the height of the ice sample, which is particularly important when utilizing the vertical shear test to measure the ice adhesion strength. For this test, where the tested surface is placed normal to the floor, the total force on the ice sample during detachment is a combination of the force probe and the effect from gravity. The effect of gravity depends wholly on the height of the sample, and the percentage of the detachment force due to gravity increases for tall ice samples on low ice adhesion surfaces [38]. For bulk water ice, and surfaces with ice adhesion strength higher than 20 kPa, the effect of gravity will not exceed 5% for ice samples with height lower than 10 cm. However, when ice sample height is above 10 cm, or the surface displays ice adhesion strengths below 10-20 kPa with a vertical shear test, so the effect of gravity should be accounted for.

4.3.3 Force probe placement and loading rate

It has been shown that the placement and loading rate of the force probe during simple vertical and horizontal shear tests greatly impact the measured ice adhesion strength [45, 53]. In Figure 9, the effect of the distance between the force probe and the surface can be seen. It shows the measured ice adhesion strength for bulk water ice on a poly(methyl methacrylate) (PMMA) surface tested with the vertical shear test for four different probe distances, where the force probe is situated from 1

mm to 4 mm away from the surface. When applying a linear fit to the data, it is seen that increasing the distance between the surface and the force probe by 1 mm, decreases the measured ice adhesion strength by 161 kPa on average. This change is illustrated in Figure 8 from b) to c). This decrease is a result of a mixed shear/tensile mode as the probe distance increases, inducing a bending moment [45].

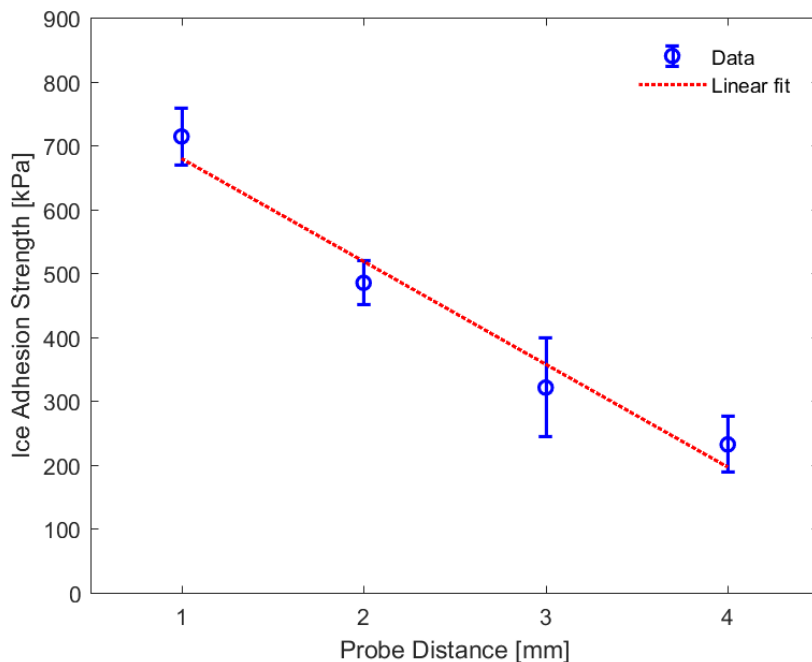


Figure 9 Dependence of ice adhesion strength on the probe distance from the surface for a vertical shear test on bulk water ice on a poly(methyl methacrylate) surface, data from [45] with linear best fit.

The distance between the force probe and the surface in a horizontal shear test for a viscoelastic surface with ice adhesion strength around 1 kPa has also been investigated recently [47]. In this study, it was observed that a small distance between the probe and surface did not induce ice detachment, but rather pushed the ice sample around on the surface. As the ice never detached from the surface, ice adhesion was not measured. Rather, the test measured a form of static friction between the ice and surface. In this study, it was recommended to keep the distance of the force probe from the surface at about 3 mm, to ensure that the ice sample detaches properly from the surface. This recommendation only applies to elastomeric low ice adhesion surfaces.

In addition to the placement of the force probe, with respect to both the distance from the surface and the induced stress distribution at the interface, the probe loading rate has been shown to impact the resulted ice adhesion strength when measured with the vertical shear test [53]. This study showed that when the probe loading rate increased, the ice adhesion increased as well. However, this effect was only apparent for some surfaces, as it could be seen for testing on Sylgard184 but not for PMMA surfaces. This differentiation on type of surface substantiates the

need for more research on the fundamental mechanisms of ice adhesion, and the different mechanisms of the available ice adhesion tests.

Table 5 gives an overview of experimental conditions for several low ice adhesion studies. As can be seen, both the probe distance, probe loading rate and temperature vary greatly, and are not always stated in the publications. Because of the great impact of these parameters, it is very difficult to directly compare these different results to each other.

5. Comparing low ice adhesion surfaces with interlaboratory tests

In 2019, the authors of this chapter undertook an interlaboratory study of ice adhesion using different techniques. The results have been published recently [61], and the experiments and results in this section are based on this publication. Additionally, in this section we will detail the need for comparison and transferability in the field of low ice adhesion surface research, and our suggestion as to how this comparability might be achieved.

5.1 The need for comparability

The need for comparability and standardization in the field of low ice adhesion has been substantiated. The definition for icephobic surfaces is not fully agreed on, and many different types of accreted ice are utilized which are created in varying ways, which affects the ice adhesion strength. Furthermore, ice adhesion strength is measured with many different set-ups where small changes in experimental parameters can have large consequences for the reported ice adhesion strength.

There is a general agreement that further development of low ice adhesion surfaces needs to include a list of criteria for comparison. As mentioned in section 4.1, several publications have suggested standard measurement techniques for ice adhesion strength, and four out of six contributions in the low ice adhesion session at the 18th International Workshop on the Atmospheric Icing of Structures (IWAIS), which was held in Reykjavik in June 2019, focused on the issue of comparability [62-65]. In short, a low ice adhesion material developed at one facility cannot be compared to another developed somewhere else. Similarly, while the ARF can be used to compare different icephobic coatings to each other by comparing to a common reference as described in section 4.2, the ARF cannot be used to compare icephobic materials in different laboratories, as their references will differ.

The ultimate goal of research in ice adhesion, and to ensure full comparability, is to understand all underlying mechanisms of the adhering of ice to different surfaces. On the other hand, these mechanisms are different for different surfaces and under different environmental conditions, and thus there is not only one true value ice adhesion which all other measurements may be compared to. Furthermore, the ideal, or true, ice adhesion value changes from application to application. Due to the complex and stochastic behavior of ice, and the many changing parameters, to uncover all the theoretical implications of ice-solid adherence is extremely complicated. Meanwhile, the ice adhesion research field is result-oriented and moves continually forward, requiring a more empirically based method of comparison between different surfaces and research facilities.

A comparison for ice adhesion must be based on real-life experimental set-ups and surfaces to be viable. Ideally, a system for comparison and transferability can be utilized to directly compare two measured ice adhesion strengths when the ice adhesion test and ice type are given, as well as all environmental conditions. As such, a variety of test methods and ice types must be considered to generate such a comparability, and multiple research groups must be involved.

The results reported in the next sections of this chapter are meant to be a beginning of such a process. In these experiments, one reference surface and one commercially available icephobic surface were tested with as similar conditions as possible in two laboratory facilities, NTNU situated in Trondheim, Norway, and AMIL situated in Chicoutimi, Quebec, Canada. The same ice type was tested, and the tests were performed at two different temperatures to compare the effect of changing environmental conditions.

5.2 Interlaboratory test procedure

The two surfaces selected for comparison in the interlaboratory test procedure were bare aluminum 6061-T6, and aluminum covered with EC-3100 that was a two-component, water-based, icephobic, non-stick coating from Ecological Coating, LLC. Both surfaces are available commercially and have been investigated in previous studies [49, 66, 67]. To ensure comparability, all surfaces were prepared at AMIL and shipped to NTNU for testing. The durability of the surfaces was not investigated, all water was created with demineralized water of resistivity 18 M Ω .cm, and temperatures of both -18°C and -10°C were tested. Several tests were performed at each configuration to generate averages. At AMIL, the averages are based on six different samples, except four samples for bulk water ice on bare aluminum at -10°C. At NTNU, the averages are for five different samples.

Two different ice types were tested at AMIL, namely precipitation ice and bulk water ice as described in Table 2 and in section 3.2 [26]. Precipitation ice as created at a temperature of -18°C can be seen in Figure 10. Bulk water ice as created at AMIL at a temperature of -18°C can similarly be seen in Figure 11. For the bulk water ice tests, unlike those described in section 3.2, the tested surfaces and water were initially at room temperature. These conditions were changed to resemble the tests performed at NTNU as much as possible. Similarly, all tests with bulk water ice in both facilities had freezing time of exactly 3 hours, to avoid discrepancies in the environmental conditions.

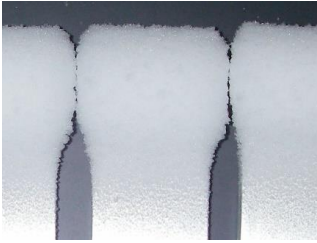


Figure 10 Picture of precipitation ice created at AMIL at test temperature of -18°C . Picture also published in [61].

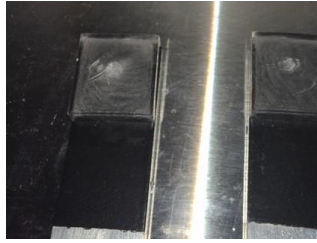


Figure 11 Picture of bulk water ice created at AMIL at test temperature of -18°C . Picture also published in [61].

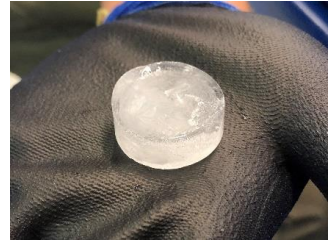


Figure 12 Picture of bulk water ice created at NTNU at test temperature of -18°C . Picture also published in [61].

At NTNU, the laboratory facility is equipped to generate bulk water ice only, by a freezer for temperature of -18°C and a separate cold room for temperature of -10°C . The bulk water ice at NTNU was generated similarly to previous studies [54, 68] in a polypropylene cylindrical tube. The ice samples generated were smaller than those created at AMIL, with circular surface area about half of that at AMIL. For both temperatures at NTNU, the ice was frozen ex situ, and required transport to the test rig. The transport from the cold room was performed with the sample in a polystyrene container to minimize the effect of the changing temperature. Additionally, the ice samples were placed in the ice adhesion test chamber for 15 minutes to ensure thermal stabilization before testing.

As mentioned in previous sections, the ice adhesion tests performed at AMIL are carried out with a centrifuge adhesion test, as described in section 4.1. The specific ice adhesion test set-up utilized is displayed in Figure 13. At NTNU, the ice adhesion tests were performed with a vertical shear test, as pictured in Figure 14. This vertical shear test is similar to the principle illustrated in Figure 6, except that it is rotated by 90 degrees. The specifications of both ice adhesion test set-ups are given with more detail in the original publication [61].

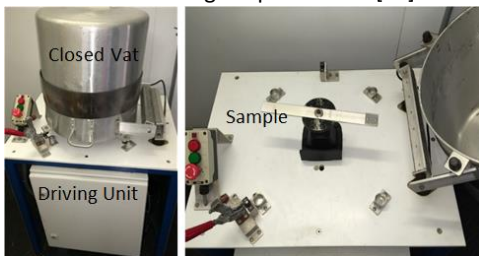


Figure 13 AMIL centrifuge adhesion test apparatus. Picture also published in [61].

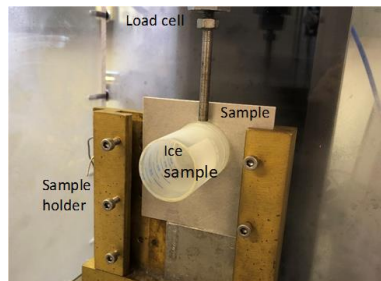


Figure 14 NTNU vertical shear test apparatus. Picture also published in [61].

5.3 Interlaboratory test results

With comparable ice types and tested surfaces, a comparison of the results obtained from AMIL and NTNU with different ice adhesion tests can be performed. The results of the experiments are shown in Figure 15, with mean values and standard deviations detailed in Table 6. This figure shows that all ice adhesion strengths are comparable, with the greatest differences for aluminum surfaces at test

temperatures of -10°C . Furthermore, the results for the different ice types from AMIL support the trends for the effect of ice type on ice adhesion strength as reported in section 3.2. Although these experiments were performed in the same laboratory facility, they were performed by different persons and at different times, which lessens the probability of systematic error due to personal habits and inclinations.

Table 6 Overview of mean values and standard deviations of ice adhesion strength measurements included in the interlaboratory study. Data from [61].

Surface / Temperature	Ice adhesion strength [kPa \pm SD (%)]		
	AMIL Precipitation ice	AMIL Bulk water ice	NTNU Bulk water ice
Aluminum / -10°C	734 \pm 75 (10%)	326 \pm 30 (9%)	509 \pm 185 (36%)
Aluminum / -18°C	340 \pm 44 (13%)	285 \pm 49 (17%)	393 \pm 124 (32%)
Coating / -10°C	83 \pm 3 (4%)	96 \pm 34 (35%)	111 \pm 19 (17%)
Coating / -18°C	78 \pm 14 (18%)	85 \pm 49 (58%)	135 \pm 38 (28%)

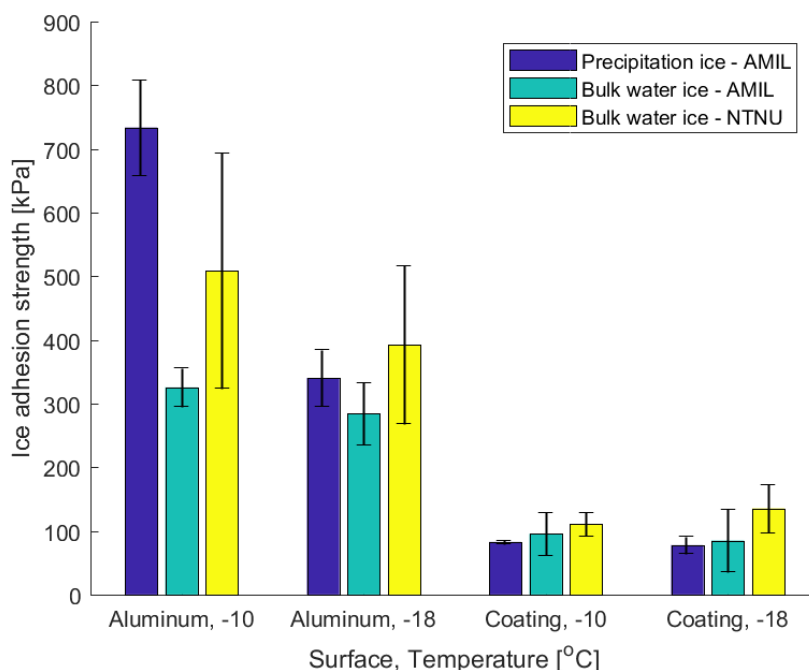


Figure 15 Measured ice adhesion strength values from the interlaboratory study between AMIL and NTNU. Data from [61].

The interlaboratory test results in Figure 15 might act as the basis for several comparisons within ice adhesion research. In addition to comparing the different ice types, as in the previous paragraph, these can be used for comparing the ice adhesion tests for the same type of ice, as well as the results for the different surfaces, the standard deviations and the effect of temperature.

When comparing the different ice adhesion tests, Figure 15 shows that for bulk water ice, the vertical shear test at NTNU systematically results in higher ice adhesion values for the same surface. However, the standard deviation depends on the type of surface. For aluminum surfaces, the

deviation is higher for vertical shear test than the centrifugal test, while the deviation is higher for the centrifugal test than for the vertical shear test. Furthermore, while the ice adhesion strengths are similar for the two test methods for low ice adhesion, the vertical shear test seems to give larger deviations than the centrifugal test. When comparing the standard deviations for the two surface types, Figure 15 shows that the aluminum surface yields larger deviations than the icephobic coating, and that the deviation seems to scale with the absolute value of the ice adhesion strength for the vertical shear test. For the centrifugal test, the largest deviations are found for bulk water ice when testing on the icephobic coating. As seen in Table 6, the standard deviations for all tests range between 4% and 58%, with a median value of 17%. This range of standard deviations coincides with other reports on the variation in ice adhesion measurements, as discussed in section 3.2. As a consequence, more ice adhesion tests for a larger range of values should be performed for more surfaces, both at several laboratories and should be repeated within each facility.

The effect of the temperature changes from -10°C to -18°C varied for the two surfaces. For the icephobic coating, the effect of decreasing temperature was very small. For aluminum, however, the effect of changing temperature was clearly visible. At AMIL, the ice adhesion on bare aluminum decreased with the decrease in temperature for both precipitation ice and bulk water ice, with a more pronounced effect for precipitation ice. This decrease is attributed to an increased occurrence of cohesive failures for the precipitation ice, which became much more common at the lower temperature. This transition from adhesive to cohesive failure has been seen for aluminum surface and precipitation ice at AMIL previously as well [40]. The same trend of decreasing ice adhesion with decreasing temperature was seen at NTNU for bulk water ice, but all failures at NTNU were adhesive. This difference indicates that the transition from adhesive to cohesive failure depends on both the ice type and the ice adhesion test method. For bulk water ice, there was very little change in the ice adhesion strength with decreasing temperature. These discrepancies substantiate the difficulty in predicting the effect of temperature on ice adhesion strength [5, 30].

As stated in the previous section, the experiments at AMIL were performed in situ, while the experiments at NTNU were performed ex situ with transportation between the freezer or cold room and the ice adhesion test chamber. However, despite the transportation which was deemed detrimental for ice adhesion, the bulk water ice adhesion tested at NTNU is higher than those tested at AMIL for both surface types for bulk water ice. This observation might indicate that the transportation did not significantly affect the ice adhesion.

Another source of discrepancies in the ice adhesion measurement is the size of the ice samples. The ice samples tested at NTNU, which had surface areas of about 590 mm², had only half the surface area of the samples tested at AMIL, which had surface areas of about 1100 mm². As seen when comparing the prepared samples for centrifugal test at AMIL in Figure 10 and Figure 11 with the size of the ice sample on the test surface at NTNU in Figure 14, there was a substantial difference in the ice coverage on the surface sample. This difference could lead to different placements of the ice sample on the tested surface, leading to possible slight changes in surface microstructure. This slight variation might contribute to the higher standard deviation measured at NTNU, especially for the bare aluminum surfaces.

The interlaboratory experiments were conceived and performed with the intent of keeping all conditions and experimental parameters in both laboratories as close and constant as possible. However, the results still show significant differences between the measured ice adhesion strengths, as well as high variations. It follows that more data are needed, and a future method of comparison

between different ice types and ice adhesion measurement methods are crucial to ensure comparability.

5.4 Requirements for a future standard and reference

As stated, the aim of a standardization process within the ice adhesion research community is not to establish a common standard method of generating and testing ice, but rather to enable comparison of performed experiments in different facilities. Ideally, this basis for comparison includes both ice type and ice adhesion test method, as well as every experimental parameter. When all parameters are specified, then comparative values should be available for different surfaces and tests.

Such a reference or standard needs to consider all parameters in ice adhesion measurements. A selection of parameters which need to be included in such a reference is displayed in Figure 16. As illustrated, a basis for comparison would need to account for differences in environmental conditions such as temperature, different variations in surface texture and chemistry, the ice adhesion strength test in use at different facilities, and all the different types of ice which are being tested for different applications. As a result, a final basis for comparison must include large amounts of data, collected from different facilities and compared in a similar manner as the interlaboratory tests from the previous section.

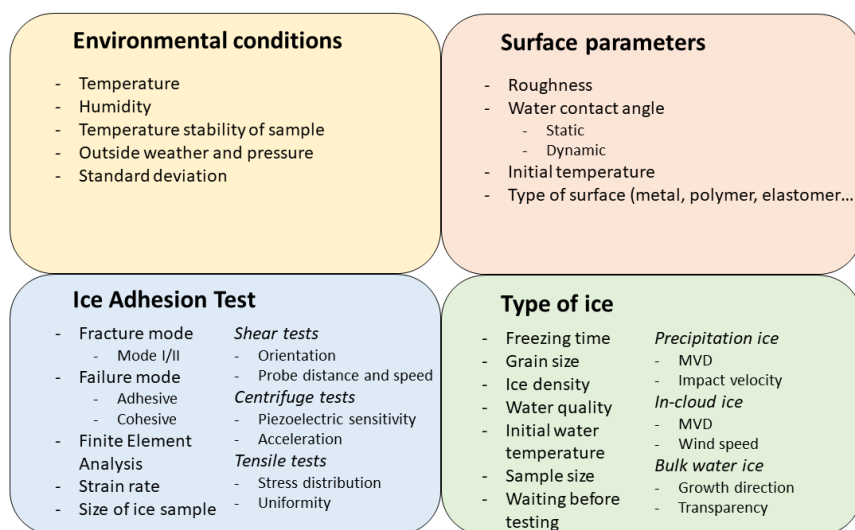


Figure 16 Selected elements and parameters of proposed experimental protocol to develop ice adhesion standard and reference basis[62].

As all research groups base their ice adhesion strength data on custom-built ice adhesion tests and ice formation processes, we recommend a common set of reference data. This reference should not be considered as the ideal test set-up or solution, but rather as a relatively easy set-up which may be implemented fast. If such a set-up could be utilized as a common reference, all other tests would only need to be compared to the reference instead of being cross-compared to all other configurations. Such a comparison set-up is suggested in Figure 17. We propose a horizontal shear

test with defined experimental parameters for testing the ice adhesion strength of bulk water ice with specific ice formation properties on aluminum surface in constant environmental conditions. For such a reference test, all parameters from Figure 16 would need to be considered.

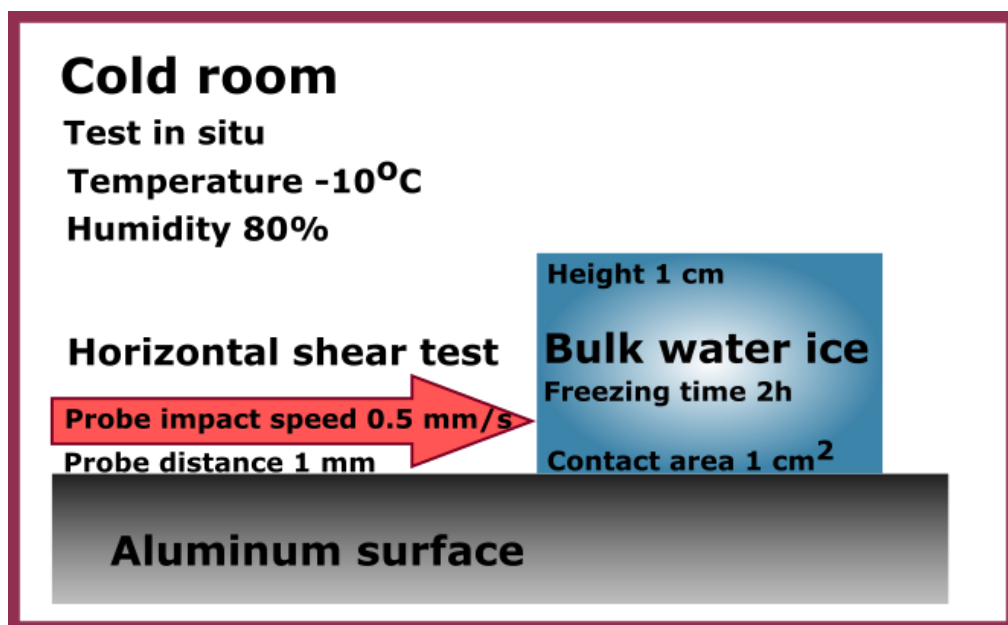


Figure 17 Schematic drawing of the proposed reference test for increased comparability within ice adhesion research.

There is already an agreement between several research facilities, including the authors of this chapter, to conduct a series of round-robins for comparing the ice adhesion strengths measured in different laboratories. These tests will be less extensive than the interlaboratory tests described here, but will include more partners, including both industry and academia. Hopefully, these round-robins will give better insight into the most critical parameters for future comparisons of ice adhesion strength.

6. Concluding remarks

The aim of this chapter was to give an overview of the status of comparison between icephobic materials to date, and to outline the possibility for direct comparison of low ice adhesion surfaces at present. It was discussed how the definition of icephobicity differs, while the most promising path towards passive anti-icing seems to be to lower the ice adhesion strength. It was shown how different atmospheric conditions induced different ice types, and the effect of ice type on the ice adhesion strength was substantiated. The most applied ice adhesion test methods were mentioned, and the centrifugal adhesion test and simplest shear tests were described in detail. In addition, the effects of changing temperature, ice sample size and force probe placement and loading rate were discussed. Finally, recently conducted interlaboratory ice adhesion tests were described, and a potential future reference basis was outlined.

The most important conclusion in this chapter was that the type of ice for ice adhesion tests needs to be based on the real-life applications to achieve realistic ice adhesion results. Furthermore, it is important to consider the applications and experimental parameters when determining which ice adhesion test to utilize, especially for super-low ice adhesion surfaces where gravity might induce a systematic error. Furthermore, when comparing ice adhesion tests performed at AMIL with a centrifugal adhesion test and at NTNU with a vertical shear test, the results display the same trends but with significant differences. For bulk water ice, the vertical shear test systematically results in higher ice adhesion strengths than the centrifugal adhesion test, although the vertical shear test overall has a higher deviation than the centrifugal test. However, the standard deviation seems to scale with the absolute value of the ice adhesion.

The interlaboratory results indicate that the type of ice accretion is less important when the ice adhesion is low. However, the ice formation is still a key parameter in predicting the ice adhesion on different surfaces, as well as for determining the underlying mechanisms of ice adhesion and ice detachment on different surfaces. To fully compare different ice adhesion measurements and to advance the field of low ice adhesion surfaces, a reference test basis should be agreed upon, and more comparative experiments should be performed.

References

- [1] J. Lv, Y. Song, L. Jiang and J. Wang, Bio-inspired strategies for anti-icing, *ACS Nano* 8, 3152-3169 (2014).
- [2] J. Brassard, C. Laforte, F. Guerin and C. Blackburn, Icephobicity: Definition and measurement regarding atmospheric icing. In: *Advances in Polymer Science*. Springer, Berlin, Heidelberg, (2017).
- [3] ISO, ISO 12494:2017 Atmospheric icing of structures, (2017).
- [4] M. Farzaneh, H. Gauthier, G. Castellana, C. Engelbrecht, Á.J. Eliasson, S.M. Fikke, C. Greyling, I. Gutmann, T. Hayashi, F. Jakl, Z. Jia, H. Lugschitz, V. Shkaptsov, L. Riera, N. Sugawara, N. Vaga and B. Wareing, CIGRE: Coatings for Protecting Overhead Power Network Equipment in Winter Conditions, report number TB631, (2015).
- [5] L. Makkonen, Ice adhesion —Theory, measurements and countermeasures, *J. Adhesion Sci. Technol.* 26, 413-445 (2012).
- [6] S. Løset, K.N. Shkhinek, O.T. Gudmestad and K.V. Høyland, *Actions from Ice on Arctic Offshore and Coastal Structures: Student's Book for Institutes of Higher Education*, "LAN", St. Petersburg, (2006).
- [7] A. Klein-Paste and J. Wåhlin, Wet pavement anti-icing — A physical mechanism, *Cold Regions Sci. Technol.* 96, 1-7(2013).
- [8] V. Hejazi, K. Sobolev and M. Nosonovsky, From superhydrophobicity to icephobicity: forces and interaction analysis, *Scientific Reports* 3, 2194 (2013).
- [9] Z. He, S. Xiao, H. Gao, J. He and Z. Zhang, Multiscale crack initiators promoted super-low ice adhesion surfaces, *Soft Matter* 13, 6562-6568 (2017).
- [10] M.J. Kreder, J. Alvarenga, P. Kim and J. Aizenberg, Design of anti-icing surfaces: smooth, textured or slippery?, *Nature Reviews Mater.* 1, 1-15(2016).
- [11] H. Sojoudi, M. Wang, N.D. Boscher, G.H. McKinley and K.K. Gleason, Durable and scalable icephobic surfaces: similarities and distinctions from superhydrophobic surfaces, *Soft Matter* 12, 1938-1963(2016).
- [12] T.M. Schutzius, S. Jung, T. Maitra, G. Graeber, M. Köhme and D. Poulikakos, Spontaneous droplet trampolining on rigid superhydrophobic surfaces, *Nature* 527, 82-85 (2015).
- [13] S. Jung, M. Dorrestijn, D. Raps, A. Das, C.M. Megaridis and D. Poulikakos, Are superhydrophobic surfaces best for icephobicity?, *Langmuir* 27, 3059-3066 (2011).
- [14] J. Chen, J. Liu, M. He, K. Li, D. Cui, Q. Zhang, X. Zeng, Y. Zhang, J. Wang and Y. Song, Superhydrophobic surfaces cannot reduce ice adhesion, *Appl. Phys. Letters* 101, 111603 (2012).
- [15] M. Nosonovsky and V. Hejazi, Why superhydrophobic surfaces are not always icephobic, *ACS Nano* 6, 8488-8491 (2012).

- [16] S. Jung, M.K. Tiwari, N.V. Doan and D. Poulikakos, Mechanism of supercooled droplet freezing on surfaces, *Nature Communi.* 3, 615 (2012).
- [17] K.K. Varanasi, T. Deng, J.D. Smith, M. Hsu and N. Bhate, Frost formation and ice adhesion on superhydrophobic surfaces, *Appl. Phys. Lett.* 97, 234102-3 (2010).
- [18] Z. Zhang and X.-Y. Liu, Control of ice nucleation: freezing and antifreeze strategies, *Chem. Soc. Reviews* 47, 7116-7139 (2018).
- [19] D. Chen, M.D. Gelenter, M. Hong, R.E. Cohen and G.H. McKinley, Icephobic surfaces induced by interfacial nonfrozen water, *ACS Appl. Mater. Interfaces* 9, 4202-4214 (2017).
- [20] D.L. Beemer, W. Wang and A.K. Kota, Durable gels with ultra-low adhesion to ice, *J. Mater. Chem. A* 4, 18253-18258 (2016).
- [21] V.F. Petrenko and R.W. Whitworth, *Physics of Ice*, Oxford University Press, Oxford, UK, (2006).
- [22] T. Bartels-Rausch, V. Bergeron, J.H.E. Cartwright, R. Escribano, J.L. Finney, H. Grothe, P.J. Gutierrez, J. Haapala, W.F. Kuhs, J.B.C. Pettersson, S.D. Price, C.I. Sainz-Díaz, D. Stokes, G. Strazzulla, E.S. Thomson, H. Trinks and N. Uras-Aytemiz, Ice structures, patterns, and processes: A view across the ice-fields, *Rev. Mod. Phys* 84, 885-944 (2012).
- [23] T. Cebeci and F. Kafyke, Aircraft icing, *Annual Rev. Fluid Mech.* 35, 11-21 (2003).
- [24] T. Armstrong, B. Roberts and C. Swithinbank, *Illustrated Glossary of Snow and Ice*, Scott Polar Research Institute, Cambridge, MA, USA (1973).
- [25] L. Makkonen, Modeling power line icing in freezing precipitation, *Atmospheric Res.* 46, 131-142 (1998).
- [26] S. Rønneberg, C. Laforte, C. Volat, J. He and Z. Zhang, The effect of ice type on ice adhesion, *AIP Advances* 9, 055304 (2019).
- [27] G. Fortin and J. Perron, Ice adhesion models to predict shear stress at shedding, *J. Adhesion Sci. Technol.* 26, 523-553 (2012).
- [28] Z.A. Janjua, B. Turnbull, K.-L. Choy, C. Pandis, J. Liu, X. Hou and K.-S. Choi, Performance and durability tests of smart icephobic coatings to reduce ice adhesion, *Appl. Surface Sci.* 407, 555-564 (2017).
- [29] A.H. Work, Jr., A.L. Gyekenyesi, R.E. Kreeger, J.A. Salem, M.M. Vargas and D.R. Drabiak, The adhesion strength of impact ice measured using a modified lap joint test, *AIAA Aviation Forum*, Atlanta, GA; United States, p. 23 (2018).
- [30] A. Work and Y. Lian, A critical review of the measurement of ice adhesion to solid substrates, *Prog. Aerospace Sci.* 98, 1-26 (2018).
- [31] M. Schulz and M. Sinapius, Evaluation of different ice adhesion tests for mechanical deicing systems, *Proceedings in SAE International*, (2015).

- [32] D.N. Anderson and A.D. Reich, Tests of the performance of coatings for low ice adhesion, NASA Technical Memorandum 14, report nr 107399, (1997).
- [33] V. Upadhyay, T. Galhenage, D. Battocchi and D. Webster, Amphiphilic icephobic coatings, *Prog. Organic Coatings* 112, 191-199, (2017).
- [34] T.M. Schutzius, S. Jung, T. Maitra, P. Eberle, C. Antonini, C. Stamatopilos and D. Poulikakos, Physics of icing and rational design of surfaces with extraordinary icephobicity, *Langmuir* 31, 4807-4821 (2015).
- [35] J.M. Sayward, Seeking low ice adhesion, U.S. Army Cold Regions Research and Engineering Laboratory, Hanover, NH USA, report nr 00197109, (1979).
- [36] AMIL Laboratory, AMIL - About us - Accreditations, 2019. (<https://amillaboratory.ca/about-us/accreditations>).
- [37] Smooth-On Inc., Mold Max TM Series Tin Cure Silicone Mold Rubber, available from <https://www.smooth-on.com/product-line/mold-max/>, accessed Jul 8, 2019.
- [38] S. Rønneberg, J. He and Z. Zhang, The need for standards in ice adhesion research: A critical review, *J. Adhesion Sci. Technol.* 34, 319-347 (2019).
- [39] R.J. Scavuzzo and M.L. Chu, Structural properties of impact ices accreted on aircraft structures, NASA, report nr 19870008688, (1987).
- [40] F. Guerin, C. Laforte, M.-I. Farinas and J. Perron, Analytical model based on experimental data of centrifuge ice adhesion tests with different substrates, *Cold Regions Sci. Technol.* 121, 93-99 (2016).
- [41] M. Vargas, H. Broughton, J.J. Sims, B. Bleeze and V. Gaines, Local and total density measurements in ice shapes, *J. Aircraft* 44, 780-789 (2007).
- [42] A.E. Carte, Air bubbles in ice, *Proc. Physical Soc.* 77, 757-768 (1961).
- [43] H. Niemelä-Anttonen, H. Koivuluoto, M. Tuominen, H. Teisala, P. Juuti, J. Haapanen, J. Harra, C. Stenroos, J. Lahti, J. Kuusipalo, J.M. Mäkelä and P. Vuoristo, Icephobicity of slippery liquid infused porous surfaces under multiple freeze–thaw and ice accretion–detachment cycles, *Advanced Mater. Interfaces* 5, 1800828 (2018).
- [44] A.J. Meuler, J.D. Smith, K.K. Varanasi, J.M. Mabry, G.H. McKinley and R.E. Cohen, Relationships between water wettability and ice adhesion, *ACS Appl. Mater. Interfaces* 2, 3100-3110 (2010).
- [45] C. Wang, W. Zhang, A. Siva, D. Tiew and K.J. Wynne, Laboratory test for ice adhesion strength using commercial instrumentation, *Langmuir* 30, 540-547 (2014).
- [46] N. Cohen, A. Dotan, H. Dodiuk and S. Kenig, Thermomechanical mechanisms of reducing ice adhesion on superhydrophobic surfaces, *Langmuir* 32, 9664-9675 (2016).
- [47] P. Irajizad, A. Al-Bayati, B. Eslami, T. Shafquat, M. Nazari, P. Jafari, V. Kashyap, A. Masoudi, D. Araya and H. Ghasemi, Stress-localized durable icephobic surfaces, *Materials Horizons* 6, 758-766 (2019).

- [48] M.R. Kasaai and M. Farzaneh, A critical review of evaluation methods of ice adhesion, Proceedings of 23rd International Conference on Offshore Mechanics and Arctic Engineering 3, 919-926 (2004).
- [49] C. Laforte and A. Beisswenger, Icephobic material centrifuge adhesion test, Proceedings of 11th International Workshop on Atmospheric Icing on Structures (IWAIS), Montreal, Canada, pp. 1-5 (2005).
- [50] R.B. Haehnel, Evaluation of coatings for icing control at hydraulic structures. Proceedings of Ice Engineering, 33 (2002).
- [51] N.D. Mulherin, R.B. Haehnel and K.F. Jones, Toward developing a standard shear test for ice adhesion, Proceedings of 8th International Workshop on Atmospheric Icing of Structures, Reykjavik, Iceland, pp. 73-79, (1998).
- [52] G. Fortin, A. Beisswenger and J. Perron, Centrifuge adhesion test to evaluate icephobic coatings, Proceedings of the 2nd AIAA Atmospheric and Space Environments Conference, Toronto, (2010).
- [53] C. Wang, M.C. Gupta, Y.H. Yeong and K.J. Wynne, Factors affecting the adhesion of ice to polymer substrates, *J. Appl. Polym. Sci.* 135, 45734 (2019).
- [54] Z. He, E.T. Vågenes, C. Delabahan, J. He and Z. Zhang, Room temperature characteristics of polymer-based low ice adhesion surfaces, *Scientific Reports* 7, 42181 (2017).
- [55] E. Mitridis, T.M. Schutzius, A. Sicher, C.U. Hail, H. Eghlidi and D. Poulikakos, Metasurfaces leveraging solar energy for icephobicity, *ACS Nano* 12, 7009-7017 (2018).
- [56] K. Golovin, A. Dhyani, M.D. Thouless and A. Tuteja, Low-interfacial toughness materials for effective large-scale deicing, *Science* 364, 371-375 (2019).
- [57] R. Dou, J. Chen, Y. Zhang, X. Wang, D. Cui, Y. Song, L. Jiang and J. Wang, Anti-icing coating with an aqueous lubricating layer, *ACS Appl. Mater. Interfaces* 6, 6998-7003 (2014).
- [58] D.S. Thompson, D. Meng, A. Afshar, R. Bassou, J. Zong, E. Bonaccorso, A. Laroche and V. Vercillo, Initial development of a model to predict impact ice adhesion stress, 2018 Proceedings of Atmospheric and Space Environments Conference, Atlanta, Georgia, (2018).
- [59] E.M. Schulson, P.N. Lim and R.W. Lee, A brittle to ductile transition in ice under tension, *Philosophical Magazine A* 49, 353-363 (1984).
- [60] L.E. Raraty and D. Tabor, The adhesion and strength properties of ice, *Proc. R. Soc. Lond. A*: 245, 184-201 (1958).
- [61] S. Rønneberg, Y. Zhuo, C. Laforte, J. He and Z. Zhang, Interlaboratory study of ice adhesion using different techniques, *Coatings* 9, 678 (2019).
- [62] S. Rønneberg, J. He and Z. Zhang, Standardizing the testing of low ice adhesion surfaces, Proceedings of International Workshops on Atmospheric Icing of Structures (IWAIS) 2019, Reykjavik, Iceland, (2019).

- [63] N. Rehfeld, B. Speckmann and S. Grünke, Durability of icephobic materials, Proceedings of International Workshop on Atmospheric Icing of Structures (IWAIS) 2019, Reykjavik, Iceland, (2019).
- [64] C. Laforte, J.-D. Brassard and C. Volat, Extended evaluation of icephobic coating regarding their field of application, Proceedings of International Workshops on Atmospheric Icing of Structures (IWAIS), Reykjavik, Iceland, (2019).
- [65] H. Niemelä-Anttonen, J. Kiilakoski, P. Vuoristo and H. Koivuluoto, Icephobic performance of different surface designs and materials, Proceedings of International Workshop on Atmospheric Icing of Structures (IWAIS), Reykjavik, Iceland, (2019).
- [66] C. Laforte and A. Beisswenger, Centrifuge Adhesion Test, Proceedings of SAE G-12 Future Deicing Technology Subcommittee, Frankfurt, (2004).
- [67] M. Susoff, K. Siegmann, C. Pfaffenroth and M. Hirayama, Evaluation of icephobic coatings— Screening of different coatings and influence of roughness, *Appl. Surface Sci.* 282, 870-879 (2013).
- [68] Y. Zhuo, V. Håkonsen, Z. He, S. Xiao, J. He and Z. Zhang, Enhancing the mechanical durability of icephobic surfaces by introducing autonomous self-healing function, *ACS Appl. Mater. Interfaces* 10, 11972-11978 (2018).

Appendix F

Conference paper

Standardizing the testing of low ice adhesion surfaces

Rønneberg, Sigríð, Jianying He, and Zhiliang Zhang. 2019. In International Workshops on Atmospheric Icing of Structures (IW AIS) 2019. Reykjavík, Iceland.

Standardizing the testing of low ice adhesion surfaces

Sigrid Rønneberg¹, Jianying He¹, Zhiliang Zhang¹

¹ Department of Structural Engineering, Norwegian University for Science and Technology (NTNU), NO-7491 Trondheim, Norway

Sigrid.Ronneberg@ntnu.no, Jianying.He@ntnu.no, Zhiliang.Zhang@ntnu.no

Abstract— Low ice adhesion surfaces are a promising strategy to develop anti-icing surfaces. At present, however, the reported ice adhesion strengths are not comparable due to a multitude of performed ice adhesion tests and types of accreted ice. Furthermore, the necessary experimental details are often not included in the published studies. In this paper, a literature review for ice adhesion tests is carried out and experiments performed at the AMIL facility for ice types are reported to show the necessity of comparability. In addition, a protocol for future experiments to help standardize the ice adhesion research is presented. This protocol includes both ice adhesion tests, types of accreted ice, environmental conditions and surface parameters. A reference is proposed with standard aluminum surface and bulk water ice as well as horizontal shear ice adhesion test at -10°C. The experiments might be performed in different facilities to avoid having to build a new, comprehensive infrastructure, but this cooperation requires a common basis of definitions and references.

Keywords— Anti-icing, Ice adhesion strength, Ice adhesion test, Ice type, Standardization

I. INTRODUCTION

Ice removal is necessary to avoid both dangerous situations and the unwanted icing of infrastructure [1], [2]. It is essential to remove the ice efficiently, either with traditional de-icing methods such as thermal, mechanical or chemical deicing or with passive anti-icing surfaces. Passive methods do not require additional energy, but utilizes natural forces such as wind, gravity or surface tension to ensure ice-free surfaces [3]. There are three main pathways to achieve passive anti-icing surfaces: removing water before freezing; the delay of ice nucleation; and the reduction of ice adhesion strength [4]. Considering long-term exposure of anti-icing surfaces in the ambient environment in cold region, the most promising strategy for durable anti-icing surfaces is the lowering of ice adhesion strength [5].

Low ice adhesion surfaces are often defined by an ice adhesion strength below 60 kPa [6]. Surfaces with ice adhesion strength below 20 kPa enables the ice to shed due to natural wind [5], and surfaces with ice adhesion below 10 kPa enables one cubic meter of ice to fall off by its own weight [4].

Research on low ice adhesion surfaces has continuously increased over the past 15 years, and there are many promising coatings available [7]. However, the available literature reports ice adhesion strengths that span three orders of magnitude, and there is no general agreement about reference values [8]. Several standard tests have been proposed earlier [9], [10], and the earliest to our knowledge was presented at IWAIS in 1998 [11]. There have also been published several reviews comparing different widely used test methods [8],

[12], [13]. However, the proposed standards do not include comparative discussions, and the comparisons between different methods do not include ice types.

In this paper, we summarize our present work on the different types of ice adhesion test methods and ice types, and propose a future protocol for standardizing ice adhesion research.

II. CURRENT STATUS OF ICE ADHESION TESTS

Although a multitude of different ice adhesion tests are available, four tests are most widely in use [14]. These are the horizontal shear test, the vertical shear test, the tensile test, and the centrifugal adhesion test, see Figure 1. For all tests, the ice adhesion strength is defined as the ratio of peak removal force to the interface area of ice, such that $\tau = F/A$. As there is no standard today, most research groups develop its own testing set-up [15], [16]. As a result, experimental results originating from different research groups are not comparable today.

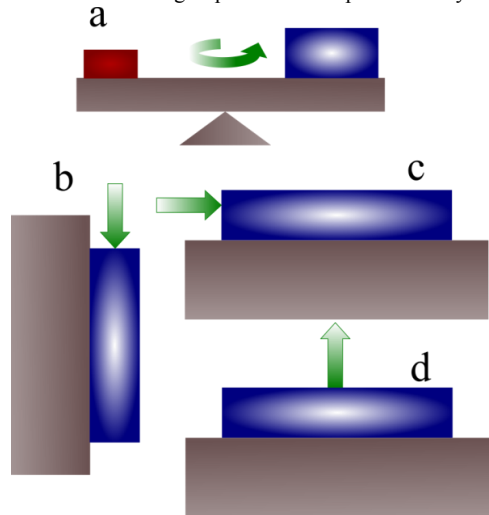


Fig. 1 Schematic illustration of the four most widely used tests for ice adhesion strength measurements: a) Centrifugal adhesion test (counterweight is red) b) Vertical shear test c) Horizontal shear test d) Tensile test.

Most publications do not include all their experimental details, such as strain rate and freezing time for ice. In Table I, it can be seen how ice adhesion measurements on a reference aluminum surface differ both within and between the ice adhesion tests. This variation substantiates the great difference between the different tests available, and the importance of a

detailed experimental section describing the experiments to ensure reproducibility. An example of the impact of experimental details on the results is the distance between the force probe and the surface for the horizontal shear tests, where a change of 3 mm alters the ice adhesion strength with almost 70% [9]. When several studies do not include this measure in their manuscripts, the results can clearly not be directly compared.

Table I Selection of Reported Ice Adhesion Strengths for a Reference Aluminum Surface.

Test Method	Ice Adhesion Strength [MPa]	Reference
Vertical shear test	0.49	He et al [6]
Horizontal shear test	0.80	Dou et al [17]
Horizontal shear test	0.11	Hejazi et al [18]
Horizontal shear test	0.7-1.0	Lou et al [19]
Centrifugal adhesion test	0.28-0.78	Rønneberg et al [20]
Centrifugal adhesion test	0.19-0.76	Guerin et al [21]
Centrifugal adhesion test	0.32	Laforte and Beisswenger [22]

Experimental details with impact on the same line as probe distance is the probe impact speed for horizontal shear tests [23], temperature [21], ice sample size [24], and stress concentrations [8], [24], among others. In Table II, eight low ice adhesion studies with bulk water ice are shown with their experimental details. As can be seen, the experimental details vary on several accounts, and although the ice adhesion tests were performed with similar ice adhesion tests and with ice frozen in a mold giving bulk water ice, the reported ice adhesion strengths are still not comparable.

Similar to the differences in ice adhesion test methods, the type of accreted ice affects the ice adhesion strength. The properties of ice are highly dependent on the environmental and mechanical conditions, such as temperature, cooling rate, grain size, and crystallization process [26]. The generation process of the ice thus determines the properties of the ice, including ice adhesion strength.

So far, no systematic investigation has been performed to test the effect of different ice adhesion test methods on similar ice types under similar conditions. However, the authors in cooperation with the Anti-icing Materials International Laboratory (AMIL) have performed a comparison of three different accreted ice types at the same temperature.

III. TESTING ICE TYPES

To test the effect of different types of accreted ice on the ice adhesion strength, three types of accreted ice widely used in ice adhesion research were tested at the AMIL facility [22]. More than 120 experiments were performed, and the ice adhesion strength was measured with the centrifugal adhesion test [20], [22]. The centrifugal adhesion test is illustrated in

Figure 1d, and utilizes centripetal acceleration as a small ice sample on a beam is rotated with an increasing acceleration. The moment of ice detachment is recorded with piezoelectric cells, and the detachment force is further calculated from the detachment angular velocity. Centrifugal adhesion tests results in more repeatable measurements and has a high probability of adhesive failure, although it can only accommodate one beam shape and can damage surface coatings [8], [14].

The three ice types tested were precipitation ice, in-cloud ice or impact ice, and bulk water ice. Precipitation ice was generated with a freezing drizzle in a cold room, as explained elsewhere [21]. Impact ice was generated in a wind tunnel of wind speed 15 m/s in a standardized procedure at AMIL [22]. Bulk water ice was generated by freezing water in a silicone mold with the aluminum bars placed on top [20]. Bulk water ice is most common on ice adhesion tests, but is not representative for several application such as aircraft icing [8], [15]. All the experiments were performed at -10°C.

The results of the ice adhesion measurements can be seen in Figure 2. The three different ice types clearly differ in their ice adhesion strength even under same environmental conditions and with the same ice adhesion test. Figure 2 clearly indicates that simply stating the ice adhesion strength of different low ice adhesion surfaces without considering the ice type gives inaccurate and flawed comparisons.

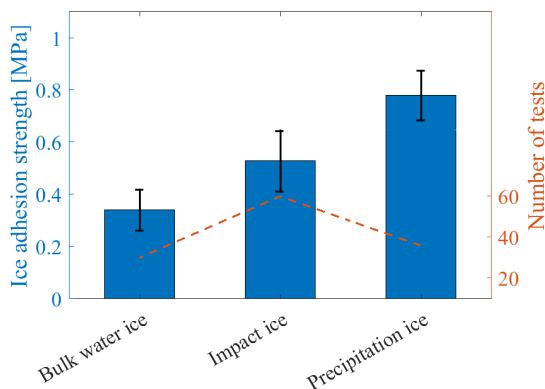


Fig. 2 Results of ice adhesion tests performed at AMIL for three different ice types, together with their standard deviation and number of tests performed [20].

IV. PROPOSAL FOR STANDARDIZING PROTOCOL

So far, we have shown that reported ice adhesion strengths cannot be directly compared due to differences in both ice generation methods and ice adhesion testing set-ups, even though the environmental conditions are similar. The goal of the low ice adhesion research is to obtain the optimal anti-icing surface with lowest possible ice adhesion strength to mitigate icing on structures. However, before the required comparisons can be made, the research community must agree upon a standard by which to perform ice adhesion strength calculations on different surfaces. Such a standard must be developed by means of international cooperation to ensure that it is applicable for all purposes.

Table II Experimental Conditions for a Selection of Low Ice Adhesion Studies with Bulk Water Ice.

Shear test	Temperature	Freezing time	Probe distance	Probe impact speed	Ice adhesion strength	Ref.
Vertical	-15°C	3 h	2 mm	0.05 mm/s	50 kPa	Wang et al [23]
Vertical	-15°C	24 h	3 mm	0.1 mm/s	5-7 kPa	He et al [6]
Horizontal	-10°C	15 h	2 mm	0.5 mm/s	165-510 kPa	Meuler et al [15]
Horizontal	-20°C	1 h	1 mm	0.8 mm/s	5-2 kPa	Beemer et al [25]
Horizontal	-25°C	1 h	3 mm	0.1 mm/s	1 kPa	Irajizad et al [10]
Horizontal	-10°C	-	1 mm	-	0.15 kPa	Golovin et al [7]
Horizontal	-20°C	-	-	-	252 kPa	Hejazi et al [18]
Horizontal	-15°C	5 h	-	-	27 kPa	Dou et al [17]

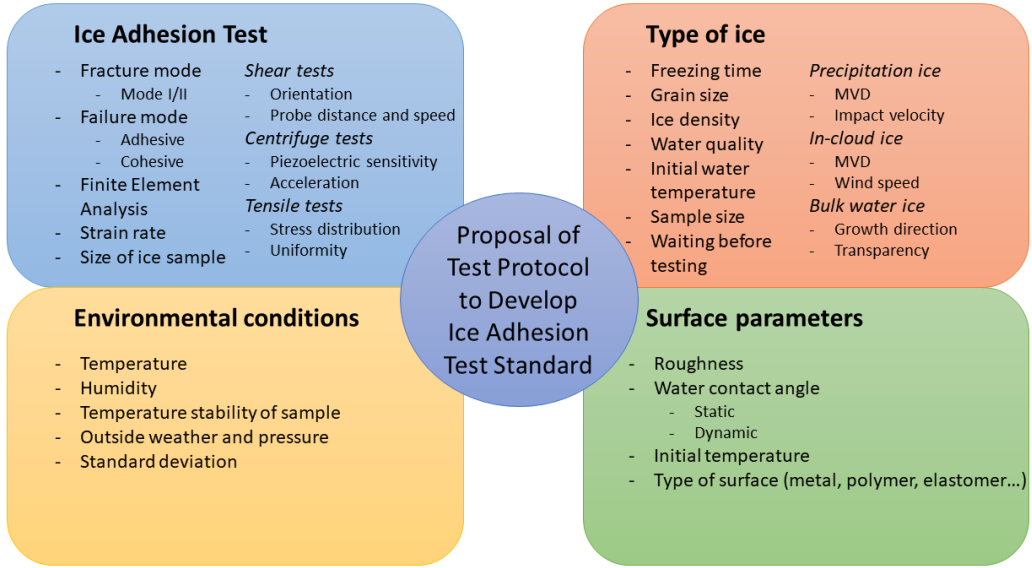


Fig. 3 Selected elements of the proposed experimental protocol to develop an ice adhesion standard.

In this paper, we propose an experimental protocol to help investigate the different parameters that must be accounted for in a standard ice adhesion measurement. Such a standard should be easy to implement, comparable for different types of ice and applicable for many anti-icing applications. Figure 3 shows an example of different parameters that will need to be included in such experiments to determine each of their impact on the ice adhesion strength. To properly explore a fitting ice adhesion standard, each parameter in Figure 3 must be tested and accounted for. The effect of each of the parameters must be tested against a reference. Based on the previous tests performed, the most commonly utilized test and ice type is the horizontal shear test with bulk water ice. This set-up is also easiest to adapt and expand upon in different laboratories and conditions. As a consequence, we propose a reference of standard aluminum surface with bulk water ice of a specific size and horizontal shear ice adhesion test with probe distance 1 mm and probe impact speed 0.5 mm/s. The temperature should be -10°C during the whole process, and the freezing time should be 2 hours. Based on this reference, all parameters in Figure 3 must be systematically changed and its effect recorded. For statistical accuracy, each set of parameters must be recorded and tested at least 5 times.

For ice adhesion test methods, all available tests should be performed, and all variable parameters must be checked. These parameters will be different for each measurement technique, for instance will the probe behavior be essential to test for shear tests but not applicable for centrifugal tests. However, for all test methods, it is important to investigate stress distribution and strain rate to fully understand the mechanisms of ice detachment, which will be different for various tests [8], [14], [24]. Also the size of the ice sample might impact the ice adhesion strength, especially for the vertical shear test where gravity affects the results. This effect is particularly important for low ice adhesion surfaces [14]. Furthermore, the failure mode is important to distinguish in the different ice adhesion tests. It is vital that failure during ice adhesion tests are adhesive failures instead of cohesive failure, and such a failure mode is more common for some tests, for instance the centrifugal adhesion test, than others such as the tensile test [14].

For types of accreted ice, bulk water ice is chosen as the reference because it is most widely used and it has the fewest controllable parameters [14]. However, bulk water ice does not occur in many realistic applications of low ice adhesion

surfaces, such as aircraft or power lines application. As a result, all types of ice must be tested with both horizontal shear test, to compare with reference, and with the other tests as well to see if all ice types are affected in the same way by the different ice adhesion tests. As grain size and ice density are thought to impact the ice adhesion strength [20], different ice generation methods must be specified to create several versions of the same accreted ice. For instance the water median volume drop diameter (MVD) will impact both the density and grain size of the ice, and must be varied. In addition, all ice types generated should be investigated specifically to determine grain size distribution and ice density, to improve our understanding of the ice adhesion mechanism.

For the environmental conditions, the same procedure must be followed of changing one parameter at a time and comparing to the reference test. It is at present unclear what environmental conditions affects the ice adhesion strength. An example can be seen in Figure 2, where the ice adhesion strength within each type of generated ice varies with up to 25 % in spite of the exact similar experimental procedures [20]. At present, it is unclear where this variation comes from, but a hypothesis is that the weather conditions outside impacted

the ice generation inside the cold room. As a result, such parameters must also be included in the recording of the experiments.

Last, for the surface parameters, properties such as surface roughness and impurities impacts the ice adhesion strength [21]. Furthermore, different materials and metals display varying ice adhesion strengths, and the effect of such variations should be compared to both the reference tests and the different tests and ices. Low ice adhesion surfaces have their own challenges that must be solved [14], and those challenges might be illuminated by testing multiple surfaces.

No laboratory facility today includes the necessary infrastructure and equipment to perform the required tests and parameter checks included in this proposed protocol. It might be possible to perform the different tests at various facilities, but these scattered experiments must have a common reference basis as well as a common language. In addition to agreeing on the parameters of the experiments, the name and definition of ice types and tests must be homogeneous. At present this agreement is lacking, as can be seen by the many definitions of the term “glaze ice” [27]-[29].

V. SUMMARY

This paper has dealt with the lack of standards within ice adhesion research, both with respect to ice adhesion strength measurements and types of accreted ice tested. Several examples have been described which shows how direct comparison between reported values of ice adhesion strengths is impossible today. Furthermore, a protocol to test the requirements of a new ice adhesion standard has been described. This protocol includes tests on ice adhesion test methods, type of ice tested, environmental conditions and surface parameters. The experiments might be performed in different facilities to avoid having to build a new, comprehensive infrastructure, but this cooperation requires a common basis of definitions and references.

ACKNOWLEDGMENT

The authors would like to thank Caroline Laforte, Christophe Volat and Caroline Blackburn at AML for their invaluable contribution in conducting the ice adhesion experiments. The authors gratefully acknowledge the financial support from the Norwegian Research Council FRINATEK project Towards Design of Super-Low Ice Adhesion Surfaces (SLICE, 250990).

REFERENCES

- [1] L. Makkonen, “Ice Adhesion —Theory, Measurements and Countermeasures”. *Journal of Adhesion Science and Technology*, vol. 26, nr 4-5, p. 413-445, 2012
- [2] M. J. Kreder, J. Alvarenga, P. Kim, and J. Aizenberg., “Design of anti-icing surfaces: smooth, textured or slippery?” *Nature Reviews Materials*, vol. 1, p. 1-15, 2016
- [3] J. Brassard, C. Laforte, F. Guerin, and C. Blackburn, *Icephobicity: Definition and Measurement Regarding Atmospheric Icing*, ser. Advances in Polymer Science. Berlin, Heidelberg, Germany: Springer, 2017.
- [4] Z. He, Y. Zhuo, J. He and Z. Zhang, “Design and Preparation of Sandwich-Like Polydimethylsiloxane (PDMS) Sponges with Super-Low Ice Adhesion”. *Soft Matter*, vol. 14, p. 4846-4851, 2018
- [5] J. Chen, J. Liu, M. He, K. Li, D. Cui, Q. Zhang, X. Zheng, Y. Zhang, J. Wang, and Y. Song, “Superhydrophobic surfaces cannot reduce ice adhesion”. *Applied Physics Letters*, vol. 101, 2012.
- [6] Z. He, E. T. Vågnes, C. Delabahan, J. He, and Z. Zhang, “Room Temperature Characteristics of Polymer-Based Low Ice Adhesion Surfaces”. *Scientific Reports*, vol. 7, p. 42181, 2017
- [7] K. Golovin, S. P. R. Kobaku, D. H. Lee, E. T. DiLoreto, J. M. Mabry, and A. Tuteja, “Designing durable icephobic surfaces”, *Science Advances*, vol. 2, nr. 3, 2016.
- [8] A. Work, and Y. Lian, “A critical review of the measurement of ice adhesion to solid substrates”, *Progress in Aerospace Sciences*, vol. 98, p. 1-26, 2018.
- [9] C. Wang, W. Zhang, A. Siva, D. Tiew, and K. J. Wynne, “Laboratory test for ice adhesion strength using commercial instrumentation”, *Langmuir*, vol. 30, nr. 2, p 540-547, 2014.
- [10] P. Irajizad, A. Al-Bayati, B. Eslami, T. Shafquat, M. Nazari, P. Jafari, V. Kashyap, A. Masoudi, D. Araya, and H. Ghasemi, “Stress-Localized Durable Icephobic Surfaces”, *Materials Horizons*, vol. 6, p. 758-766, 2019.
- [11] N. D. Mulherin, R.B. Haehnel, and K.F. Jones, “Toward developing a standard shear test for ice adhesion”, in *8th International Workshop on Atmospheric Icing of Structures*, 1998, p. 73-79.
- [12] M. R. Kasaai, and M. Farzaneh, “A critical review of evaluation methods of ice adhesion” in *23rd International Conference on Offshore Mechanics and Arctic Engineering*, 2004, paper 3, p. 919-926.
- [13] J. M. Sayward, “Seeking low ice adhesion”, U.S. Army Cold Regions Research and Engineering Laboratory, Tech. Rep. 00197109, p. 1-88, 1979.
- [14] S. Ronneberg, J. He, and Z. Zhang, “The Need for Standards in Ice Adhesion Research: A Critical Review”. *Submitted*, 2019.
- [15] A. J. Meuler, J. D. Smith, K. K. Varanasi, J. M. Mabry, G. H. McKinley, and R. E. Cohen, “Relationships between Water Wettability and Ice Adhesion”, *ACS Applied Materials & Interfaces*, vol. 2, nr. 11, p. 3100-3110, 2010.
- [16] H. Sojoudi, M. Wang, N. D. Boscher, G. H. McKinley, and K. K. Gleason, “Durable and scalable icephobic surfaces: similarities and distinctions from superhydrophobic surfaces”, *Soft Matter*, vol. 12, p. 1938-1963, 2016.
- [17] R. Dou, J. Chen, Y. Zhang, X. Wang, D. Cui, Y. Song, L. Jiang, and J. Wang, “Anti-icing Coating with an Aqueous Lubricating Layer”, *ACS Applied Materials & Interfaces*, vol. 6, nr. 10, p. 6998-7003, 2014.

- [18] V. Hejazi, K. Sobolev, and M. Nosonovsky, "From superhydrophobicity to icephobicity: forces and interaction analysis", *Scientific Reports*, vol. 3, 2013.
- [19] D. Lou, D. Hammond, and M.-L. Pervier, "Investigation of the Adhesive Properties of the Ice–Aluminum Interface", *Journal of Aircraft*, vol. 51, nr. 3, p. 1051-1056, 2014.
- [20] S. Rønneberg, C. Laforte, C. Volat, J. He, and Z. Zhang, "The effect of ice type on ice adhesion", *AIP Advances*, in press, 2019.
- [21] F. Guerin, C. Laforte, M.-I. Farinas, and J. Perron, "Analytical model based on experimental data of centrifuge ice adhesion tests with different substrates", *Cold Regions Science and Technology*, vol. 121, p. 93-99, 2016.
- [22] C. Laforte, and A. Beisswenger. "Icephobic Material Centrifuge Adhesion Test" in *11th International Workshop on Atmospheric Icing on Structures (IWAIS)*, 2005.
- [23] C. Wang, M. C. Gupta, Y. H. Yeong, and K. J. Wynne, C., "Factors affecting the adhesion of ice to polymer substrates", *Journal of Applied Polymer Science*, vol. 135, nr. 24, 2017.
- [24] M. Schulz, and M. Sinapius, "Evaluation of Different Ice Adhesion Tests for Mechanical Deicing Systems", *SAE International*. 2015.
- [25] D. L. Beemer, W. Wang, and A.K. Kota, "Durable gels with ultra-low adhesion to ice", *Journal of Materials Chemistry A*, vol. 4, p. 18253-18258, 2016.
- [26] S. Løset, K. N. Shkhinek, O. T. Gudmestad, and K. V. Høyland, *Actions from Ice on Arctic Offshore and Coastal Structures: Student's Book for Institutes of Higher Education*, St. Petersburg: "LAN", 2006.
- [27] G. Fortin, and J. Perron, "Ice Adhesion Models to Predict Shear Stress at Shedding", *Journal of Adhesion Science and Technology*, vol. 26, nr. 4-5, p. 523-553, 2012.
- [28] T. Armstrong, B. Roberts, and C. Swithinbank, *Illustrated Glossary of Snow and Ice*, Cambridge: Scott Polar Research Institute, 1973.
- [29] J. Liu, Z. Janjua, M. Roe, F. Xu, B. Turnbull, K.-S. Choi, and X. Hou, "Super-Hydrophobic/Icephobic Coatings Based on Silica Nanoparticles Modified by Self-Assembled Monolayers", *Nanomaterials*, vol 6. nr. 12, 2016.

Part III
Extra appendices

Appendix G

Future work

Future work

The future work included in this appendix is divided in two main sections, namely experimental investigations and atomistic investigations. The different projects are detailed as much as possible at the present time. All the projects are briefly mentioned in Table G.1, while more details are given in the following sections of the appendix.

Table G.1: Overview of projects for future work to uncover further fundamental mechanisms of ice adhesion strength, divided in experimental and atomistic studies.

Experimental studies
1. Standardisation experiments and protocol
2. Density of ice and measurement
3. Effect of grain size impact on ice detachment
4. Inclined plane and friction for anti-ice and solar cell applications
Atomistic studies
5. Equilibrium study of ice and water
6. Ice adhesion and wettability continues, including advancing and receding contact angles, contact angle hysteresis and macroscopic contact angles
7. Impact of surface structure on ice adhesion strength
8. Theoretical minimal ice adhesion strength for a given surface
9. Effect of ice density and ice grain size on ice adhesion strength

Experimental studies

1. Standardisation experiments

As stated in Section 3.3, a standard test to measure ice adhesion strength is not realistic to achieve. Instead, a realistic approach is to agree upon a common reference test which may be a ground for comparison across different test set-ups. A proposed reference test for this purpose is illustrated in Figure 3.7. However, for such a grounds for comparison to be valid and efficient, a database of recorded ice adhesion strength values for varying parameters should accompany the reference. A suggestion of such varying parameters are illustrated in Figure 3.6.

On the next page is an itemised list including the different elements of the proposed reference test from Figure 3.7, which is the horizontal shear test with bulk water ice on aluminium surface in specific environmental conditions. In order to create a database for changing parameters during ice adhesion testing, the different parameters must be tested against each other in a controlled environment. In other words, the relevant parameters of the reference should be tested in one facility. Each parameter should be tested individually, with at least 10 repetitions for each configuration due to the high variability of ice. For the parameters in the below list, this demand means that for instance the probe distance and the suggested values require 60 ice adhesion tests to measure the effect of probe distance on ice adhesion strength for the reference database. With 12 different parameters to test, the amount of individual ice adhesion tests that should be performed is more than 500. However, such a reference database would be invaluable when working to compare different ice adhesion test methods, and thus also develop state-of-the-art low ice adhesion surfaces.

When a reference database is present, other laboratory facilities may be included to add to the database utilising their own equipment. As long as the parameters are specifically given, they may be compared to the reference test. Such comparisons may also be performed retroactively, adding already published results to the database.

At NTNU, the current ice adhesion measurements are performed with the vertical shear test. As long as the effect of gravity is negligible (see Figure 3.2), this test method should be equivalent to the horizontal shear test and may be utilised for development of the reference database. However, the equality with a defined horizontal shear test would need to be assessed as part of the process.

- Horizontal shear test
 - Probe distance
0.5 mm, 1 mm, 2 mm, 3 mm, 4 mm, 5 mm
 - Probe loading rate
0.01 mms⁻¹, 0.025 mms⁻¹, 0.05 mms⁻¹, 0.1 mms⁻¹, 0.2 mms⁻¹, 0.3 mms⁻¹,
0.5 mms⁻¹
 - Probe size
Depends on the available equipment
- Bulk water ice
 - Ice formation temperature
–5°C, –8°C, –10°C, –15°C, –20°C, –25°C, –30°C, –40°C, –50°C
 - Ice sample size
Includes both contact area and ice sample height, depends on the
available laboratory facility
 - Water quality
Measured in resistivity, might include tap water, rain water, de-mineralised
water, among others.
 - Ice freezing time
1h, 2h, 3h, 5h, 12h, 24h
- Environmental conditions
 - Ambient temperature
–5°C, –8°C, –10°C, –15°C, –20°C, –25°C, –30°C, –40°C, –50°C
Depends on available resources and infrastructure
 - Relative humidity
Depends on available resources and infrastructure
- Surfaces
 - Aluminium
Treated with a standard process, for instance aluminium 6061-T6 pol-
ished with Walter BLENDEX Drum fine 0724 M4.
 - Sylgard 184 or similar untreated and standardised PDMS surface
 - Commercial icephobic surface, for instance EC-3100 from Ecological
Coatings [137].

2. Ice density

There is much information on the density of ice, also for different ice types. Several overviews of ice types categorise the different ice types by density, see Tables 3.4, 3.5 and 3.6. The density of pure ice crystals change very little from their reference value of 0.917 gcm^{-3} except in the presence of air pockets [95]. As such, it is the amount of air in the ice structure that determines the density of the ice, and often also the type of the ice.

In Appendix A, it can be seen that density might be a method for predicting the ice adhesion strength of a given type of ice. However, as the study only dealt with the ratio of ice mass to the ice thickness, i.e. apparent density, the trend is loose at best and cannot be fully determined.

Ice density is often calculated by measuring the dimensions of the ice with varying precision, and dividing the measured detached ice by the approximated ice volume [17, 97, 142]. A formula developed by empiric results is also often used to calculate the ice density of atmospheric ice types [91, 145], and lately a method have been developed to measure the density of ice with x-ray micrography [95, 98]. However, these methods to determine the ice density may only be applied to specific types of ice, and cannot measure the correct ice density in the field.

To enable an investigation of the effect of ice density on the ice adhesion strength, a new method for determining the ice density for typical ice samples applied to ice adhesion tests must be developed. Such a method can be developed at NTNU in cooperation with researchers at the department of civil engineering, where they apply X-ray microtomography to investigate the structure of sea ice [156]. With such a cooperation, the ice types created at AMIL as a part of the first paper of this thesis, see Appendix A, might be reproduced and further examined on at NTNU.

3. Effect of ice grain size

This future work is a continuation on the investigating density of the ice, as the grain size of the ice crystal is connected to the macroscopic density of the ice. Furthermore, the effect of grain size on mechanical properties of ice is substantial. As discussed in the first paper of this thesis (Appendix A), the observation of the grain sizes of different types of ice would enable a more thorough investigation of the mechanical properties of different ice types such as bulk water ice, in-cloud ice and precipitation ice.

As the detachment mechanisms of different ice types differ, and is often impossible to visualise, the effect of grain size is extremely interesting. The grain size helps determine whether the ice in question behaves as brittle or ductile under failure, what the elastic modulus of the ice is, and much more [107]. If the grain

size of ice was determined, the detachment mechanisms of the different types of ice could be predicted based on density. Consequently, this study could shed light on the fundamental characteristics of ice adhesion on different surfaces and for varying conditions.

4. Inclined plane and friction

As mentioned in Section 5.1, the application of tilted surfaces to determine ice adhesion strength is already under development [155], as well as similar test set-ups for snow adhesion [157]. There are several interesting dilemmas in the relation between ice adhesion strength and friction, as well as immediate advantages for instance within solar cell applications.

To characterise low ice adhesion surfaces by the tilting angle of the surfaces is ideal for solar cell applications. Solar cells and building integrated photovoltaic surfaces are impacted by accreted snow and ice, which reduces the efficiency of the photovoltaic cells [158]. If the solar cells were covered with a surface coating enabling low ice adhesion at the angle of the surface, any accreted ice and snow would slip off the surface before impacting the efficiency of the solar cells. Furthermore, as the tilting angle of many solar cells is adjustable to be able to follow the optimal path of the sun throughout the day, the surface coating could be optimally designed for the required ice adhesion strength for passive ice removal at a given angle. As a consequence, if the ice adhesion might be increased but still retain its efficacy, there is more flexibility to optimise other factors in the surface design.

Interesting items in a study focused on the ice adhesion on an inclined plane for solar cell applications is the relation between ice adhesion and friction, as well as a relation between the required ice adhesion for passive detachment of accreted ice of a given ice type and density as function of the tilted angle of the surface. Such a study would result in a list of necessary requirements for a low ice adhesion surface for solar cell applications where the surface has a given angle of tilt, and could even examine if such surface exist today or how they could be manufactured.

Atomistic studies

5. Equilibrium study of ice and water

While water and ice have both been extensively studied with atomistic simulations and molecular dynamics simulations, a study concerning the differences and similarities of water and ice have not yet been conducted. Such a comparison might

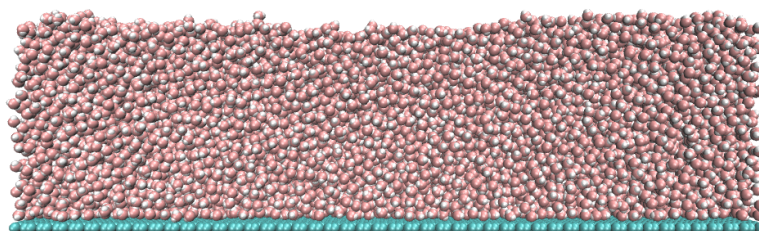


Figure G.1: Example of a system where the equilibrium properties of water and ice might be investigated, here by a water layer on an ideal graphene surface.

be performed by examining the equilibrium conditions of ice and water, and to investigate whether this information yields similarities or differences.

Atomistic simulations of water and ice at equilibrium might be performed on a relatively simple system, such as the one presented in Figure G.1. The system consists of simply a layer of water or ice on a simple surface, here represented by an ideal graphene surface. By investigating such simple systems with some modifications, fundamental similarities and differences between water and ice might be examined. Several methodologies might be utilised to investigate such differences and similarities.

The first method that can be included is a force interaction study. The force interaction gives the difference in interaction forces between the surface and water, and surface and ice. This analysis can also be expanded to include a layer-by-layer analysis of the system, looking at the interfacial energies and interfacial forces between the surface and the different layers of water molecules in both ice and water. This way, an overview of the range of the forces can be found.

Another type of analysis that can be included concerns the vibrational modes. By calculating the auto-correlation function followed by a Fourier transform on the results, the vibrational modes and phonons at the interface can be found. For different configurations of the system for both ice and water, this approach might yield water-ice similarities and differences.

In addition, the analyses should be performed for different systems and conditions. Parameters which could change are temperatures for both water and ice; the surface structure, for instance both graphene and layers of graphite, silicone or gold; the amount of water molecules in the system; the amount of vacuum above the water molecules; and the type of boundary conditions. Most of these different parameters have been checked by other publications, but this study could collect them in one study and apply the results to ice adhesion mechanisms.

This project also comes with possibilities for international cooperation. The

idea was developed in cooperation with professor Niall English at University College Dublin, who is interested in continuing the collaboration with this study. He is well versed in the application and study of molecular dynamics, and the equilibrium study of water and ice fits nicely into his ongoing work. A visit or exchange to his research group in Dublin has been encouraged.

6. Ice adhesion and wettability continued

This study is intended to be a direct continuation of the fourth paper of this thesis (Appendix D). Where the included paper includes only the contact angle and systems with different sizes, this future study should include several types of contact angles including advancing and receding contact angles, contact angle hysteresis and macroscopic contact angles.

The advancing and receding contact angles, often called dynamic contact angles, may be approached with similar simulations as the already performed study, with the sole difference that the surface is tilted to allow for droplet motion during the simulation time. When the dynamic contact angles have been calculated, the contact angle hysteresis can be calculated from their difference. By substituting the contact angle for the receding contact angle, the work of adhesion is substituted with the practical work of adhesion, which is by many hypothesised to correlate stronger with the ice adhesion strength.

Furthermore, the contact angle for a surface at nanoscale likely differs from the macroscopic and experimentally measurable contact angle. To simulate the macroscopic contact angle in atomistic simulations will give further insight into the size effect of water wettability and the relation with ice adhesion strength. One method to calculate the macroscopic water contact angle from atomistic simulations is by applying the dry surface approach [159], which utilises free energy calculations and the work of adhesion to calculate the contact angle.

7. Impact of surface structure for ice adhesion strength

This study is a further continuation of the final paper of the thesis together with the previous suggested future work. So far, the only surface investigated has been an ideal graphene surface. However, ideal surfaces are not experimentally viable, and different scales of roughness and surface texture has been found to greatly impact the ice adhesion strength [25, 33]. For this reason, an atomistic study investigating different surface structures for ice adhesion strength calculations could be useful, both incorporating different types of surfaces and different surface structures.

Several similar studies have been performed previously by members of our research group to discover the ice adhesion detachment mechanisms on given surfaces. In 2016, the effect of a liquid-like layer on graphene and silicon surfaces

with both pulling and shearing detachment of the ice [103]. In 2018, a similar study of atomistic dewetting mechanics at Wenzel and Cassie-Baxter state of wetting on a structured surface was performed [153]. By combining and expanding the procedure in these two study, it is possible to examine the effect of surface structures on different modes of ice adhesion strength.

By investigating the effect of ice adhesion through both shear and tensile detachment on multiple types of surfaces with varying surface structures, valuable information could be gained on the detachment mechanisms of ice on different types of surfaces. These mechanisms might shed light on the macroscopic detachment processes that we have not been able to determine or visualise.

8. Theoretical lowest ice adhesion strength

In Sections 2.2 and 5.1, it is described how the lowest possible ice adhesion is achieved when the electrostatic forces in the ice-solid interaction are minimised and only the van der Waals force is present. These van der Waals forces are possible to simulate with atomistic simulations based on the different atoms and their interactions. It follows that atomistic interactions may be able to predict the lowest possible ice adhesion strength for any given surface.

An interesting future study might therefore be a structured investigation of different surfaces, including metallic surfaces, polymers or structured surfaces, and their theoretical lowest ice adhesion strength. As the goal for many applied research projects is to lower the ice adhesion strength as much as possible, it is important to achieve a lower limit to how low ice adhesion strength can theoretically become.

9. Effect of ice density and grain size

The final suggested future project is a continuation of the experimental study on the effect of ice type on ice adhesion strength (Appendix A). This atomistic investigation complements the experimental project of determining the density and grain structure of the ice types experimentally by simulating similar structures and testing the ice adhesion strength of the different ice types. By creating the ice samples at nanoscale in a simulation, it is possible to observe the internal process during the ice detachment, and connect the process ice failure to experimental results.

Appendix H

Publication list

Department of Structural Engineering
Norwegian University of Science and Technology (NTNU)

**DEPARTMENT OF STRUCTURAL ENGINEERING
NORWEGIAN UNIVERSITY OF SCIENCE AND TECHNOLOGY**

N-7491 TRONDHEIM, NORWAY
Telephone: +47 73 59 47 00

"Reliability Analysis of Structural Systems using Nonlinear Finite Element Methods",
C. A. Holm, 1990:23, ISBN 82-7119-178-0.

"Uniform Stratified Flow Interaction with a Submerged Horizontal Cylinder",
Ø. Arntsen, 1990:32, ISBN 82-7119-188-8.

"Large Displacement Analysis of Flexible and Rigid Systems Considering
Displacement-Dependent Loads and Nonlinear Constraints",
K. M. Mathisen, 1990:33, ISBN 82-7119-189-6.

"Solid Mechanics and Material Models including Large Deformations",
E. Levold, 1990:56, ISBN 82-7119-214-0, ISSN 0802-3271.

"Inelastic Deformation Capacity of Flexurally-Loaded Aluminium Alloy Structures",
T. Welo, 1990:62, ISBN 82-7119-220-5, ISSN 0802-3271.

"Visualization of Results from Mechanical Engineering Analysis",
K. Aamnes, 1990:63, ISBN 82-7119-221-3, ISSN 0802-3271.

"Object-Oriented Product Modeling for Structural Design",
S. I. Dale, 1991:6, ISBN 82-7119-258-2, ISSN 0802-3271.

"Parallel Techniques for Solving Finite Element Problems on Transputer Networks",
T. H. Hansen, 1991:19, ISBN 82-7119-273-6, ISSN 0802-3271.

"Statistical Description and Estimation of Ocean Drift Ice Environments",
R. Korsnes, 1991:24, ISBN 82-7119-278-7, ISSN 0802-3271.

"Properties of concrete related to fatigue damage: with emphasis on high strength
concrete",
G. Petkovic, 1991:35, ISBN 82-7119-290-6, ISSN 0802-3271.

"Turbidity Current Modelling",
B. Brørs, 1991:38, ISBN 82-7119-293-0, ISSN 0802-3271.

"Zero-Slump Concrete: Rheology, Degree of Compaction and Strength. Effects of
Fillers as Part Cement-Replacement",
C. Sørensen, 1992:8, ISBN 82-7119-357-0, ISSN 0802-3271.

"Nonlinear Analysis of Reinforced Concrete Structures Exposed to Transient Loading",
K. V. Høiseith, 1992:15, ISBN 82-7119-364-3, ISSN 0802-3271.

"Finite Element Formulations and Solution Algorithms for Buckling and Collapse
Analysis of Thin Shells",
R. O. Bjærum, 1992:30, ISBN 82-7119-380-5, ISSN 0802-3271.

"Response Statistics of Nonlinear Dynamic Systems",
J. M. Johnsen, 1992:42, ISBN 82-7119-393-7, ISSN 0802-3271.

"Digital Models in Engineering. A Study on why and how engineers build and operate
digital models for decision support",
J. Høyte, 1992:75, ISBN 82-7119-429-1, ISSN 0802-3271.

"Sparse Solution of Finite Element Equations",
A. C. Damhaug, 1992:76, ISBN 82-7119-430-5, ISSN 0802-3271.

"Some Aspects of Floating Ice Related to Sea Surface Operations in the Barents Sea",
S. Løset, 1992:95, ISBN 82-7119-452-6, ISSN 0802-3271.

"Modelling of Cyclic Plasticity with Application to Steel and Aluminium Structures",
O. S. Hopperstad, 1993:7, ISBN 82-7119-461-5, ISSN 0802-3271.

"The Free Formulation: Linear Theory and Extensions with Applications to Tetrahedral
Elements
with Rotational Freedoms",
G. Skeie, 1993:17, ISBN 82-7119-472-0, ISSN 0802-3271.

"Høyfast betongs motstand mot piggdekkslitasje. Analyse av resultater fra prøving i
Veisliter'n",
T. Tveter, 1993:62, ISBN 82-7119-522-0, ISSN 0802-3271.

"A Nonlinear Finite Element Based on Free Formulation Theory for Analysis of
Sandwich Structures",
O. Aamlid, 1993:72, ISBN 82-7119-534-4, ISSN 0802-3271.

"The Effect of Curing Temperature and Silica Fume on Chloride Migration and Pore
Structure of High Strength Concrete",
C. J. Hauck, 1993:90, ISBN 82-7119-553-0, ISSN 0802-3271.

"Failure of Concrete under Compressive Strain Gradients",
G. Markeset, 1993:110, ISBN 82-7119-575-1, ISSN 0802-3271.

"An experimental study of internal tidal amphidromes in Vestfjorden",
J. H. Nilsen, 1994:39, ISBN 82-7119-640-5, ISSN 0802-3271.

- "Structural analysis of oil wells with emphasis on conductor design",
H. Larsen, 1994:46, ISBN 82-7119-648-0, ISSN 0802-3271.
- "Adaptive methods for non-linear finite element analysis of shell structures",
K. M. Okstad, 1994:66, ISBN 82-7119-670-7, ISSN 0802-3271.
- "On constitutive modelling in nonlinear analysis of concrete structures",
O. Fyrileiv, 1994:115, ISBN 82-7119-725-8, ISSN 0802-3271.
- "Fluctuating wind load and response of a line-like engineering structure with emphasis on motion-induced wind forces",
J. Bogunovic Jakobsen, 1995:62, ISBN 82-7119-809-2, ISSN 0802-3271.
- "An experimental study of beam-columns subjected to combined torsion, bending and axial actions",
A. Aalberg, 1995:66, ISBN 82-7119-813-0, ISSN 0802-3271.
- "Scaling and cracking in unsealed freeze/thaw testing of Portland cement and silica fume concretes",
S. Jacobsen, 1995:101, ISBN 82-7119-851-3, ISSN 0802-3271.
- "Damping of water waves by submerged vegetation. A case study of laminaria hyperborea",
A. M. Dubi, 1995:108, ISBN 82-7119-859-9, ISSN 0802-3271.
- "The dynamics of a slope current in the Barents Sea",
Sheng Li, 1995:109, ISBN 82-7119-860-2, ISSN 0802-3271.
- "Modellering av delmaterialenes betydning for betongens konsistens",
Ernst Mørtzell, 1996:12, ISBN 82-7119-894-7, ISSN 0802-3271.
- "Bending of thin-walled aluminium extrusions",
Birgit Søvik Opheim, 1996:60, ISBN 82-7119-947-1, ISSN 0802-3271.
- "Material modelling of aluminium for crashworthiness analysis",
Torodd Berstad, 1996:89, ISBN 82-7119-980-3, ISSN 0802-3271.
- "Estimation of structural parameters from response measurements on submerged floating tunnels",
Rolf Magne Larssen, 1996:119, ISBN 82-471-0014-2, ISSN 0802-3271.
- "Numerical modelling of plain and reinforced concrete by damage mechanics",
Mario A. Polanco-Loria, 1997:20, ISBN 82-471-0049-5, ISSN 0802-3271.
- "Nonlinear random vibrations - numerical analysis by path integration methods",
Vibeke Moe, 1997:26, ISBN 82-471-0056-8, ISSN 0802-3271.

- “Numerical prediction of vortex-induced vibration by the finite element method”,
Joar Martin Dalheim, 1997:63, ISBN 82-471-0096-7, ISSN 0802-3271.
- “Time domain calculations of buffeting response for wind sensitive structures”,
Ketil Aas-Jakobsen, 1997:148, ISBN 82-471-0189-0, ISSN 0802-3271.
- "A numerical study of flow about fixed and flexibly mounted circular cylinders",
Trond Stokka Meling, 1998:48, ISBN 82-471-0244-7, ISSN 0802-3271.
- “Estimation of chloride penetration into concrete bridges in coastal areas”,
Per Egil Steen, 1998:89, ISBN 82-471-0290-0, ISSN 0802-3271.
- “Stress-resultant material models for reinforced concrete plates and shells”,
Jan Arve Øverli, 1998:95, ISBN 82-471-0297-8, ISSN 0802-3271.
- “Chloride binding in concrete. Effect of surrounding environment and concrete composition”,
Claus Kenneth Larsen, 1998:101, ISBN 82-471-0337-0, ISSN 0802-3271.
- “Rotational capacity of aluminium alloy beams”,
Lars A. Moen, 1999:1, ISBN 82-471-0365-6, ISSN 0802-3271.
- “Stretch Bending of Aluminium Extrusions”,
Arild H. Clausen, 1999:29, ISBN 82-471-0396-6, ISSN 0802-3271.
- “Aluminium and Steel Beams under Concentrated Loading”,
Tore Tryland, 1999:30, ISBN 82-471-0397-4, ISSN 0802-3271.
- "Engineering Models of Elastoplasticity and Fracture for Aluminium Alloys",
Odd-Geir Lademo, 1999:39, ISBN 82-471-0406-7, ISSN 0802-3271.
- "Kapazität og duktilitet av dybelforbindelser i trekonstruksjoner",
Jan Siem, 1999:46, ISBN 82-471-0414-8, ISSN 0802-3271.
- “Etablering av distribuert ingeniørarbeid; Teknologiske og organisatoriske erfaringer fra en norsk ingeniørbedrift”,
Lars Line, 1999:52, ISBN 82-471-0420-2, ISSN 0802-3271.
- “Estimation of Earthquake-Induced Response”,
Símon Ólafsson, 1999:73, ISBN 82-471-0443-1, ISSN 0802-3271.
- “Coastal Concrete Bridges: Moisture State, Chloride Permeability and Aging Effects”
Ragnhild Holen Relling, 1999:74, ISBN 82-471-0445-8, ISSN 0802-3271.
- ”Capacity Assessment of Titanium Pipes Subjected to Bending and External Pressure”,
Arve Bjørset, 1999:100, ISBN 82-471-0473-3, ISSN 0802-3271.

“Validation of Numerical Collapse Behaviour of Thin-Walled Corrugated Panels”,
Håvar Ilstad, 1999:101, ISBN 82-471-0474-1, ISSN 0802-3271.

“Strength and Ductility of Welded Structures in Aluminium Alloys”,
Miroslaw Matusiak, 1999:113, ISBN 82-471-0487-3, ISSN 0802-3271.

“Thermal Dilation and Autogenous Deformation as Driving Forces to Self-Induced Stresses in High Performance Concrete”,
Øyvind Bjøntegaard, 1999:121, ISBN 82-7984-002-8, ISSN 0802-3271.

“Some Aspects of Ski Base Sliding Friction and Ski Base Structure”,
Dag Anders Moldestad, 1999:137, ISBN 82-7984-019-2, ISSN 0802-3271.

"Electrode reactions and corrosion resistance for steel in mortar and concrete",
Roy Antonsen, 2000:10, ISBN 82-7984-030-3, ISSN 0802-3271.

"Hydro-Physical Conditions in Kelp Forests and the Effect on Wave Damping and Dune Erosion. A case study on Laminaria Hyperborea",
Stig Magnar Løvås, 2000:28, ISBN 82-7984-050-8, ISSN 0802-3271.

"Random Vibration and the Path Integral Method",
Christian Skaug, 2000:39, ISBN 82-7984-061-3, ISSN 0802-3271.

"Buckling and geometrical nonlinear beam-type analyses of timber structures",
Trond Even Eggen, 2000:56, ISBN 82-7984-081-8, ISSN 0802-3271.

”Structural Crashworthiness of Aluminium Foam-Based Components”,
Arve Grønsund Hanssen, 2000:76, ISBN 82-7984-102-4, ISSN 0809-103X.

“Measurements and simulations of the consolidation in first-year sea ice ridges, and some aspects of mechanical behaviour”,
Knut V. Høyland, 2000:94, ISBN 82-7984-121-0, ISSN 0809-103X.

”Kinematics in Regular and Irregular Waves based on a Lagrangian Formulation”,
Svein Helge Gjørund, 2000-86, ISBN 82-7984-112-1, ISSN 0809-103X.

”Self-Induced Cracking Problems in Hardening Concrete Structures”,
Daniela Bosnjak, 2000-121, ISBN 82-7984-151-2, ISSN 0809-103X.

"Ballistic Penetration and Perforation of Steel Plates",
Tore Børvik, 2000:124, ISBN 82-7984-154-7, ISSN 0809-103X.

"Freeze-Thaw resistance of Concrete. Effect of: Curing Conditions, Moisture Exchange and Materials",
Terje Finnerup Rønning, 2001:14, ISBN 82-7984-165-2, ISSN 0809-103X

"Structural behaviour of post tensioned concrete structures. Flat slab. Slabs on ground",
Steinar Trygstad, 2001:52, ISBN 82-471-5314-9, ISSN 0809-103X.

"Slipforming of Vertical Concrete Structures. Friction between concrete and slipform panel",
Kjell Tore Fosså, 2001:61, ISBN 82-471-5325-4, ISSN 0809-103X.

"Some numerical methods for the simulation of laminar and turbulent incompressible flows",
Jens Holmen, 2002:6, ISBN 82-471-5396-3, ISSN 0809-103X.

"Improved Fatigue Performance of Threaded Drillstring Connections by Cold Rolling",
Steinar Kristoffersen, 2002:11, ISBN: 82-421-5402-1, ISSN 0809-103X.

"Deformations in Concrete Cantilever Bridges: Observations and Theoretical Modelling",
Peter F. Takács, 2002:23, ISBN 82-471-5415-3, ISSN 0809-103X.

"Stiffened aluminium plates subjected to impact loading",
Hilde Giæver Hildrum, 2002:69, ISBN 82-471-5467-6, ISSN 0809-103X.

"Full- and model scale study of wind effects on a medium-rise building in a built up area",
Jónas Thór Snæbjörnsson, 2002:95, ISBN82-471-5495-1, ISSN 0809-103X.

"Evaluation of Concepts for Loading of Hydrocarbons in Ice-infested water",
Arnor Jensen, 2002:114, ISBN 82-417-5506-0, ISSN 0809-103X.

"Numerical and Physical Modelling of Oil Spreading in Broken Ice",
Janne K. Økland Gjosteen, 2002:130, ISBN 82-471-5523-0, ISSN 0809-103X.

"Diagnosis and protection of corroding steel in concrete",
Franz Pruckner, 20002:140, ISBN 82-471-5555-4, ISSN 0809-103X.

"Tensile and Compressive Creep of Young Concrete: Testing and Modelling",
Dawood Atrushi, 2003:17, ISBN 82-471-5565-6, ISSN 0809-103X.

"Rheology of Particle Suspensions. Fresh Concrete, Mortar and Cement Paste with Various Types of Lignosulfonates",
Jon Elvar Wallevik, 2003:18, ISBN 82-471-5566-4, ISSN 0809-103X.

"Oblique Loading of Aluminium Crash Components",
Aase Reyes, 2003:15, ISBN 82-471-5562-1, ISSN 0809-103X.

"Utilization of Ethiopian Natural Pozzolans",
Surafel Ketema Desta, 2003:26, ISSN 82-471-5574-5, ISSN:0809-103X.

“Behaviour and strength prediction of reinforced concrete structures with discontinuity regions”, Helge Brå, 2004:11, ISBN 82-471-6222-9, ISSN 1503-8181.

“High-strength steel plates subjected to projectile impact. An experimental and numerical study”, Sumita Dey, 2004:38, ISBN 82-471-6282-2 (printed version), ISBN 82-471-6281-4 (electronic version), ISSN 1503-8181.

“Alkali-reactive and inert fillers in concrete. Rheology of fresh mixtures and expansive reactions.”

Bård M. Pedersen, 2004:92, ISBN 82-471-6401-9 (printed version), ISBN 82-471-6400-0 (electronic version), ISSN 1503-8181.

“On the Shear Capacity of Steel Girders with Large Web Openings”.

Nils Christian Hagen, 2005:9 ISBN 82-471-6878-2 (printed version), ISBN 82-471-6877-4 (electronic version), ISSN 1503-8181.

”Behaviour of aluminium extrusions subjected to axial loading”.

Østen Jensen, 2005:7, ISBN 82-471-6873-1 (printed version), ISBN 82-471-6872-3 (electronic version), ISSN 1503-8181.

”Thermal Aspects of corrosion of Steel in Concrete”.

Jan-Magnus Østvik, 2005:5, ISBN 82-471-6869-3 (printed version), ISBN 82-471-6868 (electronic version), ISSN 1503-8181.

”Mechanical and adaptive behaviour of bone in relation to hip replacement.” A study of bone remodelling and bone grafting.

Sébastien Muller, 2005:34, ISBN 82-471-6933-9 (printed version), ISBN 82-471-6932-0 (electronic version), ISSN 1503-8181.

“Analysis of geometrical nonlinearities with applications to timber structures”.

Lars Wollebæk, 2005:74, ISBN 82-471-7050-5 (printed version), ISBN 82-471-7019-1 (electronic version), ISSN 1503-8181.

“Pedestrian induced lateral vibrations of slender footbridges”.

Anders Rönnquist, 2005:102, ISBN 82-471-7082-5 (printed version), ISBN 82-471-7081-7 (electronic version), ISSN 1503-8181.

“Initial Strength Development of Fly Ash and Limestone Blended Cements at Various Temperatures Predicted by Ultrasonic Pulse Velocity”.

Tom Ivar Fredvik, 2005:112, ISBN 82-471-7105-8 (printed version), ISBN 82-471-7103-1 (electronic version), ISSN 1503-8181.

“Behaviour and modelling of thin-walled cast components”.

Cato Dørum, 2005:128, ISBN 82-471-7140-6 (printed version), ISBN 82-471-7139-2 (electronic version), ISSN 1503-8181.

- “Behaviour and modelling of selfpiercing riveted connections”,
Raffaele Porcaro, 2005:165, ISBN 82-471-7219-4 (printed version), ISBN 82-471-7218-6 (electronic version), ISSN 1503-8181.
- ”Behaviour and Modelling of Aluminium Plates subjected to Compressive Load”,
Lars Rønning, 2005:154, ISBN 82-471-7169-1 (printed version), ISBN 82-471-7195-3 (electronic version), ISSN 1503-8181.
- ”Bumper beam-longitudinal system subjected to offset impact loading”,
Satyanarayana Kokkula, 2005:193, ISBN 82-471-7280-1 (printed version), ISBN 82-471-7279-8 (electronic version), ISSN 1503-8181.
- “Control of Chloride Penetration into Concrete Structures at Early Age”,
Guofei Liu, 2006:46, ISBN 82-471-7838-9 (printed version), ISBN 82-471-7837-0 (electronic version), ISSN 1503-8181.
- “Modelling of Welded Thin-Walled Aluminium Structures”,
Ting Wang, 2006:78, ISBN 82-471-7907-5 (printed version), ISBN 82-471-7906-7 (electronic version), ISSN 1503-8181.
- ”Time-variant reliability of dynamic systems by importance sampling and probabilistic analysis of ice loads”,
Anna Ivanova Olsen, 2006:139, ISBN 82-471-8041-3 (printed version), ISBN 82-471-8040-5 (electronic version), ISSN 1503-8181.
- “Fatigue life prediction of an aluminium alloy automotive component using finite element analysis of surface topography”,
Sigmund Kyrre Ås, 2006:25, ISBN 82-471-7791-9 (printed version), ISBN 82-471-7791-9 (electronic version), ISSN 1503-8181.
- ”Constitutive models of elastoplasticity and fracture for aluminium alloys under strain path change”,
Dasharatha Achani, 2006:76, ISBN 82-471-7903-2 (printed version), ISBN 82-471-7902-4 (electronic version), ISSN 1503-8181.
- “Simulations of 2D dynamic brittle fracture by the Element-free Galerkin method and linear fracture mechanics”,
Tommy Karlsson, 2006:125, ISBN 82-471-8011-1 (printed version), ISBN 82-471-8010-3 (electronic version), ISSN 1503-8181.
- “Penetration and Perforation of Granite Targets by Hard Projectiles”,
Chong Chiang Seah, 2006:188, ISBN 82-471-8150-9 (printed version), ISBN 82-471-8149-5 (electronic version), ISSN 1503-8181.

“Deformations, strain capacity and cracking of concrete in plastic and early hardening phases”,

Tor Arne Hammer, 2007:234, ISBN 978-82-471-5191-4 (printed version), ISBN 978-82-471-5207-2 (electronic version), ISSN 1503-8181.

“Crashworthiness of dual-phase high-strength steel: Material and Component behaviour”, Venkatapathi Tarigopula, 2007:230, ISBN 82-471-5076-4 (printed version), ISBN 82-471-5093-1 (electronic version), ISSN 1503-8181.

“Fibre reinforcement in load carrying concrete structures”,

Åse Lyslo Døssland, 2008:50, ISBN 978-82-471-6910-0 (printed version), ISBN 978-82-471-6924-7 (electronic version), ISSN 1503-8181.

“Low-velocity penetration of aluminium plates”,

Frode Grytten, 2008:46, ISBN 978-82-471-6826-4 (printed version), ISBN 978-82-471-6843-1 (electronic version), ISSN 1503-8181.

“Robustness studies of structures subjected to large deformations”,

Ørjan Fyllingen, 2008:24, ISBN 978-82-471-6339-9 (printed version), ISBN 978-82-471-6342-9 (electronic version), ISSN 1503-8181.

“Constitutive modelling of morsellised bone”,

Knut Birger Lunde, 2008:92, ISBN 978-82-471-7829-4 (printed version), ISBN 978-82-471-7832-4 (electronic version), ISSN 1503-8181.

“Experimental Investigations of Wind Loading on a Suspension Bridge Girder”,

Bjørn Isaksen, 2008:131, ISBN 978-82-471-8656-5 (printed version), ISBN 978-82-471-8673-2 (electronic version), ISSN 1503-8181.

“Cracking Risk of Concrete Structures in The Hardening Phase”,

Guomin Ji, 2008:198, ISBN 978-82-471-1079-9 (printed version), ISBN 978-82-471-1080-5 (electronic version), ISSN 1503-8181.

“Modelling and numerical analysis of the porcine and human mitral apparatus”,

Victorien Emile Prot, 2008:249, ISBN 978-82-471-1192-5 (printed version), ISBN 978-82-471-1193-2 (electronic version), ISSN 1503-8181.

“Strength analysis of net structures”,

Heidi Moe, 2009:48, ISBN 978-82-471-1468-1 (printed version), ISBN 978-82-471-1469-8 (electronic version), ISSN 1503-8181.

“Numerical analysis of ductile fracture in surface cracked shells”,

Espen Berg, 2009:80, ISBN 978-82-471-1537-4 (printed version), ISBN 978-82-471-1538-1 (electronic version), ISSN 1503-8181.

“Subject specific finite element analysis of bone – for evaluation of the healing of a leg lengthening and evaluation of femoral stem design”,
Sune Hansborg Pettersen, 2009:99, ISBN 978-82-471-1579-4 (printed version), ISBN 978-82-471-1580-0 (electronic version), ISSN 1503-8181.

“Evaluation of fracture parameters for notched multi-layered structures”,
Lingyun Shang, 2009:137, ISBN 978-82-471-1662-3 (printed version), ISBN 978-82-471-1663-0 (electronic version), ISSN 1503-8181.

“Modelling of Dynamic Material Behaviour and Fracture of Aluminium Alloys for Structural Applications”
Yan Chen, 2009:69, ISBN 978-82-471-1515-2 (printed version), ISBN 978-82 471-1516-9 (electronic version), ISSN 1503-8181.

“Nanomechanics of polymer and composite particles”
Jianying He 2009:213, ISBN 978-82-471-1828-3 (printed version), ISBN 978-82-471-1829-0 (electronic version), ISSN 1503-8181.

“Mechanical properties of clear wood from Norway spruce”
Kristian Berbom Dahl 2009:250, ISBN 978-82-471-1911-2 (printed version) ISBN 978-82-471-1912-9 (electronic version), ISSN 1503-8181.

“Modeling of the degradation of TiB₂ mechanical properties by residual stresses and liquid Al penetration along grain boundaries”
Micol Pezzotta 2009:254, ISBN 978-82-471-1923-5 (printed version) ISBN 978-82-471-1924-2 (electronic version) ISSN 1503-8181.

“Effect of welding residual stress on fracture”
Xiabo Ren 2010:77, ISBN 978-82-471-2115-3 (printed version) ISBN 978-82-471-2116-0 (electronic version), ISSN 1503-8181.

“Pan-based carbon fiber as anode material in cathodic protection system for concrete structures”
Mahdi Chini 2010:122, ISBN 978-82-471-2210-5 (printed version) ISBN 978-82-471-2213-6 (electronic version), ISSN 1503-8181.

“Structural Behaviour of deteriorated and retrofitted concrete structures”
Irina Vasililjeva Sæther 2010:171, ISBN 978-82-471-2315-7 (printed version) ISBN 978-82-471-2316-4 (electronic version) ISSN 1503-8181.

“Prediction of local snow loads on roofs”
Vivian Meløysund 2010:247, ISBN 978-82-471-2490-1 (printed version) ISBN 978-82-471-2491-8 (electronic version) ISSN 1503-8181.

“Behaviour and modelling of polymers for crash applications”
Virgile Delhaye 2010:251, ISBN 978-82-471-2501-4 (printed version) ISBN 978-82-471-2502-1 (electronic version) ISSN 1503-8181.

“Blended cement with reduced CO₂ emission – Utilizing the Fly Ash-Limestone Synergy”,
Klaartje De Weerd 2011:32, ISBN 978-82-471-2584-7 (printed version) ISBN 978-82-471-2584-4 (electronic version) ISSN 1503-8181.

“Chloride induced reinforcement corrosion in concrete” Concept of critical chloride content – methods and mechanisms.
Ueli Angst 2011:113, ISBN 978-82-471-2769-9 (printed version) ISBN 978-82-471-2763-6 (electronic version) ISSN 1503-8181.

“A thermo-electric-Mechanical study of the carbon anode and contact interface for Energy savings in the production of aluminium”.
Dag Herman Andersen 2011:157, ISBN 978-82-471-2859-6 (printed version) ISBN 978-82-471-2860-2 (electronic version) ISSN 1503-8181.

“Structural Capacity of Anchorage Ties in Masonry Veneer Walls Subjected to Earthquake”. The implications of Eurocode 8 and Eurocode 6 on a typical Norwegian veneer wall.
Ahmed Mohamed Yousry Hamed 2011:181, ISBN 978-82-471-2911-1 (printed version) ISBN 978-82-471-2912-8 (electronic ver.) ISSN 1503-8181.

“Work-hardening behaviour in age-hardenable Al-Zn-Mg(-Cu) alloys”.
Ida Westermann , 2011:247, ISBN 978-82-471-3056-8 (printed ver.) ISBN 978-82-471-3057-5 (electronic ver.) ISSN 1503-8181.

“Behaviour and modelling of selfpiercing riveted connections using aluminium rivets”.
Nguyen-Hieu Hoang, 2011:266, ISBN 978-82-471-3097-1 (printed ver.) ISBN 978-82-471-3099-5 (electronic ver.) ISSN 1503-8181.

“Fibre reinforced concrete”.
Sindre Sandbakk, 2011:297, ISBN 978-82-471-3167-1 (printed ver.) ISBN 978-82-471-3168-8 (electronic ver) ISSN 1503:8181.

“Dynamic behaviour of cablesupported bridges subjected to strong natural wind”.
Ole Andre Øiseth, 2011:315, ISBN 978-82-471-3209-8 (printed ver.) ISBN 978-82-471-3210-4 (electronic ver.) ISSN 1503-8181.

“Constitutive modeling of solargrade silicon materials”
Julien Cochard, 2011:307, ISBN 978-82-471-3189-3 (printed ver). ISBN 978-82-471-3190-9 (electronic ver.) ISSN 1503-8181.

“Constitutive behavior and fracture of shape memory alloys”
Jim Stian Olsen, 2012:57, ISBN 978-82-471-3382-8 (printed ver.) ISBN 978-82-471-3383-5 (electronic ver.) ISSN 1503-8181.

“Field measurements in mechanical testing using close-range photogrammetry and digital image analysis”

Egil Fagerholt, 2012:95, ISBN 978-82-471-3466-5 (printed ver.) ISBN 978-82-471-3467-2 (electronic ver.) ISSN 1503-8181.

“Towards a better understanding of the ultimate behaviour of lightweight aggregate concrete in compression and bending”,

Håvard Nedrelid, 2012:123, ISBN 978-82-471-3527-3 (printed ver.) ISBN 978-82-471-3528-0 (electronic ver.) ISSN 1503-8181.

“Numerical simulations of blood flow in the left side of the heart”

Sigrid Kaarstad Dahl, 2012:135, ISBN 978-82-471-3553-2 (printed ver.) ISBN 978-82-471-3555-6 (electronic ver.) ISSN 1503-8181.

“Moisture induced stresses in glulam”

Vanessa Angst-Nicollier, 2012:139, ISBN 978-82-471-3562-4 (printed ver.) ISBN 978-82-471-3563-1 (electronic ver.) ISSN 1503-8181.

“Biomechanical aspects of distraction osteogenesis”

Valentina La Russa, 2012:250, ISBN 978-82-471-3807-6 (printed ver.) ISBN 978-82-471-3808-3 (electronic ver.) ISSN 1503-8181.

“Ductile fracture in dual-phase steel. Theoretical, experimental and numerical study”

Gaute Gruben, 2012:257, ISBN 978-82-471-3822-9 (printed ver.) ISBN 978-82-471-3823-6 (electronic ver.) ISSN 1503-8181.

“Damping in Timber Structures”

Nathalie Labonnote, 2012:263, ISBN 978-82-471-3836-6 (printed ver.) ISBN 978-82-471-3837-3 (electronic ver.) ISSN 1503-8181.

“Biomechanical modeling of fetal veins: The umbilical vein and ductus venosus bifurcation”

Paul Roger Leinan, 2012:299, ISBN 978-82-471-3915-8 (printed ver.) ISBN 978-82-471-3916-5 (electronic ver.) ISSN 1503-8181.

“Large-Deformation behaviour of thermoplastics at various stress states”

Anne Serine Ognedal, 2012:298, ISBN 978-82-471-3913-4 (printed ver.) ISBN 978-82-471-3914-1 (electronic ver.) ISSN 1503-8181.

“Hardening accelerator for fly ash blended cement”

Kien Dinh Hoang, 2012:366, ISBN 978-82-471-4063-5 (printed ver.) ISBN 978-82-471-4064-2 (electronic ver.) ISSN 1503-8181.

“From molecular structure to mechanical properties”

Jianyang Wu, 2013:186, ISBN 978-82-471-4485-5 (printed ver.) ISBN 978-82-471-4486-2 (electronic ver.) ISSN 1503-8181.

“Experimental and numerical study of hybrid concrete structures”

Linn Grepstad Nes, 2013:259, ISBN 978-82-471-4644-6 (printed ver.) ISBN 978-82-471-4645-3 (electronic ver.) ISSN 1503-8181.

“Mechanics of ultra-thin multi crystalline silicon wafers”

Saber Saffar, 2013:199, ISBN 978-82-471-4511-1 (printed ver.) ISBN 978-82-471-4513-5 (electronic ver.) ISSN 1503-8181.

“Through process modelling of welded aluminium structures”

Anizahyati Alisibramulisi, 2013:325, ISBN 978-82-471-4788-7 (printed ver.) ISBN 978-82-471-4789-4 (electronic ver.) ISSN 1503-8181.

“Combined blast and fragment loading on steel plates”

Knut Gaarder Rakvåg, 2013:361, ISBN 978-82-471-4872-3 (printed ver.) ISBN 978-82-4873-0 (electronic ver.) ISSN 1503-8181.

“Characterization and modelling of the anisotropic behaviour of high-strength aluminium alloy”

Marion Fourmeau, 2014:37, ISBN 978-82-326-0008-3 (printed ver.) ISBN 978-82-326-0009-0 (electronic ver.) ISSN 1503-8181.

“Behaviour of threaded steel fasteners at elevated deformation rates”

Henning Fransplass, 2014:65, ISBN 978-82-326-0054-0 (printed ver.) ISBN 978-82-326-0055-7 (electronic ver.) ISSN 1503-8181.

“Sedimentation and Bleeding”

Ya Peng, 2014:89, ISBN 978-82-326-0102-8 (printed ver.) ISBN 978-82-326-0103-5 (electronic ver.) ISSN 1503-8181.

“Impact against X65 offshore pipelines”

Martin Kristoffersen, 2014:362, ISBN 978-82-326-0636-8 (printed ver.) ISBN 978-82-326-0637-5 (electronic ver.) ISSN 1503-8181.

“Formability of aluminium alloy subjected to prestrain by rolling”

Dmitry Vysochinskiy, 2014:363, ISBN 978-82-326-0638-2 (printed ver.) ISBN 978-82-326-0639-9 (electronic ver.) ISSN 1503-8181.

“Experimental and numerical study of Yielding, Work-Hardening and anisotropy in textured AA6xxx alloys using crystal plasticity models”

Mikhail Khadyko, 2015:28, ISBN 978-82-326-0724-2 (printed ver.) ISBN 978-82-326-0725-9 (electronic ver.) ISSN 1503-8181.

“Behaviour and Modelling of AA6xxx Aluminium Alloys Under a Wide Range of Temperatures and Strain Rates”

Vincent Vilamosa, 2015:63, ISBN 978-82-326-0786-0 (printed ver.) ISBN 978-82-326-0787-7 (electronic ver.) ISSN 1503-8181.

“A Probabilistic Approach in Failure Modelling of Aluminium High Pressure Die-Castings”

Octavian Knoll, 2015:137, ISBN 978-82-326-0930-7 (printed ver.) ISBN 978-82-326-0931-4 (electronic ver.) ISSN 1503-8181.

“Ice Abrasion on Marine Concrete Structures”

Egil Møen, 2015:189, ISBN 978-82-326-1034-1 (printed ver.) ISBN 978-82-326-1035-8 (electronic ver.) ISSN 1503-8181.

“Fibre Orientation in Steel-Fibre-Reinforced Concrete”

Giedrius Zirgulis, 2015:229, ISBN 978-82-326-1114-0 (printed ver.) ISBN 978-82-326-1115-7 (electronic ver.) ISSN 1503-8181.

“Effect of spatial variation and possible interference of localised corrosion on the residual capacity of a reinforced concrete beam”

Mohammad Mahdi Kioumarsi, 2015:282, ISBN 978-82-326-1220-8 (printed ver.) ISBN 978-82-1221-5 (electronic ver.) ISSN 1503-8181.

“The role of concrete resistivity in chloride-induced macro-cell corrosion”

Karla Horbostel, 2015:324, ISBN 978-82-326-1304-5 (printed ver.) ISBN 978-82-326-1305-2 (electronic ver.) ISSN 1503-8181.

“Flowable fibre-reinforced concrete for structural applications”

Elena Vidal Sarmiento, 2015:335, ISBN 978-82-326-1324-3 (printed ver.) ISBN 978-82-326-1325-0 (electronic ver.) ISSN 1503-8181.

“Development of chushed sand for concrete production with microproportioning”

Rolands Cepuritis, 2016:19, ISBN 978-82-326-1382-3 (printed ver.) ISBN 978-82-326-1383-0 (electronic ver.) ISSN 1503-8181.

“Withdrawal properties of threaded rods embedded in glued-laminated timber elements”

Haris Stamatopoulos, 2016:48, ISBN 978-82-326-1436-3 (printed ver.) ISBN 978-82-326-1437-0 (electronic ver.) ISSN 1503-8181.

“An Experimental and numerical study of thermoplastics at large deformation”

Marius Andersen, 2016:191, ISBN 978-82-326-1720-3 (printed ver.) ISBN 978-82-326-1721-0 (electronic ver.) ISSN 1503-8181.

“Modeling and Simulation of Ballistic Impact”

Jens Kristian Holmen, 2016:240, ISBN 978-82-326-1818-7 (printed ver.) ISBN 978-82-326-1819-4 (electronic ver.) ISSN 1503-8181.

“Early age crack assessment of concrete structures”

Anja B. Estensen Klausen, 2016:256, ISBN 978-82-326-1850-7 (printed ver.) ISBN 978-82-326-1851-4 (electronic ver.) ISSN 1503-8181.

- “Uncertainty quantification and sensitivity analysis for cardiovascular models”
Vinzenc Gregor Eck, 2016:234, ISBN 978-82-326-1806-4 (printed ver.) ISBN 978-82-326-1807-1 (electronic ver.) ISSN 1503-8181.
- “Dynamic behaviour of existing and new railway catenary systems under Norwegian conditions”
Petter Røe Nåvik, 2016:298, ISBN 978-82-326-1935-1 (printed ver.) ISBN 978-82-326-1934-4 (electronic ver.) ISSN 1503-8181.
- “Mechanical behaviour of particle-filled elastomers at various temperatures”
Arne Ilse, 2016:295, ISBN 978-82-326-1928-3 (printed ver.) ISBN 978-82-326-1929-0 (electronic ver.) ISSN 1503-8181.
- “Nanotechnology for Anti-Icing Application”
Zhiwei He, 2016:348, ISBN 978-82-326-2038-8 (printed ver.) ISBN 978-82-326-2019-5 (electronic ver.) ISSN 1503-8181.
- “Conduction Mechanisms in Conductive Adhesives with Metal-Coated Polymer Spheres”
Sigurd Rolland Pettersen, 2016:349, ISBN 978-82-326-2040-1 (printed ver.) ISBN 978-82-326-2041-8 (electronic ver.) ISSN 1503-8181.
- “The interaction between calcium lignosulfonate and cement”
Alessia Colombo, 2017:20, ISBN 978-82-326-2122-4 (printed ver.) ISBN 978-82-326-2123-1 (electronic ver.) ISSN 1503-8181.
- “Behaviour and Modelling of Flexible Structures Subjected to Blast Loading”
Vegard Aune, 2017:101, ISBN 978-82-326-2274-0 (printed ver.) ISBN 978-82-326-2275-7 (electronic ver.) ISSN 1503-8181.
- “Behaviour of steel connections under quasi-static and impact loading”
Erik Løhre Grimsmo, 2017:159, ISBN 978-82-326-2390-7 (printed ver.) ISBN 978-82-326-2391-4 (electronic ver.) ISSN 1503-8181.
- “An experimental and numerical study of cortical bone at the macro and Nano-scale”
Masoud Ramenzanzadehkoldeh, 2017:208, ISBN 978-82-326-2488-1 (printed ver.) ISBN 978-82-326-2489-8 (electronic ver.) ISSN 1503-8181.
- “Optoelectrical Properties of a Novel Organic Semiconductor: 6,13-Dichloropentacene”
Mao Wang, 2017:130, ISBN 978-82-326-2332-7 (printed ver.) ISBN 978-82-326-2333-4 (electronic ver.) ISSN 1503-8181.
- “Core-shell structured microgels and their behavior at oil and water interface”
Yi Gong, 2017:182, ISBN 978-82-326-2436-2 (printed ver.) ISBN 978-82-326-2437-9 (electronic ver.) ISSN 1503-8181.

“Aspects of design of reinforced concrete structures using nonlinear finite element analyses”

Morten Engen, 2017:149, ISBN 978-82-326-2370-9 (printed ver.) ISBN 978-82-326-2371-6 (electronic ver.) ISSN 1503-8181.

“Numerical studies on ductile failure of aluminium alloys”

Lars Edvard Dæhli, 2017:284, ISBN 978-82-326-2636-6 (printed ver.) ISBN 978-82-326-2637-3 (electronic ver.) ISSN 1503-8181.

“Modelling and Assessment of Hydrogen Embrittlement in Steels and Nickel Alloys”

Haiyang Yu, 2017:278, ISBN 978-82-326-2624-3 (printed. ver.) ISBN 978-82-326-2625-0 (electronic ver.) ISSN 1503-8181.

“Network arch timber bridges with light timber deck on transverse crossbeams”

Anna Weronika Ostrycharczyk, 2017:318, ISBN 978-82-326-2704-2 (printed ver.) ISBN 978-82-326-2705-9 (electronic ver.) ISSN 1503-8181.

“Splicing of Large Glued Laminated Timber Elements by Use of Long Threaded Rods”

Martin Cepelka, 2017:320, ISBN 978-82-326-2708-0 (printed ver.) ISBN 978-82-326-2709-7 (electronic ver.) ISSN 1503-8181.

“Thermomechanical behaviour of semi-crystalline polymers: experiments, modelling and simulation”

Joakim Johnsen, 2017:317, ISBN 978-82-326-2702-8 (printed ver.) ISBN 978-82-326-2703-5 (electronic ver.) ISSN 1503-8181.

“Small-Scale Plasticity under Hydrogen Environment”

Kai Zhao, 2017:356, ISBN 978-82-326-2782-0 (printed ver.) ISBN 978-82-326-2783-7 (electronic er.) ISSN 1503-8181.

“Risk and Reliability Based Calibration of Structural Design Codes”

Michele Baravalle, 2017:342, ISBN 978-82-326-2752-3 (printed ver.) ISBN 978-82-326-2753-0 (electronic ver.) ISSN 1503-8181.

“Dynamic behaviour of floating bridges exposed to wave excitation”

Knut Andreas Kvåle, 2017:365, ISBN 978-82-326-2800-1 (printed ver.) ISBN 978-82-326-2801-8 (electronic ver.) ISSN 1503-8181.

“Dolomite calcined clay composite cement – hydration and durability”

Alisa Lydia Machner, 2018:39, ISBN 978-82-326-2872-8 (printed ver.). ISBN 978-82-326-2873-5 (electronic ver.) ISSN 1503-8181.

“Modelling of the self-excited forces for bridge decks subjected to random motions: an experimental study”

Bartosz Siedziako, 2018:52, ISBN 978-82-326-2896-4 (printed ver.). ISBN 978-82-326-2897-1 (electronic ver.) ISSN 1503-8181.

“A probabilistic-based methodology for evaluation of timber facade constructions”
Klodian Gradeci, 2018:69, ISBN 978-82-326-2928-2 (printed ver.) ISBN 978-82-326-2929-9 (electronic ver.) ISSN 1503-8181.

“Behaviour and modelling of flow-drill screw connections”
Johan Kolstø Sønstabø, 2018:73, ISBN 978-82-326-2936-7 (printed ver.) ISBN 978-82-326-2937-4 (electronic ver.) ISSN 1503-8181.

“Full-scale investigation of the effects of wind turbulence characteristics on dynamic behavior of long-span cable-supported bridges in complex terrain”
Aksel Fenerci, 2018:100, ISBN 978-82-326-2990-9 (printed ver.) ISBN 978-82-326-2991-6 (electronic ver.) ISSN 1503-8181.

“Modeling and simulation of the soft palate for improved understanding of the obstructive sleep apnea syndrome”
Hongliang Liu, 2018:101, ISBN 978-82-326-2992-3 (printed ver.) ISBN 978-82-326-2993-0 (electronic ver.) ISSN 1503-8181.

“Long-term extreme response analysis of cable-supported bridges with floating pylons subjected to wind and wave loads”
Yuwang Xu, 2018:229, ISBN 978-82-326-3248-0 (printed ver.) ISBN 978-82-326-3249-7 (electronic ver.) ISSN 1503-8181.

“Reinforcement corrosion in carbonated fly ash concrete”
Andres Belda Revert, 2018:230, ISBN 978-82-326-3250-3 (printed ver.) ISBN 978-82-326-3251-0 (electronic ver.) ISSN 1503-8181.

“Direct finite element method for nonlinear earthquake analysis of concrete dams including dam-water-foundation rock interaction”
Arnkjell Løkke, 2018:252, ISBN 978-82-326-3294-7 (printed ver.) ISBN 978-82-326-3295-4 (electronic ver.) ISSN 1503-8181.

“Electromechanical characterization of metal-coated polymer spheres for conductive adhesives”
Molly Strimbeck Bazilchuk, 2018:295, ISBN 978-82-326-3380-7 (printed ver.) ISBN 978-82-326-3381-4 (electronic ver.) ISSN 1503-8181.

“Determining the tensile properties of Arctic materials and modelling their effects on fracture”
Shengwen Tu, 2018:269, ISBN 978-82-326-3328-9 (printed ver.) ISBN 978-82-326-3329-6 (electronic ver.) ISSN 1503-8181.

“Atomistic Insight into Transportation of Nanofluid in Ultra-confined Channel”
Xiao Wang, 2018:334, ISBN 978-82-326-3456-9 (printed ver.) ISBN 978-82-326-3457-6 (electronic ver.) ISSN 1503-8181.

“An experimental and numerical study of the mechanical behaviour of short glass-fibre reinforced thermoplastics”

Jens Petter Henrik Holmstrøm, 2019:79, ISBN 978-82-326-3760-7 (printed ver.) ISBN 978-82-326-3761-4 (electronic ver.) ISSN 1503-8181.

“Uncertainty quantification and sensitivity analysis informed modeling of physical systems”

Jacob Sturdy, 2019:115, ISBN 978-82-326-3828-4 (printed ver.) ISBN 978-82-326-3829-1 (electric ver.) ISSN 1503-8181.

“Load model of historic traffic for fatigue life estimation of Norwegian railway bridges”

Gunnstein T. Frøseth, 2019:73, ISBN 978-82-326-3748-5 (printed ver.) ISBN 978-82-326-3749-2 (electronic ver.) ISSN 1503-8181.

“Force identification and response estimation in floating and suspension bridges using measured dynamic response”

Øyvind Wiig Petersen, 2019:88, ISBN 978-82-326-3778-2 (printed ver.) ISBN 978-82-326-377-9 (electronic ver.) ISSN 1503-8181.

“Consistent crack width calculation methods for reinforced concrete elements subjected to 1D and 2D stress states”

Reignard Tan, 2019:147, ISBN 978-82-326-3892-5 (printed ver.) ISBN 978-82-326-3893-2 (electronic ver.) ISSN 1503-8181.

“Nonlinear static and dynamic isogeometric analysis of slender spatial and beam type structures”

Siv Bente Raknes, 2019:181, ISBN 978-82-326-3958-8 (printed ver.) ISBN 978-82-326-3959-5 (electronic ver.) ISSN 1503-8181.

“Experimental study of concrete-ice abrasion and concrete surface topography modification”

Guzel Shamsutdinova, 2019:182, ISBN 978-82-326-3960-1 (printed ver.) ISBN 978-82-326-3961-8 (electronic ver.) ISSN 1503-8181.

“Wind forces on bridge decks using state-of-the art FSI methods”

Tore Andreas Helgedagsrud, 2019:180, ISBN 978-82-326-3956-4 (printed ver.) ISBN 978-82-326-3957-1 (electronic ver.) ISSN 1503-8181.

“Numerical Study on Ductile-to-Brittle Transition of Steel and its Behavior under Residual Stresses”

Yang Li, 2019:227, ISBN 978-82-326-4050-8 (printed ver.) ISBN 978-82-326-4015-5 (electronic ver.) ISSN 1503-8181.

“Micromechanical modelling of ductile fracture in aluminium alloys”

Bjørn Håkon Frodal, 2019:253, ISBN 978-82-326-4102-4 (printed ver.) ISBN 978-82-326-4103-1 (electronic ver.) ISSN 1503-8181.

“Monolithic and laminated glass under extreme loading: Experiments, modelling and simulations”

Karoline Osnes, 2019:304, ISBN 978-82-326-4204-5 (printed ver.) ISBN 978-82-326-4205-2 (electronic ver.) ISSN 1503-8181.

“Plastic flow and fracture of isotropic and anisotropic 6000-series aluminium alloys: Experiments and numerical simulations “

Susanne Thomesen, 2019:312, ISBN 978-82-326-4220-5 (printed ver.), ISBN 978-82-326-4221-2 (electronic ver.) ISSN 1503-8181

“Stress-laminated timber decks in bridges”

Francesco Mirko Massaro, 2019:346, ISBN 978-82-326-4288-5 (printed ver.), ISBN 978-82-326-4289-2 (electronic ver.) ISSN 1503-8181

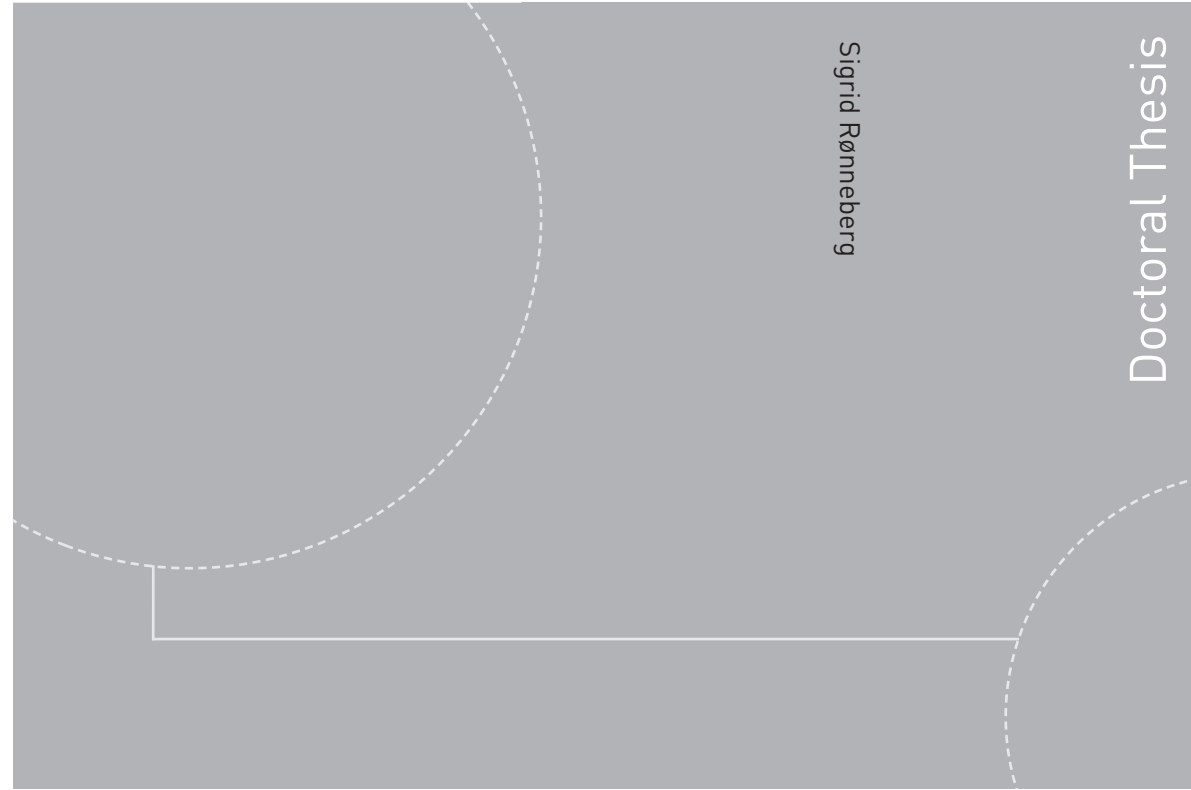
“Connections between steel and aluminium using adhesive bonding combined with self-piercing riveting: Testing, modelling and analysis”

Matthias Reil, 2019:319, ISBN 978-82-326-4234-2 (printed ver.), ISBN 978-82-326-4235-9 (electronic ver.) ISSN 1503-8181

“Designing Polymeric Icephobic Materials”

Yizhi Zhuo, 2019:345, ISBN 978-82-326-4286-1 (printed ver.), ISBN 978-82-326-4287-8 (electronic ver.) ISSN 1503-8181

ISBN 978-82-326-4527-8 (printed version)
ISBN 978-82-326-4524-5 (electronic version)
ISSN 1503-8181



Doctoral theses at NTNU, 2020:87

Sigrid Rønneberg

Fundamental Mechanisms of Ice Adhesion

Doctoral theses at NTNU, 2020:87

NTNU
Norwegian University of
Science and Technology
Faculty of Engineering
Department of Structural Engineering

 **NTNU**
Norwegian University of
Science and Technology

 **NTNU**

 **NTNU**
Norwegian University of
Science and Technology